Environmentally Benign Biodiesel Production by Heterogeneous Catalysis

by

Kathleen Francis Haigh

August 2013

A Doctoral Thesis submitted in partial fulfilment of the requirements for the award of the degree of Doctor of Philosophy in Chemical Engineering

Department of Chemical Engineering

In loving memory of my father,

Stephen Charles Haigh

Acknowledgements

Firstly I would to thank my supervisors, Professor Basu Saha and Dr Goran Vladisavljević for taking the time to guide me through this process. I have learnt a lot and your help is greatly appreciated.

I would like to thank ESPRC and Loughborough University for providing the funding and support which enabled me to do this PhD. I would also like to thank Purolite International Ltd (Mr Brian Windsor and the late Dr Jim Dale) for supplying the ion-exchange resin catalyst, Amano Enzyme Europe Ltd, UK for supplying Amano Lipase PS-IM and GreenFuel Oil Co Ltd, UK for supplying the used cooking oil. I would also like to thank Novozymes UK. Ltd. for supplying the Novozyme 435 catalyst and Dr David Cowan for technical advice and information relating to Novozyme 435.

I would like to thank the technical staff, Sean Creedon, Dave Smith, Rob Bentham, Kim Robertshaw, Monika Pietrzak, Graham Moody and Toby Vye for all the practical help, advice and a few really good laughs. In particular I would like to acknowledge the many hours Sean and Rob spend fixing the gas chromatography instrument and Dave who always knows where the important stuff is. A special mention also needs to go to Paul Izzard for all the IT support.

I would also like to thank the Mass spectrometry group in the Chemistry department for allowing me to use their instrument and helping with the method development. In particular I would like to recognise Jim Reynolds for his contribution.

A special mention needs to go to my colleague Sumaiya Zainal Abidin for helping me out in many aspects of my PhD project and Dipesh Patel.

While at Loughborough I have met a lot of interesting people who have provided me with support, good laughs and taught me about other cultures.

The people who have been most important to me are Claire Shaw and Tina Sutar who I now count as really good friends.

Last but certainly not least I would like to mention my family, particularly my mother and sister, who have been there for me no matter what.

Abstract

Process options to minimise the environmental impact and improve the efficiency of biodiesel production have been investigated. The process options considered include the use of heterogeneous catalysts and used cooking oil (UCO). An esterification pre-treatment reaction was investigated using an ion-exchange resin (Purolite D5082) and an immobilised enzyme (Novozyme 435). Another immobilised enzyme (Amano Lipase PS-IM) was investigated for transesterification. The fresh and used catalysts have been characterised. The catalytic activity of Purolite D5082, Novozyme 435 and Amano Lipase PS-IM have been investigated using a jacketed batch reactor with a reflux condenser.

Purolite D5082 has been developed for the esterification pre-treatment process and is not commercially available. Novozyme 435 has been shown to be an effective esterification catalyst for materials with high concentrations of free fatty acid but it has not been investigated for the esterification pre-treatment reaction. It was found that a high conversion was possible with both catalysts. The optimum reaction conditions identified for Purolite D5081 were a temperature of 60 °C, a methanol to free fatty acid (FFA) mole ratio of 62:1, a catalyst loading of 5 wt% resulting in a FFAs conversion of 88% after 8 h of reaction time. The optimum conditions identified for Novozyme 435 were a temperature of 50 °C, a methanol to FFA mole ratio of 6.2:1 and a catalyst loading of 1 wt% resulting in a conversion of 90% after 8 h of reaction time. These catalysts were compared to previously investigated Purolite D5081 and it was found that the highest conversion of 97% was achieved using Purolite D5081, however there were benefits to using Novozyme 435 because the reaction could be carried out using a much lower mole ratio, at a lower temperature and in much shorter reaction time.

During the Novozyme 435 catalysed esterification pre-treatment reactions it was found that the amount of free fatty acid methyl esters (FAME) formed during the reaction was greater than the amount of FFAs consumed. In order to investigate further an ultra-performance liquid chromatography mass

spectrometry (UPLC-MS) method was developed to monitor the monogclyeride (MG), diglyceride (DG) and triglyceride (TG) concentrations. This analytical method was used to show that Novozyme 435 would catalyse the esterification of FFAs as well as the transesterification of MGs and DGs typically found in UCO.

With the UPLC-MS method it was possible to separate the 1, 2 and 1, 3 DG positional isomers and from this it could be seen that the 1, 3 isomer reacted more readily than the 1, 2 isomer. The results from the UPLC-MS method were combined with a kinetic model to investigate the reaction mechanism. The kinetic model indicated that the reaction progressed with the sequential hydrolysis esterification reactions in parallel with transesterification.

Commercially available Amano Lipase PS-IM was investigated for the transesterification reaction. Enzymes are not affected by FFAs and as a result the optimisation was carried out with UCO as the raw material. An optimisation study for the transesterification of UCO with Amano Lipase PS-IM has not previously been reported. The conditions identified for the Amano Lipase PS-IM catalysed transesterification step are addition of 5 vol% water, a temperature of 30 °C, a methanol to UCO mole ratio of 3:1 and a catalyst loading of 0.789 wt% resulting in a TG conversion of 43%.

An overall enzyme catalysed process was proposed consisting of Amano Lipase PS-IM catalysed transesterification (stage 1) followed by Novozyme 435 catalysed esterification (stage 2). The previously identified optimum conditions identified for each catalyst were used for above stages. It was found that when the oil layer from stage 1 was dried the final TG conversion was 55%.

Table of Contents

List of Figures

List of Tables

List of Abbreviations

Asp	The aspartic acid amino acid residue
BCA	Bicinchoninic acid
BET	Brunauer-Emmett-Teller
DG	Diglycerides
DVB	Divinylbenzene
FAME	Fatty acid methyl esters
FEG-SEM	Field Emission Gun-Scanning Electron Microscopy
FFAs	Free fatty acids
FT-IR	Fourier Transform-Infra Red
Glu	The glutamic acid amino acid residue
His	The histadine amino acid residue
LC	Liquid chromatography
MG	Monoglycerides
PSD	Particle size distribution
Ser	The serine amino acid residue
TG	Triglycerides
UPLC-MS	Ultra Performance Liquid Chromatography Mass spectrometry
UV	Ultra Violet

Nomenclature

Al, F, T, D, M, Es, G and S	The components used for kinetic modelling being alcohol, free fatty acids, triglycerides, diglycerides, monoglycerides, esters, glycerol and substrates respectively
a_i	Area of component i
a_{is}	Area of the internal standard
AR_i	Area ratio of component i
c_i	Concentration of component I ($mg \cdot L^{-1}$)
d_{x0}	The diameter corresponding to x0 volume % on the relative cumulative particle diameter distribution curve
K_{Al}	The binding constant for Al
K_I	Inhibition constant ($mol^{-1} \cdot min^{-1}$)
K_{iAl}	The inhibition constants for Al
K_{is},	The inhibition constants for S
K_{mD}	Equilibrium constant for component D ($mol^{-1} \cdot min^{-1}$)
K_{mF}	Equilibrium constant for component F ($mol^{-1} \cdot min^{-1}$)
K_{mM}	Equilibrium constant for component M ($mol^{-1} \cdot min^{-1}$)
K_{mT}	Equilibrium constant for component T ($mol^{-1} \cdot min^{-1}$)
K_S	The binding constants for S
m_c	Mass of catalyst (g)
m_i	Mass of component i (g)
m_{is}	Mass of the internal standard (g)
MR_i	Mass ratio of component i
P_1	Pycnometer initial helium pressure (psi)
P_2	Pycnometer expanded helium pressure (psi)
RF_i	Response factor of component i
V_{cell}	Pycnometer cell volume (cm^3)
V_{eD}	Direct transesterification rate constant for D ($mol^{-1} \cdot min^{-1}$)
V_{eM}	Direct transesterification rate constant for M ($mol^{-1} \cdot min^{-1}$)
V_{eT}	Direct transesterification rate constant for T ($mol^{-1} \cdot min^{-1}$)
V_{exp}	Pycnometer expansion volume (cm^3)

V_{mD}	Hydrolysis rate constants for D ($mol^{-1}·min^{-1}$)
V_{mM}	Hydrolysis rate constants for M ($mol^{-1}·min^{-1}$)
V_{mT}	Hydrolysis rate constants for T ($mol^{-1}·min^{-1}$)
V_{sample}	Volume of catalyst sample (cm^3)

List of Greek Symbols

ρ_{H2O}	Density of water (kg·m-3)
ρ_L	Density of liquid, used cooking oil (kg·m-3)
ρ_t	True density (g·cm-3)

Description of Catalysts

Purolite D5082	A hyper-cross-linked cation exchange resin developed by Purolite International UK Ltd
Novozyme 435	*Candida antarctica* lipase B immobilised on acrylic re sin supplied by Novozymes UK Ltd
Amano Lipase PS-IM	Amano Lipase PS immobilised on diatomaceous earth. Amano Lipase is a *Pseudomanas cepacia* lipase, recently reclassified as *Burkholderia cepacia*

Chapter 1: Introduction

1.1 Motivation

Most of the energy used by the developed world is derived from fossil fuels, however there is increasing concern regarding the use of these fuels. It is generally accepted that burning fossil fuels is contributing to climate change and that these reserves are finite (Enweremadu & Mbarawa 2009; Balat & Balat 2010). In 2003 the European Union (EU) adopted a directive on biofuels for transport (Directive 2003/30/EC) which set an objective to replace 2% of energy for transport with biofuels by 2005, increasing to 5.75% in 2010 and 10% in 2020 (Melero et al. 2009a). This has subsequently been replaced with Directive 2009/28/EC, which requires 10 % of the energy used for transport to come from renewable sources by 2020.

Biodiesel is a fuel which can be used as part of the energy mix because it is derived from lipid materials such as animal fats and vegetable oils (Enweremadu & Mbarawa 2009). Animal fats and vegetable oils have a similar energy content to conventional diesel, but cannot be used directly as a fuel because of the viscosity (Knothe 2010). Methods to reduce the viscosity include heating, blending, micro emulsions, pyrolysis and transesterification, and these have all been described as methods to produce biodiesel (Meher et al. 2006a; Atadashi et al. 2013). However, the ASTM International definition will be used for this work and is “mono-alkyl esters of long chain fatty acids derived from vegetable oils or animal fats” (ASTM International, 2012), because it defines biodiesel in terms of the product composition. In addition it is slightly broader than the European standard which applies to a fatty acid methyl ester (FAME) liquid petroleum product (British Standards Online, 2013). Biodiesel can be used neat although is generally blended with conventional diesel (Balat & Balat 2010).

The conventional process to manufacture biodiesel is transesterification with methanol, using an alkaline catalysts such as sodium or potassium

hydroxide and edible vegetable oils such as rapeseed, soybean and sunflower oil (Di Serio et al. 2008; Balat & Balat 2010). Vegetable oils are composed primarily of triglyceride molecules. The transesterification reaction proceeds in a stepwise manner with triglycerides (TGs) being converted to diglycerides (DGs) and the diglycerides subsequently converted to monoglycerides (MGs) with the final products being glycerol and fatty acid alkyl esters (biodiesel) as shown in Figure 1.1 (Barakos et al. 2008; Hameed et al. 2009). There are ethical issues with regards to diverting or displacing food crops for fuel. In addition, changing the land use to cultivate fuel crops can be detrimental to the environment, because this can lead to an increased use of pesticides, a loss indigenous plants and potentially carbon release from the soil (Hara 2009). According to Directive 2009/28/EC these factors will need to be taken into account when calculating the contribution of a particular transport fuel to the target of 10%. Many of these issues can be minimised by using waste materials such as used cooking oil (UCO).

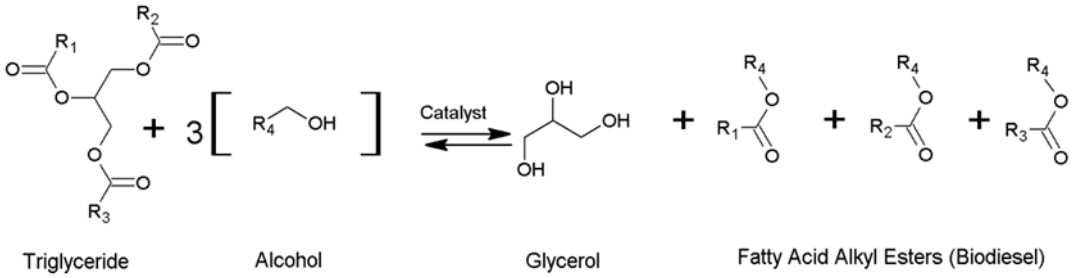

Figure 1.1. Schematic representation of the overall transesterification reaction.

A disadvantage of UCO is that it contains a significant amount of free fatty acids (FFAs), formed during the cooking process, and these react with the alkaline catalysts used during the conventional process leading to the formation of soap (Enweremadu & Mbarawa 2009). One of the solutions proposed for this problem is the use of alternative catalysts such as acid and enzyme catalysts because they are not affected by FFAs and these catalysts can simultaneously convert FFAs to biodiesel (Atadashi et al. 2013). The reaction rate is generally much slower than base catalysed transesterification and an alternative approach is a two-step process. The most common being acid catalysed esterification followed by base catalysed transesterification (Shahid &

Jamal 2011). The esterification reaction occurs when FFAs react with a short chain alcohol such as methanol to form the associated alkyl ester and the reaction scheme is shown in Figure 1.2. This is a reversible reaction with the reverse reaction being hydrolysis. When alcohol is added to a reaction mixture containing TGs and FFAs is possible for the esterification and transesterification reactions to occur simultaneously. The rate and selectivity of the reactions is determined by the catalyst and composition of the reaction mixture. The possibility of simultaneous reactions will be investigated.

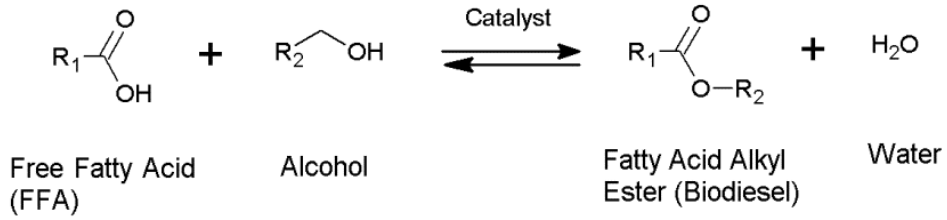

Figure 1.2. Schematic representation of the esterification reaction.

The production pathway will be taken into account when assessing the contribution of a fuel to the transport target of 10% (Directive 2009/28/EC). Homogeneous catalysts have been widely investigated for biodiesel production and are generally more efficient that the equivalent heterogeneous catalysts (Balat & Balat 2010; Atadashi et al. 2013). However, separating homogeneous catalysts from biodiesel requires additional equipment and generates a large amount of waste water (Xie & Li 2006; Caetano et al. 2009; Zabeti et al. 2009). This work will focus on assessing heterogeneous catalysts to improve the efficiency of biodiesel production. Ion-exchange resins for esterification pre-treatment and enzyme catalysts have both been shown to produce high yields at relatively benign operating conditions (Ozbay et al. 2008; Enweremadu & Mbarawa 2009). This work will focus on assessing an ion-exchange resin (Purolite D5082) and an immobilised enzyme (Novozyme 435) for the esterification pre-treatment reaction and an immobilised enzyme (Amano Lipase PS-IM) for the transesterification reaction as part of an environmentally benign process for biodiesel production.

1.2 Research Aims and Objectives

The aims and objectives of the work were to:

- Investigate the catalytic properties of the catalysts used in the work by means of various characterisation techniques. The catalysts investigated were fresh and used Purolite D5082, fresh and used Novozyme 435 and fresh Amano Lipase PS-IM. The techniques included field emission gun-scanning electron microscopy, pore size distribution, surface area measurements, elemental analysis, Fourier transform infra-red (FTIR) spectroscopy and sodium capacity determination.
- Characterise the UCO by determining the acid value, density, FFAs, FAME, water, monoglycerides (MG), diglycerides (DG) and triglycerides (TG) concentrations and the FFAs composition.
- Investigate the optimum batch reaction conditions for the esterification pre-treatment reaction and compare the catalytic activity of Purolite D5082, Novozyme 435 and previously investigated Purolite D5081.
- Develop an analytical technique to monitor the MG, DG and TG concentrations using liquid chromatography (LC).
- Develop a kinetic model to investigate the catalytic action of Novozyme 435 using the FFAs, FAME, MG, DG and TG concentrations and use this information to investigate the reaction mechanism.
- Investigate a two stage enzyme catalysed biodiesel production process focusing on the optimisation of the batch reaction conditions of the first stage catalysed by Amano Lipase PS-IM. The second stage will be catalysed using Novozyme 435.

1.3 Structure of Thesis

Brief descriptions of each chapter are summarised below:

Chapter 1: Introduction:- In this chapter the aims and objectives of the research work are discussed and the thesis structure is introduced.

Chapter 2: Literature Review:- A review of the literature pertaining to biodiesel production is presented in order to provide information on the background and context of biodiesel research. An overview of biodiesel production is provided in the first main section. The main types of catalyst investigated for biodiesel production are basic, acidic and enzymatic and these are discussed in subsequent sections. This is followed by a review of LC techniques assessed for investigating biodiesel production.

Chapter 3: Materials and Methods:- The materials and methods used for the experimental work are explained in this chapter. The main sections are materials, catalyst characterisation, batch experimental set-up and analytical techniques including the tested LC methods.

Chapter 4: Catalyst Characterisation:- Results of the characterisation of the fresh and used catalysts used in the experimental work are presented in this chapter. The physical properties of the catalysts were characterised using FEG-SEM, surface area, pore volume and diameter measurements, true density and porosity. The chemical properties were characterised using elemental analysis, FTIR measurements and sodium capacity determination. In addition the immobilised enzymes were characterised using a bicinchoninic acid (BCA) assay.

Chapter 5: Used Cooking Oil (UCO) Characterisation Batch Experiment Reproducibility:- Preparatory work essential for the batch experiments is covered in this chapter. In particular, the UCO was characterised using various chemical and physical methods and the results are

discussed. In addition, the reproducibility of the batch experiments was assessed.

Chapter 6:- Esterification Pre-treatment of Used Cooking Oil:- In this chapter, the catalytic activity of three esterification pre-treatment catalysts are compared. Optimisation studies were carried out on two types of catalysts; an ion-exchange resin (Purolite D5082) and an immobilised enzyme (Novozyme 435). The catalytic activity of these two catalysts was compared to the previously investigated ion-exchange resin, Purolite D5081.

Chapter 7: Liquid Chromatography Development Work and Kinetic Modelling:- A detailed investigation of the kinetic activity of Novozyme 435 for the esterification pre-treatment is explained in this chapter. A comparison of LC methods for monitoring biodiesel production was carried out. The most suitable method was identified as ultra performance liquid chromatography mass spectrometry (UPLC-MS) and this method used to monitor the MG, DG and TG trends of selected batch experiments. The parameters of various kinetic models were calculated and this was used to assess the reaction mechanism for Novozyme 435.

Chapter 8: Enzymatic Biodiesel Production:- In this chapter the production of biodiesel using enzyme catalysts is discussed. A two-stage process was proposed. The first stage was a transesterification reaction catalysed by Amano Lipase PS-IM and a detailed study of the optimum batch reaction conditions is discussed. The second stage was catalysed by Novozyme 435 using the optimum conditions identified in Chapter 6.

Chapter 9: Conclusions and Suggestions for Future Work:- Conclusions relating to the overall work and suggestions for future work are presented in this chapter.

Chapter 2: Literature Review

2.1 Introduction

The aim of this chapter is to review the current literature relevant to the environmentally benign production of biodiesel by heterogeneous catalysis. In order to do so it is necessary to understand the definition and composition of biodiesel. Various feedstocks can be used for biodiesel production and the choice has implications in terms of the environmental impact and type of process that can be used for biodiesel production. These issued are discussed in Section 2.2.

The catalysts investigated for biodiesel production can be classified as homogeneous and heterogeneous (Helwani B et al. 2009; Enweremadu & Mbarawa 2009). This work is focused on heterogeneous catalysts because they are readily separated and reused. The catalysts investigated for biodiesel production can also be classified as base, acid and enzyme catalysts (Semwal et al. 2011; Atadashi et al. 2013). The environmental impact of biodiesel production can be minimised by designing processes which operate at low temperatures and with a minimum amount of catalyst and reagent. On this basis enzymes are often favoured because they operate best at relatively benign conditions (Hara 2009). High conversions at relatively benign conditions can also be achieved using cation-exchange resins for esterification (Ozbay et al. 2008; Abidin et al. 2012). As a result the emphasis is on cation exchange resins and enzyme catalysts. Base catalysed biodiesel production is discussed in Section 2.3, followed by acid catalyst biodiesel production in Section 2.4 and enzyme catalysed biodiesel production in Section 2.5.

Methods to monitor the concentration of free fatty acids (FFAs) and free fatty acid methyl esters (FAME) were previously developed (Abidin 2012). However it was found that a more detailed analysis was required for some of the work with liquid chromatography identified as the most suitable analytical

technique. Potential methods for the analysis of biodiesel products with a focus on liquid chromatography are discussed in Section 2.6.

2.2 Overview of Biodiesel Production

2.2.1 What is Biodiesel?

Vegetable oils and animal fats are being investigated as an alternative to conventional diesel because they have a similar calorific value and are renewable. However vegetable oils and animal fats cannot be used directly in modern diesel engines because they are comprised of high viscosity triglycerides. The high viscosity means there is poor atomisation of the fuel leading to poor combustion and this causes deposits, a deterioration in performance and eventually engine damage (Xie & Li 2006; Demirbas 2009; Knothe 2010).

The viscosity can be changed using physical methods such as heating or blending. Diesel engines can be modified so that vegetable oil is heated prior to combustion however the chemical structure remains unchanged and as a result long term use can lead to engine damage (Demirbas 2009; Balat & Balat 2010). Blending various vegetable oils with diesel has been shown to improve engine performance and reduce emissions (Agarwal & Rajamanoharan 2009; Hazar & Aydin 2010) during short term tests. However a fuel blend of 25% sunflower oil with 75% diesel was found to be unsuitable for long term use in a direct-injection engine (Balat & Balat 2010).

The viscosity can also be reduced by chemically changing the structure of the triglycerides using a process such as transesterification or pyrolysis. Pyrolysis involves the thermal or catalytic cracking of the triglyceride molecules to form a fuel with a similar composition to conventional diesel (Maher & Bressler 2007; Knothe 2010). The product composition depends on parameters such as temperature, catalyst type and vegetable oil type (Tian et al. 2008; Knothe 2010). Alternatively, vegetable oil can be blended with crude oil at the refinery and existing processes such as cracking and hydrodeoxygentation used to convert vegetable oil to renewable diesel;

however the refinery processes and final product composition may be affected (Huber et al. 2007; Maher & Bressler 2007; Šimáček et al. 2011; Bielansky et al. 2011). Using existing processes is expected to reduce costs however the reaction kinetics and effect of vegetable oil on the refinery processes need to be better understood and modifications may be required which will increase the costs (Melero et al. 2010).

Transesterification is relatively simple and well understood, and as a result it is the preferred process for reducing the viscosity of vegetable oil (Enweremadu & Mbarawa 2009; Demirbas 2009; Balat & Balat 2010). Transesterification, also known as alcoholysis, occurs when triglycerides react with a short chain alcohol in the presence of a catalyst to form their respective fatty acid mono-alkyl esters and glycerol (Hameed et al. 2009; Caetano et al. 2009; Zabeti et al. 2009). This fuel has a different chemical structure to conventional diesel, however, the combustion properties and cetane number are similar (Knothe 2010).

Biodiesel has been described as a fuel derived from vegetable oils and animal fats which can be produced using techniques such as blending, microemulsions, pyrolysis and transesterification (Meher B et al. 2006; Atadashi et al. 2013). This definition then covers fuels with a variety of chemical structures and associated advantages and disadvantages as discussed above. Alternatively ASTM International defines biodiesel as “mono-alkyl esters of long chain fatty acids derived from vegetable oils or animals fats” (Su & Wei 2008; Enweremadu & Mbarawa 2009). Fuel produced by techniques such as pyrolysis and cracking are then known as green diesel or renewable diesel (Knothe 2010). The ASTM definition of biodiesel is more specific and meaningful and as a result it will be the definition of biodiesel used in this work. Biodiesel can be used as is or blended with conventional diesel (Ganesan et al. 2009).

The advantages of biodiesel compared to conventional diesel are given below (Helwani et al. 2009a; Russbueldt & Hoelderich 2009; Xie & Li 2006):

- They can be derived from local renewable resources.

- Improved biodegradability and non-toxicity.
- Reduction of most exhaust emissions including SOx, CO, unburnt hydrocarbons and particulate matter although there is an increase in NOx.
- Safer handling and storage due to the lower volatility and higher flash point.
- Improved lubricating properties.

2.2.2 Environmental Considerations

Biodiesel is perceived to be a renewable fuel source. However in order for it to be truly renewable the energy consumed during production needs to be less than the energy provided when biodiesel is burned as fuel. A typical example of the stages required to produce biodiesel are shown in Figure 2.1 and include the cultivation of plants, harvesting and transport of the seeds, conversion of the seeds to oil and subsequently to biodiesel (Hara 2009; Knothe 2005).

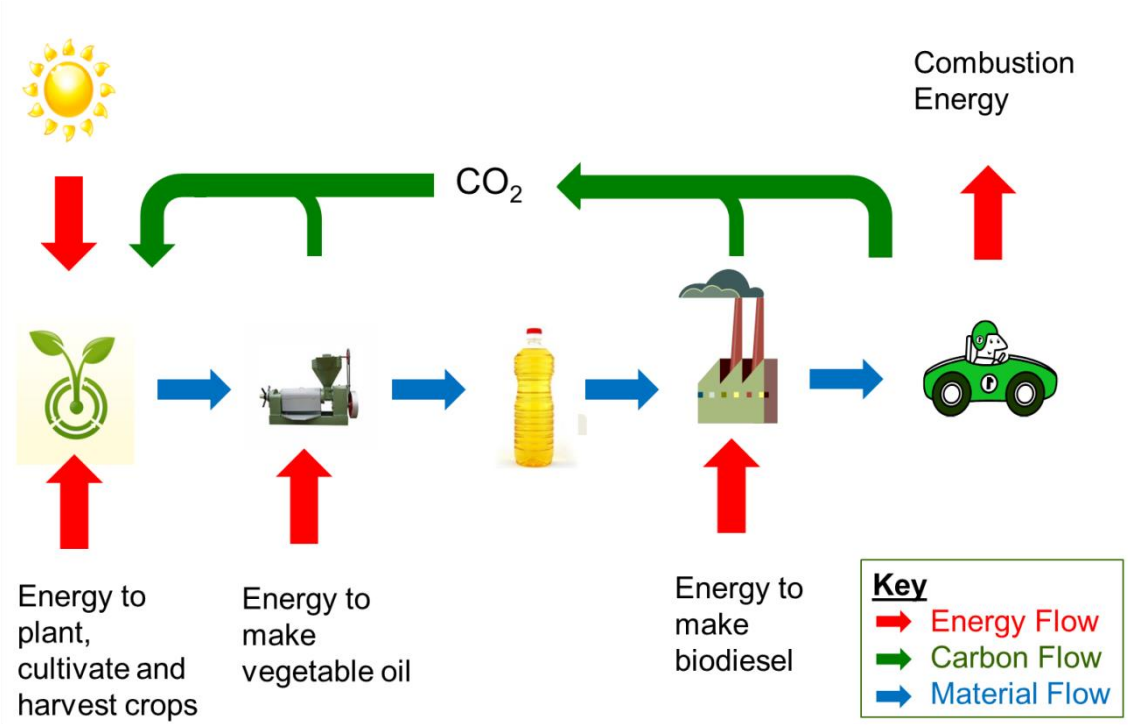

Figure 2.1. Energy and carbon cycle for the production of piodiesel.

When cultivating plants to provide fuel there are economic, environmental and social issues which need to be taken into account, that do not occur when conventional diesel is used. Oils from plants such as rapeseed

and soybean can be used as food or fuel and as a result there is direct competition between food and fuel (Hara 2009; Helwani et al. 2009a). In addition, growing crops for fuel can have detrimental effects on the environment such as contamination of surface water from the use of pesticides and herbicides, and cutting down indigenous plants to make space for agriculture (Knothe et al., 2005).

A life cycle assessment provides a systematic approach to evaluating environmental impacts although there is a subjective element because judgements need to be made regarding the importance of a given impact (Knothe 2005; Hara 2009). A life cycle assessment focused on the reduction of carbon emissions found that there was a 78% improvement from biodiesel compared to conventional diesel (Helwani et al. 2009b). An alternative approach is to use an energy balance to assess the units of energy yielded for each unit of energy required to produce a given fuel (Balat & Balat 2010). It was found that biodiesel has the highest balance when compared to liquid fuels producing a positive energy balance of 2.5 – 3.2. However some of the fossil fuel energy inputs were ignored in the assessment where a value of 3.2 was determined.

In order to ensure that biodiesel is an environmentally benign fuel all aspects of the lifecycle need to be considered. This includes minimising the consumption of energy and resources during the manufacture of biodiesel and selecting a suitable feedstock.

2.2.3 Potential Biodiesel Feedstocks

The conventional feedstock for producing biodiesel are edible vegetable oils such as rapeseed oil (Georgogianni et al. 2009a), soybean oil (Xie & Huang 2006), sunflower oil (Türkan & Kalay 2006) and palm oil (Al-Zuhair et al. 2007; Hameed et al. 2009). More than 95% of the global production of biodiesel uses edible vegetable oil as the feedstock (Balat & Balat 2010). Biodiesel produced from edible vegetable oil is sometimes (Tariq et al. 2012) referred to as a first generation biofuel.

The cost of producing biodiesel is much higher than conventional diesel, particularly when refined or virgin oil is used due to the high cost of the raw material. Haas (2005) estimated that the price of the amount of soybean oil required to make a litre of biodiesel was US$ 0.40-0.48 compared to US$ 0.21-0.24 per litre of diesel. Haas et al. (2006) developed an economic model to investigate the cost of biodiesel production with soybean oil as the raw material at a cost of 0.52 US$·kg^{-1} that the vegetable oil represented 82% of the cost. The remaining cost components were chemicals (7%), depreciation (5%), direct labour (2%), utilities (2%) and general overhead (1%). Costs not accounted for in this model include an internal rate of return, economic life, corporate tax rate salvage value and debt fraction (Haas et al. 2006).

In addition there are ethical concerns with regards to using a potential food source as a fuel. In order to overcome ethical concerns with using a potential food source as fuel the use of non-edible oils has also been investigated, i.e., *Jatropha curcas* (Su & Wei 2008; Corro et al. 2013), *Pongamia pinnata* (Meher et al. 2006a) and *babassu* oil (Da Rós et al. 2010). This type of fuel is sometimes refered to as a second generation biodiesel (Tariq et al. 2012). Plants such as *J. curcas* can grow in poor quality soil and is often used for erosion control however growing this type of crop can still lead to environmental damage and competition with food growing resources (Hara 2009; Corro et al. 2013).

Animal fats have been investigated for the production of biodiesel and include lard (Caetano et al. 2009; Huang et al. 2010) and beef tallow (Da Rós et al. 2010) Biodiesel from animal fats is not widely used because the cold flow properties are not as good as for biodiesel derived from vegetable oils such as soybean oil (Wyatt et al. 2005).

More recently microalgae have been considered as a source of oil for biodiesel production (Balat & Balat 2010; Demirbas & Fatih Demirbas 2011; Tran et al. 2012). Microalgea can be grown in a variety of aquatic environments and as result non-agricultural land can be used for cultivating microalgae. Microalgea grow rapidly with the oil content up to 40 wt%.

Microalgae consume carbon dioxide and can be used as part of a process to scrub power plant flue gasses. The microalgae species are subdivided into ten taxonomic groups which include green algae (*Chlorophyceae*), diatoms (*Bacillariophyceae*), yellow-green (*Xanthophyceae*), golden algae (*Chrysophyceae*), red algae (*Rhodophyceae*), brown algae (*Phaeophyceae*), blue-green algae (*Cyanophyceae*), dinoflagellates (*Dinophyceae*), *Prasinophyceae* and *Eustigmatophyceae* (Williams & Laurens 2010). Species which have been investigated for biodiesel production include *Chlorella protothecoides* (Williams & Laurens 2010) and *Chlorella vulgaris* (Yin et al. 2010). The cultivation of microalgae is currently not economically feasible due the costs associated with harvesting the microalgae however there is the potential to improve the economics by cultivating algae to provide additional products (Williams & Laurens 2010). Biodiesel from microalgae is sometimes referred to as third generation biodiesel (Tariq et al. 2012).

The conventional raw materials for biodiesel production are vegetable oils and animal fats with a high concentration of triglycerides, with the emphasis on converting the triglycerides to biodiesel. However FFAs can also be converted to biodiesel by means of an esterification reaction (Melero et al. 2009a). Many crude vegetable oils contain significant amounts of FFAs, which are separated from the triglycerides during refining. Palm fatty acid distillate (Talukder et al. 2009) and soybean oil deodoriser distillate (Souza et al. 2009) have been investigated as potential raw materials for biodiesel production.

Another potential raw material for the production of biodiesel is used cooking oil (UCO). The production of biodiesel from UCO has been widely investigated (Ozbay et al. 2008; Balat & Balat 2010; Lam et al. 2010) and offers numerous environmental benefits because a waste material is being recycled. There are numerous concerns with the disposal of UCO and it is often poured down the drain or dumped illegally causing water and environmental pollution (Balat & Balat 2010; Enweremadu & Mbarawa 2009). UCO generally contains FFAs and water due to the cooking process (Ozbay et al. 2008; Enweremadu & Mbarawa 2009). UCO has been selected as the feedstock for this work because it is a waste material and relatively cheap.

2.2.4 Potential Processes

There are a variety of methods available to produce biodiesel and the feedstock will influence the choice of process. The conventional process is to convert the triglycerides in refined vegetable oil to fatty acid methyl esters (FAME) using an alkali catalysed transesterification reaction with methanol as the reagent (Ganesan et al. 2009). The transesterification reaction proceeds in a stepwise manner with the triglycerides being converted to diglycerides and the diglycerides subsequently converted to monoglycerides with the final products being glycerol and fatty acid alkyl esters (biodiesel) as shown in Chapter 1, Figure 1.1 (Barakos et al. 2008; Hameed et al. 2009).

Alkali catalysed transesterification is not suitable for feedstocks where the FFAs concentration is greater than 0.5 wt%, although this can vary depending on the process (Lam et al. 2010; Melero et al. 2009a). FFAs react with the alkali catalysts leading to saponification side reactions. These side reactions reduce the amount of biodiesel produced because the catalyst is consumed and the biodiesel is difficult to separate from the reaction mixture (Balat & Balat 2010). Heterogeneous basic catalysts have been proposed as a solution however saponification is still possible with this type of catalyst (Russbueldt & Hoelderich 2009; Melero et al. 2010). In addition, the FFAs will need to be removed during the process so that the final product will meet the biodiesel specifications (Knothe 2010).

Acid catalysts can be used for the transesterification reaction because these catalysts are not affected by the presence of FFAs, in fact they simultaneously catalyse the esterification and transesterification reactions (Lam et al. 2010; Melero et al. 2009a). However, acid catalysed transesterification is slow when compared to base catalysed transesterification (Balat & Balat 2010).

Processes have been investigated for the removal of FFAs, from UCO, prior to transesterification and these include a method of steam pre-treatment followed by sedimentation, separation by column chromatography, various filtration and drying methods and neutralisation (Enweremadu & Mbarawa

2009; Russbueldt & Hoelderich 2009). Alternatively the FFAs in UCO can be converted to biodiesel by means of an esterification reaction followed by transesterification (Kulkarni & Dalai 2006; Ozbay et al. 2008).

The esterification reaction occurs when FFAs react with a short chain alcohol such as methanol to form the associated alkyl ester and the reaction scheme is shown in Chapter 1, Figure 1.2. This is a reversible reaction with the reverse reaction being hydrolysis. Esterification has been investigated as a pre-treatment step raw materials with a high FFAs content such as UCO (Russbueldt & Hoelderich 2009; Melero et al. 2009b). Raw materials containing high concentrations of FFAs such as palm fatty acid distillate and soybean oil deodoriser distillate can be converted directly to biodiesel using an esterification reaction (Souza et al. 2009; Talukder et al. 2009).

Another option is to use an enzyme catalyst to produce biodiesel. Lipases are the class of enzymes investigated for the production of biodiesel. This class of enzyme can catalyse transesterification, esterification and hydrolysis (Tongboriboon et al. 2010). The order of preference for the reactions depends on the lipase type, feedstock and composition of the reaction medium. The saponification reaction does not occur when using lipase catalysts and as result separation of glycerol is relatively easy and the methyl esters do not need purification (Balat & Balat 2010). To date lipase catalysed transesterification is relatively slow and lipases are relatively expensive.

Lipase catalysed hydrolysis reactions can be used to convert triglycerides to FFAs (Hara 2009; Melero et al. 2009a). The hydrolysis reaction proceeds in a stepwise manner similar to transesterification although the reagent is water and the final products are FFAs and glycerol as shown in Figure 2.2. The FFAs then need to be converted to biodiesel by means of an esterification reaction. This approach is generally considered for unrefined vegetable oil which contains triglycerides and high levels of FFAs (Talukder B et al. 2010).

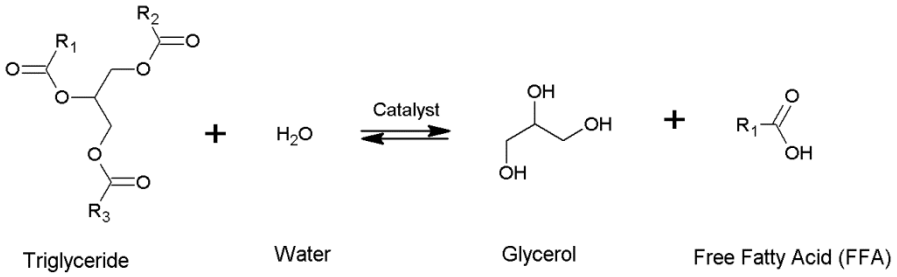

Figure 2.2. Schematic representation of the overall hydrolysis reaction, of triglycerides.

Non-catalysed processes for the manufacture of biodiesel have been investigated using supercritical methanol (Melero et al. 2009a; Zabeti et al. 2009). The reactions take place in a single phase because supercritical methanol is fully miscible in vegetable oil and as result the reaction occurs very fast with equilibrium being reached in about 2-4 min (Helwani et al. 2009a). The transesterification of triglycerides and the esterification of FFAs occur simultaneously. The disadvantage of this process is that high temperatures (250-400°C) and pressures (35–60 MPa) are required (Zabeti et al. 2009). This means that the process will be expensive to run however there may be some financial and environmental benefits as no catalyst is required.

Alcohol, particularly methanol, and vegetable oil are not very miscible leading to the formation of two liquid phases (Xie & Li 2006; Zabeti et al. 2009). One way of overcoming this problem is to use a co-solvent such as tetrahydrofuran, dimethyl sulfoxide, n-hexane and ethanol (Al-Zuhair et al. 2006; Semwal et al. 2011). An addition reason for using an co-solvent during enzyme catalysed reactions is that suitable solvents can be used to dilute the short chain alcohols which can deactivate enzymes (Su & Wei 2008). Talukder et al. (2009) assessed various solvents for improved biodiesel yield from the esterification of palm fatty acid distillate (PFAD) using an ion-exchange resin and an enzyme catalyst. It was found that isooctane increased the Novozyme 435 catalysed yield from 90 to 95% but had a negligible effect on the ion-exchange system. Organic solvents have several drawbacks such as diluting the reagents, adding mass transfer resistances and requiring additional solvent recovery (Helwani et al. 2009b; Tongboriboon et al. 2010). The addition of an

organic solvent is not in-line with an environmentally benign process and will not be considered further.

Alternative processes, such as ultrasound energy and microwave irradiation have been considered. Ultrasound energy was compared to a mechanical stirrer for the transesterification of soybean oil (Georgogianni et al. 2009b). The reaction rate increased significantly reducing the reaction time from 24h to 5h. Microwave assisted heating has been shown to increase the reaction rate. It has been shown that a conversion of 96% could be achieved using a heteropoly acid, with a reaction time of 10 min and a temperature of 60 °C (Zhang et al. 2010). Although these techniques show potential they have not been widely investigated (Atadashi et al. 2013)

A summary of the most common reaction schemes and the associated feedstocks is given in Table 2.1. UCO has been selected as the feedstock for this work and as a result chemical and enzyme catalysed esterification pre-treatment will be investigated. This will be followed by an investigation of lipase catalysed transesterification.

Table 2.1. A summary of potential reaction schemes and the associated feedstocks.

Reaction Scheme	Proposed Feedstock
Base catalysed transesterification	Rapeseed oil (Georgogianni et al. 2009a) Rapeseed oil (Komers et al. 1998)
Acid catalysed transesterification	UCO (Helwani et al. 2009b). Crude coconut oil (Jitputti et al. 2006)
Enzyme catalysed transesterification	Waste frying oil (Azócar et al. 2010) Sunflower oil (Soumanou 2003) Microalgal oil from *Chlorella vulgaris* ESP-31 (Tran et al. 2012)
Esterification - Transesterification	UCO (Ozbay et al. 2008) Crude *J. curcas* (Corro et al. 2013)
Esterification	Soybean oil deodoriser distillate (Souza et al. 2009) Palm fatty acid distillate (Talukder et al. 2009)

	Lard (Caetano et al. 2009)
Hydrolysis - Esterification	Acid oil, an oil refining by product (Watanabe et al. 2007)
	UCO (Talukder et al. 2010a)

2.3 Base Catalysed Biodiesel Production

2.3.1 The Conventional Homogeneous Process

Homogeneous alkaline catalysed transesterification has been reported using hydroxides (Hara 2009; Zabeti et al. 2009), alkaline metal alkoxides (Xie & Li 2006), sodium and potassium carbonates. Fast reaction rates are possible using methoxide catalysts however they are expensive and hydroscopic (Akoh et al. 2007; Ganesan et al. 2009). Sodium hydroxide and potassium hydroxide are generally used for industrial processes (Atadashi et al. 2013). Typical reaction conditions using a refined vegetable oil are an alcohol to oil mole ratio of 6:1, 60-65 °C, a pressure of 1.4-4.1 bar and a catalyst loading of 0.5-2 wt% (Helwani et al. 2009b). For these conditions a conversion greater than 95% can be expected after 1 h of reaction time.

Homogeneous catalysts are popular because they allow short reaction times and relatively benign conditions however there are problems with downstream processing. The homogeneous catalysts are dissolved in the transesterification products and this means that complex and expensive processing units are required which use large amounts of energy, chemicals and water to separate and neutralise the alkali catalysts generating a large amount of effluent (Cordeiro et al. 2008; Hara 2009; Caetano et al. 2009).

Another problem with using homogeneous alkaline catalysts is saponification side reactions. Water can be present as a contaminant or formed from the reaction of the hydroxide with alcohol (Hameed et al. 2009) and leads to the hydrolysis of esters to soap. Saponification can also occur when there are high levels of FFAs, which react with alkali catalyst to form soap

and water (Ozbay et al. 2008; Enweremadu & Mbarawa 2009). Saponification consumes the catalyst and the soaps form stable emulsions which cause problems with the recovery and purification of biodiesel (Enweremadu & Mbarawa 2009; Atadashi et al. 2013). Opinions vary about the upper limit of FFA that is acceptable for transesterification to avoid saponification. Yagiz et al. (2007) recommended a maximum level of 1 wt% while Ozbay et al. (2008) suggested that the FFA content should be as low as 0.5 wt% of the vegetable oil. Georgogianni et al. (2009a) found that the catalyst concentration was also a factor in saponification with soap formation occurring with a NaOH concentration of 2.5 wt% and feedstock oil with an FFA concentration of 0.9 wt%. The maximum recommended %FFAs has been found to vary from 0.5 to 3 wt% (Atadashi et al. 2013).

2.3.2 Heterogeneous Basic Catalysts

Solid basic catalysts have been proposed for biodiesel production because they are readily separated from the reaction mixture and can be reused, they are less corrosive and will not be affected by FFAs (Hara 2009; Atadashi et al. 2013). The heterogeneous basic catalysts investigated for biodiesel can be categorised as metal oxides, mixed metal oxides, supported alkali and alkaline earth metals, basic zeolites, hydrotalcites and anion exchange resins. A summary of the heterogeneous basic catalysts discussed in this section is given in Table 2.2.

Metal oxides have been investigated because they have a low solubility in the reaction mixture. The main types investigated being calcium oxide and magnesium oxide although strontium oxide has also been considered (Sharma et al. 2011). A yield of 92% has been reported using 5.0 wt% of CaO as a catalyst, a 12:1 mole ratio, after 1 h (Sharma et al. 2011). Alternatively a conversions of 91 – 97% are possible with reaction times of 10 min, a methanol to oil mole ratio of approximately 40:1 and a temperature of 300 °C (Hara 2009). However it has been found that there are problems with leaching into the reaction mixture and forming calcium diglyceroxide which catalysed the reaction (Kouzu et al. 2009)

Limmanee et al. (2013) investigated mixed metal oxides of a CaMgZn mixed oxide by varying the ratio of metals. It was found that a FAME yield of 97.5% was achieved with a Ca:Mg:Zn mole ratio of 3:1:1 using a methanol to oil ratio of 20:1, a catalyst loading of 6 wt% and a temperature of 60 °C. It was found that there was a correlation between the initial rate of FAME formation and the total basicity. A conversion of 94% was possible at similar reaction conditions using a Li-doped MgO catalyst (Wen et al. 2010). However, metal leaching was detected.

The performance of basic catalysts can be improved by using a support to increase the basicity and surface area. Examples include SrO, MgO or KCO_3 on an alumina (Al_2O_3) support (Hara 2009; Helwani et al. 2009b). Basic zeolites and alkali- or alkaline earth metal composites such as Mg/hydrotalcite and Li/hydrotalcite have also been considered. Noiroj et al. (2009) compared KOH/Al_2O_3 with KOH/NaY zeolite and found a conversion of 91% was possible for both catalysts with a reaction time of 2-3 h, 60 °C, a mole ratio of 15:1 using methanol and a catalyst loading of 3-6 wt%. There was potassium leaching from both catalysts. A calcined sodium silicate catalyst has been found to give a reasonably stable conversion of 100%, at 60 °C, after 1 h and a methanol to oil mole ratio of 7.5:1 (Guo et al. 2010).

Xie and Li (2006) compared various potassium compounds (KF, KCl, KBr, KI, K_2CO_3, KNO_3 and KOH) loaded onto an alumina support and found that with potassium iodide provided the highest conversion. In the second stage various supports were compared (ZnO_2, ZnO, NaX, KL and Al_2O_3) and it was found that the highest conversion was achieved using alumina. Xie & Li (2006) found that the best catalyst was 35 wt% KI loading on Al_2O_3 and calcined at 500 °C for 3 h. The reaction conditions, with a reflux of methanol, were a methanol to oil ratio of 15:1, a reaction time of 8h and a catalyst loading of 2.5% which resulted in a conversion of 96%. It was found that conversion increased with increasing catalyst basicity.

Hameed et al. (2009) investigated KF/ZnO because the preparation of this catalyst is easy and the materials are relatively cheap. It was found that catalyst loading was the most important parameter for this system with conversion increasing from 18 % to 87 % when the catalyst loading was increased from 1 % to 3 %. The optimum conversion of vegetable oil was 89% with a methanol to oil mole ratio of 11.43:1, a reaction time of 9.72 h and 5.52 wt% of catalyst using palm oil. These results correspond with earlier work carried out by Xie & Huang (2006) using soybean oil.

Ramos et al. (2008) assessed the catalytic activity of various basic zeolite catalysts; mordenite, beta and X. Zeolite X shown the highest transesterification activity and this was attributed to a higher concentration of super basic sites. It was found that the catalytic activity of zeolite X was improved by loading with and excess of sodium (titled 3NaX). Sodium bentonite binder was used to improve the mechanical strength of Zeolite X and it was found that this had a minimal effect on the catalytic activity, the resulting catalysts was titled 3NaXB. It was shown that a conversion of 95% was possible using 3NaXB. A reusability study showed that there was a homogeneous-like mechanism due to leaching of alkali methoxide species.

Hydrotalcite is an anionic and basic clay also known as layered double hydroxide and an example of the chemical formula is; $Mg6Al_2(OH)16CO_3{\cdot}4H_2O$ (Atadashi et al. 2013). The transesterification of refined and acidic cottonseed oil was investigated using an Mg-Al-CO_3 hydrotalcite catalyst (Barakos et al. 2008). It was found that a conversion of 98% was possible when glycerol removal stages were incorporated using temperature of 180-200 °C. It was found that simultaneous esterification and transesterification was possible when this catalyst was used for the conversion of acid cottonseed oil. Georgogianni et al. (2009b) investigated Mg/MCM-41 zeolite, MgAl hydrotalcite and mesoporous K/ZrO_2 and it was found that the highest conversion was achieved using the MgAl hydrotalcite with a conversion of 97% after 24 h.

A commercial process using a heterogeneous basic catalyst has been implemented and is based on the Esterfip-H technology developed by the

Institute Français du Petrole (Melero et al. 2009a; Limmanee et al. 2013). The catalyst used for this process is composed of a mixed oxide of zinc and aluminium. A continuous two-step process is required with intermediate glycerol removal in order to shift the equilibrium towards biodiesel formation. The reaction is carried out at a higher temperature than homogeneous processes however the final conversion is nearly 100% and with a purity greater than 99%. Although solid basic catalysts have been proposed for use with UCOs the raw material specifications require an FFAs concentration should be below 0.25% and a water concentration below 1000 ppm.

Anion exchange resins have also been considered for biodiesel production. A weak anion exchange resin (Amberlite IRC-93) was compared to a strong resin (Amberlite IRA-900) for the transesterification of yellow horn oil and it was found that conversion was substantially higher with Amberlite IRA-900 (Li et al. 2012). It was shown that while a conversion of 96% could be achieved using a microwave assisted technology, when conventional heating was used the conversion was 26%. In contrast Shibasaki-Kitakawa et al. (2007) found that the activity of PA306s was comparable to homogeneous base catalysts using a conventional batch reactor. Abidin (2012) investigated PA360s for the transesterification of pre-treated UCO and found that a conversion of 75% was possible at 55 °C, using a catalyst loading of 9 wt% and a methanol to oil mole ratio of 18:1.

There is a lot of potential to use basic catalysts for the production of biodiesel and high conversions have been reported at relatively benign operating conditions (Hara 2009; Sharma et al. 2011) although temperatures as high as 200 °C have been investigated. It has been found that conversion increases with increasing basicity (Xie & Li 2006; Georgogianni et al. 2009a; Limmanee et al. 2013) However there are still problems with this type of catalyst which include leaching of the active species, sensitivity to water and FFAs (Sharma et al. 2011; Atadashi et al. 2013). In addition the preparation of many of these catalysts is complex and calcining at high temperatures is required for some of these catalysts (Atadashi et al. 2013).

Table 2.2. A summary of the heterogeneous basic catalysts discussed

Catalyst Type	Reaction Conditions*	Conversion	Reference
Ca:Mg:Zn with the mole ratio 3:1:1, calcined at 800 °C for 2 h	Palm kernel oil, 60 °C, methanol, 20:1 mole ratio, 6 wt% catalyst	97%	Limmanee et al. (2013)
1.4 wt% Li/MgO, calcined at 550 °C for 10 h	Soybean oil, 60 °C, 9 wt% catalyst loading, methanol, 12:1 mole ratio	94%	Wen et al. (2010)
Sodium silicate, Calcined at 400 °C for 2 h	Soybean oil, 60 °C, 1 h, 3 wt% catalyst, methanol, 7.5:1 mole ratio	100%	(Guo et al. 2010)
25 wt% KOH/A_2O_3, calcined at 500 °C for 3 h	Palm oil, 60 °C, 2 h, 3 wt% catalyst, methanol, 15:1 mole ratio	91%	Noiroj et al. (2009)
10 wt% KOH/NaY, dried in air at 110 °C for 24 h	Palm oil, 60 °C, 3 h, 6 wt% catalyst, methanol, 15:1 mole ratio	91%	Noiroj et al. (2009)
35 wt% KI/ A_2O_3, calcined at 500 °C for 3h	Soybean oil, ~65 °C, 8 h, 2.5 wt% catalyst, methanol, 15:1 mole ratio	96 %	Xie & Li (2006)
35 wt% KF/ZnO, calcined at 600 °C for 5 h	Palm oil, 65 °C, 10 h, 5.5 wt% catalyst, methanol, 11:1 mole ratio	89%	Hameed et al. (2009)
15 wt% KF/ZnO, calcined at 600 °C for 5 h	Soybean oil, ~65 °C, 9h, 3 wt% catalyst, methanol, 10:1 mole ratio	87%	Xie & Huang (2006)
20 wt% K/ZrO_2, calcined at 500 °C for 3 h	Soybean oil, 24h	89%	Georgogianni et al. (2009b)
Mg/MCM-41 , calcined at 600 °C for 2 h	Soybean oil, 24h	85%	Georgogianni et al. (2009b)
NaXB Zeolite X with sodium bentonite	Sunflower oil, 60 °C, 7h, 10 wt% catalyst, methanol, 6:1 mole ratio	95%	(Ramos et al. 2008)
Mg-Al-CO_3 hydrotalcite	Transesterification and esterification, acidic cotton seed oil, 200 °C, 5 h, 1 wt% catalyst methanol, 6:1 mole ratio	84%	Barakos et al. (2008)

Catalyst Type	Reaction Conditions*	Conversion	Reference
Mg-Al hydrotalcite, calcined at 500 °C for 3 h	Soybean oil, 24h	97%	Georgogianni et al. (2009b)
Amberlite IRA-900	Yellow horn oil, 60 °C, 3 h	26%	Li et al. (2012)
PA306s	Triolein, 5 h, ethanol, 10:1 mole ratio	90%	Shibasaki-Kitakawa et al. (2007)
PA306s	UCO, 55 °C, 8 h, 9 wt%, methanol, 18:1 mole ratio	75%	Abidin (2012)

* mole ratio refers to the alcohol to vegetable oil mole ratio

2.4 Acid Catalysed Biodiesel Production

Acid catalysts have been investigated for the esterification and transesterification of UCOs and crude vegetable oils which contain a significant amount of FFAs. Acidic catalysts are not affected by the presence of FFAs in the raw material (Melero et al. 2009a; Enweremadu & Mbarawa 2009; Zabeti et al. 2009) and they can simultaneously catalyse esterification and transesterification. Acids considered for biodiesel production include sulphuric acid, sulphonic acid and hydrochloric acid (Ganesan et al. 2009; Balat & Balat 2010). When compared to the conventional alkali catalysed transesterification, homogeneous acid catalysis are typically 4000 times slower (Balat & Balat 2010; Atadashi et al. 2011). High conversions are possible using acid catalysts, however reaction times of 3-48 h, at temperatures above 100 °C with high alcohol to oil mole ratios have been reported.

Homogeneous acids are highly corrosive and need to be separated from the reaction mixture and heterogeneous catalysts have been investigated as a potential solution (Helwani et al. 2009a; Lam et al. 2010). The types of solid acids catalysts investigated for biodiesel production include acidic zeolites, heteropoly acids, cation exchange resins, and sulphated and mixed metal oxides. Although it is possible to synthesize zeolites with varying chemical and physical properties the catalyst activity remains low (Lam et al. 2010). The highest reported conversion is 26.6%, using Zeolite Y, at a temperature of 460

°C after 22 min of reaction time. Zeolites can be functionalised with organic species to alter their activity (Helwani et al. 2009a). Shu et al. (2007) found that zeolite beta modified with Lanthanum could be used with soybean oil to achieve a conversion of 48.9 wt%, after 4h, at 60 °C, with a mole ratio of 14.5:1 and a catalyst loading of 1.1 wt%.

Heteropoly acids have also been considered for biodiesel production. Typical heteropoly acids are $H_3PW_{12}O_{40}$, H_4SiWO_{40}, $H_3PMo_{12}O_{40}$ and H_4SiMoO_{40}. Heteropoly acids have been shown to have a high activity at relatively low temperatures (Melero et al. 2009a; Hara 2009). The surface area can be increased by adding a salt such as caesium, ammonium and silver. The transesterification of waste frying oil using $H_3PW_{12}O_{40}{\cdot}6H_2O$ was investigated (Cao et al. 2008). It was found that a conversion of 87% was possible at a temperature of 65 °C, a methanol to oil mole ratio of 70:1 and a reaction time of 14 h.

Metal oxides investigated for transesterification include zirconium oxide (zircona), titanium oxide and tin oxide (Lam et al. 2010). It has been found that the catalytic activity of these metal oxides can be enhanced by incorporating anions such as sulphate and tungstate into the structure (Melero et al. 2009a). For example the conversion of palm kernel oil was increased from 64.5% to 90.3% when sulphated zirconia was used in place of zircona (Jitputti et al. 2006). These catalyst often lose activity due to sulphur leaching (Helwani et al. 2009a; Melero et al. 2009a). A silica-supported sulphated titania catalyst was found to result in a conversion greater than 90 % using an oleic acid-refined cotton seed mixture. The reaction conditions were 50 wt% FFAs, 200 °C, 3 wt% of catalyst methanol to oil ratio of 9:1 and after four reusability cycles there was a small reduction in activity (Melero et al. 2009a). A sulfonic acid modified mesostructured catalyst was investigated for the transesterification of refined and crude vegetable oil (Melero et al. 2009b). It was found that a conversion close to 100% was possible at 180 °C, a methanol to oil mole ratio of 10:1 and a catalyst loading of 6 wt%. It was also found that increasing the mole ratio too much leads to a loss in catalytic activity.

A series of zinc and lanthanum mixed oxides were investigated for simultaneous esterification and transesterification of crude and waste vegetable oils (Yan et al. 2009). A yield of 96 % was obtained using a temperature range of 170-220 °C and a reaction time of 3 h. Di Serio et al. (2007) investigated a vanadyl phosphate catalyst for the production of biodiesel from soybean oil. They found that a maximum conversion of 80% was possible at 180 ºC after about 30 min after this time the catalyst started to deteriorate. A similar conversion was possible with a temperature of 150 ºC after 90 min with less catalyst degradation. Catalyst activity was recovered by calcination in air. In addition it was established that leaching of the active species did not occur.

Cation-exchange resins have been investigated for transesterification. Commercially available sulphonic acid resins investigated for transesterification include Amberlyst 15, Amberlyst 35, Nafion SAC13 and Nafion NR50. It has been found that some sulphonic acid resins are more active for esterification than transesterification (Lam et al. 2010). It has been shown that a high conversion of FFAs in UCO is possible using Purolite D5081 (Abidin et al. 2012) however when tested for transesterification there was no biodiesel formation (Abidin 2012). Similarly Russbueldt & Hoelderich (2009) found that after 24 h of reaction time less that 1% of the triglycerides were converted by transesterification. Cation-exchange resins for esterification are discussed in Section 2.4.2.2.

A disadvantage of acid catalysts is that they are less active when compared to their alkaline and basic counterparts. The reaction times are much slower typically about 48-96h and a high mole ratio of methanol to oil is required of about 30-150:1 (Xie & Li 2006). A conversion greater than 90% is possible at a temperature of 60 ºC, a methanol to oil mole ratio of 6:1, 3 wt% of sulphuric acid and 96h (Helwani et al. 2009a). Another disadvantage of acid catalysts is that water concentration is more critical than for basic catalysts, with water concentrations as low as 0.1 wt% being shown to affect ester yields (Helwani et al. 2009a).

It has been proposed that a two stage process would be suitable for UCOs. The FFAs would first be removed from UCOs by means of an acid catalysed esterification reaction followed by an alkali catalysed transesterification reaction (Canakci & Gerpen 2001). It was found that when this process was used to treat yellow grease with 12% FFAs and brown grease with 33% FFAs the acid levels could be reduced to less than 1%. Sulphuric acid was used as the catalyst. The transesterification was then carried out using an alkaline catalyst to produce fuel grade biodiesel. As discussed there are problems associated with homogeneous catalysts and it has been proposed that the two-stage process could be carried out using heterogeneous catalysts (Enweremadu & Mbarawa 2009; Atadashi et al. 2013). On this basis the esterification pre-treatment of biodiesel using an acid catalyst will be investigated.

2.4.1 Esterification Reaction Mechanism

Esterification can be catalysed by Lewis and Brønsted-type acids. Inorganic heterogeneous acid catalysts, such as mixed and sulphated oxides, generally act as Lewis type-acids with an acid metal sharing an electron pair with the FFAs carboxyl group (Melero et al. 2009a; Corro et al. 2013). This leads to the formation of an oxonium ion which is attacked by the alcohol. This leads to a proton loss by the alcohol and the corresponding ester and water are formed as a result. The mechanism for esterification with a Lewis-type acid is shown in Figure 2.3.

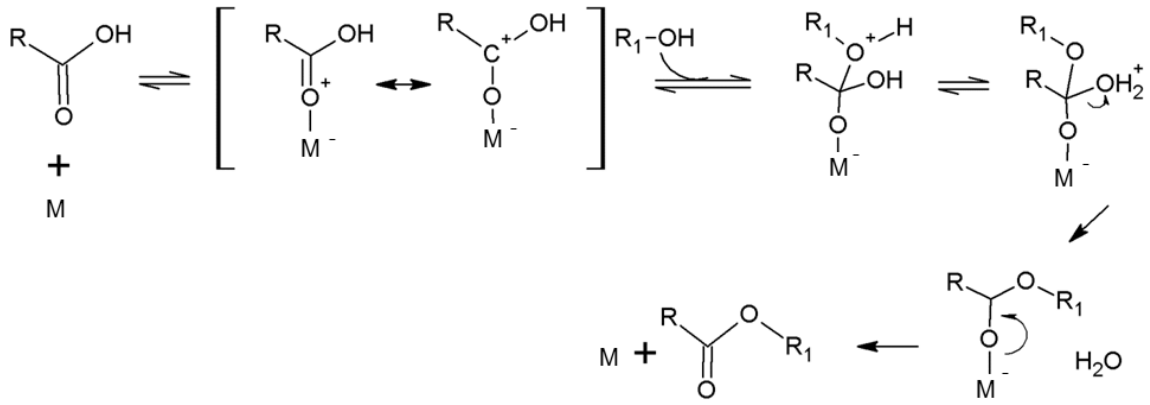

Figure 2.3. The mechanism for Lewis acid-type esterification (Melero et al. 2009a).

Sulphuric acid and sulfonated resins have been widely investigated for esterification and these catalysts act as Brønsted-type acids (Melero et al. 2009a; Tesser et al. 2010). In this case the oxonium ion is formed when a proton donated by the acid reacts with the carboxyl group of the FFAs. The mechanism for esterification using a Brønsted-type acid is shown in Figure 2.4.

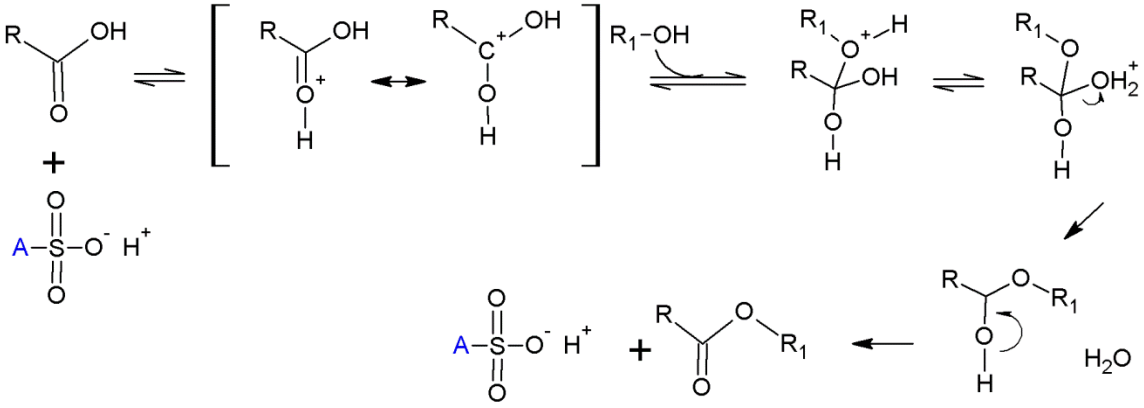

Figure 2.4. The mechanism for Brønsted acid-type esterification (Melero et al. 2009a).

2.4.2 Heterogeneous Catalysts Assessed for the Esterification Reaction to Produce Biodiesel

Homogeneous catalysts such as sulphuric acid, hydrochloric and p-toluenesulphonic acid (Ozbay et al. 2008; Feng et al. 2010) have been investigated for esterification pre-treatment. However these catalysts are corrosive and separating them from the final product is expensive and generates a lot of waste. In addition sulphuric and sulphonic acid catalysts often results in a high sulphur content in the final product (Melero et al. 2009a). In order to overcome these difficulties numerous heterogeneous acid catalysts have been investigated for esterification pre-treatment. Acid catalysts have been shown to catalyst transesterification and esterification however this section focuses on heterogeneous acid catalysts assessed for the esterification reaction to produce biodiesel.

2.4.2.1 Inorganic Heterogeneous Acid Catalysts

Mixed metal oxides such as modified zirconia and zinc hydroxide nitrate have been investigated for esterification. Y.-M. Park et al. (2010) found that a conversion of 98% could be achieved using tungsten oxide zircona (WO_3/ZrO_2) for the esterification of 4 wt% oleic acid in soybean oil. This conversion was achieved after 2 h at 200 °C, and with mole ratio of 1:9. The effect of WO_3 loading was investigated and it was found that from 10 wt% to 20 wt% the FFAs conversion increased from 78% to 93% however when the loading was increased to 30 wt% the conversion decreased to 89%. Temperature programmed desorbtion of nitrogen showed that the 20 wt% WO_3/ZrO_2 catalyst had the strongest acid sites indicating that the activity of acid catalysts increased with increasing acidity. Sulphated zircona (SO_4^{2-}/ZrO_2) was shown to achieve a conversion of approximately 93% (after 2 h, at 75 °C, a mole ratio of 1:9 and 0.29 g of catalyst per gram ml of oil), however there were concerns about sulphur leaching and as a result a detailed study was not carried out.

Cordeiro et al. (2008) investigated the esterification of lauric acid using a zinc hydroxide nitrate catalyst. With this catalyst a conversion of 97% achieved after 2 h at 140 °C, using a methanol to acid mole ratio of 4:1 and a catalyst wt% (to lauric acid) of 2 wt%. Commercially available acid catalysts CBV-780 and niobic acid were compared to the synthesised catalysts SAPO-34 and niobia with CBV-780 for the esterification of soybean oil deodoriser distillate (Souza et al. 2009). CBV-780, a zeolite type catalyst, was found to be the most active with conversion of 49% using 9 wt% of catalyst, at 100 °C after 2.5 h.

Recently a photocatalytic process under ultraviolet radiation (UV) using a Zn/SiO_2 catalyst has been assessed (Corro et al. 2013). It was found that a FFAs conversion of 96% could be achieved with a reaction time of 4 h, and catalyst loading of 15 wt%, with a methanol to oil mole ratio of 12:1 and a temperature of 20 °C. This step was followed by a conventional alkali catalysed process and it was shown that the resulting biodiesel product met the required standards for use as a fuel.

The effect of calcination temperature on the catalytic activity of titania zirconia, sulphated zirconia and tungstated zirconia was investigated (López et al. 2008). It was found that the optimum temperature for titania zirconia and sulphated zirconia was 500 °C with 800 °C for tungstated zirconia. Sulphated zirconia being the most sensitive to changes in the calcination temperature with the loss of activity at higher temperatures attributed to sulphur loss.

2.4.2.2 Organic Heterogeneous Acid Catalysts

Various organic acid catalysts have been investigated and while there are examples of organosulfonic acid immobilised on inorganic supports the focus has been on sulphonated ion exchange resins (Melero et al. 2009a). A summary of the acid catalysts investigated for the esterification reaction is given in Table 2.3.

Organosulfonic acid-functionalised mesoporous silicas were investigated for the esterification of palmitic acid in soybean oil (Mbaraka 2003). It was found that increasing the acidity of the organosulfonic acid group increased the activity of the mesoporous catalyst. These catalysts showed a similar catalytic performance to sulphuric acid and a higher catalytic performance than Amberlyst-15. Many sulphated catalysts have been shown to leach sulphur however it appears a reusability study was not carried out. In addition Amberlyst-15 may have suffered some thermal degradation at the temperatures investigated.

Sulfonated ion-exchange resins have been widely investigated for the esterification reaction (Melero B et al. 2009; Russbueldt & Hoelderich 2009) with high conversions possible at relatively benign conditions. These resins generally consist of sulfonated polystyrene cross-linked with divinylbenzene (DVB) (Ozbay et al. 2008; Zagorodni 2007). The extent of DVB cross-linking determines textural properties such as surface area, pore size distribution and swelling. Sulfonic acid acts as the cation-exchanger and forms strongly acidic, brønsted acid, catalytic sites.

Ozbay et al. (2008) investigated the esterification of waste cooking oil with an initial FFA content of 0.4 wt% FFA using Amberlyst-15, Amberlyst-35, Amberlyst-16 and Dowex HCR-W2. The catalyst with the highest activity was Amberlyst-15 which had the largest surface area, porosity, pore diameter and degree of cross-linking which corresponds to the highest number of accessible active sites. The gelular resin (Dowex HCR-W2) had the lowest activity. The highest conversion was 46% after 3 h using Amberlyst-15 at 60 °C with 2 wt% catalyst and 20 vol% methanol. Park et al. (2010) showed that a conversion of 98% could be achieved using Amberlyst-15 after 2 h, at 75 °C, a mole ratio of 1:9 and 0.29 g of catalyst per gram ml of oil, using a simulated waste cooking oil comprised of 4 wt% oleic acid in soybean oil. Amberlyst-15 has also been investigated for the esterification of palm fatty acid distillate and it was found that a conversion of 97% was possible using 12 wt% methanol, at 60 °C, a catalyst loading of 30 wt% (Talukder et al. 2009).

Russbueldt & Hoelderich (2009) investigated non-commercially available, strongly acidic, ion exchange resins EBD-100, EBD-200 and EBD-300. A variety of potential feedstocks were investigated with a FFAs content of 10-16 wt%. In contrast to Ozbay et al. (2008) it was found that the gelular resin (EBD-100) had a higher activity compared to the macroporous resins (EBD-200 and EBD-300). The activity of the geluar resin was attributed to a poor uptake of methanol by the macroporous materials which meant that the reaction could only take place on the surface of the macroporous material while sites inside the gelular material were accessible for transesterification. It was found that a conversion of approximately 100% was possible after 6 h, at 120 ºC using an FFA to methanol ratio of 1:19.7 and a catalyst loading of 1 wt% with EBD-100. The reusability of EBD-100 was investigated and the loss of activity was attributed to ion-exchange with alkaline cations present in waste oils due to salt.

Feng et al. (2010) compared NKC-9, 001 x 7 and D61 for the esterification of waste frying oil and lauric acid. NKC-9 had the highest catalytic activity and this was attributed to the fact that this resin had the highest pore diameter and a low moisture content allowing it to absorb water formed during

the reaction. Conversion increased when the catalyst loading was increased from 6 wt% to 20 wt% however when the loading was further increased to 24 wt% the change in conversion was negligible. The highest FFA conversion was approximately 90% after 3 h, 66 °C, using 18 wt% of NKC-9 catalyst and methanol to oil mole ratio of 3:1.

Caetano et al. (2009) compared commercially available sulfonated polystyrene cross-linked with DVB (D50w8 and D50w2) with PVA with varying degrees of sulfosuccinic acid crosslinking (PVA, PVA_SSA20 and PVA_SSA40) for the esterification of palmitic acid. The degree of crosslinking was compared to conversion and it was found that with D50w8 and D50w2 conversion decreased with an increase in cross-linking because the cross-linking agent (DVB) is hydrophobic. In addition the surface area decreased, reducing the number of accessible active sites. In the case of PVA. PVA_SSA20 and PVA_SSA40 conversion increased with increasing cross-linking due to an increase in the amount of sulfonic acid due to the cross-linking agent. PVA_SS40 was found to have the highest catalytic activity with a conversion of 90%, after 2 h, using a temperature of 60 °C and a methanol to oil ratio of 1:63.

A sulfonated microcrystalline cellulose catalyst has recently been reported for the esterification of palm fatty acid distillate and it was found that this catalyst could be reused (Chabukswar et al. 2013). It was found that his catalyst had a better catalytic activity than Ambelyst-15 although it was worse than sulphuric acid.

Table 2.3. A summary of acid catalysts investigated for the esterification reaction to product biodiesel

Catalyst Type	Reaction Conditions*	Conversion	Reference
Organosulfonic acid-functionalised mesoporous silicas	Palmitic acid in Soybean Oil, 85 °C, 20:1 mole ratio, 10 wt% catalyst	92%	Mbaraka (2003)
Amberlyst-15 (macroporous resin)	UCO, 3 h, 60 °C, 2wt% catalyst and 20 wt%	46%	Ozbay et al. (2008)
Amberlyst-15 (macroporous resin)	4 wt% oleic acid in soybean oil, 2 h, 75 °C and 9:1 mole ratio	98%	Park et al. (2010)
Amberlyst-15 (macroporous resin)	Palm fatty acid distillate, 60 °C, 6 h 12 wt% 30 wt% catalyst loading	97%	Talukder et al. (2009)
EBD-100 (gelular resin)	UCO with a salt removal pre-treatment, 120 °C, 6 h, 19:1 mole ratio, 1 wt% catalyst loading	100%	Russbueldt & Hoelderich (2009)
NK-9 (cation exchange resin)	Simulated UCO, 66 °C, 3 h, 3:1 mole ratio, 18 wt% catalyst loading	90%	Feng et al. (2010)
PVA_SS40 (polyvinyl alcohol with sulfosuccinic acid crosslinking)	Palmitic acid, 60 °C, 2 h, 63:1 mole ratio	90%	Caetano et al. (2009)
Sulfonated microcrystalline cellulose	Palm fatty acid distillate, 60 °C, 3 h, 3:1 mole ratio, 7wt% catalyst loading	90%	Chabukswar et al. (2013)

*mole ratio refers to the methanol to vegetable oil (or FFAs) mole ratio

2.4.3 Effect of Mole Ratio and Alcohol Type on the Esterification Reaction

Esterification can be carried out using short chain alcohols. The main alcohols considered are methanol (Ozbay et al. 2008) and ethanol (Marchetti et al. 2007; López et al. 2008) although propanol and butanol have also been considered (Zabeti et al. 2009). The type of alcohol used influences type of esters formed with methanol leading to the formation of fatty acid methyl esters (FAME) and ethanol leading to the formation of fatty acid ethyl esters (FAEE). It has been found that the diesel properties of FAME and FAEE are similar (Issariyakul et al. 2007). However FAEE has a slightly higher cetane number

and the cloud an pour points are lower which means this fuel is more suitable for cold climates (Tongboriboon et al. 2010).

The advantages of using ethanol are that it can be derived from renewable sources, it is less toxic and it is less harmful to the environment (Marchetti et al. 2007; Zabeti et al. 2009; Caetano et al. 2009). In addition ethanol is more soluble in vegetable oil than methanol (Tongboriboon et al. 2010). However ethanol is less active for the esterification reaction. Methanol and ethanol were compared for the esterification of lauric acid and it was found that at a temperature of 100 °C the ester concentration increased from 20.6 wt% to 39.4 wt% when ethanol was replaced with methanol (Cordeiro et al. 2008). When the temperature was increased to 140 °C there was a smaller increase from 77.2 wt% to 87.1 wt% when ethanol was replaced with methanol. The esterification of palmitic acid was investigated and a conversion of 75% was possible using methanol compared to a conversion of 1% using ethanol at 60 °C (Caetano et al. 2009). When the reaction temperature was increased to 80 °C the conversion with ethanol reached 19%.

Esterification is an equilibrium reaction with one mole of alcohol required to convert one mole of FFAs to one mole of FAME and thus increasing the mole ratio should increase the amount of FAME formed (Yan et al. 2009). There is a large variation in the mole ratios reported for esterification. Feng et al. (2010) found that the highest conversion could be achieved with a mole ratio of 6:1 with no further increase at higher mole ratios and Chabukswar et al. (2013) reported that a mole ratio of 4:1 was sufficient. In contrast, Caetano et al. (2009) showed that conversion increased for mole ratios up to 63:1.

The aim of this work is to investigate the environmentally benign production of biodiesel. Ethanol can be derived from renewable sources however it is more expensive and less active when compared to methanol. While methanol is derived from less environmentally benign sources higher conversions can be achieved by using less alcohol at lower temperature and as

a results there are potential environmental benefits when using methanol. Methanol will be the reagent used for this work.

2.4.4 The Effect of Temperature and Reaction Time on the Esterification Reaction

As a general rule it is expected that conversion will increase with increasing temperature and reaction time. In the case of equilibrium reactions the conversion will increase until the conversion value is reached and after this increasing the reaction time will not increase the conversion. However increasing the temperature will shift the equilibrium position and can result in an increase in conversion (Feng et al. 2010).

The esterification reaction has been investigated using temperatures in the range of 50 – 200 °C (Ozbay et al. 2008; Park et al. 2010). The boiling point of methanol is 64.7 °C and of ethanol is 78 °C at standard conditions. A reflux condenser is generally used for reactions carried out below the boiling point of the alcohol in order to prevent alcohol loss (Ozbay et al. 2008). As the temperature approaches the boiling point of the alcohol, bubbles are formed and this inhibits mass transfer and thus reducing conversion (Zabeti et al. 2009; Abidin et al. 2012). A pressure vessel is used to carry out experiments at temperatures above the boiling point of alcohol (Park et al. 2010; Cordeiro et al. 2008). It was found that increasing the temperature, for the esterification of lauric acid, from 100 °C to 140 °C could increase the ester content from 39.4 wt% to 87.1 wt%.

Cation-exchange resin experiments are carried out at relatively low temperatures, typically 50 – 65 °C (Ozbay et al. 2008; Feng et al. 2010) because ion-exchange resins have a low temperature stability (Singare et al. 2011). Desulphonation occurs when conventional sulphonated styrene-divinylbenzene are used for extended period at temperatures of 150 ºC and above (Caetano et al. 2009; Zagorodni 2007). In contrast inorganic acid catalysts are stable at much higher temperature and as a result the activity has been investigated for temperatures as a high as 200 °C (Park et al. 2010).

2.5 Enzymatic Biodiesel Production

Enzyme catalysts have also been considered for biodiesel production. Enzyme catalysts are often considered in order to reduce the environmental impact of chemical processes because high conversions are possible at relatively benign operating conditions (Shahid & Jamal 2011). The class of enzyme catalysts used to investigate biodiesel production are lipases (Semwal et al. 2011; Akoh et al. 2007). Another advantage of enzymes is that the saponification side reaction does not occur.

2.5.1 Enzymatic Reaction Mechanism

The biological function of lipases is to catalyse the breakdown of lipids as part of the metabolism of living cells which generally exist in a water rich environment. This leads to the formation of carboxylic acids and short chain alcohols (Paiva et al. 2000). One of the defining characteristics of lipases is that they operate at the interface between a hydrophilic and a hydrophobic phase, with a hydrophobic active sited covered by a helical structure (or lid) with a hydrophilic external surface (Ganesan et al. 2009). When lipases are in contact with a hydrophilic/hydrophobic interface the helical lid rolls back to expose the electrophilic region or oxyanion hole (Paiva et al. 2000; Akoh et al. 2007). The reaction takes place inside the oxyanion hole, where the active site is a catalytic triad composed of non-sequential serine (Ser)-histadine (His)–aspartic acid (Asp) or Ser-His-glutamic acid (Glu) residues (Orçaire et al. 2006).

Lipases have been designed by nature to catalyse the cleavage of ester bonds by means of a hydrolysis reaction in water rich environments (Paiva et al. 2000). However the reverse esterification reaction is possible depending on the reaction environment. The active site targets carboxyl groups which are a characteristic functional group on lipids such monoglycerides (MG), diglycerides (DG), triglycerides (TG), FFAs and esters, including FAME. The structural conformation of the enzyme and lipid will determine if the carboxyl group is able to reach the active site. This feature was described by Emil Fischer's "lock-and-key" model and refined by Daniel Koshland Jr who introduced the "induced-fit" model (Bommarius & Riebel 2002). Lipases can catalyse esterification, transesterification and hydrolysis involving MGs, DG, TGs, FAME

and FFAs depending on the type of lipase and the reaction medium (Tongboriboon et al. 2010).

Lipase catalysed reactions follow a Ping Pong Bi Bi mechanism (Paiva et al. 2000; Al-Zuhair et al. 2006; Willis & Marangoni 2008). For simplicity the esterification reaction has been discussed however the same mechanism applies to enzyme catalysed hydrolysis and transesterification. The overall schematic for the Ping Pong Bi Bi mechanism is shown in Figure 2.5 with an FFA first reacting with the enzyme (E) to form a complex (E·FFA) leading to the formation of water (H_2O). Methanol (MeOH) can then react with the surface to form the E·FAME and the FAME is subsequently released.

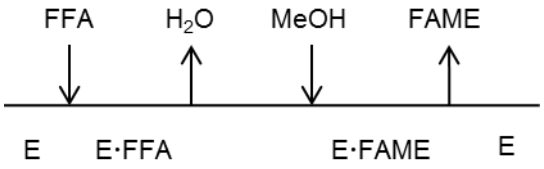

Figure 2.5. Schematic representation of the Ping Pong Bi Bi mechanism for enzyme catalysed esterification.

A detailed Ping Pong Bi Bi mechanism for the lipase catalysed esterification of FFAs with methanol is shown in Figure 2.6 (adapted from Willis & Marangoni 2008). The reaction is initiated by a nucleophilic attack on the carbonyl carbon by the Ser residue. The His and Asp (Glu) residues increase the nucleophilic strength of the serine residue by sharing electrons across this imidazole ring of the histadine residue. This leads to the formation of a tetrahedral intermediate, stabilised by two hydrogen bonds formed with the oxyanion-stabilising residues. The FFA's carbon-oxygen bond breaks to release a water molecule and this leads to a nucleophilic attack by methanol. A hydroxyl group is added to the carbonyl carbon, forming a tetrahedral intermediate. A rearrangement leads to the formation of a methyl ester which is released and the serine residue is regenerated.

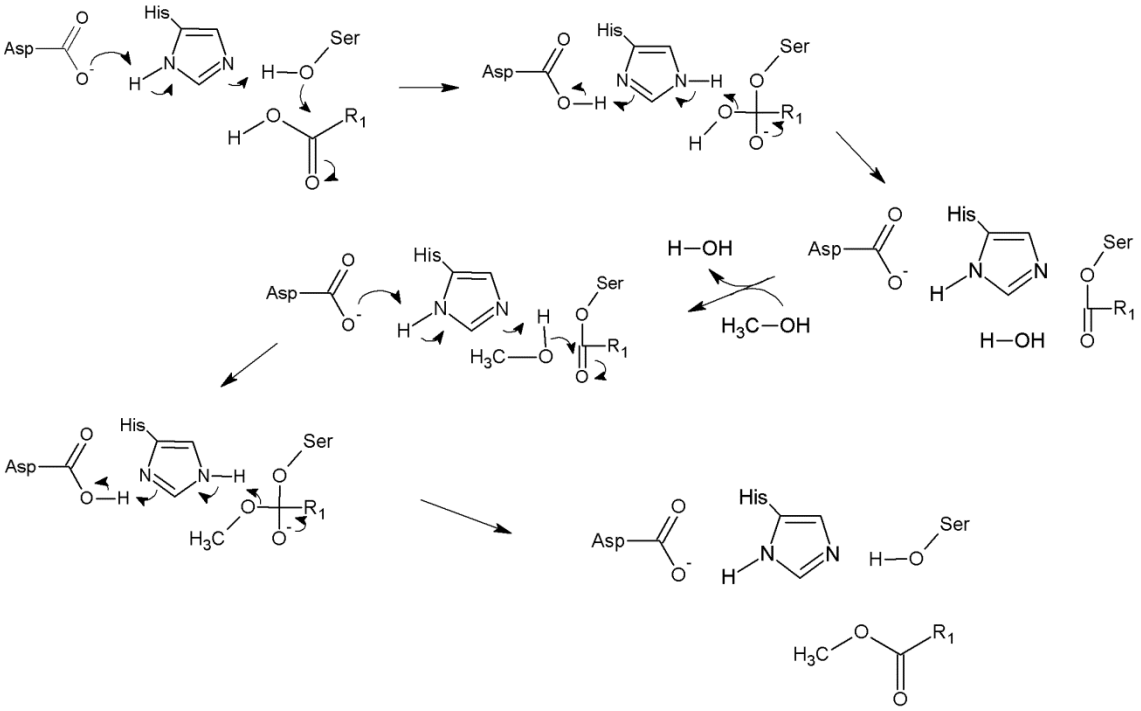

Figure 2.6. The detailed mechanism for enzyme catalysed esterification (adapted from Willis & Marangoni 2008). R_1 represents a fatty acid group.

2.5.2 Kinetics of Enzyme Reactions

Biodiesel production can be modelled using Michaelis-Menten kinetics (Gog et al. 2012) and this has been used to compare the kinetics of free and immobilised enzymes (Dossat et al. 2002; Da Rós et al. 2010). However the intrinsic kinetics of lipase catalysed reactions are generally regarded as a following a Ping Pong Bi Bi mechanism with competitive inhibition by alcohol and the resulting model is (Al-Zuhair et al. 2006; Halim & Harunkamaruddin 2008):

$$v = \frac{V_{\max}}{1 + \frac{K_S}{[S]}\left[1 + \frac{[Al]}{K_{iAl}}\right] + \frac{K_{Al}}{[Al]}} \qquad \textbf{2.1}$$

where v is the initial rate of reaction, V_{max} is the maximum rate of reaction, K_S and K_{Al} are the binding constants for the substrate (S) and the alcohol (Al) respectively, and K_{iAl} is the inhibition constant for alcohol.

The Ping Pong mechanism with competitive inhibition of alcohol was assessed for the esterification of *n*-butyric acid with methanol catalysed by a lipase from *Mucor miehei* in an *n*-hexane microaqueous system (Al-Zuhair et al. 2006). It was shown that FFAs did not inhibit conversion when the modelling was carried out using initial reaction rates. The same model was applied to a microaqueous system of *n*-hexane/water to show that the initial reaction rate increased at higher water concentration although the conversion after 1 h was lower.

The esterification of oleic acid with 1-butuanol was also found to follow the Ping Pong Bi Bi mechanism with competitive inhibition by 1-butanol (Kraai et al. 2008). The model was amended to allow for a biphasic system by describing the reaction rate in terms of the interfacial area. Foresti et al. (2008) found that the classic monophasic model did not adequately describe the effect of water on the experimental results on ethyl oleate synthesis. A biphasic reactor model was developed which allowed for simultaneous esterification and mass transfer between phases. It was found that the biphasic model fitted the experimental data well and as a result a simplified model was developed which could be used to provide a fast estimation of conversion.

Mahmud et al. (2010) investigated the esterification of oleic acid with ethanol and Novozyme 435 as the catalyst. A sigmoidal response curve indicated the presence of allosteric effects due to a change in enzyme conformation and a modified Ping Pong Bi Bi model was found to fit the experimental data.

The transesterification of simulated oil from triolein with ethanol and catalysed by Lipozyme MM IM was investigated and the model was developed using the King-Altman geometric approach. For this system it was found that there was competitive inhibition of alcohol only and there were no internal or external mass transfer limitations (Calabrò et al. 2010). Novozyme 435 catalysed transesterification of UCO has also been shown to follow this model (Halim & Harunkamaruddin 2008) Previously (Dossat et al. 2002) had shown

that the transesterification of sunflower oil with butanol fitted the Ping Pong mechanism with competitive alcohol inhibition.

However it was proposed that it would be more suitable to describe transesterification using a Ping Pong mechanism with competitive inhibition by both alcohol (Al) and substrate (S) (Al-Zuhair et al. 2006):

$$v = \frac{V_{\max}}{1 + \frac{K_S}{[S]}\left[1 + \frac{[Al]}{K_{iAl}}\right] + \frac{K_{Al}}{[Al]}\left[1 + \frac{[S]}{K_{iS}}\right]} \qquad \textbf{2.2}$$

where K_{iS} is the inhibition constant for the substrate and the other components are the same as equation 2.1.

It was found that this was a more suitable model for the transesterification of palm oil using methanol, a lipase from *M. miehei* as the catalyst, in *n*-hexane as the solvent (Al-Zuhair et al. 2007). This model assumed direct transesterification of the vegetable oil and provided a reasonable fit to experimental data. The progress of the reaction was determined by monitoring the FAME concentration. The model was extended to allow for internal and external mass transfer resistances as a result of using in immobilised lipase and applied to a simulated waste cooling oil (Al-Zuhair et al. 2009) and it was found that the model gave a good predication of the experimental data.

Two models were proposed for the deactivation of *Pseudomanas cepacia* (Torres et al. 2008). Model A described irreversible deactivation according to first order kinetics while Model B proposed two parallel processes with one leading to an inactive form and the other leading to another active and stable form. Experimental data for the transesterification of sunflower oil with ethanol showed that Model B could be used to describe lipase deactivation.

To date most of the modelling work, investigating the kinetics of biodiesel production has focused on either esterification or transesterification and the

modelling has been carried out by monitoring either the substrate (TG or FFAs) or the final product (biodiesel) and alcohol. Xu et al. (2005) found that a simplified model based on the Ping Pong Bi Bi mechanism with substrate competitive inhibition could be used to describe the transesterification of soybean oil with methyl acetate. However this model did not account for MGs and DGs detected during the reaction and a model describing the transesterification as a series of three consecutive steps was found to fit the data.

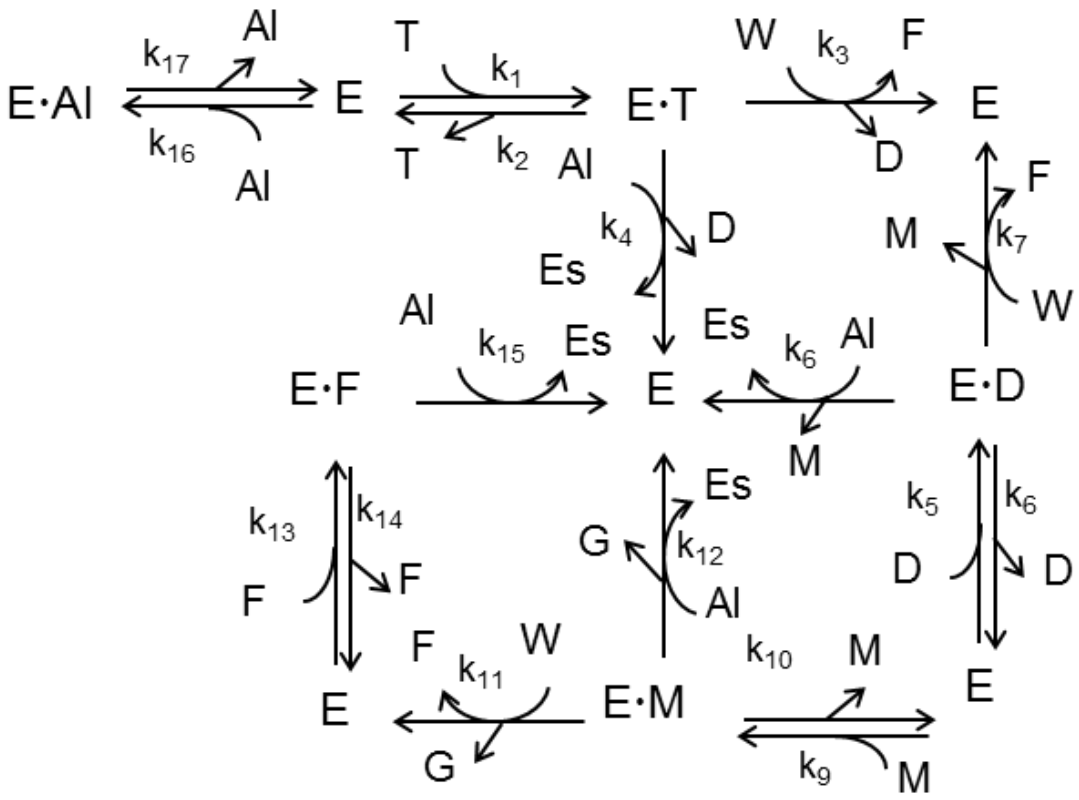

Figure 2.7. The conceptual scheme of mechanism 3 proposed by Cheirsilp et al. (2008).

In order to investigate if the transesterification reaction proceeded according to hydrolysis followed by esterification or by direct transesterification three mechanisms have been assessed (Cheirsilp et al. 2008). This was used to investigate the transesterification of palm oil, using an immobilised lipase from *Pseudomonas* sp. and ethanol based on the variation of the TG, MG, DG, biodiesel and alcohol concentrations. Mechanism 1 assumed hydrolysis

followed by esterification with the overall reaction following a Ping Pong Bi Bi mechanism. Mechanism 2 assumed that the complexes bound the enzyme surface react fast and was a simplified version of mechanism 1. Mechanism 3 assumed that transesterification (direct alcoholysis) of the triglycerides occurred in parallel with the hydrolysis esterification reaction sequence. The mechanism which best fitted the experimental data was Mechanism 3 and the conceptual scheme is shown in Figure 2.7. With this approach it is possible to describe the change of all species involved in the transesterification reaction.

2.5.3 Reaction Parameters affecting Enzymatic Biodiesel Production

The biodiesel yield when using enzyme catalyst varies based on a number of factors which include the enzyme source, immobilisation technique, the type of feedstock, water addition, alcohol type and mole ratio, reaction time and reaction temperature.

2.5.3.1 Effect of Enzyme Source

Lipases investigated for biodiesel production include lipases derived from *Pseudomanas fluorescens*, a commercial version is Lipase AK, *Candida rugosa,* a commercial version is Lipase AY, *Rhizomucor miehei*, commercial immobilised version is Lipozyme RM IM, *Candida antarctica*, a commercial immobilised version is Novozyme 435, *Thermomyces lanuginosa*, a commercial immobilised version is Lipozyme TL IM and *P. cepacia*, a commercial version is Lipase PS. Recently a novel lipase from *Ralstonia* sp. CS274 has been shown to produce biodiesel from soybean oil and palm oil (Yoo et al. 2011) and a lipase from *Penicillium expansum* has been considered for the transformation of waste cooking oil (Li et al. 2009). Another recent development is the use of whole-cell biocatalysts for biodiesel production such as *Rhizopus orzae*, and *Aspergillus orzae* expressing *Fusarium heterosporum* lipase (Koda et al. 2010).

Various lipases were compared for the transesterification of sunflower oil the highest conversion of 90 % was achieved using a lipase from *P. fluorescens*

(Soumanou 2003) when compared to *R. miehei*, *T. lanuginosa* and *P. cepacia*. In contrast when lipases were compared for the transesterification of oil from *Madhuca indica* with a high FFAs content it was found that *P. cepacia* gave the highest conversion followed by *R. miehei* and then *P. fluorescens* (Kumari et al. 2007). Novozyme 435 (immobilised *C. antarctica* lipase B), Lipozyme TL IM (immobilised *T. lanuginose*), and Lipozyme RM IM (immobilised *R. miehei*) were shown have a similar activity for the transesterification of UCO with Novozyme 435 having the greatest activity (Halim & Harunkamaruddin 2008). Lipozyme TL IM was investigated for the transesterification of crude palm oil and it was found that a conversion of 96% was possible after a 4 h reaction time, a loading of 6.67 wt% and 40 °C. This suggests that the oil type can affect the activity of various lipases.

A lipase from *P. cepacia* (recently reclassified as *Burkholderia cepacia*) (Torres et al. 2008) has been widely investigated for transesterification for simplicity the name *P .cepacia* will be used for this work. A conversion of 98% with a reaction time of 8 h was reported for *P. cepacia* immobilised on celite (a type of diatomaceous earth) (Shah & Gupta 2007). *P. cepacia* immobilised on a polyacrylonitrile nanofibrous membrane was investigated for the transesterification of soybean oil and a conversion of 90% was possible after a 24 h (Li et al. 2011). The catalyst was shown to retain 91% of its activity after 10 reusability cycles.

Novozyme 435 has been shown to catalyse the transesterification of waste frying oil (or UCO) using the response surface methodology which predicted a conversion of 100% after 12 h, at 44.5 °C, a catalyst loading of 15 wt% and mole ratio of 3.8:1 using stepwise addition of methanol (Azócar et al. 2010). This compares well to previous results where the conversion of canola oil was 97.9% after 12 h, at 38 °C, an enzyme concentration of 42%, a mole ratio of 3.5:1 and addition of 7.2% water (Chang et al. 2005). With similar reaction conditions reported for the transesterification of UCO and cotton seed oil using methanol (Köse et al. 2002) It has been shown that Novozyme 435 can be repeatedly reused (Shimada et al. 2002; Talukder et al. 2009).

Novozyme 435 has also been investigated for esterification and it was found that a conversion of 90% was possible for the esterification of oleic acid (Trubiano et al. 2007). Novozyme 435 was compared to Amberlyst-15 (an ion-exchange resin) for the esterification of palm fatty acid distillate which contains 97% FFA (Talukder et al. 2009) and shown to have a specific activity 50 times greater than Amberlyst-15. It was found that both catalysts could be reused up to 15 times with a minimal loss of activity. Novozyme 435 was washed with *tert*-butanol and freeze-dried. In a similar study it was found that lipase catalysts (Lipozyme RM-IM, Lipozyme TL-IM and Novozyme 435) were more active for the esterification of soybean oil deodoriser distillate when compared to selected acid catalysts (Zeolite CBV-780, SAPO-34, niobia and niobic acid) (Souza et al. 2009). Novozyme 435 was found to be the most active lipase catalyst with a conversion of 84% after 2 h. Novozyme 435 has been investigated for a continuous flow process for the esterification of palm fatty acid distillate and it was found that approximately 3500 kg palm fatty acid / kg Novozyme 435 could be treated in the first reaction before the catalyst started losing activity (Brask et al. 2011)

Biodiesel production from acid oil, a by-product of vegetable oil refining contains mainly free fatty acids has been investigated using hydrolysis followed by esterification. Soluble *C. rugosa* was used to catalyse the hydrolysis reaction, followed by two esterification steps using an immobilised *C. antarctica* An overall conversion of 91% was achieved by repeating the process every 24 h for 40 days (Watanabe et al. 2007). A similar process was proposed for the conversion of crude palm oil to biodiesel (Talukder et al. 2010b) Alternatively UCO was converted to biodiesel using *C. rugosa* catalysed hydrolysis followed by esterification with an ion-exchange resin, Amberlys-15 with a maximum conversion of 99%.

It has been proposed that mixtures of lipases can be used do decrease costs (Souza et al. 2009) and improve conversion (Tongboriboon et al. 2010). A series of immobilised lipases were screened and it was found that Lipase AY resulted in the highest hydrolysis conversion with very low conversions for

esterification and transesterification (Tongboriboon et al. 2010). The highest conversions for transesterification were achieved using immobilised Lipase PS and immobilised Lipase AK while Novozyme 435 showed the highest activity for esterification. Various combinations of these enzymes were investigated with a two-step process resulting in improvements. The best improvement was with a one-step process using an equal mass two lipases, immobilised Lipase AY and immobilised Lipase AK. A reusability study was carried out and it was found the activity of the lipases decreased by 50% after 15 cycles. This was attributed to glycerol accumulating on the surface of the catalyst. Similarly it was shown that conversion could be enhanced by using a mixture of Novozyme 435 and Lipozyme TL IM for the transesterification of lard (Huang et al. 2010).

2.5.3.2 Effect of Immobilisation and Support Type

One of the disadvantages of enzyme catalysts is that they are expensive. In order to overcome this various immobilisation techniques have been investigated to improve stability, reusability and reduce the cost (Li et al. 2011). Techniques available for immobilisation include covalent bonding, adsorption, cross-linking methods, entrapment and encapsulation (Paiva et al. 2000; Al-Zuhair et al. 2009). A summary of the immobilised enzymes reported for biodiesel production is presented in Table 2.4.

A popular technique is to formulate the lipase catalyst into protein coated microcrystals. For example Lipase PS immobilised on K_2SO_4 crystals was compared to free Lipase PS with the immobilised lipase showing a much greater thermal stability with an optimum conversion of 99.8% at 60 °C compared to an optimum conversion of 57% at 50 °C (Zheng et al. 2012). Lipase PS immobilised on K_2SO_4 could be reused when washed with a solvent such as hexane and *tert*-butanol. A cross-linked protein coated microcrystalline lipase incorporating *T. lanuginosus* lipase with glycerol as the core matrix was developed and assessed for the esterification of palm fatty acid distillate (Raita et al. 2011). *P. cepacia* was immobilised on accurel, and formulated into protein coated microcyrstals, and a cross-linked enzyme aggregate were compared to the free enzyme for the transesterification of oil from *Madhuca*

indica with a high FFA content. It was found that the highest conversion of 99% in 2.5 h was achieved using the *P. cepacia* coated microcrystals (Kumari et al. 2007).

In some cases the immobilisation technique and support have been shown to improve the catalytic activity of enzyme. Lipase PS immoblised in a sol-gel material increased conversion compared to the free enzyme and this was attributed to the lipophilic microenvironment created by the sol-gel material (Noureddini et al. 2005). The increased yield for *P. cepacia* immobilised on celite was attributed to a higher surface area which meant there were more accessible active sites (Shah & Gupta 2007). In contrast the activity of *P. cepacia* immobilised on polyacrylonitrile nanofibrous membrane was shown to be 79.5% of the free enzyme (Li et al. 2011). Similarly *C. antarctica* and *P. cepacia* encapsulated in aerogels had a lower activity than the free enzymes due to substrate diffusion limitations inside the aerogels (Orçaire et al. 2006). Conversion improved when using *iso*-octane as a solvent.

Hydrotalcite and four types of zeolite were compared as immobilisation supports for Lipozyme TL and it was found that the hydrotalcite was the most suitable support with a higher protein loading that the zeolites (Yagiz et al. 2007). A conversion of 93% was achieved compared to 95% for the commercially immobilised Lipozyme TL IM. 36% activity was retained by the reusability cycle 7 at a temperature of 40 °C. The effect of a styrene-DVB copolymer was compared to styrene-DVB containing polyglutaraldehyde for the immobilisation of *T. lanuginosus* by physical adsorbtion and covalent attachment. It was found that the that the activity was 85% for the polymer containing polyglutaraldehyde compared to an activity of 60% (Dizge et al. 2009). *T. lanugnosus* has also been found to be more effective immobilised by polyurethane foams incorporating polygluraraldehyde than those without (Dizge & Keskinler 2008) A conversion of 97% was possible at 50 °C for a reaction time of 24 h with the catalyst retaining activity for 10 reusability cycles. Niobium oxide (Nb_2O_5) and polysiloxane-polyvinyl alcohol (SiO_2-PVA) were compared as immobilised supports for Lipase PS and compared for the transesterification of

babassu oil and beef tallow (Da Rós et al. 2010). The best performance was from the SiO_2-PVA support with a conversion of 89% in 48 h and this was attributed to more suitable textural and chemical properties.

Immobilised lipases are suitable for use in continuous flow reactors. A series of fixed bed reactors using a lipase derived from *Candida* sp. immobilised on textile cloth to produce biodiesel from UCO has been shown to produce biodiesel from UCO that meets the biodiesel specifications (Chen et al. 2009). Similarly a packed bed reactor with integrated glycerol removal using Novozyme 435 as the catalyst has been shown to produce biodiesel from UCO, that meets the required biodiesel specifications (Hama et al. 2011). A 1:1 mixture of immobilised *C. rugosa* and *Rhizopus orzae* resulted in a conversion above 90% for the transesterification of biodiesel when operated for 108 h in a continuous system (Lee et al. 2010). An enzymatic reactor using lipase immobilised on a monolithic polymer support using glyceryl tributyrate showed that the activity was retained after treating 1000 reactor volume and it was shown that soybean oil could also be treated (Urban et al. 2012).

Table 2.4. A summary of the immobilised enzymes reported for biodiesel production

Immobilisation support	Enzyme Source	Substrate	Reaction Conditions*	Conversion	Reusability	Reference
K_2SO_4 microcrystals	*P. cepacia*	Soybean Oil	60 °C, 12 h, ethanol, 4:1 mole ratio**	99.8%	Relatively stable for 8 cycles (washed with hexane)	Zheng et al. (2012)
Glycine based microcrystals, prepared using cross-linked protein	*T. lanuginosus*	Palm fatty acid distillate	Esterification, 50 °C, 6 h, 20 wt% catalyst, ethanol, 1:4 mole ratio, *tert*-butanol solvent	81%	Relatively stable for 8 cycles	Raita et al. (2011)
Microcrystals	*P. cepacia*	*Madhuca indica* oil	40 °C, 2.5 h, ethanol, 4:1 ratio	99%	None reported	Kumari et al. (2007)
Cross-linked enzyme aggregate	*P. cepacia*	*Madhuca indica* oil	40 °C, 2.5 h, ethanol, 4:1 ratio	92%	None reported	Kumari et al. (2007)
Accurel MP 100	*P. cepacia*	*Madhuca indica* oil	40 °C, 6 h, ethanol, 4:1 ratio	96%	None reported	Kumari et al. (2007)
Acrylic Resin	*C. antarctica* lipase B (Novozyme 435)	Soybean Oil	40 °C, 12 h, ethanol,4:1 mole ratio	99.0%	None reported	Zheng et al. (2012)
Celite (a type of diatomaceous earth)	*P. cepacia*	*Jatropha* seed oil	50 °C, 8 h, 5 wt% water, ethanol,4:1 mole ratio	98%	Stable for 4 cycles	Shah & Gupta (2007)

Immobilisation support	Enzyme Source	Substrate	Reaction Conditions*	Conversion	Reusability	Reference
Hydrophobic sol-gel	*P. cepacia*	Soybean oil	35 °C, 1 h, 0.5 g water and 475 mg lipase for 10g oil, methanol, 1:7.5 mole ratio	67%	Steady decline over 12 cycles	Noureddini et al. (2005)
Hydrophobic sol-gel	*P. cepacia*	Soybean oil	35 °C, 1 h, 0.3 g water and 475 mg lipase for 10g oil, ethanol, 1:15.2 mole ratio	65%	Relatively stable for 11 cycles	Noureddini et al. (2005)
Silica aerogel reinforce with silica quartz fibre	*P. cepacia*	Sunflower oil	Methyl acetate reagent, 3:1 mole ratio, *iso*-octane solvent	~56%	None reported	Orçaire et al. (2006)
Silica aerogel reinforce with silica quartz fibre	*C. antarctica*	Sunflower oil	Methyl acetate reagent, 3:1 mole ratio, *iso*-octane solvent	~56%	None reported	Orçaire et al. (2006)
Polyacrylonitrile nanofibrous membrane	*P. cepacia*	Soybean oil containing 50-75% FFAs	24 h, 30 °C, 0.035g catalyst in 10g of oil, methanol, 6.6:1 mole ratio	90 %	91% of activity retained after 10 cycles	Li et al. (2011)
Accurel EP-100	A 1:1 mixture of *C. rugosa* and *P. fluorescens*	Used palm oil	12 h, 45 °C, 2% water, 10% catalyst loading, ethanol, 3.1 mole ratio	67%	Steady decline, 50% of activity retained after 15 cycles	Tongboriboon et al. (2010)

Immobilisation support	Enzyme Source	Substrate	Reaction Conditions*	Conversion	Reusability	Reference
styrene-DVB-polyglutaraldehyde	*T. lanuginosus*	Canola oil	24 h, 50 °C, stepwise methanol, 6:1 total mole ratio	97%	Activity retained for 10 cycles	Dizge et al. (2009)
Hydrophilic polyurethane foam incorporating polyglutaraldehyde	*T. lanuginosus*	Canola oil	40 °C, 0.5 wt% water, stepwise methanol, 6:1 mole ratio	90%	Activity retained for 10 cycles (washed with *tert*-butanol)	Dizge & Keskinler (2008)
Not specified	A 1:1 mixture of *C. rugosa* and *R. oryzae*,	Soybean oil	4 h, 45 °C, 10% water, 20% catalyst loading, stepwise methanol	98%	90% activity retained in a continuous flow reactor for 108 h	Lee et al. (2010)
Acrylic Resin	*C. antarctica* lipase B (Novozyme 435)	Canola oil	12 h, 38 °C, 42.3% catalyst loading, 7.2% water, methanol, 3.5:1 mole ratio	98%	None reported	Chang et al. (2005)
Acrylic Resin	*C. antarctica* lipase B (Novozyme 435)	UCO	48 h, 30 °C, 4 wt% catalyst, stepwise methanol, 3:1 mole ratio	90%	Activity retained in a continuous flow reactor for 100 days	Shimada et al. (2002)
Acrylic Resin	*C. antarctica* lipase B (Novozyme 435)	UCO	12 h, 40 °C, 4 wt% catalyst to oil, methanol, 4:1 mole ratio *tert*-butanol solvent	88%	None reported	(Halim & Harunkamaruddin 2008)

Immobilisation support	Enzyme Source	Substrate	Reaction Conditions*	Conversion	Reusability	Reference
Acrylic Resin	*C. antarctica* lipase B (Novozyme 435)	UCO	12 h, 44.5 °C, 15 wt% catalyst, stepwise methanol 3.8:1 mole ratio	100%	None reported	Azócar et al. (2010)
Acrylic Resin	*C. antarctica* lipase B (Novozyme 435)	Cotton seed oil	7 h, 50 °C, 30 wt% catalyst, methanol, 4:1 mole ratio	92%	None reported	Köse et al. (2002)
MgAl Hydrotalcite	*T. lanuginosa*	UCO	105 h, ~24 °C, methanol, 4:1 mole ratio	93%	36% of activity retained by cycle 7 at 45 °C	Yagiz et al. (2007)
Various zeolites (13-x, 5A, FM-8 and AW-300)	*T. lanuginosa*	UCO	105 h, ~24 °C, methanol, 4:1 mole ratio	~0%	None reported	2007)
Polysiloxane-polyvinyl alcohol (SiO_2-PVA)	*P. cepacia*	*babassu* oil	50 °C, 48 h, ethanol, 12:1 mole ratio, 20 wt% catalyst	100%	None reported	Da Rós et al. (2010)
Niobium oxide (Nb_2O_5)	*P. cepacia*	*babassu* oil	50 °C, 48 h, ethanol, 12:1 mole ratio, 20 wt% catalyst	74%	None reported	Da Rós et al. (2010)

*Unless otherwise specified the reaction investigated is transesterification
**In all cases this refers to the mole ratio of alcohol to substrate

2.5.3.3 Effect of Oil Type

It was found for the same conditions the conversion of UCO was 90.4 % compared to 95.9 % for vegetable oil (Shimada et al. 2002). The difference was attributed to contaminants in the oil which would have been produced during cooking such as epoxides, aldehydes and polymers. Conversely a higher conversion was achieved with UCO compared to rapeseed oil and this was attributed to the increase in concentration of MGs, DGs and FAME in the mixed vegetable oil (Azócar et al. 2010).

2.5.3.4 Effect of Water Concentration

It is often necessary to add water in order to activate lipases because the reactions are catalysed at the oil/water interface (Tongboriboon et al. 2010; Gog et al. 2012). In addition water is believed to increase protein flexibility by forming multiple hydrogen bonds with the enzyme molecule in organic solvents thus improving the activity of enzymes (Yadav & Manjula Devi 2004). When too much water is added the hydrolysis reaction can be catalysed (Tongboriboon et al. 2010).

The effect of water addition on Lipozyme TL IM catalysed transesterification of crude palm oil was investigated (Khor et al. 2010). It was found that as the water concentration increased from 0 to 6 wt% of substrate, the reaction rate and FAME yield increased however further increases in the water concentration resulted in a decrease in the reaction rate and FAME yield. A similar trend was observed by Noureddini et al. (2005) using Lipase PS entrapped in a sol-gel material and *P. cepacia* immobilised on celite (Shah & Gupta 2007). In contrast for a Lipase AY and Lipase AK catalysed reaction with used palm oil and ethanol, it was found that as the water increased from 2% to 20% the amount of FAEE formed decreased. However in this case Lipase AY is more suitable for the hydrolysis reaction.

Water addition is not required for Novozyme 435 catalysed esterification and increasing the amount of water can be detrimental to conversion (Talukder

et al. 2009; Trubiano et al. 2007). Water is formed during the esterification reaction.

2.5.3.5 Effect of Oil to Alcohol Mole Ratio and Type of Alcohol

Methanol (Li et al. 2011; Dizge et al. 2009) and ethanol (Tongboriboon et al. 2010; Souza et al. 2009) are the alcohols most frequently investigated for enzymatic biodiesel production although propanol, butanol and isopropanol have been considered (Köse et al. 2002). As discussed in Section 2.4.3 advantages of ethanol for biodiesel production are that it can be derived from renewable resources, the resulting FAEE biodiesel has slightly superior properties and it is more soluble in vegetable oil.

Methanol has a higher activity than ethanol for lipase catalysed production of biodiesel (Ferrão-Gonzales et al. 2011; Noureddini et al. 2005). However many lipase catalysts are deactivated by high alcohol concentrations and it has been found that lipases are more readily deactivated by methanol than ethanol. This deactivation has been described by the kinetic models as a competitive inhibition which means that the active sites are deactivated due to attachment by the alcohol. On this basis deactivation can be linked to the affinity of the alcohol to the active site and it has been shown that lipases are more readily deactivated by short chain alcohols (Köse et al. 2002; Chen & Wu 2003; Ferrão-Gonzales et al. 2011). Deactivation of lipases has also been attributed to dehydration which leads to denaturation of the lipase (Trubiano et al. 2007; Souza et al. 2009).

Alcohol is sparingly soluble in vegetable oil with ethanol being more soluble than methanol and it has been shown that lipase are deactivated by contact with insoluble alcohol (Shimada et al. 2002). Co-solvents to dilute the alcohol have been proposed as a solution (Halim & Harunkamaruddin 2008; Kraai et al. 2008; Gog et al. 2012). As discussed in Section 2.2.4 there are disadvantages when using a co-solvent and alternative solution is stepwise addition of alcohol (Shimada et al. 2002). However it was found that for the stepwise addition of ethanol to a system containing a mixture of lipases,

conversion only increased from 89% to 91% (Tongboriboon et al. 2010). Shah et al. (2004) also observed there was no additional benefit from the stepwise addition of ethanol.

Alcohols act as acyl acceptors in the transesterification reaction and alternative acyl acceptors have been proposed which do not deactivate lipases. For example methyl acetate leads to the formation of FAME and triacetylglycerol (Xu et al. 2005). More recently dimethyl carbonate has been investigated for the transesterification of palm oil using Novozyme 435 and kinetic modelling showed that competitive inhibition does not occur (Sun et al. 2013).

In addition it has been found that immobilised enzymes are more stable and able to tolerate higher alcohol concentrations when compared to free enzymes (Soumanou 2003). It has been found that *P. cepacia* has a high tolerance for alcohol when compared to other enzymes such as Novozyme 435 (Soumanou 2003; Shah et al. 2004; Kaieda et al. 2001).

In the case of chemical catalysed reactions the conversion can be increased by increasing the alcohol to oil mole ratio however this is more difficult in the case of enzyme catalysed biodiesel production. The range of mole ratios proposed for transesterification is 3-4:1 (Halim & Harunkamaruddin 2008; Tongboriboon et al. 2010; Lee et al. 2010). The minimum mole ratio for complete conversion is 3:1 as shown in Chapter 1, Figure 1.1. Similarly a typical mole ratio for esterification is 1:1 (Trubiano et al. 2007; Talukder et al. 2009; Souza et al. 2009).

2.5.3.6 Effect of Reaction Time

High conversions of biodiesel have been reported however the reaction time is generally much greater than required for the alkaline catalyst process. Conversions of 90-99 % have been reported for enzyme catalysed transesterification however the reaction times are typically 12-24 h (Tongboriboon et al. 2010; Li et al. 2011; Zheng et al. 2012). There are

execptions with a reaction time of 8 h reported for *Chromobacterium viscosum* lipase immobilised on Celite-545 with a conversion of 92 % (Shah et al. 2004) and 2.5 h for *P. cepacia* coated microcrystals with a conversion of 99 % (Kumari et al. 2007).

The reaction times reported for enzyme catalysed esterification of free fatty acid materials are typically 1.5–2h (Talukder et al. 2009; Souza et al. 2009; Trubiano et al. 2007).

2.5.3.7 Effect of Reaction Temperature

Conversion generally increases with increasing temperature until an optimum value is reached. As the temperature increases further the conversion drops rapidly due to deactivation of the catalyst (Souza et al. 2009; Köse et al. 2002). Typical temperatures investigated for enzymatic biodiesel production are 30–80 °C with the optimum generally falling in the range of 40-50 °C (Ganesan et al. 2009; Soumanou 2003; Sim et al. 2010).

Immobilisation can increase the thermal stability of enzymes and it was found that the conversion of soybean oil using *P. cepacia* immobilised on a polyacrylonitrile nanofibrous membrane remained approximately the same for temperatures of 30 – 50 °C (Li et al. 2011). Trubiano et al. (2007) investigated the effect of temperature in the range of 25-60 °C on Novozyme 435 and found that conversion increased from 69.6% to 80.4% with no evidence of catalyst deactivation.

The effect of temperature on the immobilised enzyme, Lipozyme TL IM, with *tert*-butanol as the solvent for the transesterification of crude palm oil with methanol was investigated (Khor et al. 2010). It was found that the optimum temperature was 40 °C and the activation energy was 22.15 kJ·mol^{-1} compared to a deactivation energy of 45.18 kJ·mol^{-1}. This is similar to the value of 26.0 kJ·mol^{-1} calculated for transesterification of palm oil with dimethyl carbonate as the regent and catalysed by Novozyme 435. The value for activation energy is similar to the value calculated by Mahmud et al. (2010) of 22.4 kJ·mol^{-1} using a

temperature range of 25-45 °C for Novozyme 435 catalysed esterification of oleic acid.

2.6 Liquid Chromatography to Monitor Biodiesel Production

Numerous methods have been investigated to monitor the formation of biodiesel depending on the process selected. In most cases the relevant fatty acid alkyl ester formation is monitored (Khor et al. 2010) although the FFAs concentration can be monitored during esterification (Ozbay et al. 2008). Depending on the nature of the investigation other components which may need to be monitored are MGs, DGs TGs, glycerol, methanol and water.

The FFA concentration is generally determined using a recognised titration method (Souza et al. 2009; Feng et al. 2010). such as ASTM D 974-08. Methods which have been developed to quantify the other components include thin layer chromatography (TLC), gas chromatography (GC), high performance liquid chromatography (HPLC), gel permeation chromatography (GPC), 1H nuclear magnetic resonance (1H NMR) and near-infrared spectroscopy (NIR) (Arzamendi et al. 2006), with GC and HPLC being the methods used most often (Li et al. 2008).

The American and European biodiesel standards are based on GC techniques with separate methods for analysing FAMEs (EN 14103:2003) and MG, DG, TGs and glycerol (EN 14105:2003). However substances with high molecular weights, high boiling points and low volatility are not easily vaporised and separated by GC and as a result the GC method for MG, DG, TG and glycerol includes a derivitisation method and internal standards (Holcapek et al. 1999). An alternative solution for investigating mixtures containing compounds with a low volatility is to use liquid chromatography.

2.6.1 Types of Liquid Chromatography

In liquid chromatography the separation is achieved by injecting a dissolved sample into a stream of solvent which is pumped through a column packed with solid separating material. Differences in polarity, size, shape, charge, specific affinity for a site, sterio and optical isomerism can be used to achieve the separation (McMaster 2007).

Size exclusion chromatography was investigated by Arzamendi et al. (2006) with a refractive index (RI) detector to analyse transesterification samples. Three columns, connected in series, were required to separate components in the following order TG>DG>MG>FAME>glycerol>methanol. FFAs have a similar molecular weight to FAMEs when compared to the other components, however FFAs were not investigated. This method is not particularly useful if the methyl esters and FFAs are co-eluting, particularly when using a raw material such as UCO which contains FFAs. In addition this method is expensive compared to other types of liquid chromatography.

Polarity differences are more commonly used when carrying out separations involving vegetable oil. For example Hishamuddin (2009) used reverse-phase chromatography to separate the triglycerides in palm oil. An isocratic elution with the mobile phase composed of actetone:acetonitirile 63.5:36.5 (v/v) was used with a non-polar column. This method achieved a good separation of triglycerides however MGs and DGs were not considered.

The separation can be improved by using a gradient method to vary the polarity of the mobile phase, by varying the solvent composition. Holcapek et al. (1999) developed a method based on a ternary gradient variation of solvents. According to this method; reservoir A contained water, reservoir B contained acetonitrile and reservoir C contained 2-propanol:hexane (5:4 v/v). Two linear steps were used with the first being 30% A + 70% B in 0 min, 100% B in 10 min, 50% B + 50% C in 20 min followed by an isocratic elution with 50% B + 50% C for the last 5 min. This method resulted in a good resolution of the various component classes and nearly complete resolution of the individual

components with the order of elution being FFAs<MGs<MEs<DGs<TGs. Ternary gradients increase the analysis time and most laboratory equipment is restricted to a binary pump. In order to simplify the analysis Holcapek et al. (1999) proposed a rapid analysis method. According to this method; reservoir A contained methanol and reservoir B contained a mixture of 2-propanol-hexane (5:4 v/v). A linear gradient from 100% A to 50% A + 70% in 15 min was used. This method gave a reasonable separation of the FAMEs from the TGs although the DGs were obscured by baseline noise.

Di Nicola et al. (2008) investigated a similar method to Holcapek et al. (1999) using non-aqueous reversed phase liquid chromatography, with a binary gradient and a UV detector at 210 nm. The optimal method proposed is with a mobile phase A consisting of acetonitrile:methanol 4:1 (v/v) and mobile phase B consisting of n-hexane:isopropanol 8:5 (v/v). The linear gradient started with 100% A from time 0 min till 2.2 min then 34% A and 66% B after 25.5 min followed by and isocratic elution of 34% A and 66% B till 30 min. There was good separation of most of the components although there was some co-elution of the monoglycerides and methyl esters. The order of elution was MGs<MEs<DGs<TGs. FFAs were not investigated.

Türkan & Kalay (2006) investigated reversed-phase HPLC. The binary method selected for further study started with 100% acetonitrile to 30% acetonitrile and 70% acetone over 3 min followed by a 25 min isocratic elution although there was some co-elution of components. It was found that better separation was achieved using a linear gradient elution from 100% acetonitrile to 50% acetonitrile + 50% acetone over 3 min followed by 12 min isocratic elution and then a step gradient to 30% acetonitrile + 70% acetone and a 25 min isocratic elution.

A recent modification of liquid chromatography is ultra performance liquid chromatography (UPLC) which uses columns with small particles and a high pressure in order to speed up the analysis time (McMaster, 2007). Li et al. (2008) investigated a UPLC method using acetonitrile-water (3:1 v/v) as the mobile phase and a phenyl C18 column. With this method it was found that a

good separation of eleven fatty acids and methyl esters was possible however MGs, DGs, TGs and glycerol were not considered. Lee & Di Gioia (2007) developed a UPLC method starting with 90% acetonitrile and 10% 2-propanol to 10% acetonitrile + 90% 2-propanol in 22 min. With this method it was found that separation of the MG, DG and TG, as well as fatty acids and methyl esters was possible.

Vegetable and waste vegetable oil consists of many different components and in many cases it was found that some of the components co-elute. For example it was shown that for the method used by Lee & Di Gioia (2007) there was co-elution of various components including linoleic acid and monoolein, oleic and palmitic acid as well as methyl oleate and methyl palmitate. Co-elution of similar components can be observed from the method proposed by Di Nicola et al. (2009). Turkan and Kalay (2006) showed co-elution of some di- and triglyceride species.

2.6.2 Types of Liquid Chromatography Detectors

Detectors reported for HPLC biodiesel analysis include ultraviolet/visible (UV/vis) (Holcapek et al. 1999; Lee & Di Gioia 2007; Di Nicola et al. 2008), refractive index (RI) (Arzamendi et al. 2006; Hishamuddin 2009), evaporative light scattering detectors (ELSD) (Lee & Di Gioia 2007; Li et al. 2008) and mass spectrometry (MS) (Holcapek et al. 1999; Türkan & Kalay 2006).

Refractive index detectors have been found to show a good response to the components found in vegetable oil (Arzamendi et al. 2006; Hishamuddin 2009) however they can only be used for isocratic elutions. As a result UV/vis and ELSD detectors have been considered for the investigation of biodiesel production. Holcapek et al. (1999) found that UV/vis was more sensitive compared to ELSD however a recent study carried out by Lee & Di Gioia (2007) showed that the ELSD was more sensitive. Li et al. (2008) was also able to get a good response using ELSD. One of the problems with the UV/vis detector is that the response is low with saturated lipids and as a result these components are not readily detected (McMaster 2007).

Mass spectrometry is used to detect compounds based on the mass to charge ratio (m/z) and this method can be used to quantify and identify the components of a given mixture. Various methods exist to ionise the samples. Holcapek et al. (1999) and Türkan & Kalay (2006) used an atmospheric-pressure chemical ionisation spray (APCI) which fragments the molecules into a predictable set of ions. An alternative type of mass spectrometer which has recently been used in conjunction with liquid chromatography is time-of-flight (TOF). In this case a low energy electrospray is used to charge compounds without fragmenting them (Gay et al. 2011).

2.7 Conclusions

Biodiesel has been defined as “mono-alkyl esters of long chain fatty acids derived from vegetable oils or animals fats” according to the ASTM International definition. Feedstocks which have been investigated for biodiesel production include edible and non-edible vegetable oils, animal fats, oil refining by-products, algal oil and UCO. UCO has been selected as the raw material for this work because it is expected to minimise the environmental impact.

Base, acid and enzyme catalysts have been considered for biodiesel production. The focus of this work is on heterogeneous forms of these catalysts because they are readily separated from the reaction mixture and can be reused. Basic catalysts have been shown to have the highest activity; however, there are problems which include leaching of the active species, sensitivity to water and FFA. In addition the preparation of many of these catalysts is complex and calcining at high temperatures is sometimes required.

Acid catalysts have been proposed as an alternative type of catalyst for processes involving UCO because these catalysts are not affected by FFAs and can simultaneously catalyse the esterification and transesterification reactions. Acid catalysed transesterification is slow when compared to base catalysed transesterification. In order to overcome this problem a two-step process has been proposed with esterification followed by transesterification. Ion-exchange resins have shown to be effective for the esterification pre-

treatment of UCO for the preparation of biodiesel, at relatively benign reaction conditions. Purolite D5082 is an ion-exchange resin recently developed for the esterification pre-treatment of biodiesel. The optimisation of this catalyst for the esterification pre-treatment process has not been reported and will be investigated.

Enzyme catalysts have been proposed for biodiesel production because they can catalyst esterification, transesterification and hydrolysis at relatively benign operating conditions and there are no saponification side reactions. Novozyme 435 has been widely reported for the esterification of lipid materials with a high FFAs content however it has not been considered for the esterification pre-treatment of UCO.

Various forms of the lipase *P. cepacia* (recently reclassified as *B. cepacia*) have been investigated for the production of biodiesel. To date the focus has been in assessing various techniques and supports for immobilising this lipase. An optimisation study with UCO as the raw material and the commercially available, immobilised form of this lipase, Amano Lipase PS-IM, has not been reported in the literature and it proposed to carry out this study.

Chapter 3: Materials and Methods

3.1 Introduction

This chapter details the materials and experimental methods used to carry out the research work. Section 3.2 of the chapter provides information on the materials used. This is followed by a description of the catalyst characterisation techniques in Section 3.3. The experimental set-up and procedures are discussed in Section 3.4. In Section 3.5 the analytical techniques used for monitoring the progress of the various reactions and the characterisation of the UCO are discussed and this includes all the liquid chromatography methods that have been tested.

3.2 Materials

Purolite D5082 (ion-exchange resin), was donated by Purolite International UK Ltd and received in a dry form. The ion-exchange resin was washed with methanol, dried in a vacuum oven at 373 K for 6 h and stored in a desiccator prior to use. Novozyme 435 (immobilised enzyme, *Candida antarctica* lipase B) was donated by Novozymes UK Ltd and Amano Lipase PS-IM (immobilised enzyme, lipase from *Pseudomanas cepacia*, recently reclassified as *Burkholderia cepacia*) was donated by Amano Enzyme Europe Ltd, UK. The immobilised enzymes were stored in a refrigerator and used as supplied.

The UCO, used as the raw material for producing biodiesel, was supplied by GreenFuel Oil Co Ltd., UK. Methanol (>99.9%) was used as the reagent for bidiesel and cleaning Purolite D5082 was purchased from Fisher Scientific UK Ltd.

The 0.1 M standardised solution of potassium hydroxide in 2-propanol and α-Naphtholbenzein indicator, used for the FFA titration, were purchased from Sigma Aldrich, UK.

The methyl oleate (>99.0%), methyl palmitate (>99.0%), methyl linoleate (>99.0%), methyl stearate (>99.5%) methyl heptadecanoate (>99.0%) were used as the standards for FAME analysis and *n*-hexane (>97.0%), and purchased from Sigma Aldrich, UK. Methyl linolenate was also used as a standard for determining the FAME concentration and purchased from Fischer Scientific UK Ltd.

DL-α-palmitin (>99%), 1,3 diolein (>99%), dipalmitin (>99%) and glycerol trilinoleate (>98%), glycerol tripalmitate (>99%) were used as standards to determine the MG, DG and TG concentrations and were purchased from Sigma Aldrich, UK.

Hydranal® Coulomat Oil, Hydranal® Coulomat GC and Hyranal® Water standard 1.00 (0.1% water) were used for determining the water concentration and were purchased from Sigma Aldrich, UK.

Toluene (>99%), 2-propanol (>99.8%), acetone (>99.8%) and acetonitrile (>99.9%) were used as solvents for various analysis and *tert*-butanol (>99%) was used for washing Novozyme 435. These solvents were purchased from Fisher Scientific UK Ltd.

The palm oil was originally supplied by the Malaysian Palm Oil Board and is palm oil sample series 4.

3.3 Catalyst Characterisation

3.3.1 Field Emission Gun-Scanning Electron Microscopy

A field emission gun-scanning electron microscope (Carl Zeiss, Leo 1530 VP) (FEG-SEM) was used to study the morphology of the ion exchange resins. The FEG-SEM analysis was carried out a room temperature and used

accelerating voltages of 1-30 kV. Prior to analysis samples of each catalyst were crushed using a mortar and pestle. Fresh catalyst beads and ground powder were then mounted on aluminium stubs using double sided adhesive carbon conductive dots. Silver paint was placed at both sides of the samples to act as a conductor and the samples were coated with gold in an argon atmosphere prior to observation. The results are given in Chapter 4.

3.3.2 Elemental Analysis

The elemental analysis was used to investigate the elemental composition of the catalysts and to determine if this changed when the catalyst was used. In particular sulfonic acid is the active species on the ion-exchange resin catalyst so a reduction in the sulphur percentage would indicate a loss of sulfonic acid. The ion-exchange resin catalyst (Purolite D5082) was analysed for carbon (C), hydrogen (H), nitrogen (N) and sulphur (S).

The immobilised enzymes (Novozyme 435 and Amano Lipase PS-IM) are composed of C, H and N and as a result were analysed for C, H and N. In the case of lipases the catalytic activity is based on the conformation of specific functional groups known as the catalytic triad. The catalytic triad is composed of the serine, aspartic acid and histidine amino acid residues (Paiva et al. 2000).

The catalyst samples were crushed and dried before being sent for elemental analysis. The elemental analysis was carried out using a Thermoquest EA1110 Elemental Analyser by OEA Laboratories Ltd (Cornwall). The samples were combusted in pure oxygen with a catalyst to ensure complete combustion to form elemental nitrogen, carbon dioxide, water vapour and sulphur dioxide. These gases were separated using gas chromatography and quantified using a thermal conductivity detector. The analysis was carried out in duplicate and the results are given in Chapter 4.

3.3.3 Fourier Transform-Infrared Measurements

The Fourier Transform-Infrared Transform (FT-IR) spectroscopy analysis was carried out to investigate the functional groups present on the various catalysts. A sample of each catalyst was ground into a powder using a mortar and pestle, and subsequently mixed with potassium bromide (KBr). The powder was pressed under a constant 10 T pressure for 5 min to form a pellet.

The analysis was carried out using an FTIR 8500S SHIMADZU analyser. Each pellet was placed in the sample holder and 64 scans carried out. A spectral range (wavenumbers) from 4000 - 600 cm^{-1} was used and the transmittance recorded. The results are discussed in Chapter 4.

3.3.4 True Density Measurement

The true density (ρ_t) was measured using a Micromeritics Multivolume Pycnometer 1305 with helium as the gas. A known mass of catalyst (m_c, g) was placed in the pycnometer cell with known volume (V_{cell}, cm^{-3}) and helium was passed through the cell several time in order to purge the sample. The volume of the sample was determined by measuring the pressure of helium permitted to flow into the cell (P_1, psi) and the pressure when the helium was permitted to expand (P_2, psi) to a known volume (V_{exp}, cm^{-3}). The volume of the sample (V_{sample}, cm^{-3}) and the density could then be calculated:

$$V_{sample}, cm^{-1} = \frac{V_{cell} - V_{exp}}{\frac{P_1}{P_2} - 1} \quad \textbf{(3.1)}$$

$$\rho_t = \frac{m_c}{V_{sample}} \quad \textbf{(3.2)}$$

For each sample five measurements were made and the average values have been reported. The results are reported in Chapter 4.

3.3.5 Particle Size Distribution Measurement

Particle size distribution (PSD) analysis was carried out using a Coulter LS 130 particle analyzer with particle size measurements over the range 0.1 - 900 μm. The Fraunhofer optical model was used for the measurement of the distribution pattern. The samples were introduced into the dispersion module with isopropyl alcohol as the solvent. The results are given in Chapter 4.

3.3.6 Surface Area, Total Pore Volume and Average Pore Diameter Measurement

Surface area, pore volume and average pore diameter were determined from adsorption isotherms using a Micromeritics ASAP 2020 surface analyser as follows: The samples were degassed by means of a two-stage temperature ramping under a vacuum of <10 mmHg, followed by sample analysis at 77 K using nitrogen gas. The Brunauer–Emmett–Teller (BET) method was used to calculate the surface area, average pore diameter and total pore volume.

3.3.7 Sodium Capacity Determination

The acid capacity was determined using a conventional titration method. A known amount of catalyst (~0.5 g) was placed in a conical flask and contacted with 50 mL of 0.1 M sodium hydroxide for 72 h using an orbital shaker. After shaking, 5 mL aliquots of the filtered solution were titrated with 0.1 M hydrochloric acid and methyl red as the indicator. The samples were analysed in triplicate.

3.3.8 Bicinchoninic Acid Protein Assay

The catalytic activity of enzymes is linked to the amount of enzyme immobilised on the support. A bicinchoninic acid (BCA) assay is used to determine the amount of protein immobilised on various surfaces, with enzymes a type of protein. By analysing fresh and used catalyst the BCA assay can be used to determine if the amount of protein changes during use. The BCA assay was carried out using a commercially available Pierce BCA protein determination kit. The kit contains copper II which is reduced to copper I by the

protein. The copper I then reacts with BCA to form a purple copper-BCA complex.

100 μL of deionised water was added to a known mass of sample. The BCA standards and reagents were prepared in accordance with the manufacturer's instructions. 1.9 mL of the reagent solution was added to 0.1 mL of sample or standard and incubated for 2 h on a 3-D rocking platform (60 RPM) at room temperature. The optical density was measured at a wavelength of 562 nm using a UV-VIS spectrophotometer UV mini (Shimadzu, Milton Keynes, UK). The samples were calibrated against an albium standard solution in deionised water.

3.4 Batch Experimental Set-up

The esterification reactions were carried out using a five-neck, 500 mL jacketed batch reactor with a reflux condenser and baffles. The stirrer motor was a Eurostar Digital IKA-Werke. The temperature was monitored by means of a Digitron, 2751-K thermocouple and this information was used to set the temperature on the Techne, TE-10D Tempette water bath. The sample tube was fitted with metal gauze to prevent withdrawal of catalyst when taking a sample and the samples withdrawn by means of a syringe. A schematic representation of the batch experimental set-up is shown in Figure 3.1.

Most reactions were carried out using a liquid volume of 300 mL. The exception being the reusability studies when the volume had to be adjusted to allow for a smaller or larger amount of catalyst. When parameters such as the mole ratio were investigated the ratio of the volumes was varied to meet the required mole ratio, keeping the total volume constant. The reactants were added to the reactor and heated to the required temperature, after which the catalyst was added to initiate the reaction. The point at which all the catalyst had been added was defined at the start point for the reaction or time, t=0. The catalyst mass was determined based on the total mass of the reactants. Samples were taken at regular intervals.

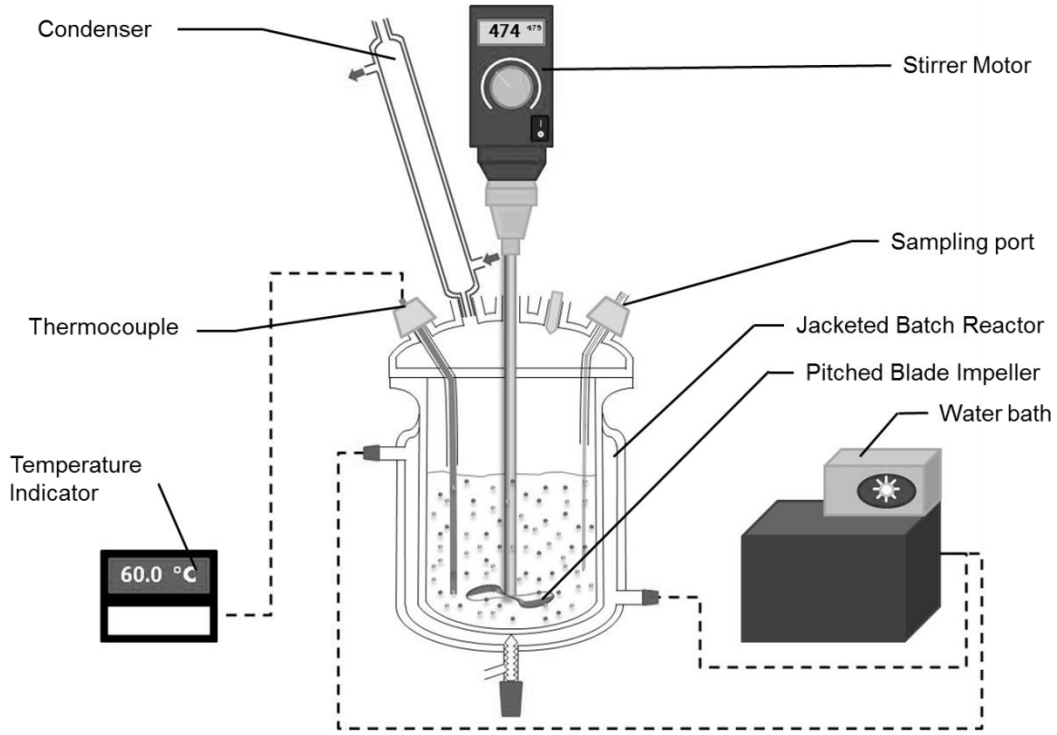

Figure 3.1. Schematic representation of the batch experimental set-up.

3.4.1 Esterification Pre-treatment Experiments

The aim of the esterification pre-treatment experiments was to investigate the esterification of FFAs in UCO to FAME. The esterification reaction schematic is shown in Chapter 1, Figure 1.2. Typical reaction conditions for the esterification reaction are shown in Table 3.1. All optimisation reactions were carried out using the same liquid volume (0.3 L). When the mole ratio was varied the Excel function “goal seek” was used to find the new conditions by varying the amount of methanol and UCO to be added. The catalyst was calculated based on the total mass of liquids added to the reactor. In the case of the reusability studies it was necessary to amend the total reactor volume depending on the amount of catalyst available for the experiment.

For the esterification reaction the effect of stirring speed (external mass transfer resistance), particle size (internal mass transfer resistance), catalyst loading, temperature and mole ratio on conversion were investigated. A blank run, without catalyst, was also carried out at the optimum conditions for Purolite

D5082 and it was found that the change in FFA and FAME concentrations was negligible after 8 h. These conditions were selected because it was expected that the uncatalysted reaction was most likely to occur at these conditions. As a result it was concluded that the esterification and transesterification reactions were only possible in the presence of a suitable catalyst.

Table 3.1. Typical reaction conditions for the esterification pre-treatment experiments

Parameter	Purolite D5082	Novozyme 435
Temperature (°C)	60	50
Stirring speed (rpm)	450	650
Methanol to FFAs mole ratio (-)	62:1	6.2:1
Methanol		
Molar Mass Basis ($g \cdot mol^{-1}$)	278.0	278.0
Mass (g)	83.07	12.13
Volume (L)	0.105	0.0153
UCO		
Mass (g)	180.2	263.1
Volume (L)	0.195	0.284
Total volume (L)	0.300	0.300
Total mass (g)	263.3	275.3
Catalyst loading (%)	5.00	1.00
Catalyst mass (g)	17.55	2.753

All samples were analysed for the FFAs. In order to understand the extent of the side reactions samples from selected experiments were analysed for the FAME concentration. Samples from a small number of experiments were also analysed for the MG, DG, and MG concentrations in order to investigate the reaction mechanism. The conversion of FFAs at any time was calculated according to equation 3.3.

$$\text{Conversion of FFAs, } X_{FFAs} = \frac{c_{FFAs,0} - c_{FFAs}}{c_{FFAs,0}} \quad \textbf{(3.3)}$$

where $c_{FFAs,0}$ is the initial concentration of FFAs (wt%), at time, t=0 and c_{FFAs} is the concentration of FFAs (wt%), at any time, t=t.

After the experiments the catalyst was separated from the reaction mixture by filtration. Selected samples were kept for the reusability studies detailed in sections 3.4.1.1 and 3.4.1.2. The reaction mixture was left in a separating funnel overnight allowing the mixture to separate into two layers; a non-polar oil layer and a polar layer. The density and composition of these layers was measured and the results are discussed in Chapter 5.

The reproducibility of the esterification reactions are discussed in Chapter 5 and the results are discussed in Chapter 6. The results of the batch experiments which included monitoring the MG, DG and TG concentrations and the associated kinetic modelling are presented in Chapter 7.

3.4.1.1 Ion-exchange Resin catalyst (Purolite D5082) Reusability Study

The aim of this study was to compare the effect of methanol washing using an ultrasonic bath and regeneration using sulphuric acid on the reusability of Purolite D5082.

The batch experiments for this study were carried out using the optimum reactions conditions identified for Purolite D5082. After cycle 1 the catalyst was separated from the reaction mixture by filtration. This catalyst was washed using methanol and an ultrasonic bath (Fisherbrand, FB11003) set at 60% power. The methanol was changed regularly until no further discolouration of the methanol could be observed. The catalyst was then dried in the vacuum oven at 100 °C for 6 h. The resulting catalyst is referred to as Purolite D5082, Cycle 2 and a second reusability cycle carried out.

After cycle 2 the catalyst was again separated from the reaction mixture by filtration, washed using methanol and the ultrasonic bath and then dried in the vacuum oven. After drying 1 M sulphuric acid was added to the catalyst and this was left in the orbital shaker overnight. The catalyst was then washed using a continuous flow of deionised water through a column. The progress was monitored by measuring the conductivity of the water. Methanol was used to displace water from the catalyst and it was then dried in the vacuum oven at 100 °C for 6 h. This sample of catalyst is referred to as Purolite D8082, Cycle 3. Reusability cycle 3 was carried out using this catalyst.

In order to investigate the results further a sample of Purolite D5082, Cycle 2 and a sample of Purolite D5082 were regenerated with 1 M sulphuric acid overnight and washed with deionised water through a column as above. These catalyst samples were then soaked in methanol with regular changes until no further discolouration of the methanol could be observed. The catalyst was then dried in the vacuum oven 100 °C for 6 h. These catalyst samples were labelled Purolite D5082, Cycle 1-2, Purolite D5082, Cycle 2-2 and Purolite D5082, Cycle 3, and the reusability batch experiments carried out.

3.4.1.2 Immobilised Enzyme (Novozyme 435) Reusability Study

It is known that methanol damages enzyme catalysts (Talukder et al. 2009; Shimada et al. 2002). *Tert*-butanol was selected to clean this catalyst because it has been shown to be effective.

The catalyst was soaked in *tert*-butanol with regular solvent changes until no further colour change could be observed. *Tert*-butanol has a melting point of 25.7 °C and as a result it was necessary to immerse the conical flasks containing the solvent and catalyst in a water bath at 26 °C. The catalyst was then separated from the solvent by filtration and placed in a refrigerator for 1 h. Freeze-drying was used to remove the residual solvent.

3.4.2 Enzymatic Biodiesel Production

The production of biodiesel using immobilised lipases has been investigated. Lipases are able to catalyse the esterification, transesterification and hydrolysis reactions. The order of preference depends on the lipase type and reagents. The enzymatic biodiesel production has been carried out in two stages with the first stage focused on the transesterification reaction using Amano Lipase PS-IM as the catalyst. The second stage was carried out using Novozyme 435 as the catalyst and was focused on the esterification reaction.

3.4.2.1 Enzymatic Biodiesel Production Stage 1

Initially the esterification reaction was intended as a pre-treatment process to remove FFAs prior to transesterification however an advantage of enzyme catalysts is that they are not affected by the presence of FFAs. As a result stage 1 is regarded as a transesterification process and the overall transesterification reaction scheme is shown in Chapter 1, Figure 1.1.

Stage 1 was carried out with UCO as the raw material and Amano Lipase PS-IM as the catalyst. It was found that it was necessary to add water to the transesterification reaction mixture. Water can cause problems with GC-MS analysis and the samples were centrifuged to separate most of the water from the oil. The non-polar oil layer was analysed for FAME and FFA. The work carried out to investigate the composition of the final product layers has shown that the amount of FAME and FFA in the polar layers is negligible. This is discussed in Chapter 5. The amount of material added was calculated using the same approach for esterification as discussed in Section 3.4.1. Typical reaction conditions for enzymatic biodiesel production are given in Table 3.2.

At the end of the experiments, the catalyst was separated from the reaction mixture by filtration. The reaction mixture was left in a separating funnel overnight allowing the mixture to separate into two layers; a non-polar oil layer and a polar layer. The density and composition of these layers was measured and the results are presented in Chapter 5. In addition the oil layer

at the optimum conditions was used to investigate enzymatic biodiesel production stage 2, as discussed in Section 3.4.2.2.

Table 3.2. Typical reaction conditions used for enzymatic biodiesel production stage 1

Parameter	Amano Lipase PS-IM
Temperature (°C)	40
Stirring speed (rpm)	500
Methanol to oil mole ratio (-)	3:1
Methanol	
Mass (g)	25.9
Volume (L)	0.032
UCO	
Molar Mass Basis ($g \cdot mol^{-1}$)	867.4
Mass (g)	233.2
Volume (L)	0.253
Water	
Volume percentage (%)	5
Mass (g)	15
Volume (L)	0.015
Total volume (L)	0.300
Total mass (g)	274.0
Catalyst loading (%)	0.786
Catalyst mass (g)	2.154

For the transesterification reaction the effect of water addition, mole ratio, external mass transfer resistance, catalyst loading and temperature on conversion were investigated. The reproducibility of the transesterification reactions are discussed in Chapter 5 and the results are discussed in Chapter 8.

3.4.2.2 Enzymatic Biodiesel Production Stage 2

The reaction product from the transesterification reaction contained a significant amount of FFAs. In addition given the FAME conversion it was expected that a significant amount of unreacted TGs, DGs and MGs were present in the reaction product. Novozyme 435 has been shown to catalyse esterification, transesterification and hydrolysis. As a result Novozyme 435 has been investigated to determine if it could be used after the transesterification reaction to convert the FFAs, DGs and MGs to FAME thus increasing the conversion.

A sample of oil was used directly for the Stage 2 investigation. A second sample of oil was dried using rotary evaporation at 60 °C. The aim of the rotary evaporation was to remove any residual water and methanol however it was possible that FAME would also be removed and a sample was taken before and after drying to monitor the FAME concentration. The batch experiments were carried out at the optimum conditions identified for Novozyme 435 as an esterification pre-treatment catalyst (Chapter 6) and the results are discussed in Chapter 8.

3.5 Analytical Methods

3.5.1 Determination of the FAME Concentration

The FAME concentration was determined using gas chromatography mass spectrometry (GC-MS) according to the procedure described in Abidin et al. (2012). The GC-MS analysis was carried out using a Hewlett Packard HP-6890 instrument, equipped with a DB-WAX (J & W Scientific) capillary column, (30 m x 0.25 mm) packed with polyethylene glycol (0.25 µm film thickness); Helium at a flow rate of 1.1 mL·min^{-1} was used as the carrier gas. The amount of sample injected was 2 µL and the temperature of the injector and detector was 250 °C. The initial oven temperature was 70 °C held for 2 min, then increased at 40 °C·min^{-1} up to 210 °C, then increased at 7 °C·min^{-1} up to 230 °C and the final temperature held for 11 min. Methyl heptadecanoate was used as the internal standard.

In order to determine the response factors, stock solutions were prepared, using the 5 components and the internal standard, to a concentration of approximately 5000 mg·L^{-1}, with hexane as the solvent. These stocks could be stored for up to a week in the refrigerator, in an amber glass bottle. The calibration standards were made up by adding a known mass of each stock to a 2 mL amber vial. This was done in triplicate for each analytical run. The standards were used to determine the response factor according to equations 3.4-3.6.

$$\text{Response factor of the } i^{th} \text{ component, } RF_i = \frac{\text{Mass ratio of component } i,\ MR_i}{\text{Area ratio of component } i,\ AR_i} \quad \textbf{(3.4)}$$

Where:

$$MR_i = \frac{\text{mass of component } i,\ m_i}{\text{mass of the internal standard, } m_{is}} \quad \textbf{(3.5)}$$

$$AR_i = \frac{\text{area of component } i,\ a_i}{\text{area of the internal standard, } a_{is}} \quad \textbf{(3.6)}$$

The samples were prepared by adding a known mass of sample and internal standard solution to a 2 mL amber vial. This was diluted with hexane. The calibration information could then be used to calculate the component masses according to equation 3.7. The mass and molar concentrations were subsequently calculated according to equations 3.8 and 3.9.

$$m_i = RF_i \times m_{is} \times AR_i \quad \textbf{(3.7)}$$

$$\text{mass concentration, } g \cdot g = \frac{\sum m_i}{m_s} \cdot \quad \textbf{(3.8)}$$

$$\text{molar concentration, } mol \cdot m^{-3} = \frac{\text{mass concentration}}{M_{oil}} \times \rho \quad \textbf{(3.9)}$$

Where m_s is the sample mass (g); M_{oil} is the molar mass of the oil (g·mol^{-1}) and ρ is the calculated reaction mixture density (g·m^{-3}).

3.5.2 Liquid Chromatography Methods Investigated for Monitoring Biodiesel Production

Various liquid chromatography methods were investigated for their potential use to monitor biodiesel reaction products. The justification for assessing each method is discussed in Chapter 7.

3.5.2.1 The High Performance Liquid Chromatography (HPLC) Instrument

The HPLC work was carried out using a Hewlett Packard model 1100 HPLC system with a binary pump, a variable loop injector system, a column oven, a refractive index detector and a diode array detector.

A Waters NovaPak© C18 with a 3.9 mm internal diameter, 300 mm in length and preloaded with 4 μm silica particles was used for the separation. For Method 1 two columns were used and one column was used for Method 2.

3.5.2.2 The Liquid Chromatography-Mass Spectrometry (LC-MS) Instrument

The LC-MS work was carried out using a Waters Acquity ultra performance liquid chromatography (UPLC) system interfaced to a Waters Synapt HDMS quadrupole time-of-flight (TOF) mass spectrometer, using positive ion. A Phenomenex Kinetix C18 UPLC column (150 mm x 2.1 mm x 2.1 μm) was used for the separation.

3.5.2.3 LC Method 1

Method 1 was carried out using the HPLC instrument. An isocratic elution was used with the mobile phase consisting of acetone:acetonitrile 63.5:36.5 (v/v) with a flow rate of 1 $mL \cdot min^{-1}$ and the run time was set at 130 min. The injection volume was 10 μL of 5% (w/v) oil in chloroform and the oven temperature was set at 25 ºC. Attenuation was fixed at 500 x 103 RI units and

the refractive index detector was maintained at a temperature of 35 ºC (Hishamuddin 2009).

3.5.2.4 LC Method 2

Method 2 was carried out using the HPLC instrument. The chromatography used a binary gradient with mobile phase A consisting of acetonitrile:methanol 4:1 (v/v) and mobile phase B consisting of n-hexane:isopropanol 8:5 (v/v). The separation started with 100% A from 0 min till 2.2 min then 34% A and 66% B after 25.5 min followed by an isocratic elution of 34% A and 66% B ending at a run time of 30 min and a total flow rate of 1.3 mL·min^{-1}. The oven was set at a temperature of 30 ºC and the UV detector was set at a wavelength of 210 nm. The injection volume was 10 μL of sample of varying concentrations dissolved in mobile phase B (Di Nicola et al. 2008; Santori et al. 2009).

3.5.2.5 LC Method 3

Method 3 was carried out using the LC-MS instrument. The chromatography used a binary method with acetonitrile as solvent A and 2-propanol as solvent B. The separation was carried out using a binary gradient with a flow rate of 0.15 ml·min^{-1} starting with 90% A and 10% B changing to 90% B in 22 min. An injection volume of 2 μL was used (Lee & Di Gioia 2007).

3.5.2.6 LC Method 4

Method 4 was carried out using the LC-MS instrument. The chromatography used a binary method with acetonitrile as solvent A and 2-propanol as solvent B. The separation was carried out using a binary gradient with a flow rate of 0.15 ml·min^{-1} starting with 90% A and 10% B changing to 70% B in 20 min. An injection volume of 10 μL was used

The calibration was carried out using external standards. UCO has many components and in order to simplify the method it has been assumed that each component of a given species gives a similar mass spectrometric

response. Two calibration standards were used for each of the MG, DG and TG species.

The external standard method was used for the LC-MS calibration. Stock solutions of each component were prepared using 2-propanol as the solvent. Specified volumes were added to a 25 mL volumetric flask and the volume made up using a solvent of acetonitirile:2-propanol (90:10 v/v) which corresponds to the initial conditions for the analysis. 500 μL of this solution was transferred to a 10 mL flask and further diluted with the acetonitrile:2-propanol solvent. This solution was the highest concentration for the calibration curve. A series of 1:1 dilutions were carried out to form a calibration series of 6 standards. An aliquot of each standard was transferred to a 2 mL clear vial for analysis.

The linear portion of the calibration curve was used to determine the calibration constants according to equation 3.10. In theory the intercept should be zero however it was found that this was not the case for all components due to interaction with the solvents. The linear equation used is:

$$a_i = RF_i \times c_i + \text{intercept} \qquad \textbf{(3.10)}$$

Where a_i is the area of component i and c_i is the concentration of component I ($mg \cdot L^{-1}$) and RF_i is the response factor for component i.

In order to prepare the samples a known mass of approximately 0.5 g was added to a 10 mL volumetric flask and diluted using 2-propanol. From there 50 μL of each solution was diluted by 1:100 using the acetonitrile: 2-propanol solution. A portion of this was transferred to a 2 mL vial for analysis. Equation 3.10 was then rearranged in order to calculate the concentration according to equation 3.11.

$$c_i = \frac{a_i - \text{intercept}}{RF_i} \qquad \textbf{(3.11)}$$

This method was selected for monitoring the MG, DG and TG concentrations and the results are discussed in Chapter 7.

3.5.3 Determination of the FFAs Concentration

The FFAs concentration was determined by titration using ASTM D974 (ASTM standard D974-08), specifically developed to determine the acidic or basic constituents of highly coloured oils. In order to determine the acid content 2 ± 0.2 g of sample was dissolved in 100 mL of a solution of toluene:2-propanol:water (100:99:1 v:v:v). The resulting solution was titrated at room temperature using a standardised 0.1 M solution of potassium hydroxide (KOH) in 2-propanol and *p*-naphtholbenzein indicator. A colour change from orange to green indicated that the end point had been reached. The acid value of the oil could then be calculated using equation 3.12.

By assuming that all the acid present in the samples is FFAs it is possible to calculate the wt% of FFAs in the oil using equation 3.13. The calculation to determine the molar concentration of FFAs is shown in equation 3.14.

$$\text{Acid Value, mg KOH/sample} = \frac{[(A - B) \times M \times 56.1]}{W} \quad \textbf{(3.12)}$$

$$\text{FFA wt\%} = \frac{[(A - B) \times M \times 28.2]}{W} \quad \textbf{(3.13)}$$

$$\text{FFA concentration, mol.m}^{-3} = \frac{[(A - B) \times M]}{W} \times \frac{\rho}{1000} \quad \textbf{(3.14)}$$

Where, A is the volume of KOH solution required for the titration and B is the volume of KOH for the blank (mL); M is the molar concentration of the KOH solution; W is the mass of sample (g) and ρ is the density ($g \cdot m^{-3}$).

3.5.4 Determination of Water Concentration

The water content was determined using the Karl Fisher titration method and a Mitsubishi Moisture Meter (CA-20) as the analytical instrument. Hydranal® Coulomat Oil was used as the anode solution and Hydranal® Coulomat GC was used as the cathode solution.

A micropipette was used to add a known mass of sample to the cell. The water content was determined automatically by the cell.

3.5.5 Oil Derivitisation

In order to determine the fatty acid composition of the UCO, a sample of oil was first derivatized. A 100 mg was dissolved in 10 mL hexane and then derivitized using 100 µL of a 2 M potassium hydroxide in methanol solution. Components were mixed using a vortex mixer and then centrifuged. The supernatant was analysed by GC-MS for the FAME composition which could then be used to determine the fatty acid composition.

3.5.6 Measurement of Liquid Bulk Density

The density of the UCO was determined using a pycnometer. A pycnometer is a glass bottle with a close fitting glass stopper with a capillary tube through it to ensure a precise volume is added. Water was used as the reference material to determine the density of the UCO. The pycnometer was filled with deionised water with the volume calculated according to equation 3.15:

$$\text{Volume of water, } V = \frac{m_{H_2O}}{\rho_{H_2O}} \qquad \textbf{(3.15)}$$

Where m_{H2O} is the experimentally determined mass of water and ρ_{H2O} is the density of water. The procedure was repeated for UCO and the mass of sample was experimentally determined. The volume in the pycnometer was

assumed to be the same as the water volume. The density of oil (ρ_L) was then calculated according to equation 3.16:

$$\text{Density of liquid}, \rho_L = \frac{m_L}{\left(m_{H_2O} \times \rho_{H_2O}\right)} \quad \textbf{(3.16)}$$

where m_L is the mass of the liquid sample, UCO (kg).

3.5.7 UCO-Methanol Solubility Analysis

The solubility of methanol in oil was investigated using a similar set up to the batch experiments described in Section 3.4. However a smaller, 100 mL jacked batch reactor was used in place of the 500 mL reactor. A known mass of UCO (approximately 40g) was added to the batch reactor. Once the oil reached 30 °C a known amount of methanol was added in increments using a micropippette. The mixture changed from transparent to cloudy when the saturation point was reached. The temperature was then increased by 10 °C. As the temperature increased, excess methanol dissolved in the UCO and the mixture became transparent. The process was then repeated for the new temperature. The results of this work are reported in Chapter 5.

Chapter 4: Characterisation of Fresh and Used Catalysts

4.1 Introduction

This chapter details the results of the catalyst characterisation, carried out on the catalysts investigated for biodiesel production. The catalysts investigated are Purolite D5082, Novozyme 435 and Amano Lipase PS-IM. Field emission gun – scanning electron microscopy (FEG-SEM), elemental analysis, Fourier transform – infrared (FT-IR), surface area, pore volume, average pore diameter and sodium capacity were used to characterise the fresh and used catalyst samples. In addition a bicinchoninic acid (BCA) assay was carried out on the immobilised enzymes. The true density and particle size distribution of the fresh catalysts was also measured.

Purolite D5082 is a cation exchange resin developed by Purolite International UK Ltd for the esterification pre-treatment of biodiesel. This catalyst has been developed in conjunction with Purolite D5081. Purolite D5081 has been studied in detail by Abidin et al. (2012) and a limited number of experimental results have been presented for comparison. These cation-exchange resins consist of sulphonated polystyrene cross-linked with divinylbenzene (DVB) with sulphonic acid as the cation exchanger (Andrijanto et al. 2012). This catalyst has a high degree of DVB cross-linking and as a result exhibits very little volume change (swelling), has a dense matrix and improved oxidation resistance. Esterification pre-treatment was investigated using Purolite D5082.

Novozyme 435 and Amano Lipase PS-IM are immobilised enzymes and the class of enzymes investigated for biodiesel production are lipases (Souza et al. 2009). Novozyme 435 is supplied by Novozymes UK Ltd and consists of *Candida antarctica* lipase B immobilised on acrylic resin. Amano Lipase PS-IM consists of Amano Lipase PS immobilised on diatomaceous earth. Amano

Lipase is a lipase from *Pseudomanas cepacia*, recently reclassified as *Burkholderia cepacia* (Torres et al. 2008). The catalytic activity of lipases is due to the structure of the polypeptide chains which form a catalytic triad composed of the Serine, Aspartate and Histidine amino acid residues (Orçaire et al. 2006).

A high conversion is possible using Novozyme 435 to catalyse the esterification reaction of material with a high concentration of free fatty acids such as palm fatty acid distillate and soybean oil deodoriser distillate (Talukder et al. 2009; Souza et al. 2009). It was expected that a high conversion would be possible if Novozyme 435 was used for the esterification pre-treatment of UCO. Amano Lipase PS-IM has been shown to be active for the transesterification reaction (Tongboriboon et al. 2010; Li et al. 2011) is comprised of a lipase from *Pseudomanas cepacia* (recently reclassified as *Burkholderia cepacia*) immobilized on diatomaceous earth (Orçaire et al. 2006; Kataoka et al. 2010). Diatomaceous earth is composed of the crushed remains of fossilised algae. It has been shown that Amano Lipase PS-IM gives the highest conversion of the commercially available lipase catalysts for transesterification of vegetable oil and as a result it was investigated for the transesterification reaction of UCO (Tongboriboon et al. 2010).

4.2 Field Emission Gun-Scanning Electron Microscopy (FEG-SEM) Analysis

FEG-SEM images of the fresh catalysts are shown in Figures 4.1 – 4.3. Structural changes to the fresh and used Purolite, D5082 and Novozyme 435 could not be observed using FEG-SEM.

Purolite D5082 and Novozyme 435 are supplied as beads and the surface morphology of a single bead is shown in Figures 4.1(a) and 4.2(a). From this it can be seen that there are differences in the surface morphology with Purolite D5082 having a very smooth surface and very few features in comparison to Novozyme 435 which has a large number of surface features.

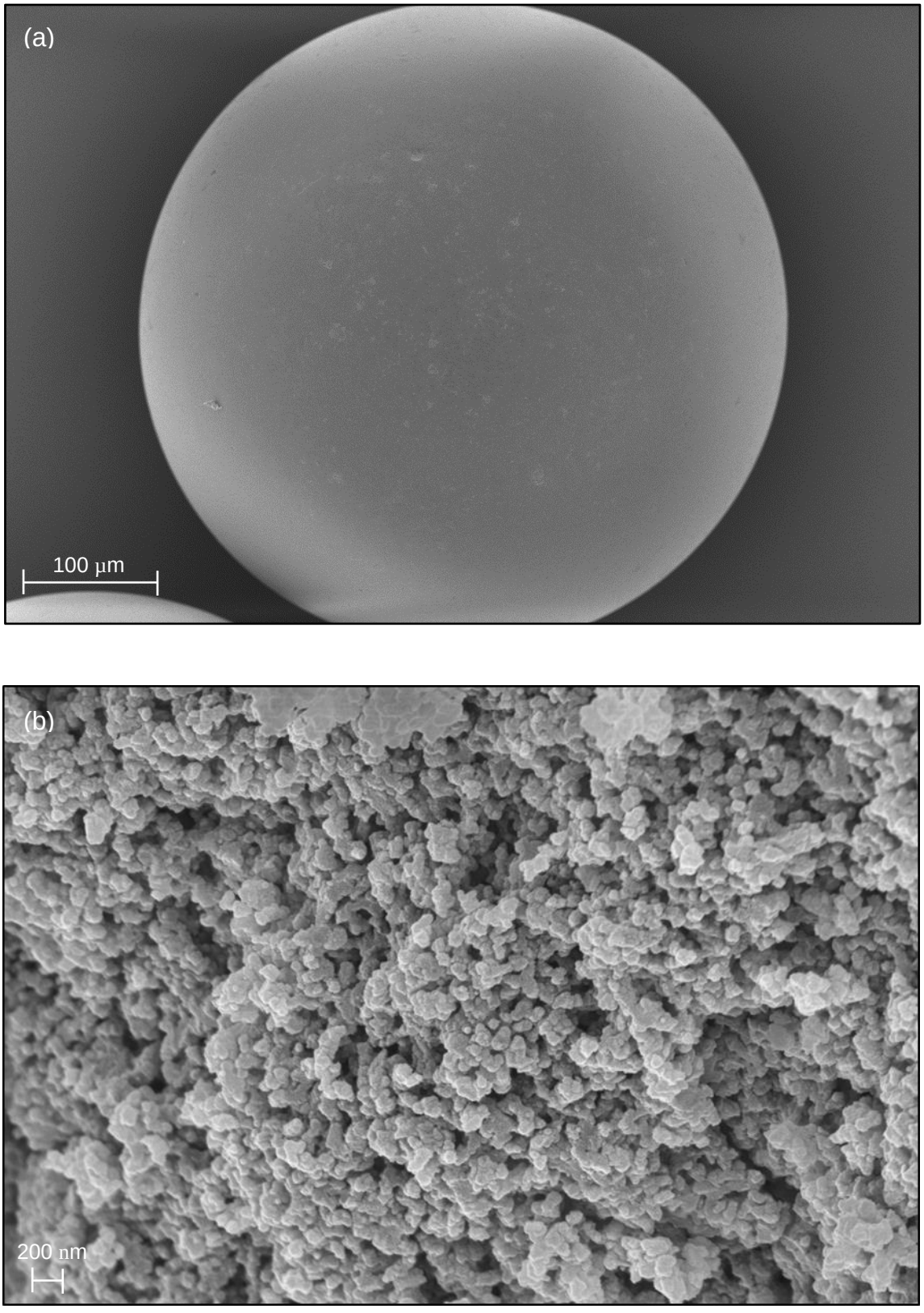

Figure 4.1. The FEG-SEM images of Purolite D5082. Where (a) shows a catalyst bead at a magnification of 450 X and (b) shows a sample of crushed catalyst at a magnification of 50 000 X.

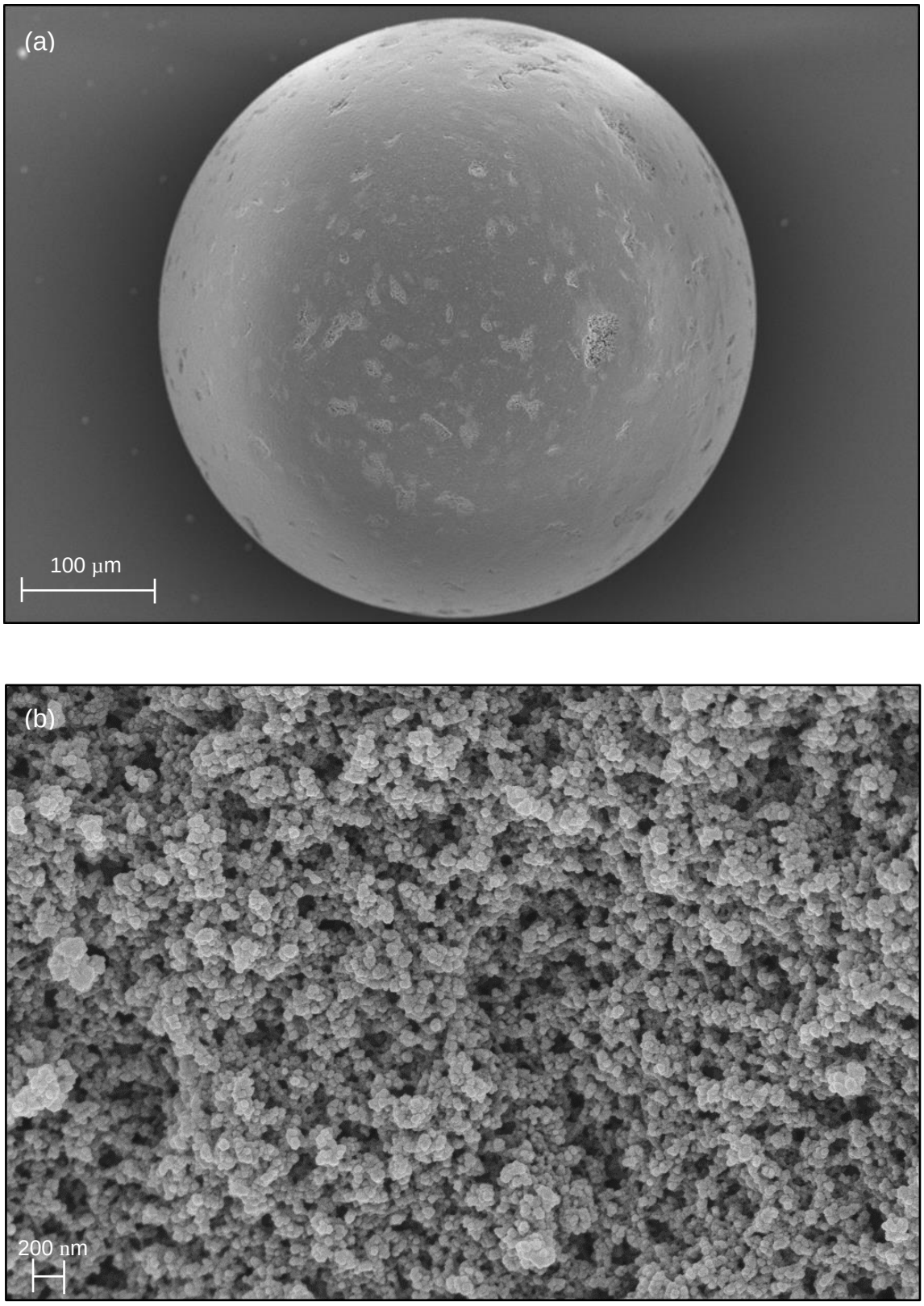

Figure 4.2. The FEG-SEM images of Novozyme 435 with (a) showing a single bead with a magnification of 450 X and image (b) showing a sample of crushed catalyst with a magnification of 50 000 X.

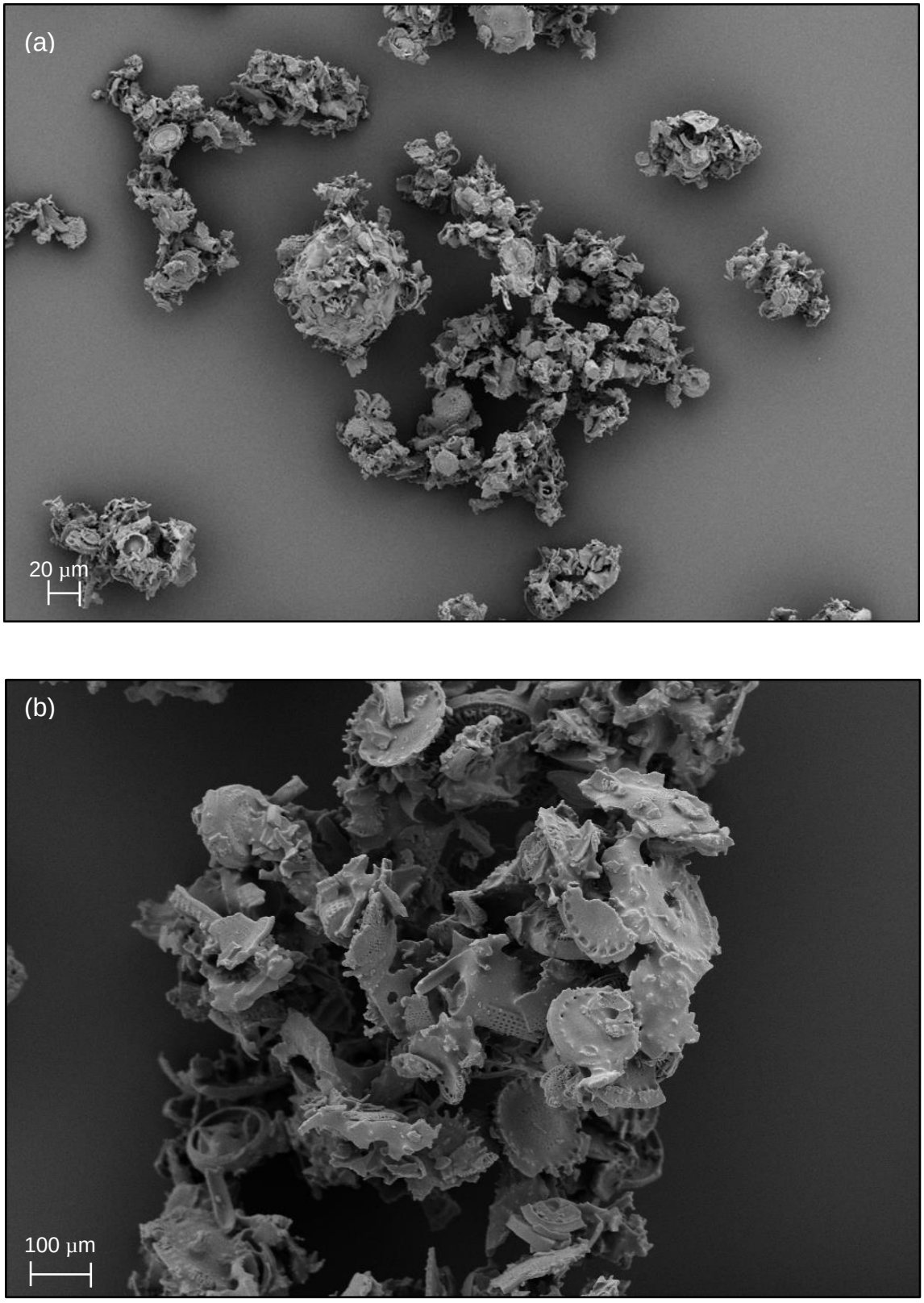

Figure 4.3. FEG-SEM images of Amano Lipase PS-IM with (a) a magnification of 500 X and (b) a magnification of 2000 X.

A sample of Purolite D5082 and Novozyme 435 were crushed in order to view the internal structure of these catalysts and these images are shown in

Figures 4.1(b) and 4.2(b). From this it can be seen that the two catalysts have a very similar structure. Purolite D5081 appears to have the largest spheres, which allow for the formation of the largest pores, which indicates that the internal mass transfer resistance may be lower when compared to Purolite D5082. Novozyme 435 appears to have the most porous internal structure.

Amano Lipase PS-IM was supplied as a powder and the structure of this catalyst at two different magnifications is shown in Figure 4.3. From these data it can be seen that the morphology of this catalyst is very different. Diatomaceous earth is comprised of crushed, fossilised algae and various parts of the algal structure can be seen, particularly in Figure 4.3(b).

4.3 Particle Size Distribution

The cumulative particle size distribution of the fresh catalysts is shown in Figures 4.4 – 4.6. It was observed that the particle size of the catalysts remained similar at the end of the experiments indicating that there was no mechanical damage to the catalyst. It is expected that the particle size distribution will be similar for fresh and used catalyst.

From the data it can be seen that Purolite D5082 and Novozyme 435 have relatively similar average particle sizes with d_{50}'s of 519 and 588 μm (d_{50} is the diameter corresponding to 50 volume % on the relative cumulative particle diameter distribution curve). However Novozyme 435 has a much broader size distribution with a relative span of 0.858 when compared to Purolite D5082 with a relative span of 0.476. In comparison Amano Lipase PS-IM has a much smaller average particle size with a d_{50} of 63.6 μm and the narrowest particle size distribution with a relative span of 1.058.

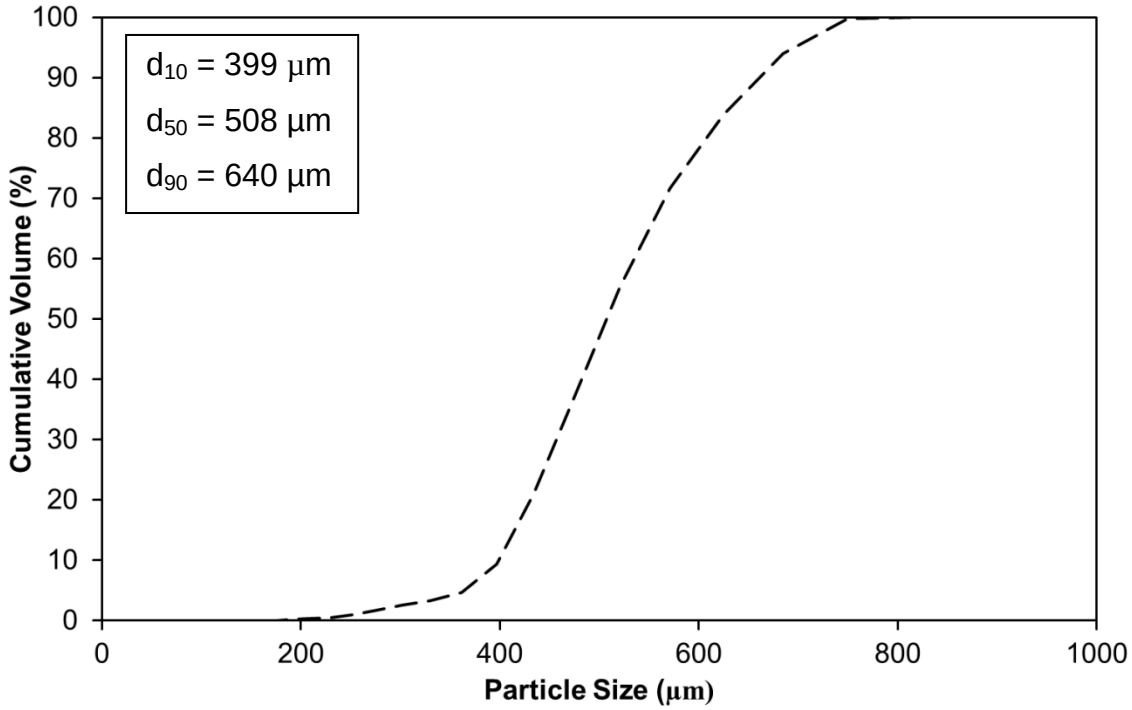

Figure 4.4. The cumulative particle size distribution for Purolite D5082. d_{x0} is the diameter corresponding to x0 volume % on the relative cumulative particle diameter distribution curve.

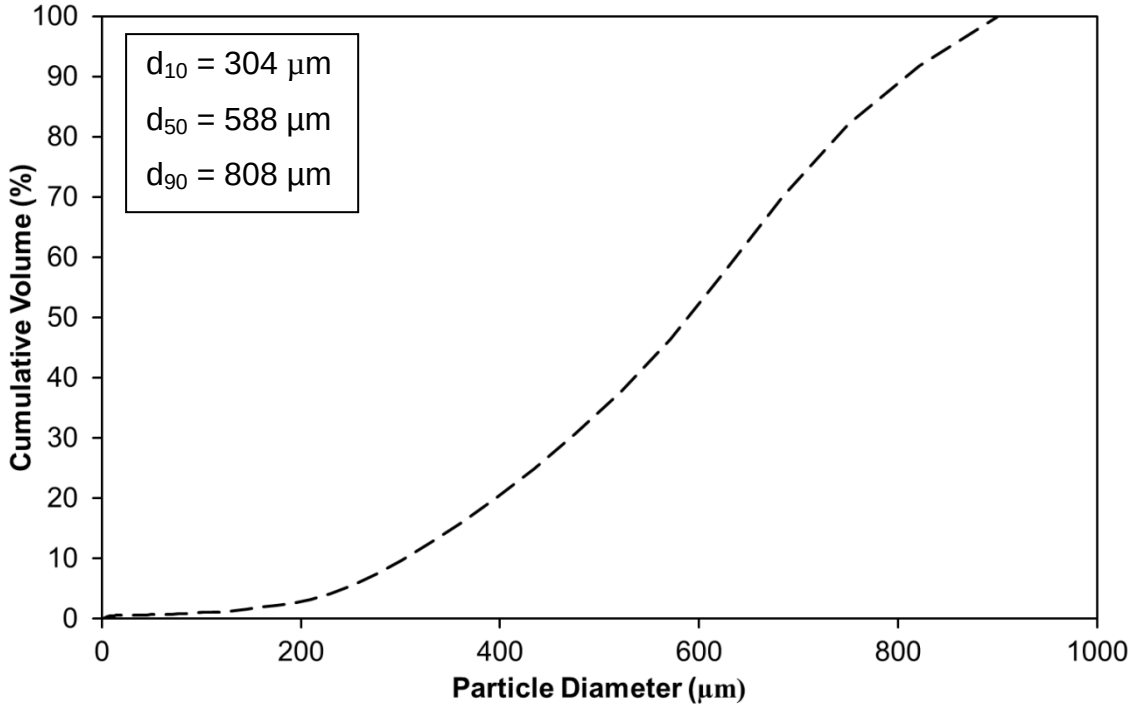

Figure 4.5. The cumulative particle size distribution for Novozyme 435. d_{x0} is the diameter corresponding to x0 volume % on the relative cumulative particle diameter distribution curve.

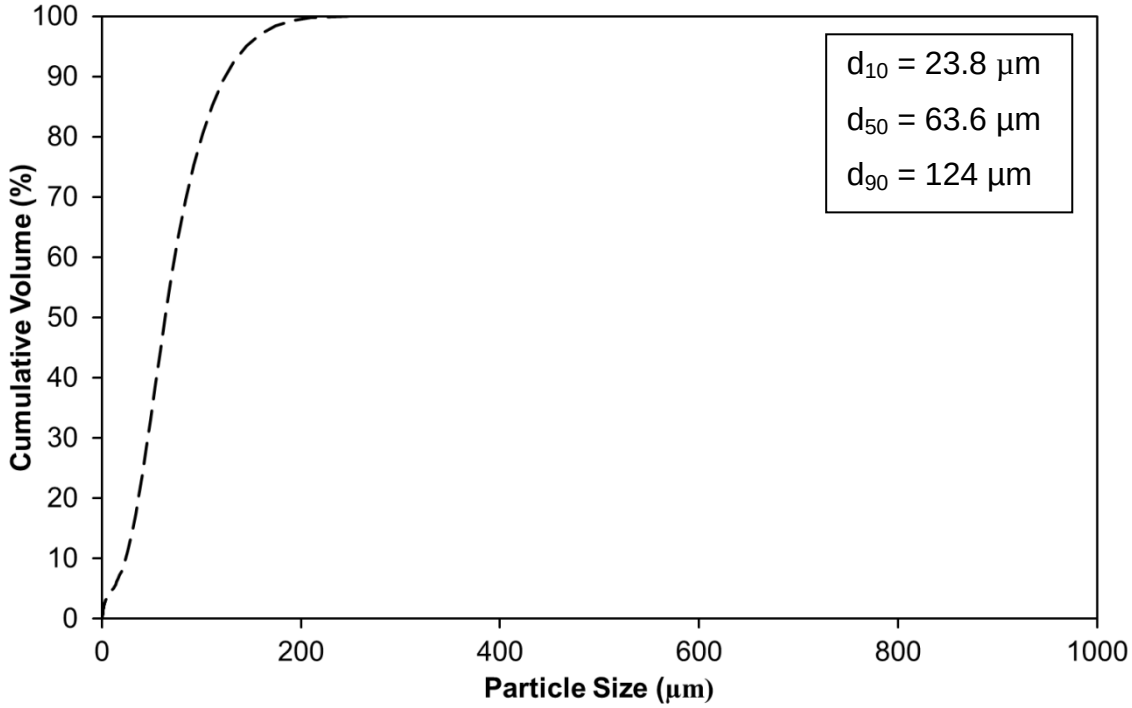

Figure 4.6. The cumulative particle size distribution for Amano Lipase PS-IM. d_{x0} is the diameter corresponding to x0 volume % on the relative cumulative particle diameter distribution curve.

4.4 Surface Area, Pore Volume and Average Pore Diameter

The surface area, pore volume and average pore diameter has been compared for the fresh and used catalysts and the results are given in Table 4.1. These measurements are useful for developing an understanding of the number of active catalytic sites which can be reached by the reagents.

Novozyme 435 has the largest pores and total pore volume. Amano Lipase PS-IM is a fine powder and there are no measurable pores. Purolite D5082 has the largest surface area followed by Novozyme 435 while Amano Lipase PS-IM has a substantially smaller Brunauer-Emmett-Teller (BET) surface area. A substantial portion of the surface areas for porous catalysts is due to the internal surface area and the small surface area for Amano Lipase PS-IM can be attributed to the lack of measurable pores.

The reusability of Purolite D5082 was investigated by comparing the effect of washing with methanol in an ultrasonic bath only and using sulphuric acid to regenerate the catalyst, as detailed in Chapter 3, Section 3.4.1.1. Purolite D5082, Fresh and Cycle 2 were washed with methanol and Purolite D5082, Cycle 1-2, Cycle 2-2 and Cycle 3 were regenerated using sulphuric acid. The fresh catalyst has the largest surface area, with a steady decrease after each reusability cycle. In addition it can be seen that there is a slight increase in the pore diameter after each use with a corresponding increase in the total pore volume. These data indicate that there are changes to the structural properties after each cycle however differences as a result of the two cleaning regimes is negligible.

In terms of Novozyme 435 it can be seen that the BET surface area and total pore volume have increased for the fresh catalyst when compared to Cycle 2, while the average pore diameter has decreased by approximately 12%. This suggests that there has been some damage to the surface area during use which has resulted in the formation of additional smaller pores. The reduction in pore diameter could also be due to pore blockage.

Table 4.1. Surface area, pore volume and average pore diameter

Catalyst	BET Surface Area ($m^2.g^{-1}$)	Average Pore Diameter (nm)	Total Pore Volume ($cm^3.g^{-1}$)
Purolite D5082, Fresh	483	3.13	0.240
Purolite D5082, Cycle 1-2	526	3.33	0.303
Purolite D5082, Cycle 2	464	3.31	0.263
Purolite D5082, Cycle 2-2	474	3.41	0.292
Purolite D5082, Cycle 3	461	3.40	0.274
Novozyme 435, Fresh	81.6	17.7	0.449
Novozyme 435, Cycle 2	116	15.5	0.533
Amano Lipase PS-IM	0.0717	n/a	n/a

4.5 True Density and Porosity

The true density of the catalysts is given in Table 4.2. The true density was determined using gas pycnometry (Chapter 3, Section 3.3.4). The porosity was calculated using the true density and the pore volume, Section 4.4. From these data it can be seen that Novozyme 435 has the lowest density while

Amano Lipase PS-IM has the highest true density. Srivastava & Albertsson (2005) reported a bulk density of 0.43 $g \cdot cm^{-3}$ for Novozyme 435. The bulk density is expected to be lower than the true density because bulk density applies to the packing of beads and thus incorporates air.

Amano Lipase PS-IM has no measurable pores and as a result the porosity is zero. The porosity of Purolite D5082 is greater than Novozyme 435. The porosity for Novozyme 435 and Purolite D5082 are similar with Purolite D5082 having a slightly larger value.

Table 4.2. True density of the fresh catalysts

Catalyst	True Density ($g.cm^{-3}$)	Porosity (-)
Purolite D5082	1.39	0.354
Novozyme 435	1.22	0.250
Amano Lipase PS-IM	2.24	0

4.6 Elemental Analysis

The elemental analysis was used to investigate the elemental composition of the catalysts and to determine if this changed when the catalyst was used for biodiesel production. The results of the elemental analysis are given in Table 4.3.

From these data it can be seen that the Purolite D5082 samples contain a trace amount of nitrogen although this is not typical of the chemical structure. The levels is low (<1%) and it has been assumed that this is a contaminant in the sample. The percentage nitrogen appears to be increasing with reusability cycles however this can be attributed to the decrease in sulphur. The changes in carbon, hydrogen and oxygen are relatively small and have been attributed to experimental error. There is a drop in the percentage sulphur with a drop of 2% after the first cycle and 8% after the second cycle. It was expected that there would be a loss of sulphur after the first cycle because this type of catalyst has been shown to leach sulphur (Abidin et al. 2012). After the second cycle the catalyst was left in sulphuric acid overnight in order to regenerate the catalyst.

The decrease in percentage sulphur indicates that the catalyst was not regenerated.

From the data in Table 4.3 it can be seen that Novozyme 435 contains nitrogen. In this case it is expected because lipases are composed of a long chain of amino acids which include nitrogen as part of the chemical structure. The elemental composition for the used catalyst remains approximately constant and changes in the catalytic activity cannot be attributed to a single element.

Table 4.3. The elemental analysis data for the fresh and used catalysts

Catalyst	wt% C	wt% H	wt% S	wt% N	wt% O*
Purolite D5082, Fresh	64.27	5.13	5.17	0.09	25.36
Purolite D5082, Cycle 2	64.05	5.11	5.04	0.10	25.71
Purolite D5082, Cycle 3	64.47	5.17	4.67	0.12	25.58
Novozyme 435, Fresh	68.53	8.14	n/a	1.31	22.02
Novozyme 435, Cycle 2	68.98	8.15	n/a	1.23	21.64
Novozyme 435, Cycle 3	68.14	8.11	n/a	1.35	22.41
Amano lipase PS-IM	4.50	0.65	n/a	0.19	n/a

* Oxygen by difference

The percentage carbon, hydrogen and nitrogen are low for Amano Lipase PS-IM however this catalyst is immobilised on diatomaceous earth which is comprised mainly of silica and alumina (Korunic 1998). In this case the percentage carbon, hydrogen and nitrogen can be attributed to the lipase with the remaining elemental composition being silicon and aluminium from the diatomaceous earth support and oxygen from both the support and the lipase.

4.7 Fourier Transform-Infra Red Measurements

Fourier transform-infra red (FT-IR) measurements were used to investigate the functional groups present on the various catalysts and to determine if changes could be observed on used catalyst samples.

The infrared absorbance spectra for Purolite D5082 Fresh and used are given in Figures 4.7-4.9. From these spectra it can be seen that all the Purolite D5082 samples have peaks at the same wavenumbers indicating that the same

functional groups are present. The infrared wavenumber assignments for Purolite D5082 are summarised in Table 4.4 (Stuart 2004; Smith 1999).

Table 4.4. The infrared wavenumber assignment for Purolite D5082

Wavenumber (cm^{-1})	Assignment
3461-3430	O-H stretching vibration of hygroscopic water
2924	C-H_2 stretching vibration (asymmetric)
2853	C-H_2 stretching vibration (symmetric)
2362-2332	Atmospheric CO_2
1631 - 1629	C=C aromatic stretch and C-H deformation and skeletal vibrations in DVB
1449 - 1442	C-CH_3 bending vibration (asymmetric)
1224 – 1215	SO_3^- stretching vibrations (asymmetric)
1185 - 1020	SO3- stretching vibrations (symmetric) (Singare et al. 2011)
902-671	C-H out-of-plane deformation vibrations of monosubstituted and disubstituted benzene rings

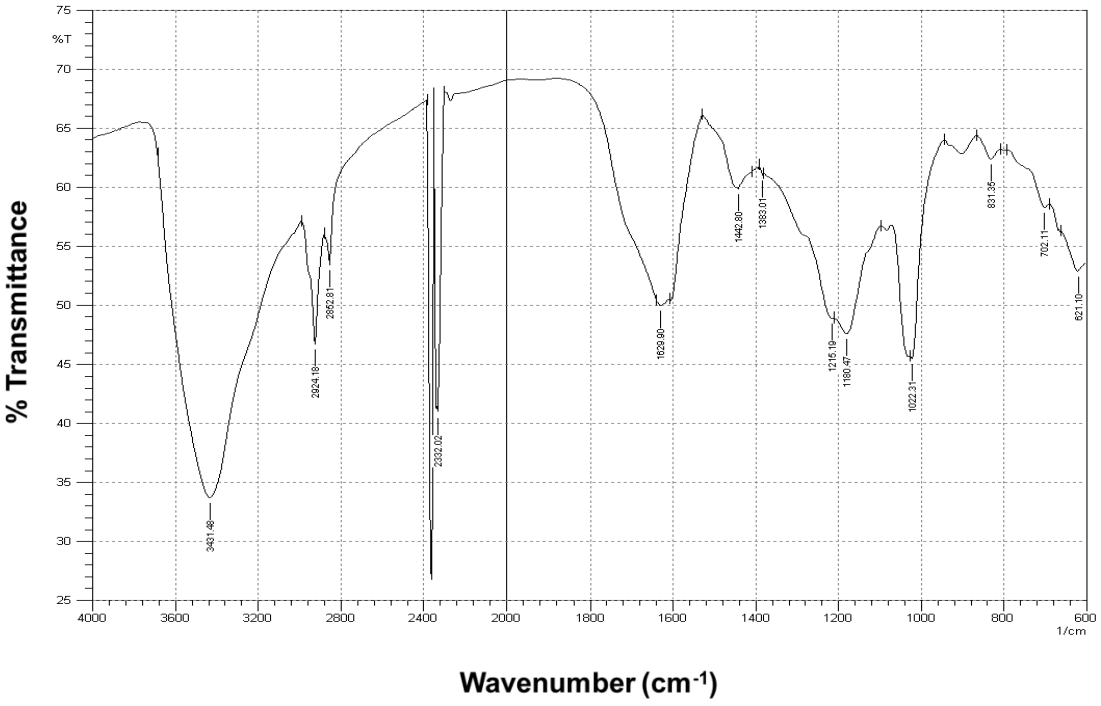

Figure 4.7. The infrared absorbance spectrum of Purolite D5082, Fresh.

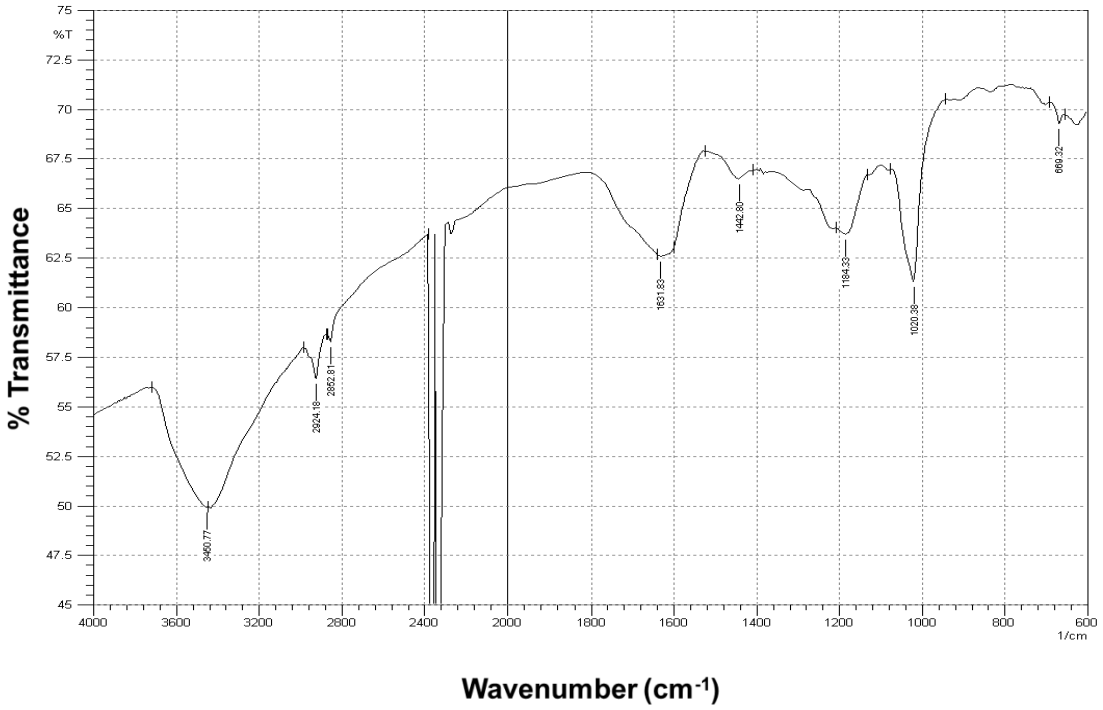

Figure 4.8. The FT-IR absorbance spectrum of Purolite D5082, Cycle 2.

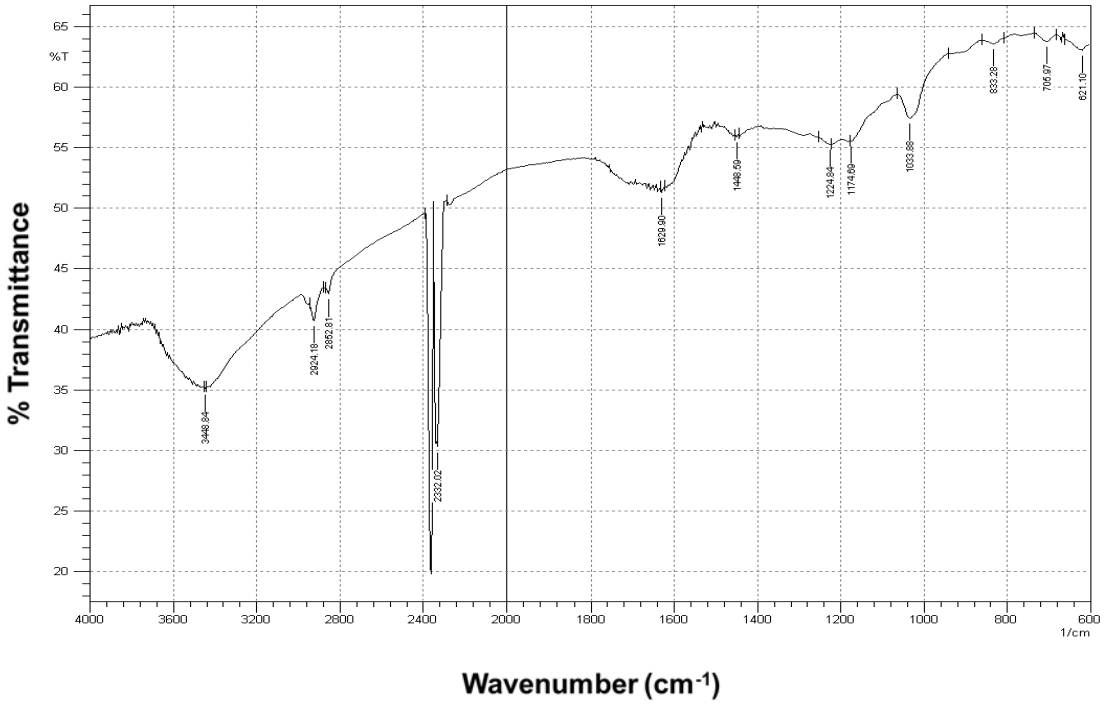

Figure 4.9. The infrared absorbance spectrum of Purolite D5082. Cycle 3.

The infrared absorbance spectra for Novozyme 435 are given in Figures 4.10 and 4.11, and the infrared wavenumber assignments are given in Table

4.5. Novozyme 435 consists of *Candida antarctica* lipase B immobilised on acrylic resin and as a result is expected that the spectra will consist of the sum of the spectra for the lipase and the acrylic resin. Given the complex nature of the sample it has been found that some of the peaks could be attributed to more than one functional group and where appropriate more than one assignment has been listed.

From Figures 4.10 and 4.11 it can be seen that the spectra for the fresh and used catalyst are very similar with both catalysts having peaks for the same wavenumbers. This indicates that there are no significant changes to the structure after a single use.

Table 4.5. The infrared wavenumber assignment for Novozyme 435

Wavenumber (cm^{-1})	**Assignment**
3435-3389	N-H stretching
2951	C-H_2 stretching vibration (asymmetric)
2362-2332	Combination C-H stretching and atmospheric CO_2
1730-1713	C=O stretching
1659-1656	80% C=O stretching, 10% C-N stretching and 10% N-H bending (Stuart 2004)
1546-1512	60% N-H bending and 40% C-N stretching (Stuart 2004)
1452	CH_3 bending (asymmetric)
1385	C-H bending (symmetrical)
1269	O-H bending, C-C-O stretching
1196	C-N stretching
1147-1143	C-N stretching and C-O-C bending
991 - 704	C-H out-of-plane deformation vibrations of mono- and disubstituted benzene rings

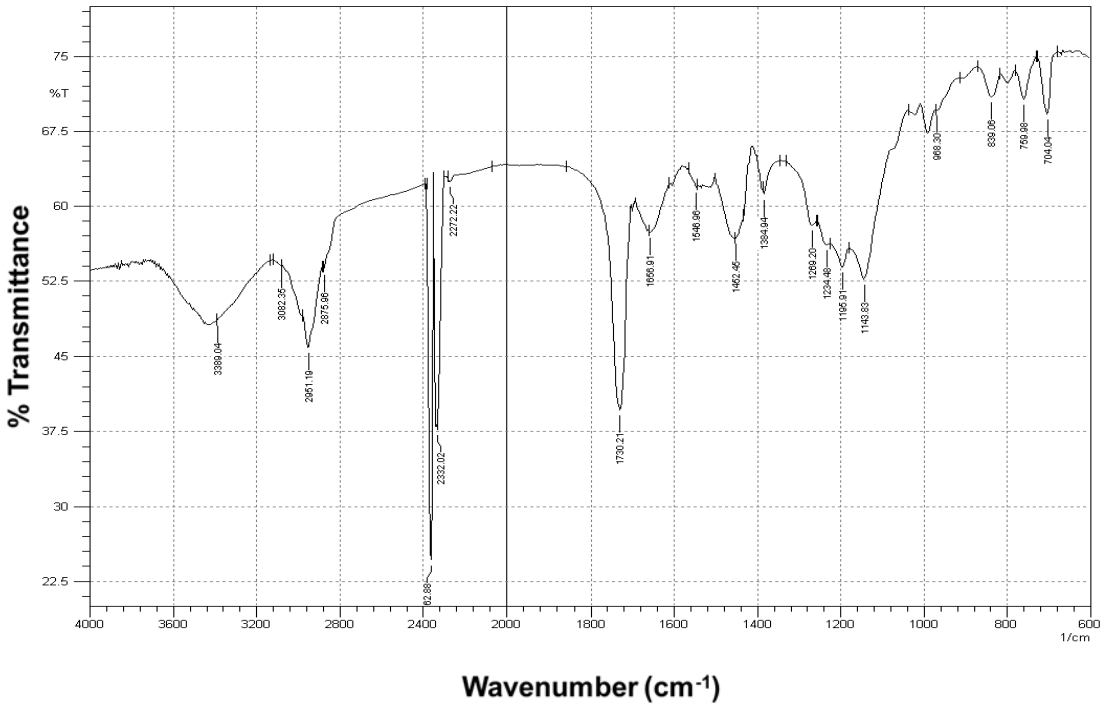

Figure 4.10. The infrared absorbance spectrum of Novozyme 435, Fresh.

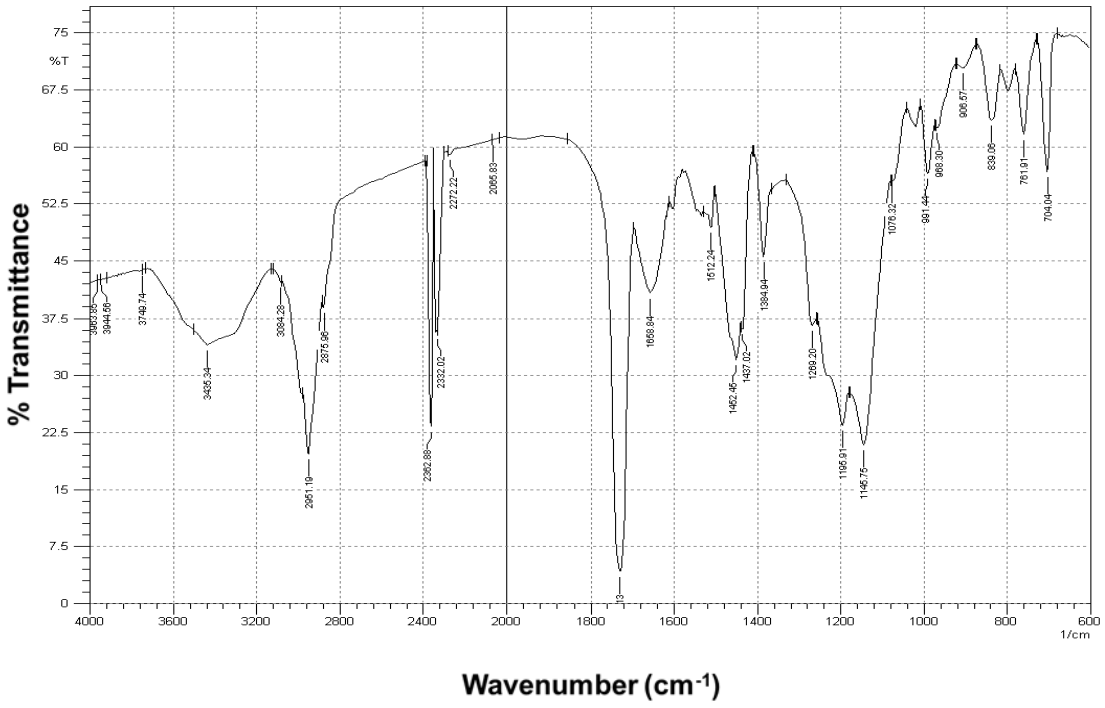

Figure 4.11. The infrared absorbance spectrum of Novozyme 435, Cycle 2.

The spectra for Amano Lipase PS-IM is given in Figure 4.12 and the wavenumber assignment is given in Table 4.6. In this case it is expected that

the spectrum is a sum of the lipase and the diatomaceous earth components. Due to the complex nature of the sample it is possible to assign more than one function group to a peak. In particular it is expected that the peak with a wavenumber of 1086 cm^{-1} represents the sum of numerous functional groups because this peak is large and broad.

Table 4.6. The infrared wavenumber assignment for Amano Lipase PS-IM

Wavenumber (cm^{-1})	Assignment
3416	N-H stretching
2930	C-H_2 stretching vibration (asymmetric)
1881	C=O stretch (symmetric)
1641	80% C=O stretching, 10% C-N stretching and 10% N-H bending (Stuart 2004)
1086	Si-O-Si stretch (asymmetric) Si-O silanol stretch C-H bending (symmetrical) O-H bending C-N stretching C-H stretching in aliphatic and aromatic compounds
793	Si-O-Si stretch (symmetric) N-H stretching
617	C=O bending

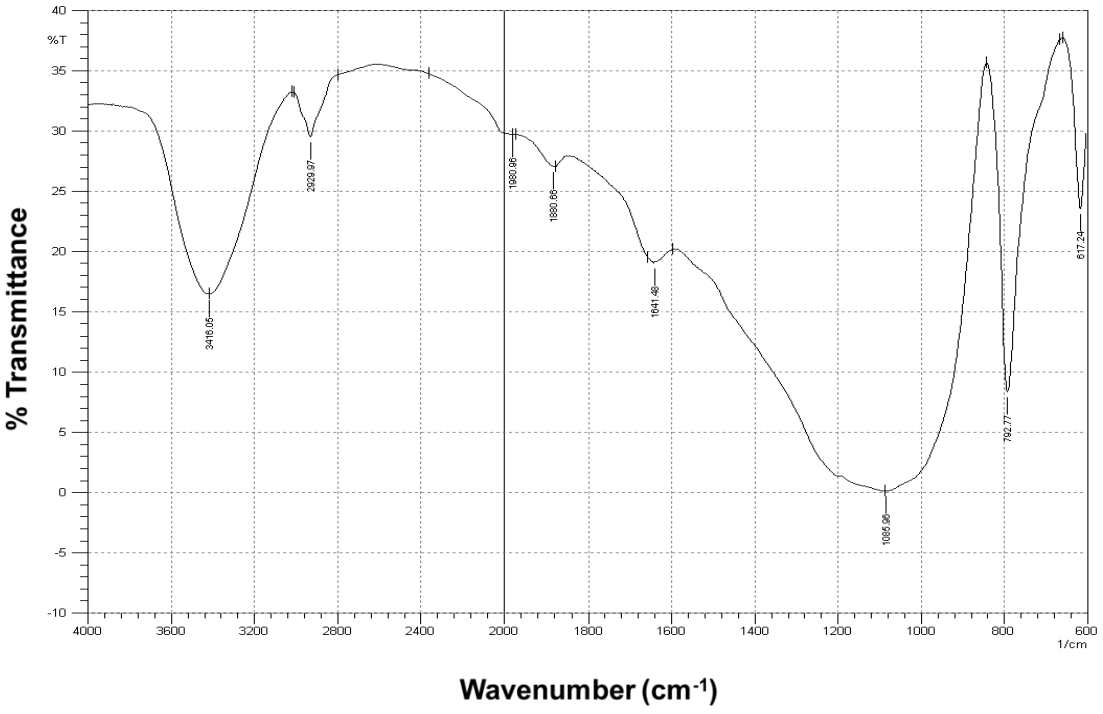

Figure 4.12. The infrared absorbance spectrum of Amano Lipase PS-IM.

4.8 Sodium Capacity

Sodium capacity is a measure of the ion-exchange capacity of solids. The sodium capacity of the fresh and used catalysts is given in Table 4.7. From the data it can be seen that the ion-exchange resin catalyst, Purolite D5082 has the highest sodium capacity.

From these data it can be seen that there is a decrease in the sodium capacity of Purolite D5082, Cycle 2 when compared to Purolite D5082, Fresh. Purolite D5082, Cycle 2 was washed in methanol and it can be seen that there is also a decrease in the percentage sulphur, Section 4.6 and this corresponds with previous findings showing sulphur leaching (Abidin et al. 2012; Andrijanto et al. 2012). Purolite D5082, Cycle 2-2 and Purolite D5082, Cycle 3 were both regenerated using sulphuric acid and have a higher sodium capacity than fresh Purolite D5082. These catalysts were washed extensively with water in order to remove the sulphuric acid. However the increase in sodium capacity indicates that some sulphuric acid remained in the pores of the catalyst.

The sodium capacity of the immobilised enzymes is lower than the ion-exchange resin however the catalytic action of enzymes is based on specific structural properties and is not dependant on the sodium capacity. Novozyme 435, Fresh and Amano Lipase PS-IM have similar acid capacities. There is a reduction in the sodium capacity of the used Novozyme 435 suggesting there is a loss of enzyme during the reaction.

Table 4.7. The sodium capacity of fresh and selected used catalyst

Catalyst	Sodium Capacity (mmol·g^{-1})
Purolite D5081, Fresh	1.82
Purolite D5082, Cycle 2	1.72
Purolite D5082, Cycle 2-2	2.73
Purolite D5082, Cycle 3	2.56
Novozyme 435, Fresh	0.436
Novozyme 435, Cycle 2	0.189
Amano Lipase PS-IM	0.330

4.9 BCA Assay

The results of the BCA Assay are shown in Table 4.8. From these data it can be seen that the initial protein loading on the fresh Novozyme 435 is much higher than Amano Lipase PS-IM.

In the case of Novozyme 435 it can be seen that there is a substantial reduction in the amount of immobilised protein after the first cycle. The amount of protein lost in subsequent samples is considerably smaller.

Table 4.8. Results of the BCA Assay

Catalyst	Mass of immobilised enzyme ($mg \cdot g^{-1}$ support)
Fresh Amano Lipase PS-IM	20.68
Fresh Novozyme 435	39.47
Novozyme 435, after Cycle 1	7.16
Novozyme 435, after Cycle 3	6.84

4.10 Conclusions

Three catalysts, investigated for biodiesel production, have been characterised and they are Purolite D5082, Novozyme 435 and Amano Lipase PS-IM. The physical properties have been characterised using FEG-SEM, surface area, pore volume and diameter measurements, true density and porosity. The chemical properties have been characterised using elemental analysis, FTIR measurements and sodium capacity. In addition the immobilised enzymes have been characterised using a BCA assay.

From the FEG-SEM it could be seen that Purolite D5082 and Novozyme 435 have similar internal and external structures as both catalysts are porous beads. In contrast Amano Lipase PS-IM is immobilised on diatomaceous earth and part of the algal structure could be observed. This fits with the results of the particle size distribution measurements which showed that Purolite D5082 and Novozyme 435 had similar average sizes while the average particle size for Amano Lipase PS-IM was considerably smaller.

It was found that Purolite D5082 has the largest BET surface area followed by Novozyme 435 and then Amano Lipase PS-IM which had a much smaller BET surface area. In addition Novozyme 435 has the largest pores and total pore volume while Amano Lipase PS-IM has no measurable pores.

From the elemental analysis it could be seen that with Purolite D5082 there was a reduction in the percentage sulphur which would lead to a reduction in catalytic activity. It was found that the sodium capacity of used Purolite D5082 was higher than the fresh, indicating that some of the sulphuric acid used to regenerate the catalyst remained behind in the pores. This sulphuric acid would have been removed when samples of catalyst were crushed and dried prior to elemental analysis.

The catalytic activity of Novozyme 435 is due to structural properties of the lipase and as result changes to the catalytic activity cannot be attributed to a single element or functional group. The BCA assay showed a loss of protein after one use and this could explain the reduction in catalytic activity and the reduction in sodium capacity although the sodium capacity may not be a direct measure of catalytic activity.

Significant differences in the chemical structure of the three catalysts could be observed using FT-IR. However changes to the functional groups could not be observed with FT-IR.

Chapter 5: Used Cooking Oil Characterisation and Batch Experiment Reproducibility

5.1 Introduction

Key aspects relating to the development of the experimental procedures are discussed in this chapter. The results of the used cooking oil (UCO) characterisation are discussed in Section 5.2. This is followed by a discussion of the various sampling procedures for the experiments including why it was necessary and how this would have affected reproducibility in Section 5.3.

5.2 UCO Characterisation

Various methods have been used to characterise the UCO and the results are given in Table 5.1. From these data it can be seen that the UCO is composed mainly of triglycerides (TG), however water is usually introduced as part of the cooking process leading to hydrolysis of the TGs to form diglycerides (DG), monoglycerides (MG), free fatty acids (FFAs) and fatty acid methyl esters (FAME) as a result of the cooking process.

Due to the complex composition of the oil there are a number of methods available to express the molar mass which can be used to calculate the mole ratio. A common method for determining the oil composition is to convert all the lipid components to FAME using a sodium hydroxide derivitisation method, Chapter 3, Section 3.5.5. The FAMEs can readily be separated and quantified by GC-MS although the results are generally expressed in terms of the fatty acid composition. The fatty acid composition varies depending on the type of vegetable oil and the UCO used for this work has a similar composition to soybean oil (Akoh et al. 2007).

The fatty acid composition can be used to estimate a molar mass by assuming the oil is comprised totally of FFAs. This information combined with the FFA% was used to calculate the mole ratio for esterification. Alternatively it could be assumed that the oil is comprised of just triglycerides. In this case the average FFAs molar mass can be combined with the glycerol components to calculate the average molar mass of triglycerides. This molar mass was used to calculate the mole ratio for the transesterification experiments.

Table 5.1. Results of the UCO characterisation

Property	Value
Fatty Acid Composition (wt%)	
Linoleic acid	43
Oleic acid	36
Palmitic acid	13
Stearic acid	3.8
Linolenic acid	3.6
Molar Mass, average FFAs ($g \cdot mol^{-1}$)	278.0
Molar Mass, average TGs ($g \cdot mol^{-1}$)	867.4
FAME Concentration ($mol \cdot m^{-3}$)	17.42
FFA (%wt/wt)	8.42
Acid Value (mg $KOH \cdot g^{-1}$)	16.6
Water (%wt/wt)	0.531
TG concentration (%)	84
DG concentration (%)	7.0
MG concentration (%)	0.3
Density ($kg \cdot m^{-3}$)	924

5.3 Solubility of Methanol in Oil

Methanol has been used as the reagent to convert UCO to biodiesel. The UCO for these experiments is a translucent, dark brown liquid; a typical example is the UCO rich layer shown in Figure 5.2. Methanol and vegetable oil are sparingly soluble leading to the formation of an emulsion when sufficient

methanol is added. Heterogeneous catalysts are being used to investigate the production of biodiesel and this means that depending on the amount of methanol added this leads to the formation of a two or three phase system. This can lead to poor contacting between the phases and affect the extent of conversion. A co-solvent can be used to improve contacting (Talukder et al. 2009; Su & Wei 2008) and thus conversion however heterogeneous catalysts are being investigated to simplify product recovery. In addition it can be more difficult to take a representative sample when an emulsion is formed

The solubility of methanol in oil has been investigated and the solubility curve is given in Figure 5.1. The solubility experiment was carried out in triplicate. A temperature range of 30 – 60 °C was used because this was the expected temperature range for the experiments. The methanol concentration has been expressed as a mole ratio, rather than the conventional mass concentration, because mole ratio is the measure used for the experiments, and these units have been deemed more useful.

From Figure 5.1 it can be seen that the solubility of methanol in UCO at 60 °C corresponds to a methanol to FFA mole ratio of 22:1 and a concentration of 0.17 $g \cdot g^{-1}$. This is substantially higher than the solubility of methanol in *Jatropha curcas* oil reported by Y. Liu et al. (2009) as 0.070 $g \cdot g^{-1}$ at 60 °C and a value of 0.075 $g \cdot g^{-1}$ reported by Zhou et al. (2006). In contrast Shimada et al. (2002) found that the solubility of methanol in vegetable oil (a mixture of soybean and rapeseed) corresponds to a mole ratio of 23:1. The composition of UCO in this study has a similar composition to soybean oil. These data indicate that there is substantial variation of methanol solubility in vegetable oils.

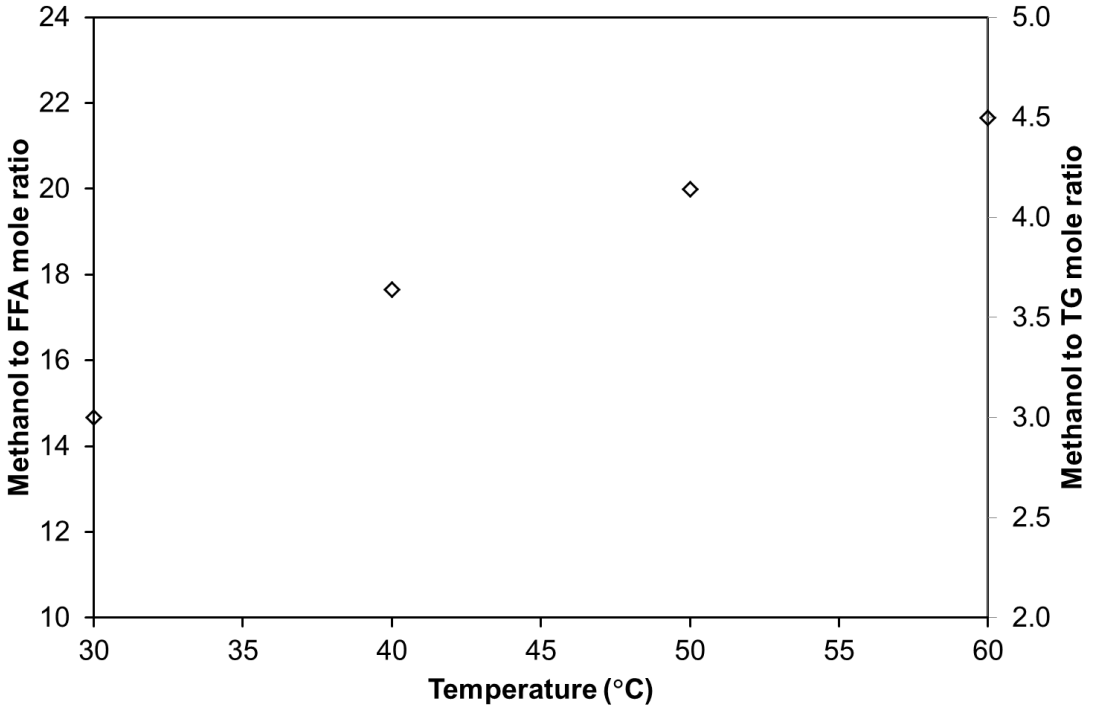

Figure 5.1. The solubility curve for methanol in UCO.

5.4 Batch Experiment Reproducibility

There are a number of factors which affect experimental reproducibility with the most significant factor being the instrument used for the analysis, followed by the experimental protocol and then the skill of the person carrying out the work. A number of figures have been presented in this section in order to discuss and compare reproducibility of the different experiment types. A more detailed discussion of the results in terms of conversion is presented in the relevant sections later in the thesis.

5.4.1 Reproducibility of the Experiments Catalysed by the Ion-exchange Resin, Purolite D5082

The experiments using the ion-exchange resin, Purolite D5082, were carried out using relatively high mole ratios (an optimum conditions 83 g of methanol was mixed with 180 g of UCO) leading to the formation of a pale yellow emulsion. An example of the final reaction product is shown in Figure 5.2. Methanol has a lower specific gravity when compared to UCO and as a

result the top layer contains mostly methanol with a trace of water and glycerol. In comparison the non-polar components can be found in the UCO rich layer.

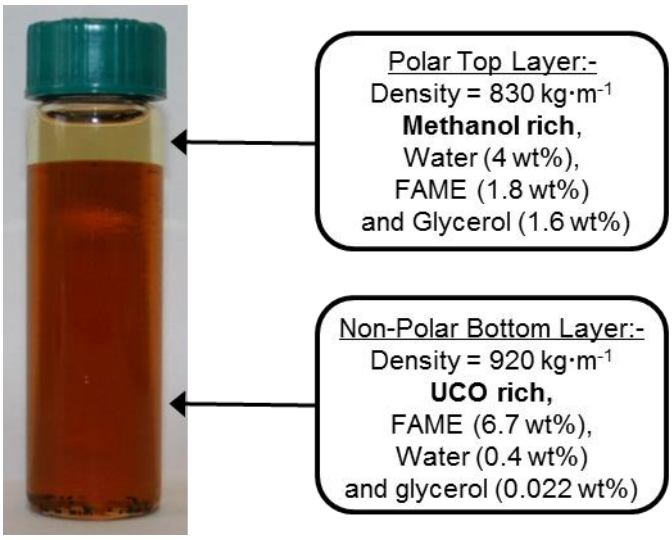

Figure 5.2. An example of the reaction product composition when Purolite D5082 is used as the catalyst.

The progress of esterification using Purolite D5082 was monitored primarily using a titration to determine the FFAs concentration. A relatively large sample of (2.00 ± 0.20) g was used for the analysis. Three experiments were carried out at the optimum conditions in order to investigate reproducibility. The result of these experiments is shown in Figure 5.3. From these data it can be seen that the largest error is at 80 min where the difference is 9% however overall the difference between the highest and lowest value is within 5.5%. This shows there is reasonably good reproducibility from this type of experiment and analysis. In this case the sample size was large enough to minimise errors associated with getting a representative sample from an emulsion. It was assumed that a similar error applied to the FFAs conversion for all esterification reactions catalysed by Purolite D5082.

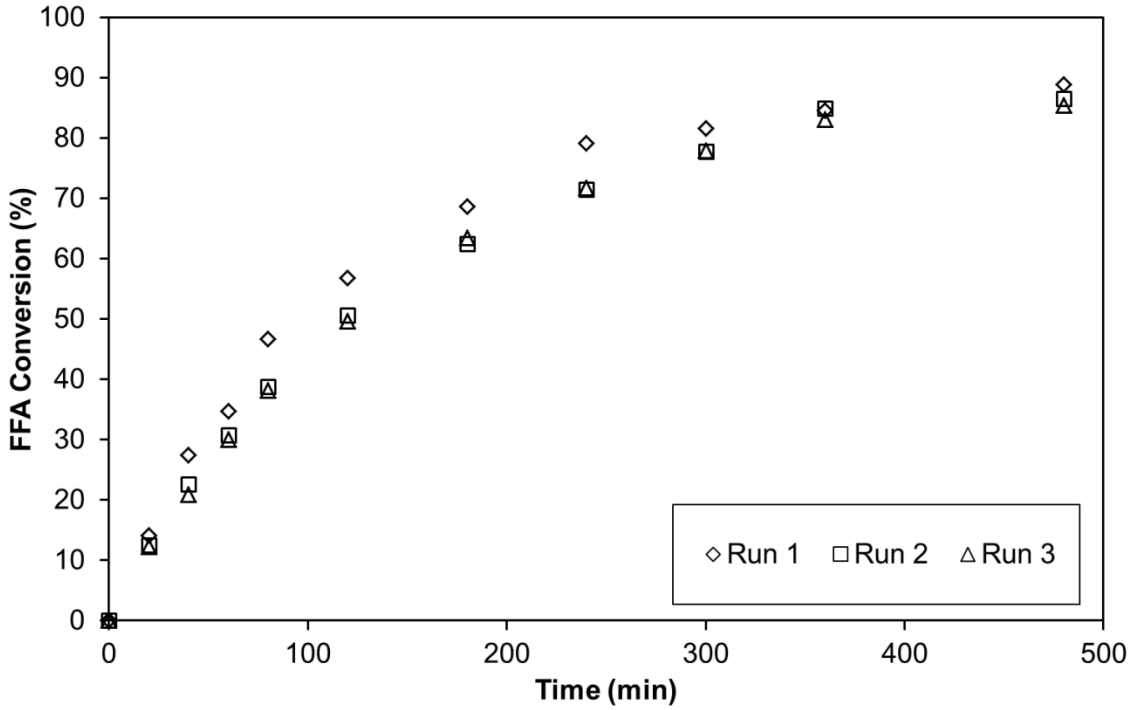

Figure 5.3. Investigation of the reproducibility of the FFA conversion results for the ion-exchange resin catalysts. (With a temperature of 60 °C, Purolite D5082 as the catalyst with a loading of 5 wt%, a methanol to FFA mole ratio of 62:1 and a stirrer speed of 450 rpm)

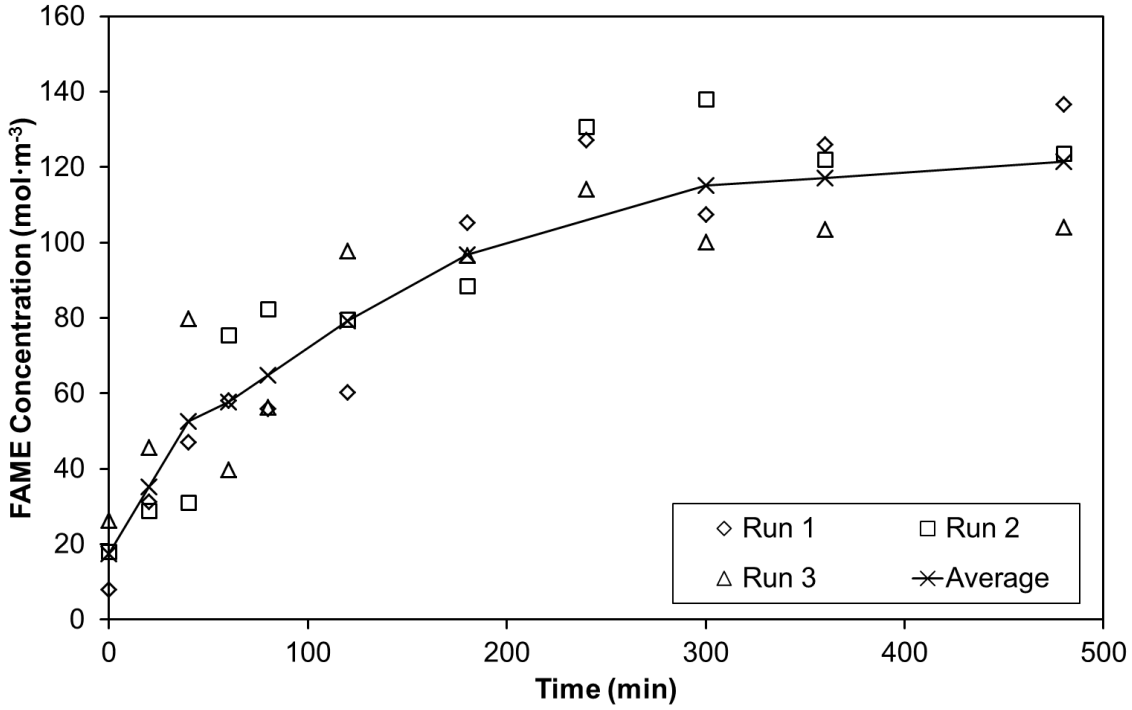

Figure 5.4. Investigation of the reproducibility of the FAME concentration results for Purolite D5082. (With a temperature of 60 °C, a catalyst loading of 5 wt%, a methanol to FFA mole ratio of 62:1 and a stirrer speed of 450 rpm)

The FAME concentration was also determined for these experiments and the results are shown in Figure 5.4. From Figure 5.4 it can be seen that the data are more scattered than the FFA conversion data. The FAME concentration has been analysed by GCMS and a single drop with a weight of approximately 0.01g is sufficient for the analysis. It is difficult to ensure that a single drop is a representative sample, particularly when the reaction mixture forms an emulsion. In addition there will be a larger error from weighing when compared to the FFA titration samples. It can be seen that when the analysis is carried out in triplicate it is possible to obtain a reasonable trend as this compensates for the difficulties getting a representative sample.

5.4.2 Reproducibility of the Experiments Catalysed by Novozyme 435

The experiments carried out using Novozyme 435 used the lowest mole ratios (at optimum conditions 12 g of methanol was mixed with 263 g of UCO) and at the reaction temperature the methanol was fully dissolved in the oil. An example of the final reaction product is shown in Figure 5.5. In this case the polar phase is composed mainly of glycerol which forms during the reaction. It was observed that, for reaction conditions where the conversion was negligible the polar layer did form at the end of the experiment.

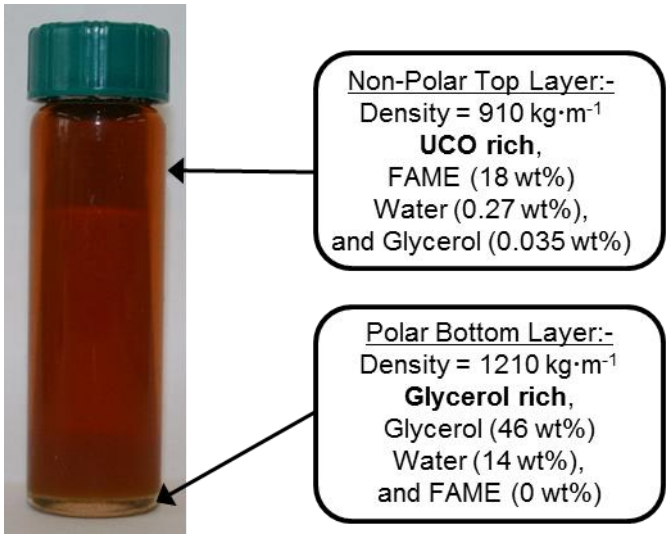

Figure 5.5. An example of the reaction product composition when Novozyme 435 is used as the catalyst.

A figure showing the typical reproducibility of the FFAs conversion using Novozyme 435 as the catalyst is shown in Figure 5.6 and the FAME concentration reproducibility is shown in Figure 5.7. In terms of the FFAs conversion it appears there for the first 2 h of reaction time there is a lot of scatter in the data after which the FFAs tend toward the same value. However it can be seen that the FFAs conversion for Run 2 are below the average value while for Run 4 they are greater than this average. This suggests that the variation is due to a small error in the initial reaction conditions. These data indicate that overall there is good reproducibility of the FFAs conversion data, however, care must be taken comparing results in the first 2 h of reaction time. In addition it can be seen that the conversion of FFAs reduce after 5 h of reaction time. This is due to side reactions which will be discussed in Chapters 6 and 7.

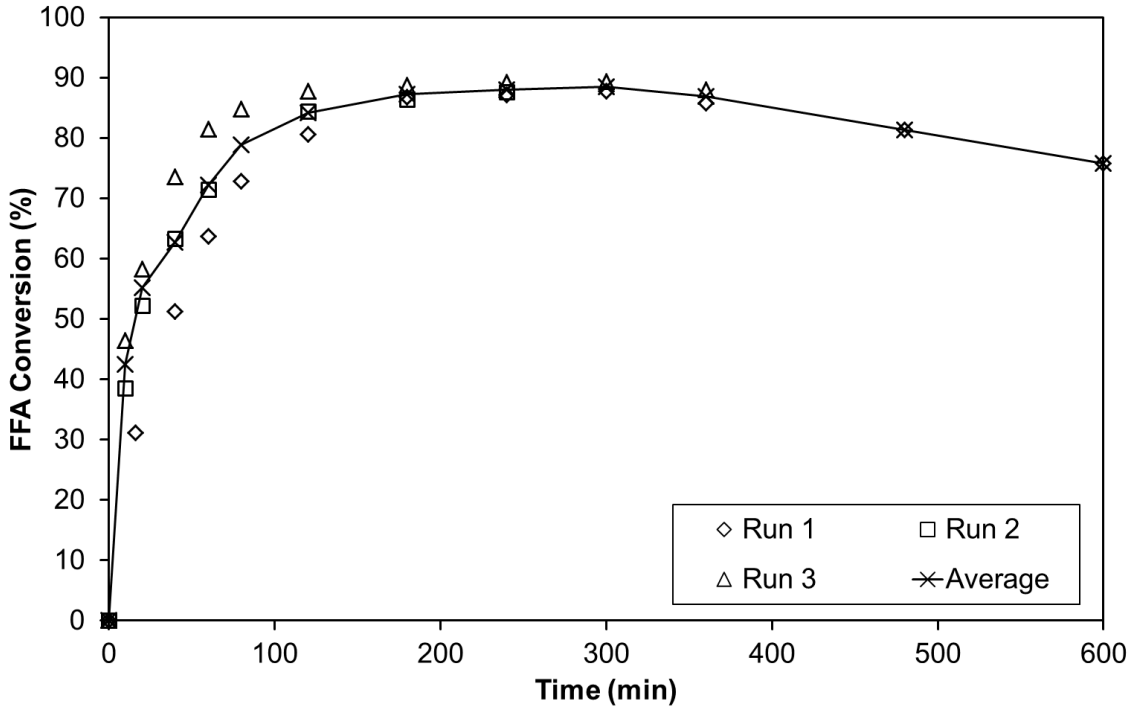

Figure 5.6. Reproducibility of the FFA% when using Novozyme 435 as the catalyst. (With a temperature of 60 °C, a catalyst loading of 1 wt%, a methanol to FFA mole ratio of 6.2:1 and a stirrer speed of 650 rpm)

Generally lipases are only active at the interface between a polar and a non-polar phase, typified by an emulsion. The existence of an interface causes the lid covering the active site of a lipase to open. This allows the substrate to reach the active site and a reaction to occur (Paiva et al. 2000). A possible explanation for this is that Novozyme 435 is an immobilised enzyme and it is possible to immobilise enzymes in the open conformation (Willis & Marangoni 2008). In addition investigations of lipase structures have found that the lid on the Novozyme 435 lipase (*Candida antacrtica* lipase B) is very small.

In terms of the FAME concentration it can be seen that there is some scatter although as expected the differences are smaller when compared to Figure 5.4. Overall there is an error of approximately 20 %. Novozyme 435 was used primarily as an esterification catalyst and the results were monitored based on the FFAs conversion. There were a small number of experiments where the FAME was important and these experiments were repeated to confirm the trend.

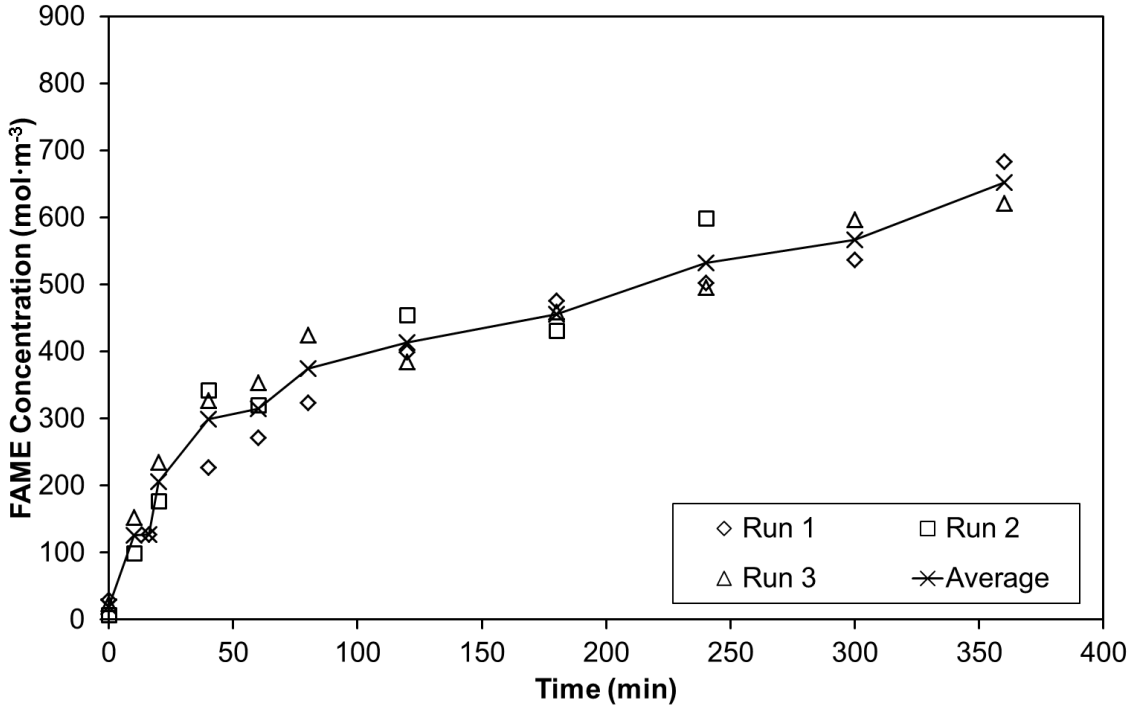

Figure 5.7. Reproducibility of the FAME concentration when using Novozyme 435 as the catalyst (With a temperature of 60 °C, a catalyst loading of 1 wt%, a methanol to FFA mole ratio of 6.2:1 and a stirrer speed of 650 rpm)

5.4.3 Reproducibility of the Experiments Catalysed by Amano Lipase PS-IM

Amano Lipase PS-IM has a greater methanol tolerance when compared to Novozyme 435. The amount of methanol used was greater than for Novozyme 435 and less than Purolite D5082 (at optimum conditions 26 g of methanol was mixed with 233 g of UCO). In addition it was found that it was necessary to add water to the reaction mixture. As a result when using Amano Lipase PS-IM as the catalyst, an emulsion was formed. Two examples of the final reaction product are shown in Figure 5.8 and these show the comparison for a high conversion and no conversion. The main components of the polar phase are methanol, water and glycerol. Water and glycerol have a higher specific gravity than UCO while methanol has a lower specific gravity. When the conversion is high methanol is consumed and glycerol is formed and as a result the density of the polar layer increases steadily with increasing conversion.

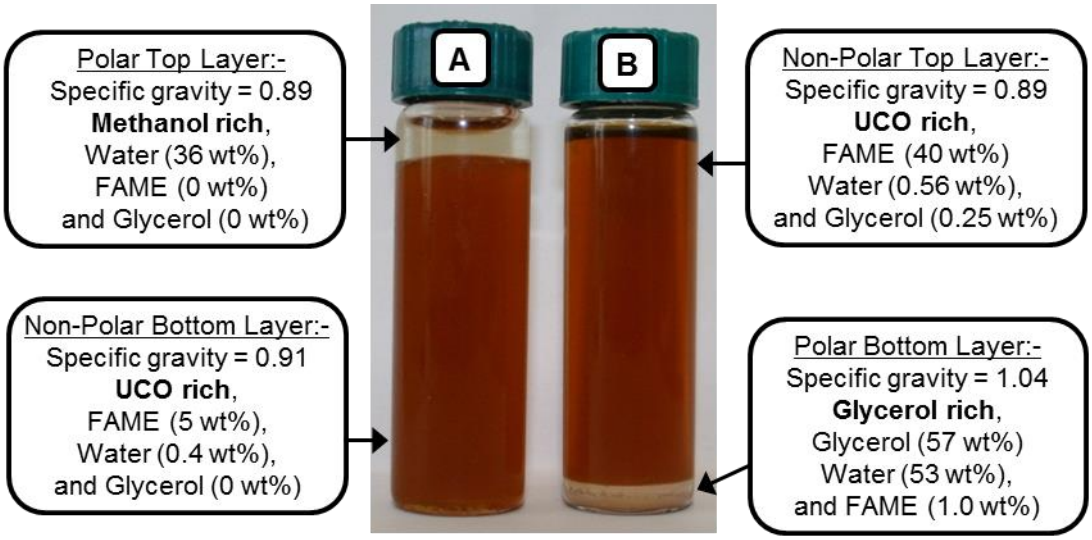

Figure 5.8. Examples of the reaction product composition when Amano Lipase PS-IM is use as the catalyst. Vial A contains an example of the reaction product when the conversion is low with Vial B an example at high conversion.

Injecting samples containing water onto a GC column is generally avoided because it is detrimental to the analysis and the column. It was expected that the FAME and FFAs would be in the non-polar layer and as a

result the samples were centrifuged and the non-polar layer analysed for FAME and FFAs. The polar and non-polar layers from selected experiments were analysed and the average results are given in Figure 5.8. From this it can be seen that the non-polar layer contains approximately 40 wt% FAME compared to 1 wt% in the polar layer. In addition the polar layer is approximately 4.5 % of the total mass. This shows that the FAME in the polar layer can be regarded as negligible.

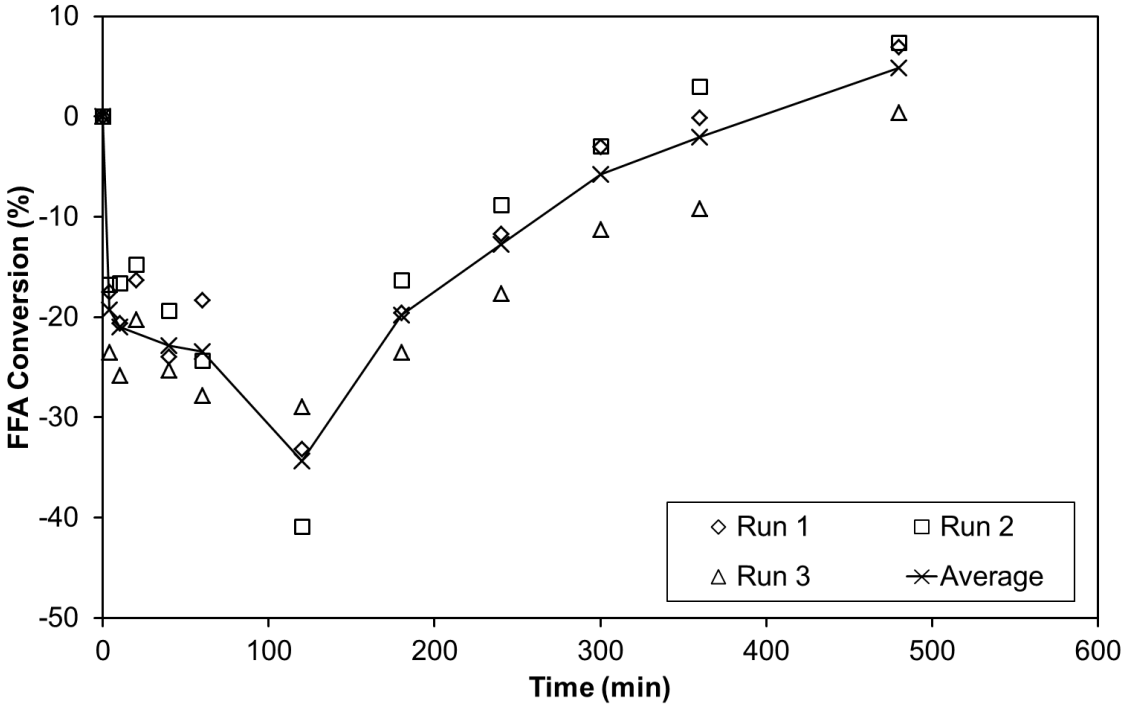

Figure 5.9. Reproducibility of the FFAs data when using Amano Lipase PS-IM as the catalyst. (With a temperature of 40 °C, a methanol to triglycerides mole ratio of 3.12:1, a catalyst loading of 0.786 wt%, 5 vol% of water added and a stirrer speed of 500 rpm)

The reproducibility of the FFAs concentration is shown in Figure 5.9 and from this it can be seen that the scatter is relatively low. This is particularly true for Runs 1 and 2. There are some substantial differences in the data for Run 3 however it is consistently low relative to the other two runs. This suggests there was a problem with the initial reaction conditions rather than the analytical technique. As discussed in previous sections (Sections 5.3.2 and 5.3.3) is possible to obtain a more consistent data set with this analysis because a relatively large sample is analysed. From the data it can be seen that the FFAs

are a reaction intermediate with FFAs formed due to the addition of water and subsequently consumed by the esterification reaction.

In contrast it can be seen that there is a large scatter in the FAME concentration data, Figure 5.10. In this case the reaction mixture forms an emulsion and this makes it more difficult to take consistent samples particularly when the amount of sample required is small. It can be seen that when the results of three experimental trends are averaged the overall trend is reasonable. Amano Lipase PS-IM was used as a transesterification catalyst and the FAME analysis was important for monitoring the amount of product formed. The FAME analysis was carried out in triplicate in order to minimise the error.

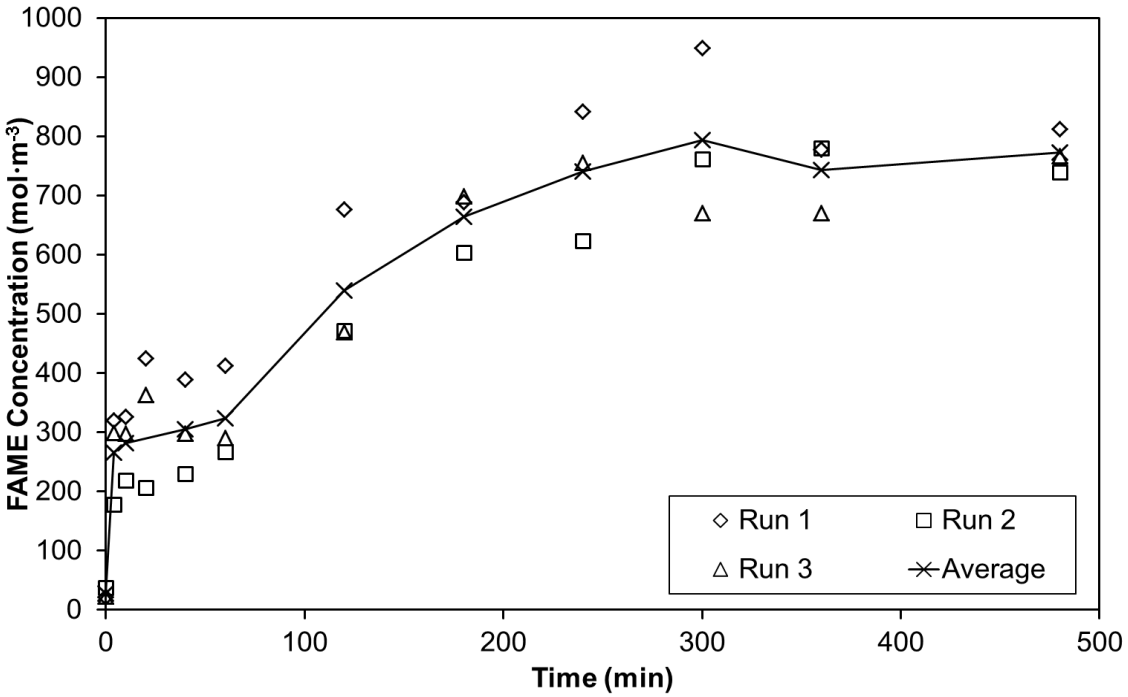

Figure 5.10. Reproducibility of the FAME data when using Amano Lipase PS-IM as the catalyst. (With a temperature of 40 °C, a methanol to triglycerides mole ratio of 3.12:1, a catalyst loading of 0.786 wt%, 5 vol% of water added and a stirrer speed of 500 rpm)

5.5 Conclusions

In this chapter methods used for the UCO characterisation were discussed with the main emphasis on their reproducibility of the methods. It was shown that as expected the TGs had stared to break down during the cooking process and the UCO contained approximately 8.42 wt% FFAs.

It has been shown that there was a high degree of reproducibility in the FFAs concentrations even when the reaction mixture formed an emulsion. However it was more difficult to achieve reproducible data for the FAME concentrations. This has been attributed to the small sample size used for analysis, particularly when the reaction mixture forms an emulsion. In order to compensate for this the experiments using Novozyme 435 were repeated to confirm the overall trend and for the transesterification experiments using Amano Lipase PS-IM the FAME analysis was carried out in triplicate.

Chapter 6: Esterification Pre-treatment of the Free Fatty Acids in Used Cooking Oil

6.1 Introduction

The conventional transesterification process is generally carried out using vegetable oil as the raw material (Balat and Balat 2010; Atadashi et al. 2013). Vegetable oil is an expensive raw material (Park et al. 2010; Zabeti et al. 2009) and there are ethical concerns regarding the use of a potential food source as fuel (Enweremadu and Mbarawa 2009). Alternative raw materials have been investigated and these include non-edible oils such as *Jatropha curacas* (Patil et al. 2009), by-products from oil refining such as palm fatty acid distillate (Talukder et al. 2009), animal fats (Da Rós et al. 2010), algal oil (Semwal et al. 2011) and used cooking oil (UCO) (Enweremadu and Mbarawa 2009; Akoh et al. 2007). UCO is a waste material and this means that it is possible to reduce the amount of waste going to landfill and use a relatively cheap material.

UCO contains free fatty acids (FFAs), which form due to hydrolysis of triglycerides during cooking (Ozbay et al. 2008) and this results in an unwanted saponification side reaction during transesterification, when a base catalyst is used (Di Serio et al. 2008). In addition, most biodiesel specifications impose an upper limit on the FFAs content (Knothe 2005) as they can cause engine damage due to deposit formation. FFAs can be converted to biodiesel by means of an esterification reaction using a short chain alcohol such as methanol and an acid catalyst. A schematic of the reaction is shown in Chapter 1, Figure 1.2. Currently most esterification processes use homogeneous catalysts such as sulfuric or sulfonic acid (Enweremadu and Mbarawa 2009; Melero et al. 2009a), however, homogenous catalysts are difficult to separate from the products, generate large amounts of waste water, and require expensive materials to prevent associated corrosion (Caetano et al. 2009). As

a result, solid acid catalysts such as ion-exchange resins have been investigated as heterogeneous esterification catalysts with high FFA conversions reported (Ozbay et al. 2008; Feng et al. 2010; Abidin et al. 2012).

Advances in enzyme technology are providing a greater choice of catalysts with research to date focusing on transesterification (Halim and Harunkamaruddin 2008; Al-Zuhair et al. 2009), however hydrolysis and esterification (Akoh et al. 2007; Talukder et al. 2009) reactions can also be used to form biodiesel. It has been shown that Novozyme 435 can be used to catalyse transesterification and hydrolysis reactions for the production of biodiesel, however the fastest reaction rates are achieved when Novozyme 435 is used to esterify free fatty acids (Tongboriboon et al. 2010). The work to date has focused on the esterification of material with a high concentration of free fatty acids such as palm fatty acid distillate which contains more than 93 wt% FFAs (Talukder et al. 2009) and soybean oil deodorizer distillate containing 80 wt% FFAs (Souza et al. 2009). Reports on the use of Novozyme 435 to convert the FFAs in UCO to biodiesel prior to transesterification are limited.

Although acid and enzyme catalysts catalyse both esterification and transesterification, the reaction rates for transesterification are often much slower compared to using a basic catalyst (Lam et al. 2010). In this chapter the esterification pre-treatment of UCO to transform FFAs using batch kinetic studies is discussed. Two catalysts, Purolite D5082 and Novozyme 435, have been investigated in detail and the results are presented in Sections 6.2 and 6.3, respectively. Purolite D5081 has been studied in detail by Abidin et al. (2012). High conversions are possible using Novozyme 435, Purolite D5082 and Purolite D5081 to catalyse the esterification reaction, however, there were significant differences in the optimum conditions identified. A comparison of the optimum conditions and conversions is provided in Section 6.4.

6.2 Optimisation of Purolite D5082

6.2.1 Effect of Catalyst Loading

The initial experimental conditions were based on the work by Abidin et al. (2012) using Purolite D5081 and catalyst loadings of 0.75 – 1.5 wt%. However the initial conversion was relatively low and it was found that it was necessary to increase the loading to 5 wt%, in order to increase the conversion. The results of this work are shown in Figure 6.1.

From these data it can be seen that a catalyst loading of 5 wt% was required in order to reach an equilibrium conversion of 90% within 8 h and as a result this loading was selected as the optimum catalyst loading for subsequent experiments.

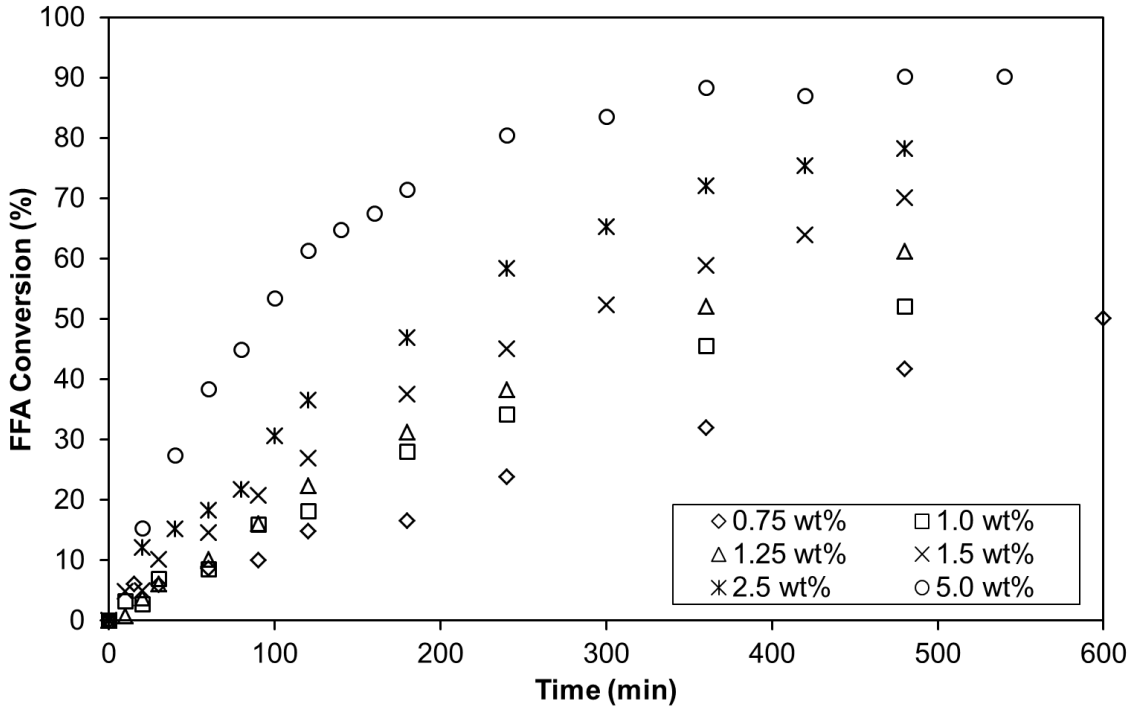

Figure 6.1. Effect of catalyst loading on the FFA conversion. (With a temperature of 60 °C, mole ratio of 93:1 and a stirrer speed of 450 rpm)

6.2.2 Effect of the Methanol to FFA Mole Ratio

The esterification reaction is an equilibrium limited reaction with one mole of methanol required to convert one mole of FFA to one mole of FAME.

The reaction scheme is given in Chapter 1, Figure 1.2. It is expected that conversion will increase with an increase in mole ratio. The effect of the mole ratio on FFA conversion using Purolite D5082 is shown in Figure 6.2(a) and (b).

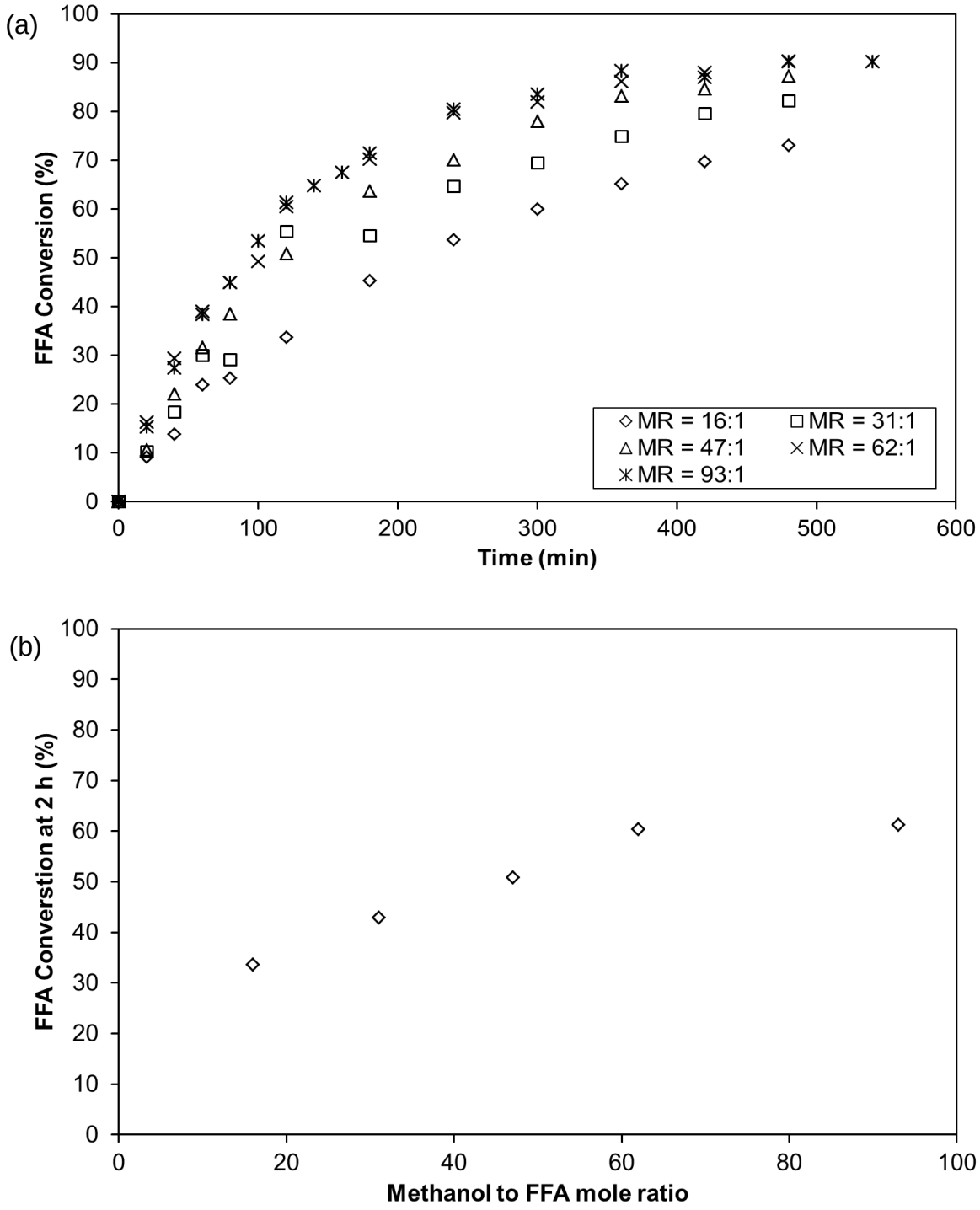

Figure 6.2. Effect of the methanol to FFA mole ratio on the FFA conversion with (a) showing the overall conversion trend and (b) showing the conversion at 2h. (With a temperature of 60 °C, a catalyst loading of 5 wt% and stirrer speed of 450 rpm)

From Figure 6.2 it can be seen that conversion increases with increasing mole ratio until a ratio of 62:1 after which no further increase is observed. On this basis a mole ratio of 62:1 has been selected as the optimum mole ratio because it gives the maximum conversion without using excess methanol.

Methanol is sparingly soluble in UCO, leading to the formation of an emulsion at high mole ratios. The solubility of methanol in oil is shown in Chapter 5, Section 5.3.1 and at 60 °C the solubility of methanol in oil corresponds to a mole ratio of 22:1. For the experiment with a mole ratio of 16:1 the methanol would have been fully dissolved compared to the rest of the experiments, where an emulsion formed. The mole ratio trend indicates that this change in the nature of the reaction mixture does not affect conversion.

6.2.3 Effect of Temperature

Conversion is expected to increase with increasing temperature. However the maximum recommended temperature for Purolite D5082 is 120 °C and methanol has a boiling point of 65 °C. Abidin et al. (2012) reported concerns regarding methanol loss at temperatures close to the boiling point of methanol and as a result 60 °C has been selected as the maximum temperature for investigation. The effect of temperature on conversion is shown in Figure 6.3.

From these data it can be seen that conversion increases with increasing temperature. However the increase is small because small increments in temperature were used. A temperature of 60 ºC has been selected as the optimum because it results in the fastest reaction rate and highest conversion although the difference is small.

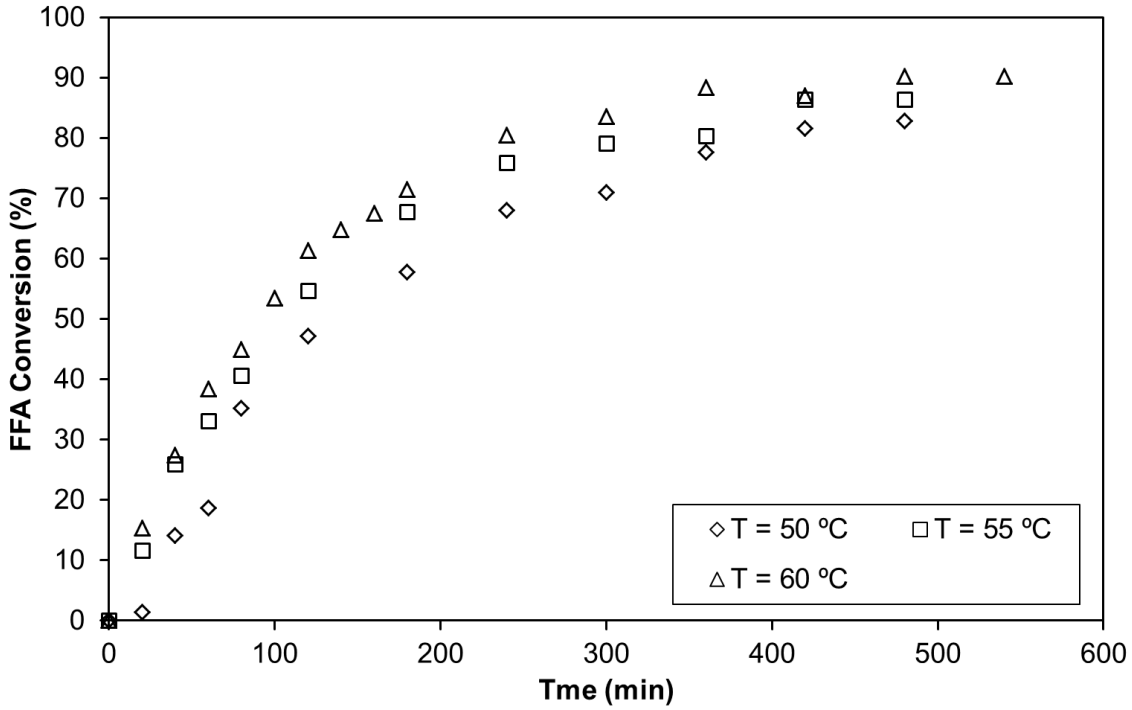

Figure 6.3. Effect of temperature on the conversion of FFA. (With catalyst loading of 5 wt%, a mole ratio of 62:1 and a stirrer speed of 450 rpm)

6.2.4 A Comparison of FFA and FAME Concentrations

For the optimisation of the reaction conditions for Purolite D5082 it has been assumed that the only reaction taking place is esterification. In order to investigate this further, FAME formation at the optimum reaction conditions has been investigated. The results of this comparison are shown in Figure 6.4. From these data it can be seen that the amount of FAME formed during the experiment is similar to the amount of FFA consumed. There are small differences and these have been attributed to experimental error. In particular, while the FFAs concentration is determined by means of a titration, the FAME concentration is measured using GCMS and the error for these methods will be different. This indicates that there are no side reactions occurring.

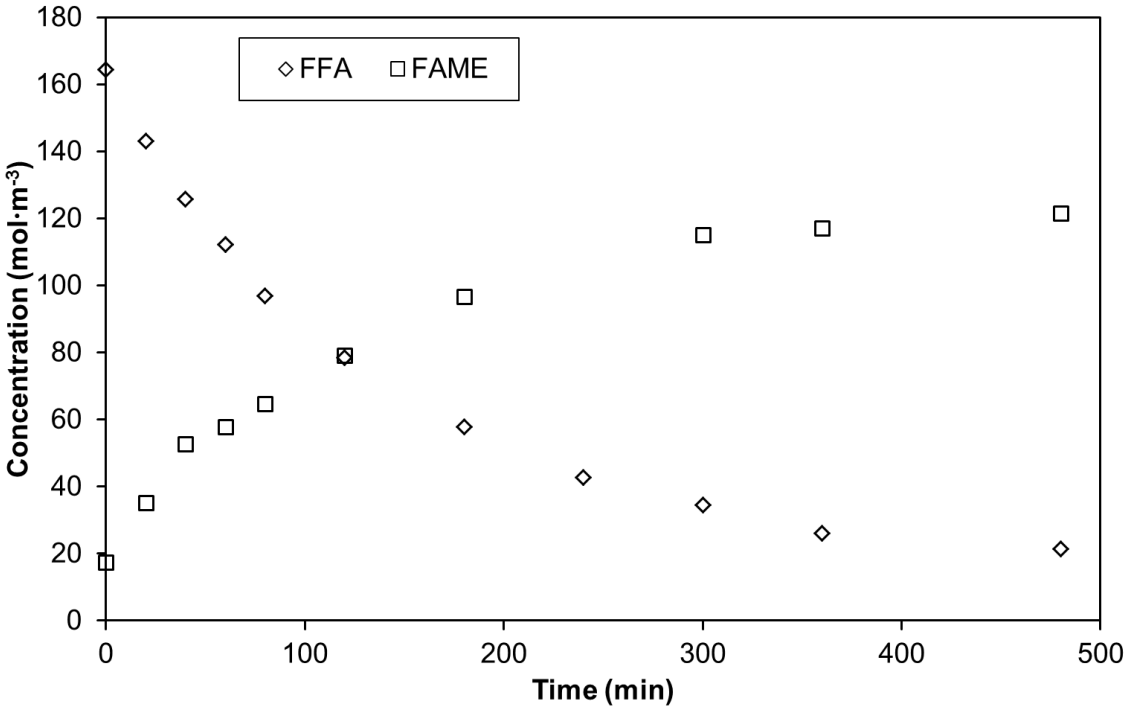

Figure 6.4. Comparison of the FFA and FAME concentrations when using Purolite D5081 as the catalyst. (With a temperature of 60 °C, a mole ratio of 4:1 a catalyst loading of 5 wt% and a stirrer speed of 450 rpm)

6.2.5 Reusability Study

Reusability studies are conducted to investigate the long term stability of heterogeneous catalysts. The effect of reused cycles and two types of cleaning regime, on FFAs conversion, is shown in Figure 6.5. From the data in Figure 6.5 it can be seen that when Purolite D5082 was washed with methanol the FFA conversion decreased relative to the conversion using fresh catalyst. It has been shown that pore blockage contributes to the loss of activity in Purolite D5082 and a similar catalyst, Purolite D5081 (Abidin et al. 2012; Andrijanto et al. 2012). In order to improve the cleaning process, Purolite D5082 was washed with methanol in conjunction with ultrasonic irradiation. The BET surface area, after washing, was similar to the fresh catalyst (Chapter 4, Section 4.4). In contrast Andrijanto et al. (2012) washed Purolite D5081 with methanol (no ultrasonic irradiation) and found that there was a substantial drop in conversion and BET surface area. These results indicate that washing with methanol is not sufficient to remove vegetable oil from this type of catalyst.

Ultrasonic irradiation will help with the removal of the reagent, however this would be difficult to apply on an industrial scale.

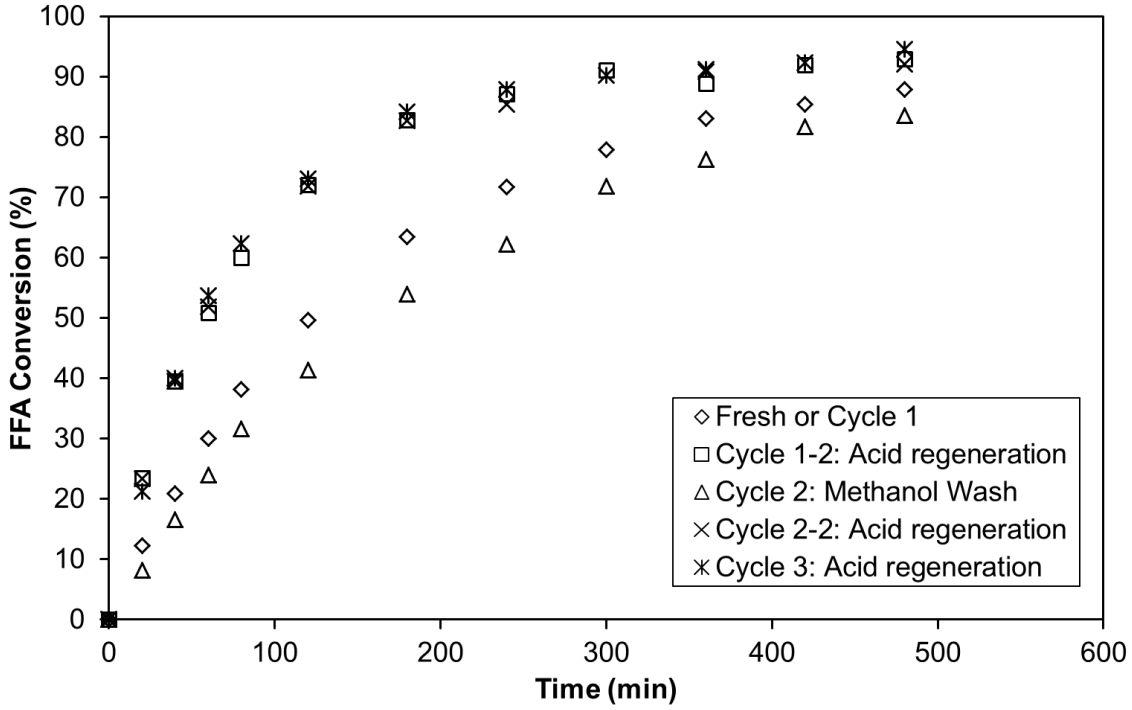

Figure 6.5. Investigation of the reusability and regeneration of Purolite D5082. (With a temperature of 60 °C, a mole ratio of 4:1 a catalyst loading of 5 wt% and a stirrer speed of 450 rpm)

Previous studies have found that while pore blockages contributes to a loss of activity, sulphur leaching occurs during esterification leading to a further loss of activity (Abidin et al. 2012). It has been proposed that these catalysts can be regenerated by contacting with sulphuric acid (Andrijanto et al. 2012). Purolite D5082 used for cycles 1-2, 2-2 and 3-2 was contacted with sulphuric acid and it can be seen that the conversion is the same for each cycle. In addition, the conversion is higher than the fresh catalyst.

From the sodium capacity data in Chapter 4, Section 4.8 it can be seen that sodium capacity values for the acid regenerated catalysts are higher than the fresh catalyst, while the methanol washed catalyst is lower. In contrast, the elemental analysis data indicate a steady decrease in the sulphur composition of Purolite D5082 with increasing reusability cycle (Chapter 4, Section 4.6). While these data may appear contradictory, the sodium capacity determination

analysis was carried out directly with the catalyst, while it was necessary to crush and then dry the samples used sent for elemental analysis. It is probable that the sulphuric acid remaining the pores of the acid regenerated catalyst would have been removed during this process. These data indicate that contacting with sulphuric acid residual does not necessarily regenerate Purolite D5082 and the increase in activity is due to sulphuric acid in the pores of the catalyst.

6.3 Optimisation of Novozyme 435

6.3.1 Effect of the Methanol to FFA Mole Ratio

The effect of the methanol to FFA mole ratio on conversion with Novozyme 435 as the catalyst is shown in Figure 6.6. From these data it can be seen that the effect of the mole ratio varies significantly for the two catalysts. In the case of Purolite D5082, conversion increases with an increase in mole ratio tending towards a maximum above which further increase in mole ratio will not increase FFA conversion. This is a typical trend for chemical catalysts.

In comparison, Novozyme 435 catalysis is more sensitive to changes in the mole ratio and a high conversion is possible with much lower mole ratios. In this case it can be seen there is an optimum methanol to FFA mole ratio of 6.2:1. Mole ratios below this value suggest there is insufficient methanol for the reaction and increasing the methanol above this range results in a decrease in conversion due to poisoning of the catalyst. Methanol is known to poison enzymes including Novozyme 435 (Talukder et al. 2009; Shimada et al. 2002) and in the case of transesterification where much larger quantities of methanol are required the issue has been mitigated by stepwise addition of methanol. A large reduction in the methanol requirement results in a higher throughput and increased process safety.

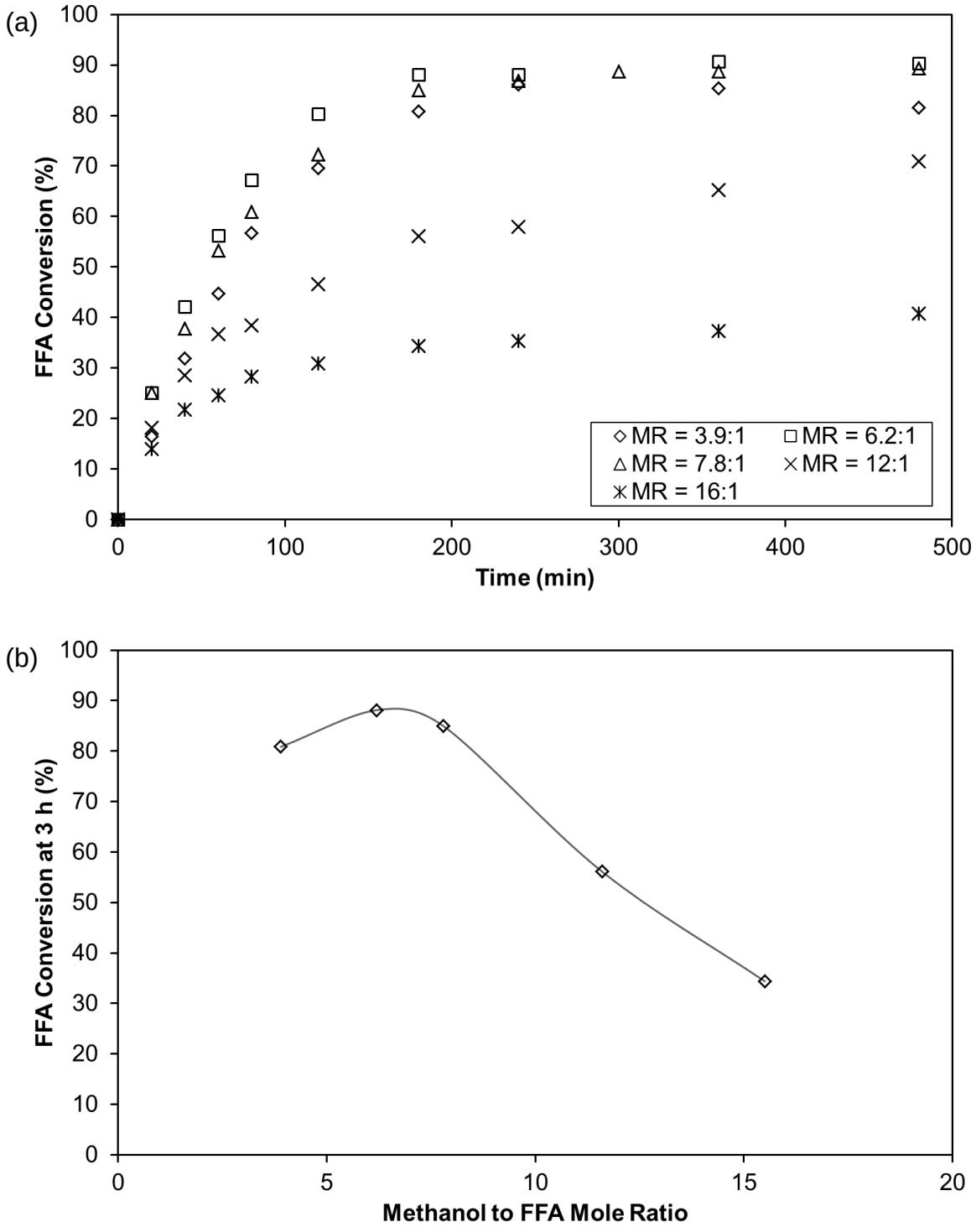

Figure 6.6. Effect of the methanol to FFA mole ratio on the FFA conversion with (a) showing the overall conversion trend and (b) showing the conversion at 2h. (With a temperature of 40 °C, a catalyst loading of 1 wt% and stirrer speed of 450 rpm)

6.3.2 Investigation of the External Mass Transfer Limitations

Vegetable oil and methanol are poorly miscible and the use of a heterogeneous catalyst leads to the formation of a three phase system with limited mass transfer between the three phases (Zabeti et al. 2009), reducing the reaction rate. An organic solvent can be used to improve contacting. However this will need to be removed from the final product (Talukder et al. 2009) thus eliminating the process step saving of using a heterogeneous catalyst. External mass transfer resistance refers to the resistance across the solid-liquid interface in heterogeneous catalyst systems due to the formation of a boundary layer around catalyst particles. Increasing the stirring speed of the impeller in a batch reactor reduces the thickness of the boundary layer and improves solid suspension. The effect of increasing the stirring speed for Novozyme 435 is shown in Figure 6.7. From Figure 6.7 it can be seen that the increase in conversion is small with increasing stirrer speed, however, in order to be certain that mass transfer limitations have been eliminated a stirrer speed of 650 rpm was selected for subsequent work.

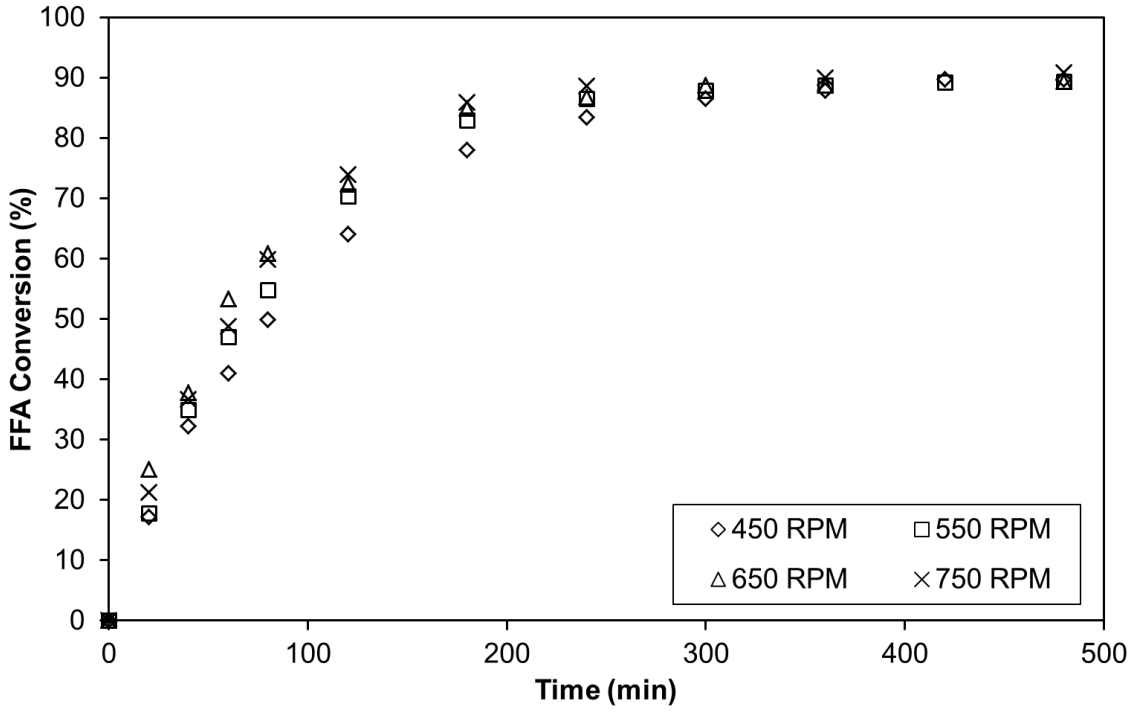

Figure 6.7. Effect of the stirrer rotational speed on conversion. (With a temperature of 40 °C, an FFA mole ratio of 6.2:1 a catalyst loading of 1 wt%)

6.3.3 Investigation of the Internal Mass Transfer Limitations

Internal mass transfer resistance is due to the resistance of flow inside the particles. The internal mass transfer resistance can be reduced by decreasing the particle size because this reduces the diffusion path length. The internal mass transfer resistance from Novozyme 435 was investigated by sieving the beads supplied by the manufacturer[1] (d_{50} = 588 µm) into a large size fraction (d_{50} = 845 µm) and a small size fraction (d_{50} = 430 µm) as shown in Figure 6.8 (a).

The effect of various particles sizes on FFA conversion is shown in Figure 6.8 (b). From these data it can be seen that there are intra-particle diffusion limitations when using the large size fraction. When the overall size fraction supplied by the manufacturer is compared to the small size fraction it can be seen that the difference in conversion is small. These data indicate that with the catalyst supplied by the manufacturer there are some intra-particle diffusion limitations due to larger beads. However, the effect on conversion is small and as a result the internal mass transfer limitations are small, particularly when the smaller size fractions are compared.

[1] d_{50} is the diameter corresponding to the 50% volume on a relative cumulative particle diameter distribution curve.

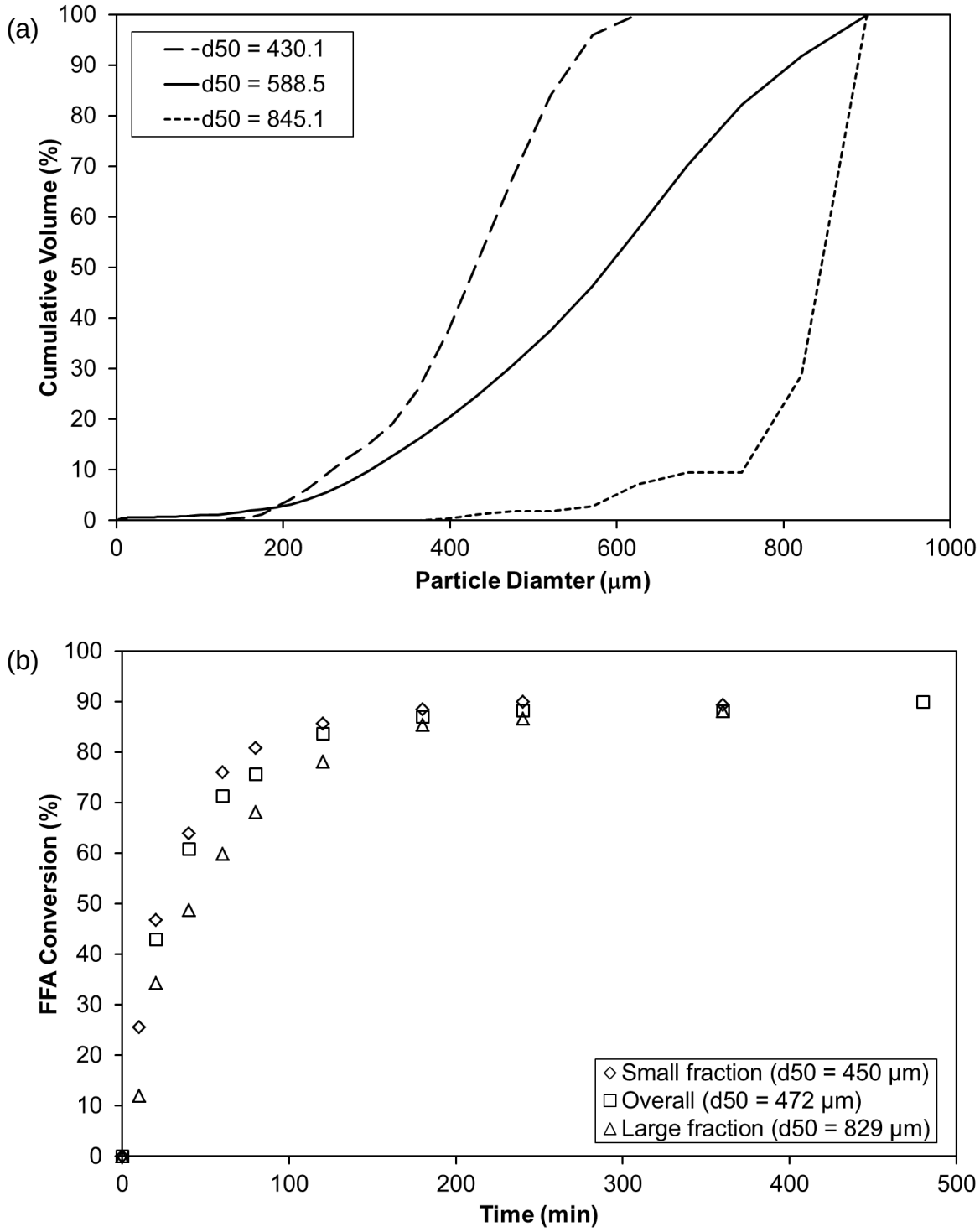

Figure 6.8. Effect of internal mass transfer limitations on conversion with (a) showing the cumulative size distribution of the sieved fractions investigated and (b) showing the effect of these size distributions on FFA conversion. (With a temperature of 50 °C, and FFA mole ratio of 6.2:1, a catalyst loading of 1 wt% and a stirrer speed of 650 rpm)

6.3.4 Effect of Temperature

As discussed in Section 6.2.3 the maximum possible temperature for this system has been set at 60 °C based on the boiling point of methanol. The maximum recommended reaction temperature for Novozyme 435 is 70 °C, (manufacturer's data). Figure 6.9 (a) shows the effect of temperature on FFA conversion. From these data it can be seen that it is possible to achieve a relatively high initial reaction rate with temperatures as low as 30 °C. Hence this reaction could be carried out in warmer countries without additional heating. From Figure 6.9 (a) it can be seen that for temperatures of 50 °C and above, the conversion reaches a maximum and then has decreased significantly after 24 hours. The effect of temperature on the FAME concentration is shown in Figure 6.9 (b). This is compared to the expected FAME concentration, calculated based on the change in the FFA concentration according to the esterification reaction schematic shown in Chapter 1, Figure 1.2. From these data it can be seen that the amount of FAME formed is higher than expected and increasing with an increase in temperature. The active catalytic site of lipases target the carboxyl groups of lipids including monoglycerides (MG), diglycerides (DG), triglycerides (TG), FAME and FFAs allowing for reactions with water or methanol (MeOH) (Paiva et al. 2000). Schematics of the possible reactions, including esterification are shown in Chapter 2, Figures 2.2 to 2.4. The order of preference for the reactions is esterification > transesterification > hydrolysis reaction (Tongboriboon et al. 2010). The reaction mechanism and side reactions have been investigated and this is discussed in Chapter 7.

The formation of additional biodiesel is beneficial, however, the main purpose of this work is to reduce the FFAs concentration in order to avoid downstream processing problems and ensure the final biodiesel specification is met. The reduction in FFAs conversion at longer reaction times has been attributed to the increase in water driving the hydrolysis side reactions. As a result the optimum temperature was defined as the temperature at which the highest conversion was achieved, combined with a high initial reaction rate and this was determined to be 50 °C. The possibility of a more efficient process involving the reaction of the MG, DG and TGs will be discussed in Chapter 7.

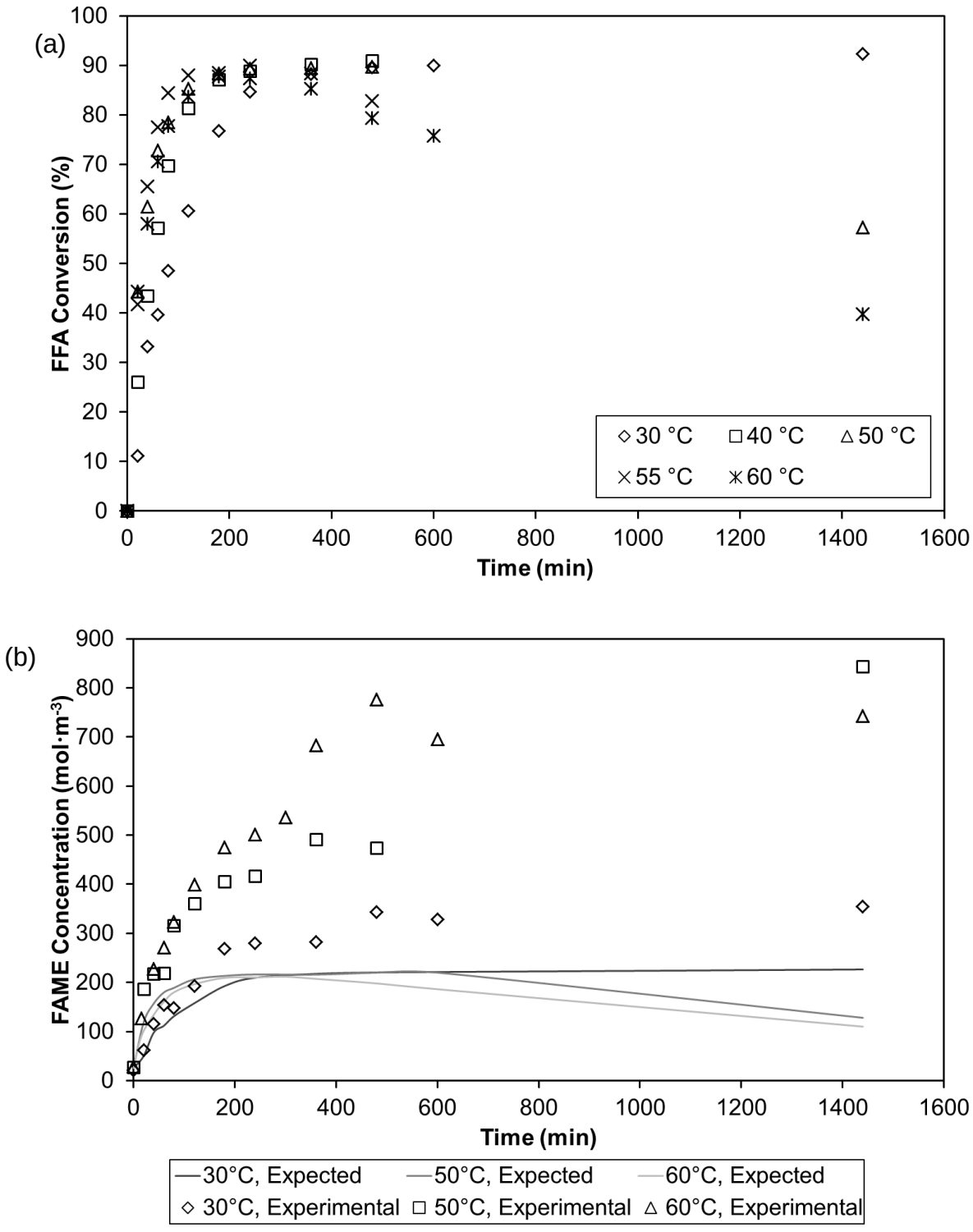

Figure 6.9. The effect of temperature on esterification reaction with (a) showing the FFA conversion and (b) showing a comparison between the expected and experimental FAME formation. (With a FFA mole ratio of 6.2:1, a catalyst loading of 1wt% and a stirrer speed of 650 rpm)

6.3.5 Effect of Catalyst Loading

Figure 6.10 shows the catalyst loading. From these data it can be seen that conversion is lower with a loading of 0.75 wt% while the conversion for the other three loadings investigated, 1.0, 1.25 and 1.50 wt % are very similar. This shows that with a loading of 1.0 wt% there is sufficient catalyst present for the reaction with no additional benefits to adding more catalyst.

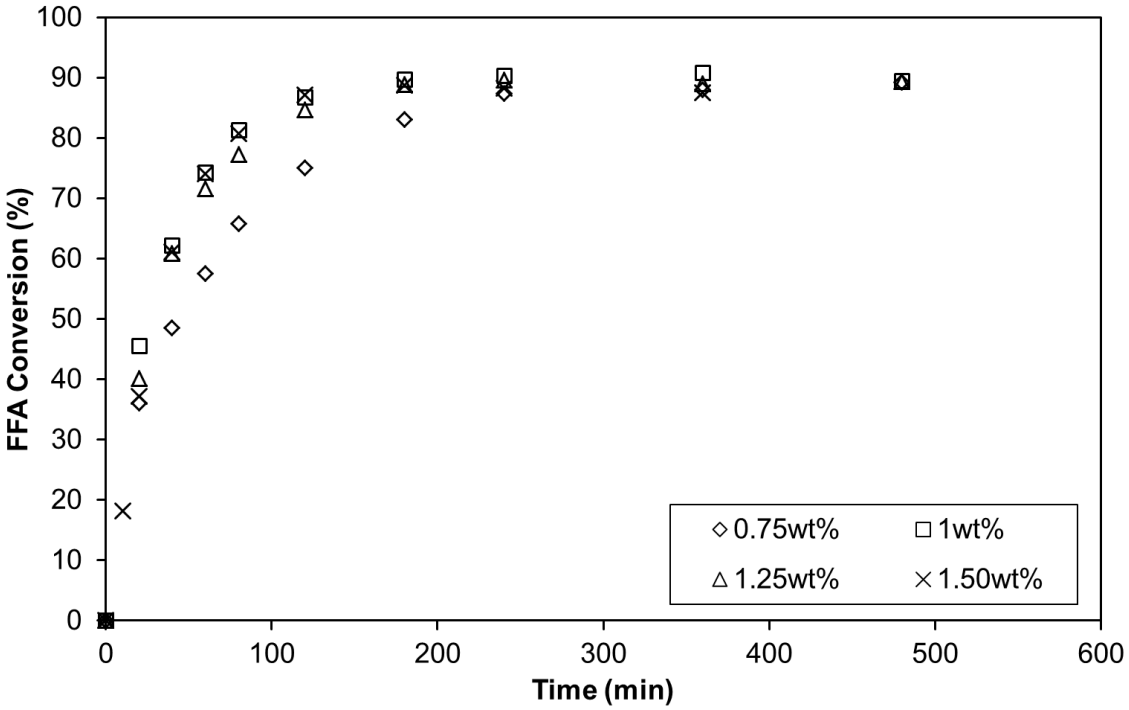

Figure 6.10. Effect of catalyst loading on conversion. (With a temperature of 50 °C, a methanol to FFA mole ratio of 6.2:1 and a stirrer speed of 650 rpm)

6.3.6 Reusability Study

The effect of reusing Novozyme 435 on conversion is shown in Figure 6.11. From these data it can be seen that after the first use there is an overall reduction in conversion. The trend for cycles 2-4 is similar indicating that the largest loss in catalytic activity occurs due to the first cycle (Fresh catalyst). From the BCA Assay results (Chapter 4, Section 4.9) it can be seen that there is a substantial reduction in the amount of protein bonded to the surface of the catalyst after cycle 1.

In addition the trend for cycles 2-4 is not following the expected equilibrium trend as conversion increases to a maximum and then decreases. Analytical and kinetic modelling work detailed in Chapter 7 has confirmed the existence of side reactions including hydrolysis. The MGs and DGs found in UCO can be converted by the hydrolysis reaction to FFAs, and glycerol or DGs according the reaction scheme in Chapter 2, Figure 2.2. The FFAs are subsequently converted to FAME. The trend in cycles 2-4 is typical of a reaction intermediate. These data indicate that overall the catalytic activity of Novozyme 435 is decreasing with the esterification activity decreasing at a faster rate than hydrolysis. One potential explanation is water accumulation in the pores of the catalysts with the water not fully removed during the washing and drying process.

From the data in Figure 6.11 it can be seen that the maximum conversion occurs between 180 and 240 min and in this range the decrease in conversion is approximately 5% per cycle

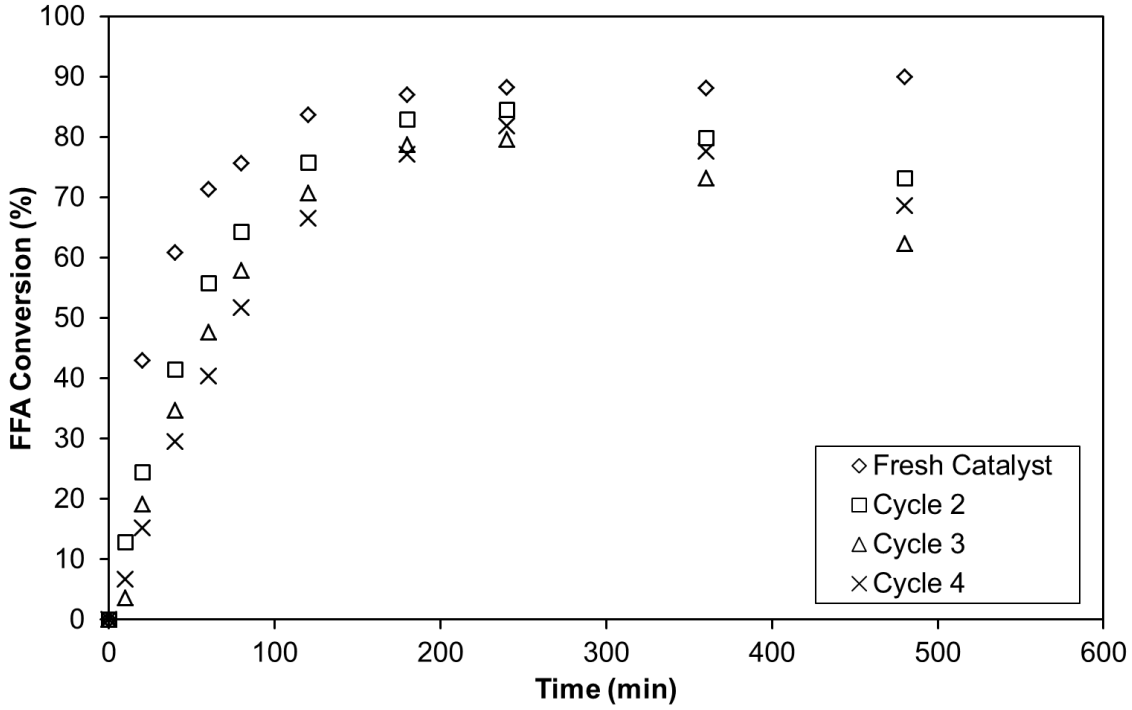

Figure 6.11. Investigation of the reusability of Novozyme 435. (With a temperature of 50 °C, a FFA mole ratio of 6.2:1, a catalyst loading of 1wt% and a stirrer speed of 650 rpm)

6.4 A Comparison of Novozyme 435, Purolite D5082 and Purolite D5081

The optimum conditions have been identified for Purolite D5081 (Abidin et al. 2012), Purolite D5082 (Section 5.2) and Novozyme 435 (Section 5.3) and a summary is given in Table 6.1.

Table 6.1. Comparison of the optimum reaction conditions

Catalyst	Purolite D5081	Purolite D5082	Novozyme 435
FFA to methanol Mole Ratio	93	62	6.2
Temperature (°C)	60	60	50
Catalyst Loading (wt%)	1.25	5.00	1.00
Stirrer speed (rpm)	350	450	650

One of the most noticeable differences is the effect of the mole ratio on conversion and the resulting optimum mole ratios. In the case of both ion-exchange resins, conversion increased with increasing FFA mole ratio until the optimum mole ratio was reached and at that point conversion remained approximately constant. In contrast with Novozyme 435 there was a clear peak in conversion, identified as the optimum mole ratio with conversion decreasing for values above and below this optimum. This is because Novozyme 435 is poisoned by high levels of methanol. Purolite D5081 had the highest optimum FFA mole ratio of 93:1. Purolite D5082 had a slightly lower optimum mole ratio of 62:1 which offsets somewhat the much higher catalyst loading required. For Novozyme 435 the mole ratio was an order of magnitude lower with a value of 6.2:1.

The differences in optimum mole ratios affect the composition and nature of the reaction mixture. This in turn affects the formation of a boundary layer around the catalyst. The methanol dissolves fully in oil at a mole ratio of 6.2:1 as this is below the solubility of methanol in oil. However, mole ratios of 62:1 and 93:1 are above the solubility point and an emulsion is formed. The solubility of methanol in UCO is given in Chapter 5, Section 5.3. This was found to affect the stirrer speed required to eliminate external mass transfer

limitations. In the case of Purolite D5081 a stirrer speed of 350 rpm was sufficient to eliminate mass transfer limitations, while with Novozyme 435 a stirrer speed of 650 rpm was required. The other factor to consider with stirrer speed is that the catalyst should be fully suspended in the reaction medium and this is affected by the size and density of the catalyst particles.

Novozyme 435 has been shown to have a much lower selectivity for the esterification reaction compared to Purolite D5082. A comparison of the FAME and FFA concentrations using Novozyme 435 and Purolite D5082 showed that Purolite D5082 catalyses only the esterification reaction, whilst Novozyme 435 catalyses the esterification, transesterification and hydrolysis reactions. In this case the side reactions are beneficial because this leads to the formation of the desired product. However, a poorly controlled process will result in a low FFAs conversion.

A comparison of conversion for the three catalysts at their optimum conditions is shown in Figure 6.12. Given that there is a large difference in the effect of mole ratio on conversion, depending on the choice of catalyst, it would not be meaningful to compare these catalysts at the same reaction conditions. From these data it can be seen that with Novozyme 435 the initial reaction rate is the fastest, followed by Purolite D5081, however the conversion after 600 min of reaction time is slightly lower with Novozyme 435 reaching 90% compared to 94% with Purolite D5081. The esterification reaction is an equilibrium limited reaction and as a result increasing the mole ratio and thus the amount of methanol will affect the equilibrium position. As a result, the conversion after 600 min of reaction time should be regarded as a function of both the catalyst type and mole ratio. In addition, a higher impeller stirring speed is required with Novozyme 435 in order to mitigate external mass transfer limitations. The conversion from Purolite D5082 remains the lowest throughout the reaction.

Novozyme 435 offers numerous benefits over Purolite D5081 and Purolite D5082 because a high conversion is achieved at a much lower mole ratio, lower temperature and catalyst loading. In particular, the significant

reduction in methanol requirements suggests that for the same equipment size a much higher capacity is possible and the process will be safer. In addition, the side reactions with Novozyme 435 mean that better process control is required in order to prevent FFA formation. A disadvantage is that the cost of enzymes tends to be much greater than that for ion-exchange resins.

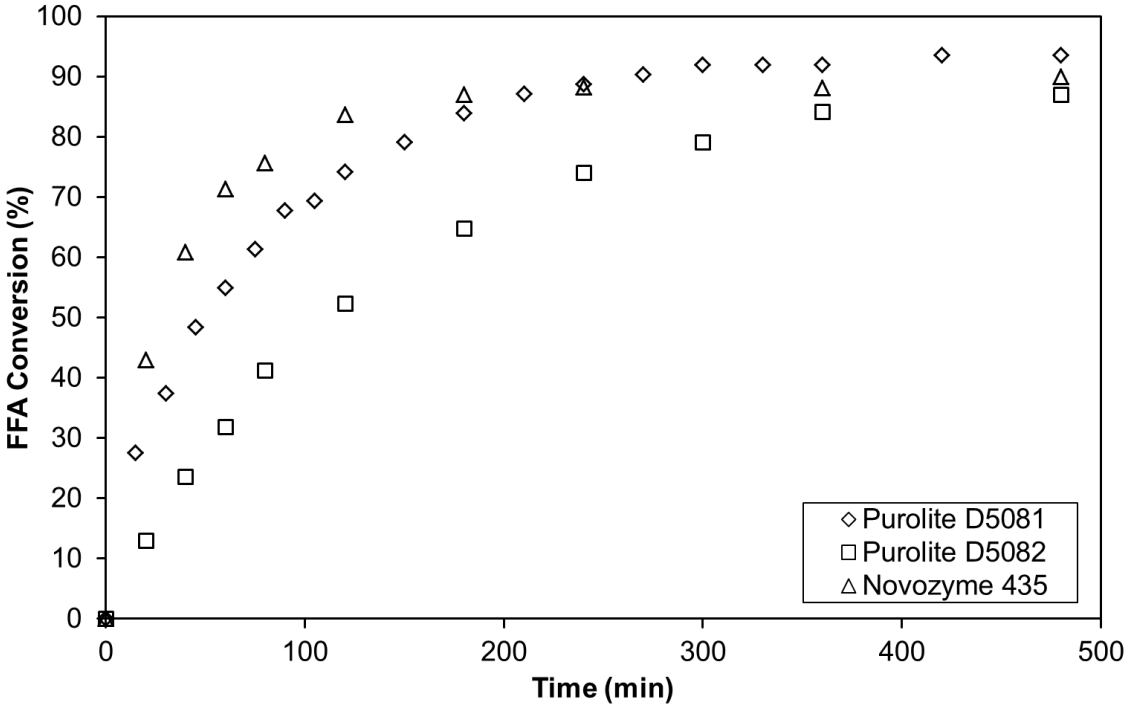

Figure 6.12. Comparison of catalytic performances of the three catalysts at their optimum reaction conditions.

6.5 Conclusions

The catalytic action of two types of catalysts, ion-exchange resins (Purolite D5082 and Purolite D5081) and an immobilized enzyme (Novozyme 435) were compared for the esterification pre-treatment of UCO for the preparation of biodiesel. A high conversion of FFAs to biodiesel was achieved with Purolite D5081, Purolite D5082 and Novozyme 435 with the optimum reaction conditions summarised in Table 6.1. The optimum reaction conditions have been identified for Purolite D5082 and Novozyme 435 using batch kinetic studies. A detailed investigation of Purolite D5081 has been previously reported (Abidin et al. 2012).

The highest conversion of 94% is possible with Purolite D5081 compared to 90% conversion of FFAs using Novozyme 435 and 88% with Purolite D5082 after 8h of reaction time. This difference can be explained in part because the higher mole ratio used with Purolite D5081 will have affected the equilibrium. Purolite D5082 did not reach equilibrium in the reaction time. It was found that using Novozyme 435 as the catalyst resulted in a large reduction in the amount of methanol required with the optimum FFA mole ratio going from 98:1 with Purolite D5081 to 6.2:1 with Novozyme 435. Purolite D5082 required a lower mole ratio of 62:1 when compared to Purolite D5081 which compensates for the higher catalyst loading required. The decrease in the mole ratio, for Novozyme 435, changed the composition in the reaction medium and as a result a much higher stirring speed was required to eliminate mass transfer limitations.

Relatively high reaction rates were possible with Novozyme 435 at a temperature of 30 °C indicating that this reaction could be carried out without heating in some parts of the world. Side reactions with Novozyme 435 at vigorous reaction conditions such as high temperatures and during the reusability study did occur. One of the advantages of a heterogeneous catalyst is that they can be reused and in the case of Novozyme 435 it was found that there is a lot of potential to reuse this catalyst providing the reaction time is less than 4 h.

Chapter 7: Liquid Chromatography Development and Kinetic Modelling

7.1 Introduction

It was found that when Novozyme 435 is used for the esterification pre-treatment of cooking this leads to the formation of additional fatty acid methyl esters (FAME) at high temperatures, as discussed in Chapter 6. It has been shown that Novozyme 435 can be used to catalyse hydrolysis and transesterification reactions (Ganesan et al. 2009; Tongboriboon et al. 2010; Lam et al. 2010) although the reaction rate is very low. In order to investigate this hypothesis further it was necessary to develop a method to monitor the MG, DG and TG concentrations.

Gas Chromatography (GC) and liquid chromatography (LC) are the most common methods for investigating the production of biodiesel (Li et al. 2008). LC was selected for further investigation because the substances under investigation, particularly the triglycerides (TG), diglycerides (DG) and monoglycerides (MG) have high molecular weights, high boiling points and low volatilities. As a result they are not readily vaporised and separated by GC and need to be derivitised (Li et al. 2008; Holcapek et al. 1999).

The concentration data can then be analysed using a kinetic model to investigate the reaction mechanisms. Cheirslip et al. (2008) developed a series of models to investigate if lipases catalyse the reaction according to the hydrolysis esterification series or if this reaction occurs in parallel with transesterification.

In this chapter, the work carried out to develop an LC method for monitoring the MGs, DGs and TGs is discussed in Section 7.2. Once an LC method had been developed a series of batch experiments were monitored for

the MG, DG, TG, FFAs and FAME concentrations and these results are presented in Section 7.3. The results in section 7.3 were used to carry out some kinetic modelling in order to investigate the reaction mechanism and these results are presented in Section 7.4.

7.2 Development of a Liquid chromatography (LC) Method

Various methods have been investigated for the analysis of the reaction mixture for the production of biodiesel.

7.2.1 Results of LC Method 1

This method was selected because it was used in the department by Hishamuddin (2009) and as a result all the equipment, columns and necessary data were readily available making it possible to rapidly assess the results and determine if this method could be adapted for the analysis of biodiesel. A comparison of the results for palm oil and used cooking oil (UCO) is shown in Figure 7.1. The trend for palm oil corresponds to the results reported by Hishamuddin (2009), although Hishamuddin (2009) applied a baseline correction algorithm. For the UCO trend many of the peaks correspond to the palm oil data although the areas are different. The UCO was derived from soybean oil which has different composition of triglycerides.

Hishamuddin (2009) reported the peaks for components eluting in the first 10 min as ‘other’ and these components would have been primarily MGs and DGs with the first TG component eluting at about 35 min. In the case of UCO there are lot of peaks in the first 35 min and this was expected because the UCO is known to contain significant quantities of FFAs, MGs and DGs.

These data show that it is possible to assess the composition of biodiesel using liquid chromatography although Method 1 is not suitable because the resolution of the FFA, MG and DG peaks is low.

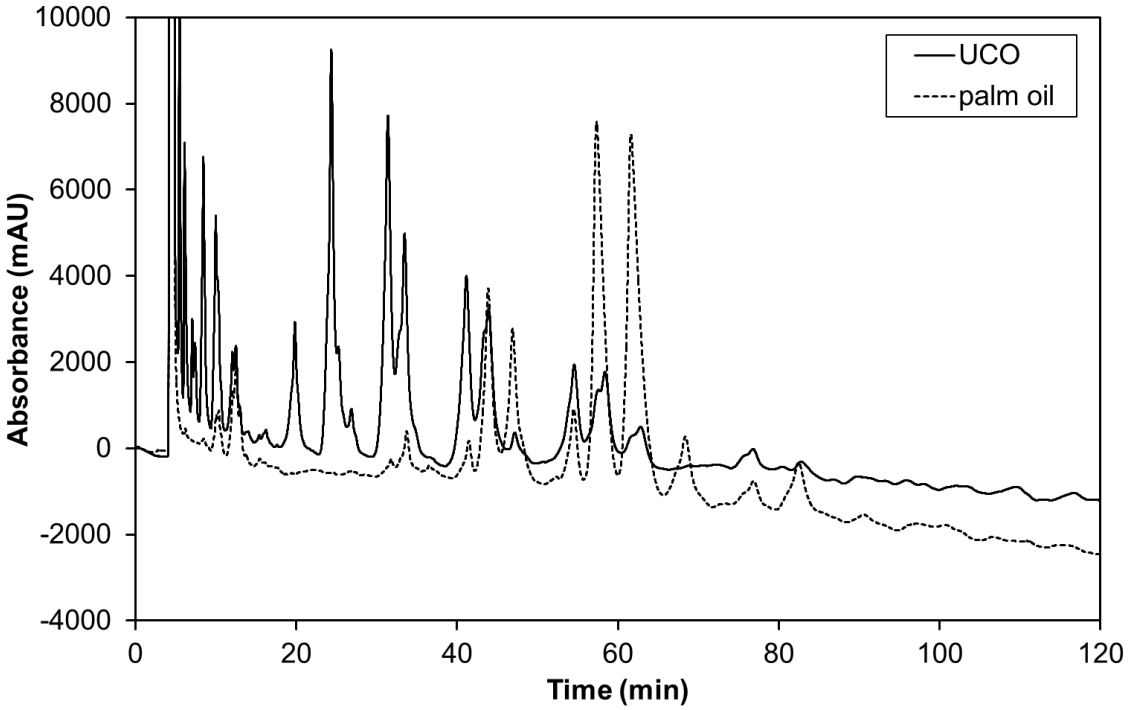

Figure 7.1. Comparison of chromatograms for UCO and palm oil using LC method 1.

7.2.2 Results of LC Method 2

Method 2 was based on the method reported by Santori et al. (2009) and Di Nicola et al. (2008). This method was selected because it was designed to analyse a broad range of components involved in the manufacture of biodiesel, achieving a reasonable separation without the additional complexity of the ternary gradient required in the method used by Holcapek et al. (1999). A comparison of the chromatograms generated using UCO and palm oil is shown in Figure 7.2.

In the case of palm oil there is a cluster of peaks between 19 – 22 min and these are expected to be TGs. The elution times reported by Santori et al. (2009) for TGs are 24 to 28 min. There are peaks along the length of the chromatogram for UCO due to the range of components. The resolution of the peaks is better than Method 1 although there is no clear distinction between all peaks. Santori et al. (2009) was able to obtain a peak resolution, however, a different column was used for the separation.

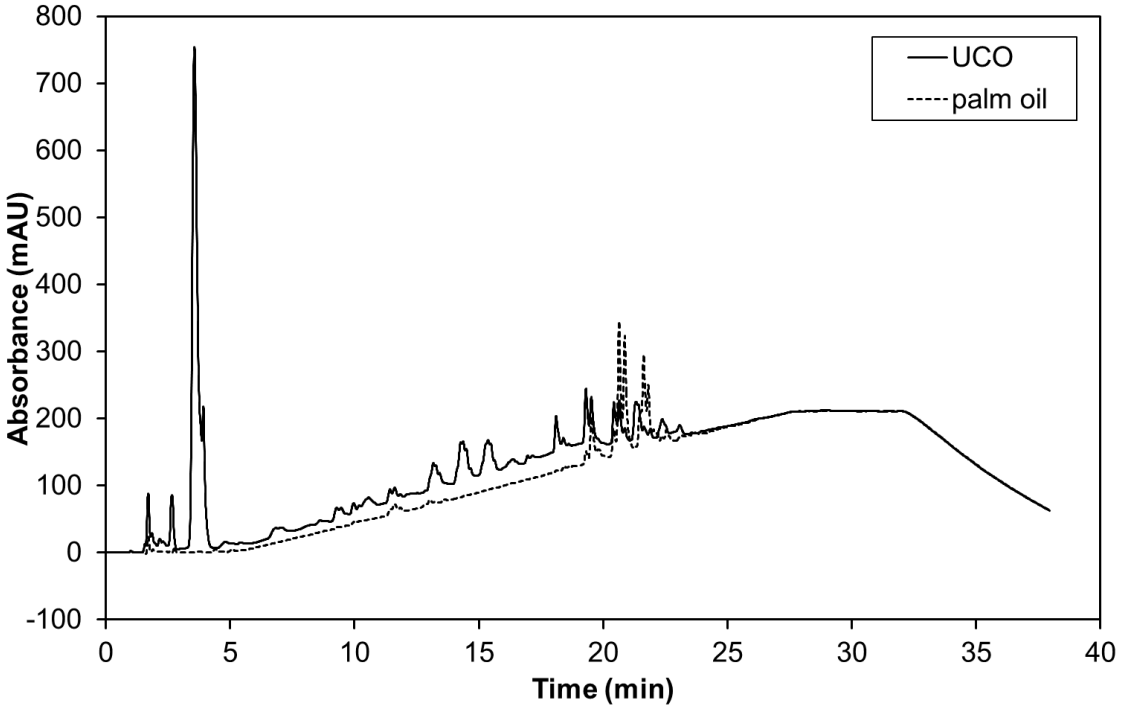

Figure 7.2. Comparison of the chromatograms for UCO and palm oil using LC Method 2

From Figure 7.2 it can be seen that there was potential to adapt this method for biodiesel analysis. In order to assess if this method could be used to quantify the biodiesel components, the possibility of characterising the FAME composition of UCO was investigated. The retention times for the FAME standards are given in Table 7.1 alongside those reported by Di Nicola et al. (2008). From Table 7.1 it can be seen that the components are eluting in the same order as that reported in the literature for this method although the elution times are roughly half those reported by Di Nicola *et al.* (2008). This fits with the experimental retention time for the TGs, suggesting the components have a lower affinity for the column in use, compared to the column used by Di Nicola et al. (2008).

Table 7.1. Retention times for methyl esters, experimentally determined and from literature

Component Name	Experimental Retention time (min)	Literature Retention time (min)*
Methyl linolenate	3.0	6.03
Methyl linoleate	4.0	7.60
Methyl oleate	5.4	10.06
Methyl palmitate	5.7	10.15
Methyl stearate	7.8	13.73

*Di Nicola *et al.*, 2008

The response factor used to determine concentrations with an external standard is defined in equation 7.1 and assumes the response is linear in the selected concentration range.

$$\text{Response Factor}\left((\text{mAU})^2.\text{L.mg}^{-1}\right) = \frac{\text{Peak Area}(\text{mAU}^2)}{\text{Concentration}(\text{mg.L}^{-1})} \quad \textbf{(7. 1)}$$

Initially the calibration was carried out with a concentration range of 1000 – 10, 000 mg/L. However, it was found that there was a strong response with methyl linolenate with a linear response for the concentration range of 100 – 1000 mg/L and this range was used for calibration. Methyl palmitate and methyl oleate co-eluted as reported by Di Nicola et al. (2008) and a combined response factor was estimated for these two components. A plot of the calibration data is shown in Figure 7.3 and the response factors are given in Table 7.2.

From these data it can be seen that there is a large variation in response factors for the methyl esters and this is inversely proportional to the number of double bonds. Methyl stearate and methyl palmitate have no double bonds and different carbon chain lengths and the response factors are very similar. The value of the response factors are a measure of the detection limit with a small response factors due to small peaks resulting from poor UV absorbance. This

indicates that the limit of detection for saturated compounds is relatively high and this was also observed by Türkan & Kalay (2006).

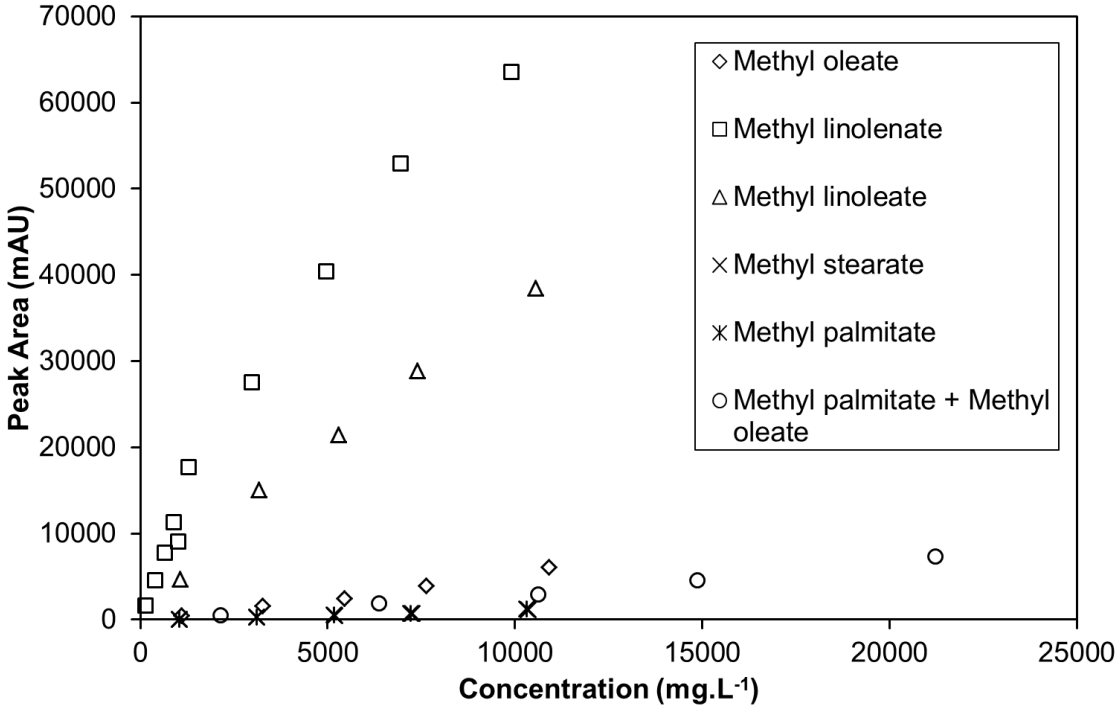

Figure 7.3. Calibration data for the determination of the methyl ester concentrations using LC Method 2.

Table 7.2. Response factors for the methyl esters

Component	CN:DB*	Response factor ($(mAU)^2.L.mg^{-1}$)
Methyl linolenate	C18:3	14.03**
Methyl linoleate	C18:2	3.484
Methyl oleate	C18:1	0.5704
Methyl palmitate	C16:0	0.1227
Methyl stearate	C18:0	0.1134
Methyl palmitate + Methyl oleate	n/a	0.3527

*CN is the carbon number and DB is the number of double bonds in the acyl chain (Santori et al., 2009)
**For the concentration range 100 – 1000mg/L

In order to characterise the FAME composition of UCO a sample was derivitised to FAMEs and analysed by GC and HPLC and a comparison of the FAME compositions are given in Table 7.3.

Table 7.3. Comparison of the methyl ester composition of UCO using HPLC and GC Analyses

	FAME Composition (%)				
Component	**HPLC Run 1**	**HPLC Run 2**	**HPLC Run 3**	**GC***	**GC**
Methyl linoleate	32.2	32.6	32.6	43.2	43.2
Methyl oleate	n/a	n/a	n/a	n/a	35.9
Methyl palmitate	n/a	n/a	n/a	n/a	13.5
Methyl oleate + methyl palmitate	65.1	66.2	64.2	49.4	n/a
Methyl stearate	1.49	0.00	2.05	3.8	3.8
Methyl linolenate	1.23	1.23	1.16	3.7	3.7

*These data were modified by adding the methyl palmitate and methyl oleate concentrations together for comparison with HPLC

From Table 7.3 it can be seen that the results for each HPLC run are similar indicating good reproducibility with the HPLC method. The biggest difference between the results is for methyl stearate, however this component has the smallest response factor and one of the lowest concentrations for the sample resulting in small to non-existent peaks. In order to determine the concentration of methyl palmitate and methyl oleate it was necessary to estimate a combined response factor. When the GC and HPLC results are compared it can be seen that there is a reasonable agreement between the results.

From these data it can be seen that there is potential to use liquid chromatography to investigate the production of biodiesel. However, improvements to the method are still required because there is co-elution of the components. In addition the UV/vis detector is not suitable because of the low response from saturated lipids meaning that calibration would be difficult.

7.2.3 Results for LC Method 3

Ultra high performance liquid chromatography (UPLC) was used to separate the components based on the method proposed by Lee & Di Gioia (2007) for Method 3. The components were detected using a time-of-flight (TOF) mass spectrometer (MS) and the resulting chromatogram for UCO is

shown in Figure 7.4. From these data it can be seen that there is some separation of the components, however, the peaks are tightly clustered in the first part of the run. In order to improve the quality of the data, changes were made to the solvent gradient, sample concentration and injection, creating Method 4.

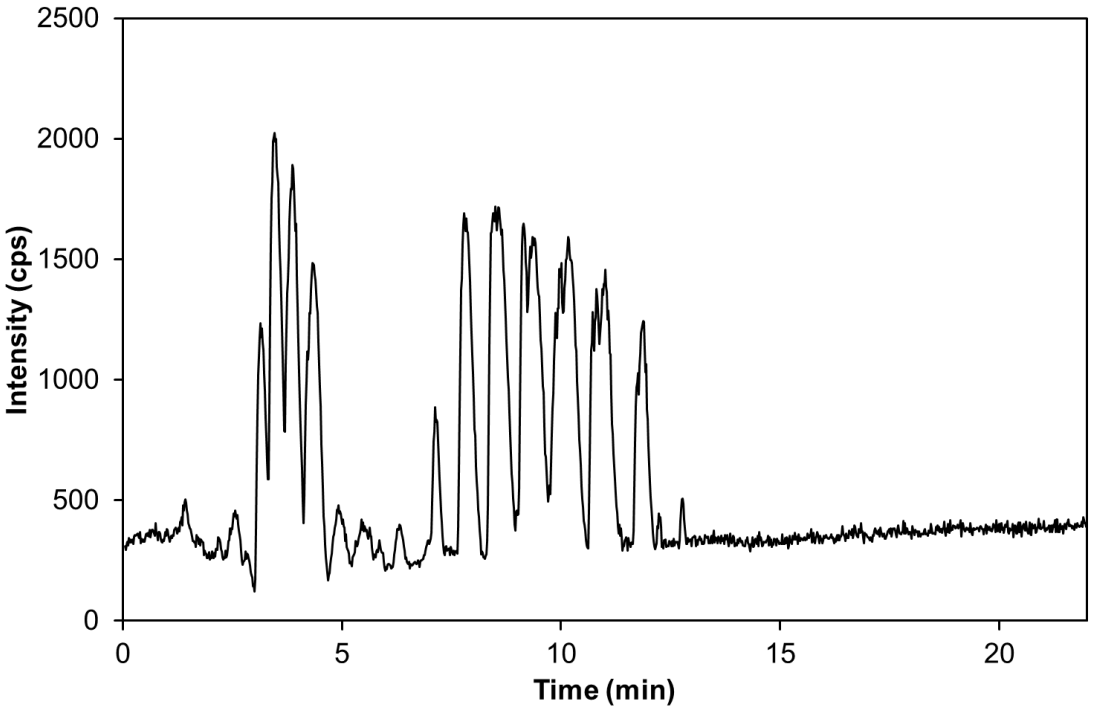

Figure 7.4. The UPLC chromatogram for UCO chromatogram using method 3 and the base peak ion (BPI) setting.

7.2.4 Results for Method 4

The amendments to Method 3 improved the separation of the components; however there is still some co-elution of the components. A typical chromatogram for UCO, using Method 4, is shown in Figure 7.5 using the base peak ion (BPI) setting.

In order for components to be detected, by the TOF mass spectrometer, they need to be charged. Based on the standards it was found that a Na^+ ion was incorporated into the MG, DG and TGs and these components were detected based on the mass-to-charge ratio (*m/z*). The FAMEs and glycerol

could not be analysed using this method because they do not charge readily. The FFAs lose a proton to become negatively charged and can be detected when the TOF detector is run in the negative mode. However, the FFAs were not well separated by the column and formed broad peaks that were not suitable for calibration. As robust methods existed for the analysis of the FAME and FFAs concentrations it was decided to continue using these methods.

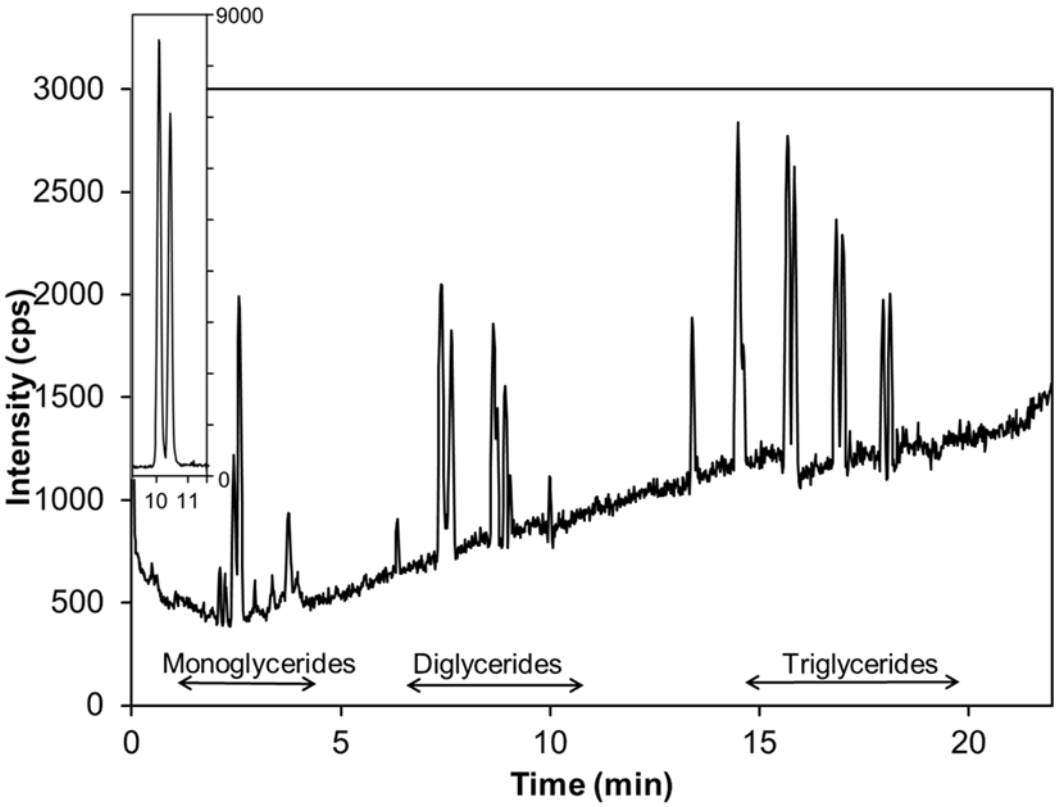

Figure 7.5. A typical UPLC chromatogram of used cooking oil (UCO) using the base peak ion (BPI) setting from Method 4. The inset shows the extracted ion chromatogram for the 1, 2 and 1, 3 isomers of dioleoyl-glycerol which gives a sodiated molecular ion $[M+Na]^+$ at m/z 643.5.

The time-of-flight (TOF) detector can be used to further separate the components based on the individual mass-to-charge ratios (*m/z*). The extracted ion chromatogram for dioleoyl-glycerol is shown as an inset in Figure 7.5. This chromatogram has two significant peaks that correspond to two isomers of dioleoyl-glycerol separated by the UPLC column.

UCO has a complex composition and in order to simplify the method it has been assumed that each component of a given species provides a similar mass spectrometric response. In addition, given the size of the molecules it is possible there is carbon 13 present and molecules with one additional carbon 13 have also been included in the concentration calculations. Two calibration standards were used for each of the MG, DG and TG species. It can be seen from the inset in Figure 7.5 that many of the components form multiple peaks due to isomers and as a result the total area under all peaks for the relevant component was used as the peak area. A typical calibration curve for trilinoleate is shown in Figure 7.6. From this figure it can be seen that the calibration curves are linear for the concentration investigated.

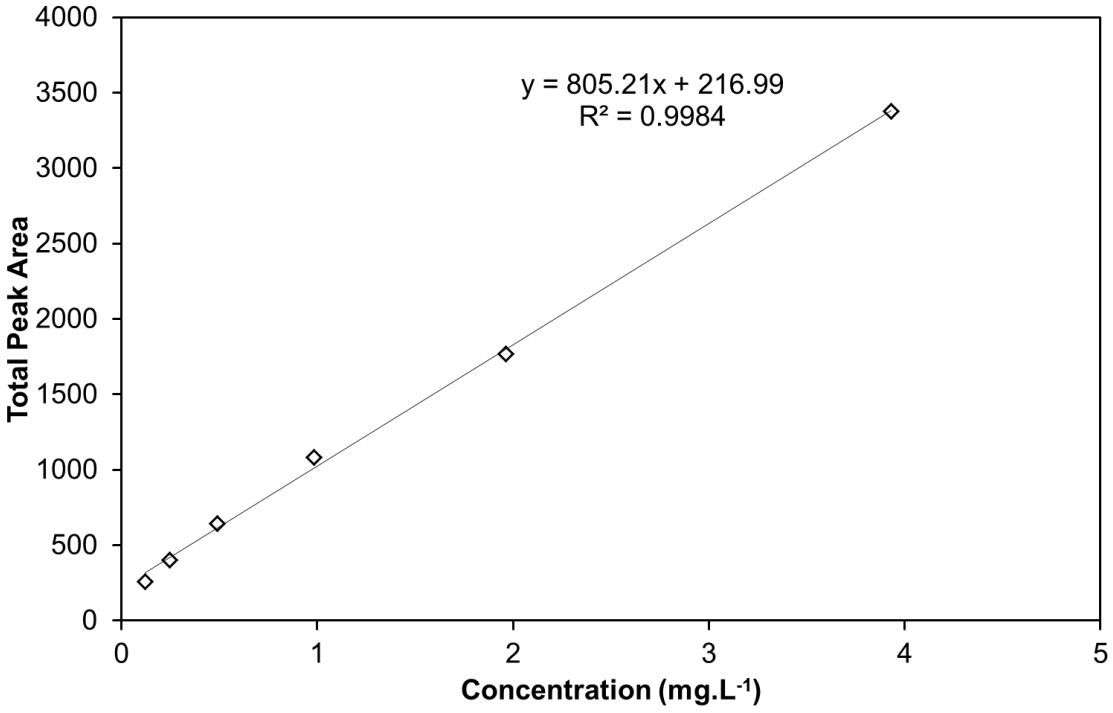

Figure 7.6. Typical calibration curve for trilinoleate

It has been found that individual diglycerides can be separated into two peaks corresponding to the 1, 2 and 1, 3 positional isomers of the diglyeceride. During the reaction these peaks disappear at different rates, an example of this is shown in Figure 7.7. The peaks at two reaction times for dioleoyl-glycerol have been compared to the 1, 3 dioleoyl-glycerol standard which is composed predominantly of the 1, 3 isomer. The second peak corresponds to the 1, 2

isomer. From the data it can be seen that the 1, 3 isomer is transesterified preferentially over the 1, 2 isomer by the Novozyme 435 enzyme catalyst. A comparison of the concentration of two palmitoyl-oleoyl-glycerol isomers during the reaction is shown in Figure 7.8. The concentration has been calculated for these two species because there is better separation of the isomers than dioleoyl-glycerol and it has been assumed that the isomers elute in the same order. Novozyme 435 was used to catalyse the reaction and these data show that this catalyst has some stereoselectivity. Enzymes have been investigated for biodiesel production, but these data indicate that information on the fatty acid composition of a particular oil may not be sufficient to determine how well the enzyme will catalyse a particular reaction. The isomer composition can also determine the rate and the extent of reaction.

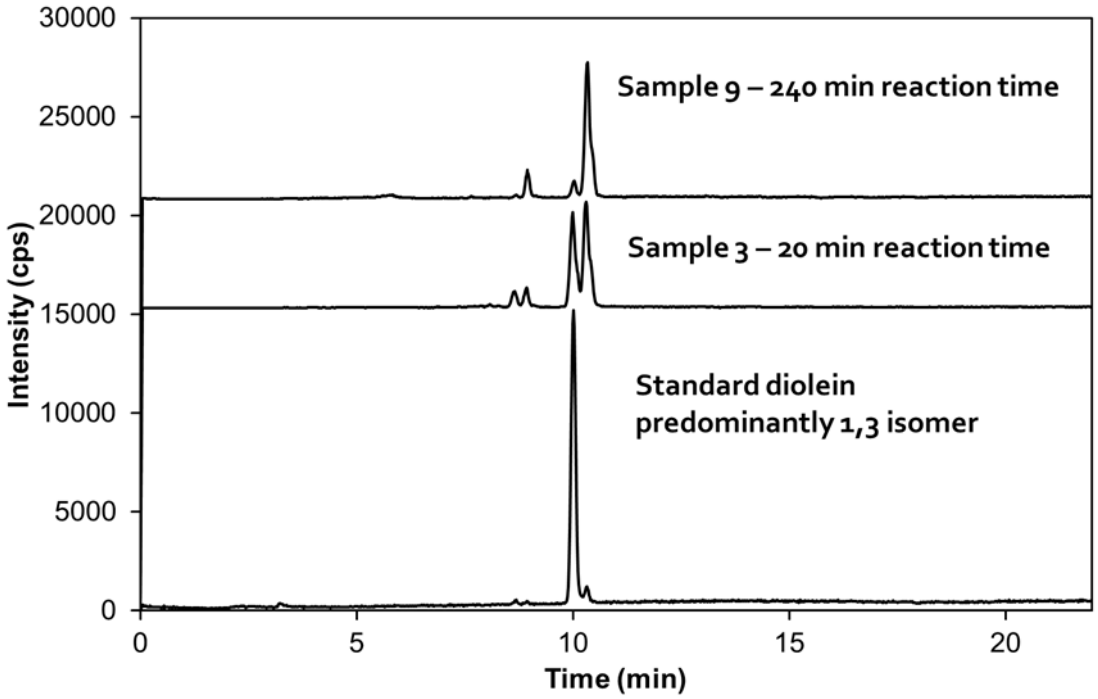

Figure 7.7. Selected ion LC-MS chromatograms showing depletion of 1,3 positional isomer of dioleoyl-glycerol [M+Na]+ ion at m/z 643.5 and comparison with the dioleoyl-glycerol standard containing predominantly 1, 3 positional isomers.

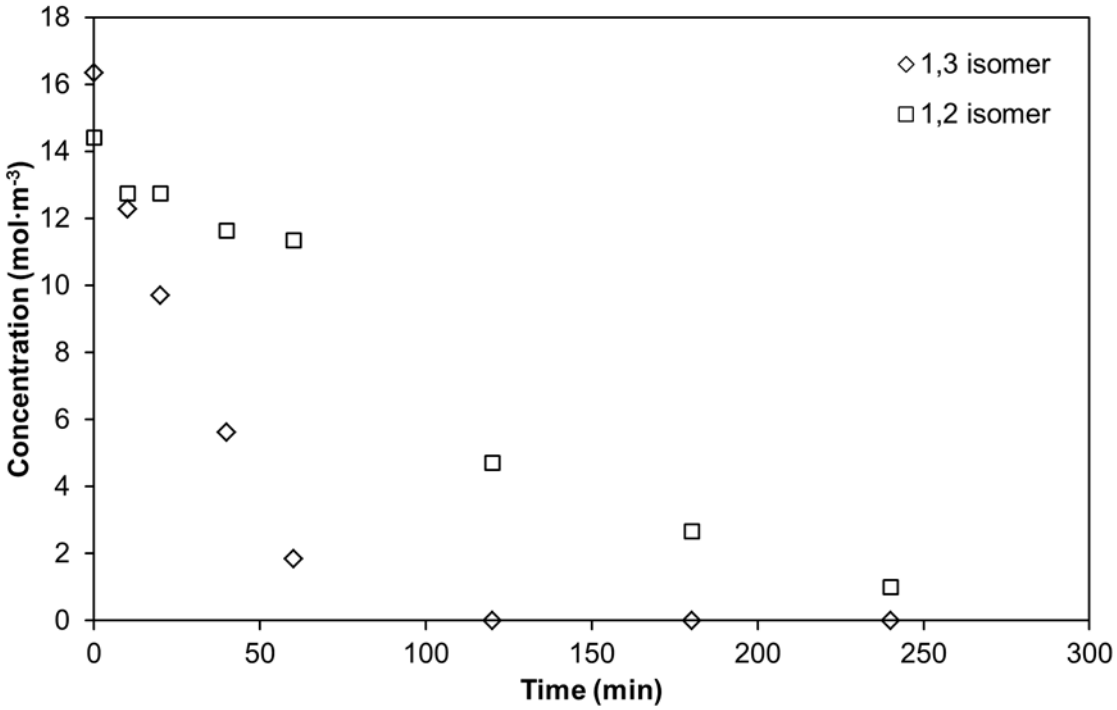

Figure 7.8. A comparison of the rate of disappearance of diglyceride peaks (palmitoyl-oleoyl-glycerol)

It was found that there was some scatter in the concentration results using Method 4, particularly with regard to the TG concentrations. As a result, a quality control sample was injected at regular intervals to ensure the instrument behaved consistently. The quality control sample was made by adding 100 μL of each sample to a vial to make up a mixture of all samples. A typical plot of the concentration with injection time is shown in Figure 7.9. The quality control sample was injected repeatedly at the start of the sequence as part of the column conditioning procedure. From Figure 7.9 it can be seen that initially there was some scatter, however, the results settled and overall the results were consistent, indicating that the instrument was behaving consistently.

It has been found that while Method 4 can be used to quantify the MG, DG and TG concentrations, it was not possible to use Method 4 to analyse other components found in the UCO. The FAMEs and glycerol could not be analysed because they do not charge well and the FFAs are not well separated by the column.

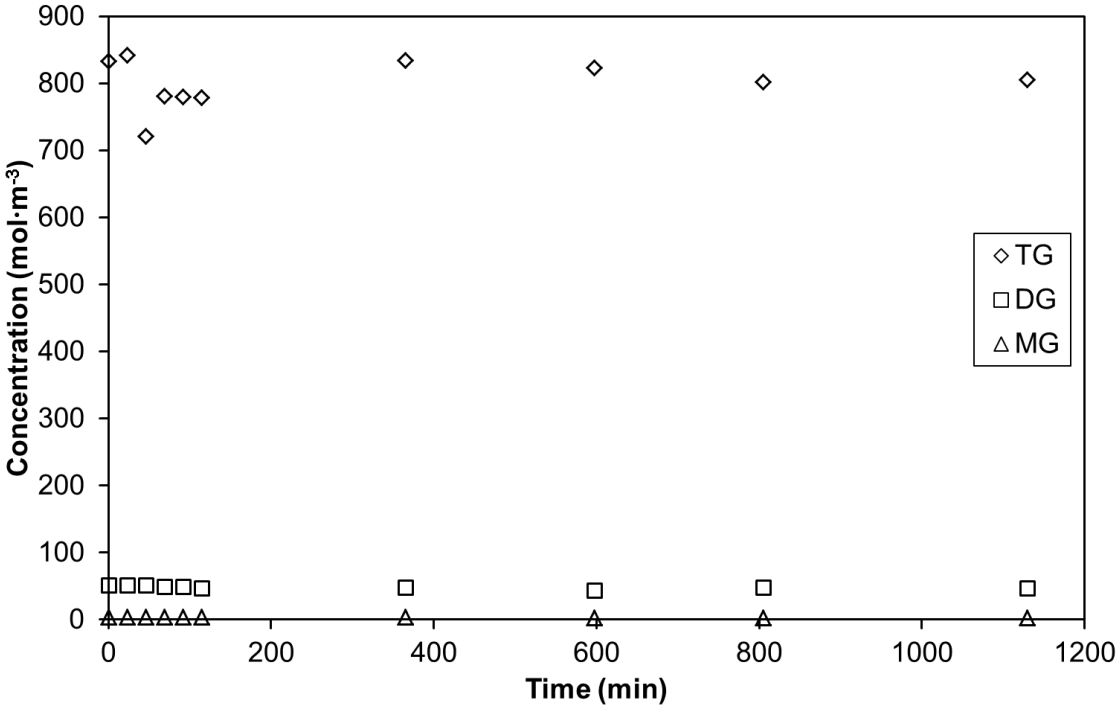

Figure 7.9. A typical comparison of concentrations from the quality control sample and various intervals during the analysis

7.2.5 Liquid Chromatography Applied to Batch Experiments

It was proposed that the additional FAME formation that occurred when Novozyme 435 was used to catalyse the esterification pre-treatment of UCO (Chapter 6) was due to transesterification side reactions. In order to investigate this further a method has been developed to determine the MG, DG and TG concentrations. A comparison of the change in concentration of the MG, DG, TG, FAME and FFAs is shown in Fig. 7.10.

From the data in Figure 7.10 it can be seen that the MG concentration increases slightly and then decreases, which is typical of a reaction intermediate. The DG concentration decreases steadily during the course of the reaction. At the end of the 6 h reaction time most of the MG and DGs have been consumed and this would account for the additional FAME formation. In contrast, the change in TG concentration is very small. Overall, there is a slight decrease in the concentration of triglycerides. Thus, while the TGs will react,

the rate is much slower when compared to the MGs and DGs. This is consistent with previous experiments where it was found that when Novozyme 435 was used as a transesterification catalyst, the transesterification of triglycerides was the rate limiting step with no accumulation of MG or DGs during the reaction (Türkan & Kalay 2006).

It was found that the extent of FAME formation varied with temperature (Chapter 6) and the change in concentrations at 60 °C is shown in Figure 7.11. From these data it can be seen that the trends for most of the components is similar to Figure 7.10. However, the TG concentration is decreasing faster at the higher temperature.

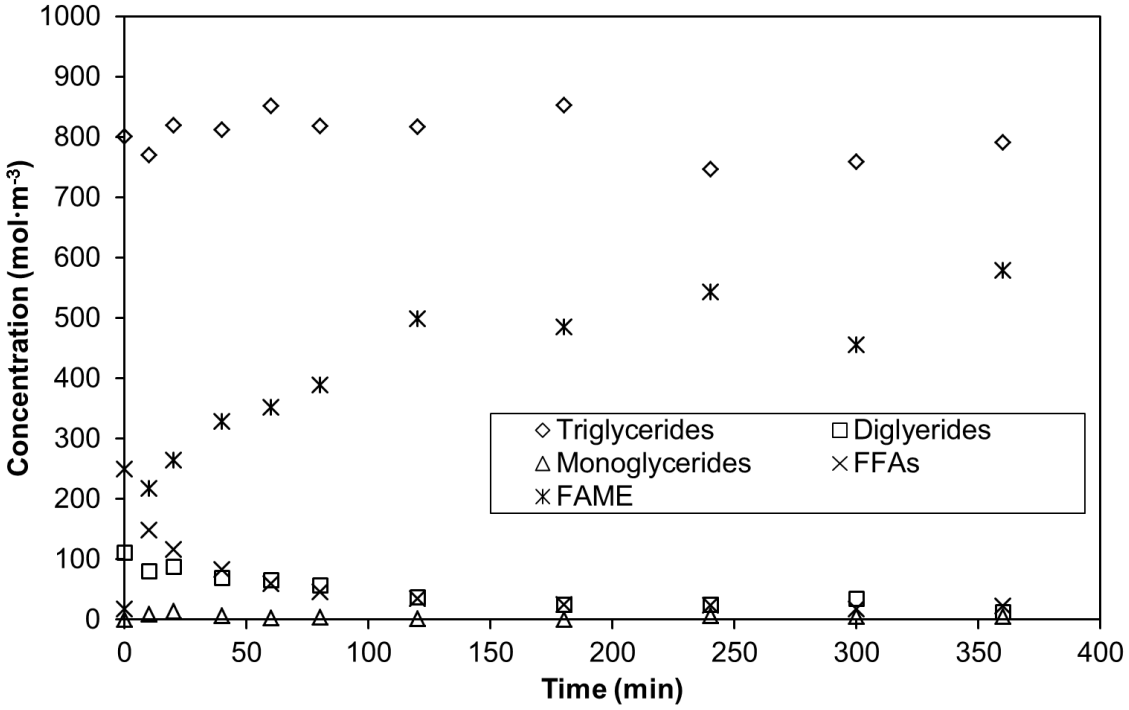

Figure 7.10. Change in the concentration of the triglycerides (TG), diglycerides (DG), monoglycerides (MG), fatty acid methyl esters (FAME / biodiesel) and fatty acids (FFAs) during the pre-treatment of UCO for biodiesel production. This experiment was carried out using Novozyme 435 as the catalyst at 50 °C.

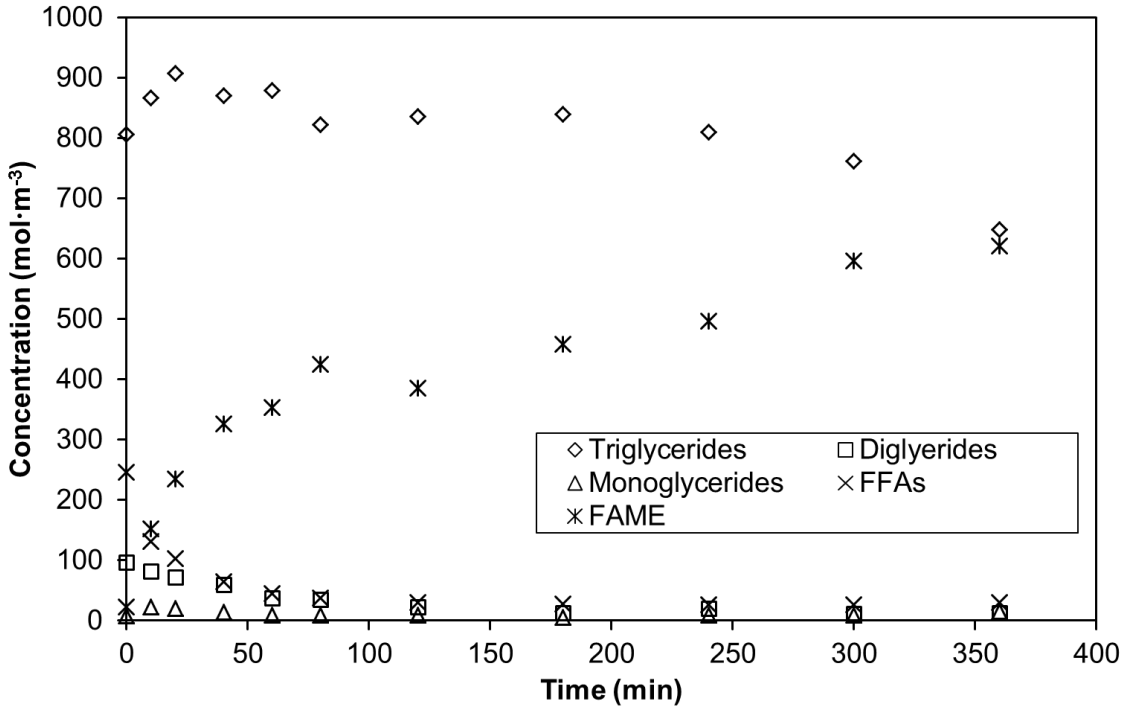

Figure 7.11. Change in the concentration of the triglycerides (TG), diglycerides (DG), monoglycerides (MG), fatty acid methyl esters (FAME / biodiesel) and fatty acids (FFAs) during the pre-treatment of UCO for biodiesel production. This experiment was carried out using Novozyme 435 as the catalyst at 60 °C.

7.3 Kinetic Modelling

7.3.1 Results using the Literature Model

Various mechanisms for the reactions catalysed by enzymes to form biodiesel were investigated by Cheirsilp et al. (2008). It was found that mechanism 3, which allowed for the simultaneous transesterification and esterification hydrolysis reactions gave the best fit to the experimental data.

The differential equations proposed by Cheirsilp et al. (2008) were solved by means of the MATLAB “ode23s” function. This was combined with the MATLAB “fminsearch” function to minimise the residual of the sum of squares, ie., the difference between the experimental and calculated values. The difference between the model and experimental data was condensed into a single value, using the sum of squares, for the “fminsearch” and weighting has not been applied. The program code is given in Appendix A. It was found that

the model predicted a reasonable fit for most of the components. The comparison for the MG, DG and TG concentrations is shown in Figure 7.12.

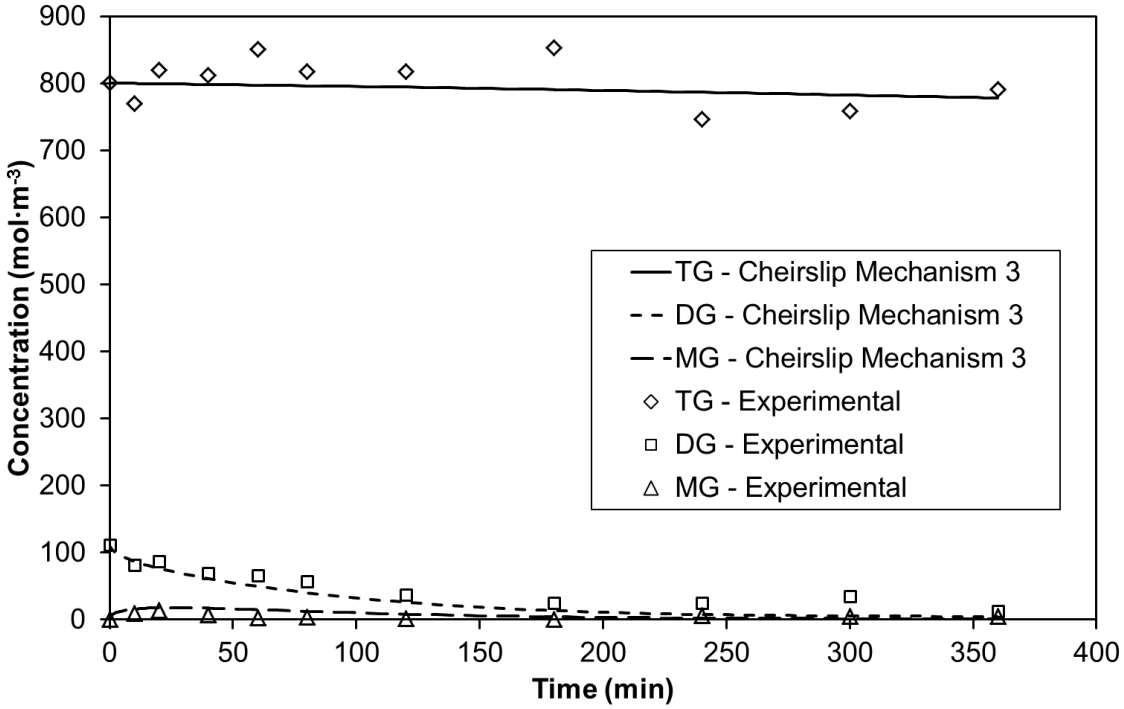

Figure 7.12. A comparison of the MG, DG and TG concentration trends predicted by Cheirsilip et al. (2008) Mechanism 3 and the experimentally determined concentrations. Using Novozyme 435 at 50 °C.

However it was found that there was a substantial difference between the predicted and experimental water concentrations as shown in Figure 7.13. This is because the model developed by Cheirslip et al. (2008) does not allow for water formation. The system investigated by Cheirslip et al. (2008) required the addition of water as a part of the transesterification reaction. In contrast the system investigated as part of this work using Novozyme 435 did not require water addition for the reaction to proceed.

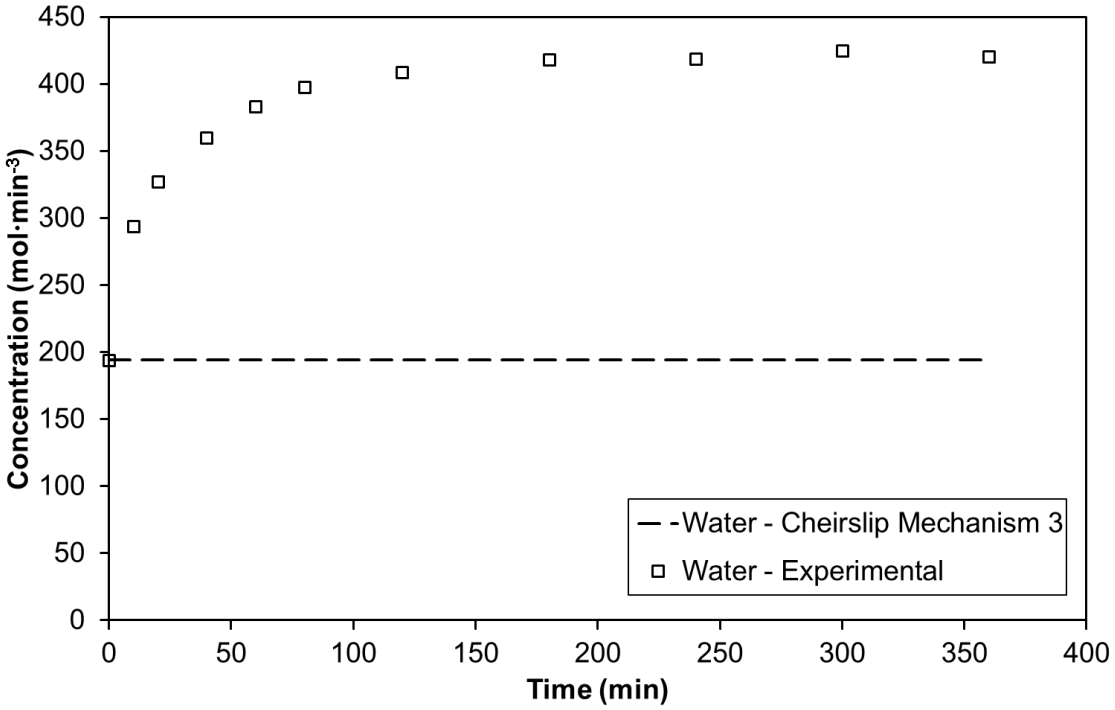

Figure 7.13. A comparison of the water concentration trends predicted by Cheirslip Mechanism 3 and the experimentally determined concentrations. Novozyme 435 at 50 °C.

7.3.2 Development of the Kinetic Model

The model developed by Cheirsilp et al. (2008) was amended to allow for water formation and the resulting conceptual scheme is shown in Figure 7.14. In order to simplify the model it was assumed that the components can be grouped together. It was also assumed that the inhibition of the enzyme by alcohol followed the competitive inhibition model. It has been shown that for the reaction conditions investigated there are no mass transfer limitations (Haigh et al. 2013) and as a result this model applies to the intrinsic reaction kinetics.

The reactions are expected to follow a Ping Pong Bi Bi mechanism as detailed in Chapter 2, Section 2.5. A schematic representation and detailed mechanism for the esterification reaction are shown in Figures 2.7 and 2.8. According to this reaction scheme, the free enzyme (E) reacts with alcohol (Al), triglycerides (T), diglycerides (D), monoglycerides (M) and FFAs (F) to form the associated complexes; E·Al, E·T, E·D, E·M and E·F respectively. The hydrolysis and esterification reactions are then expected to occur in parallel

with the E·T, E·D and E·M complexes reacting with water (W) to form F or with Al to form esters (Es) eventually leading the formation of glycerol (G).

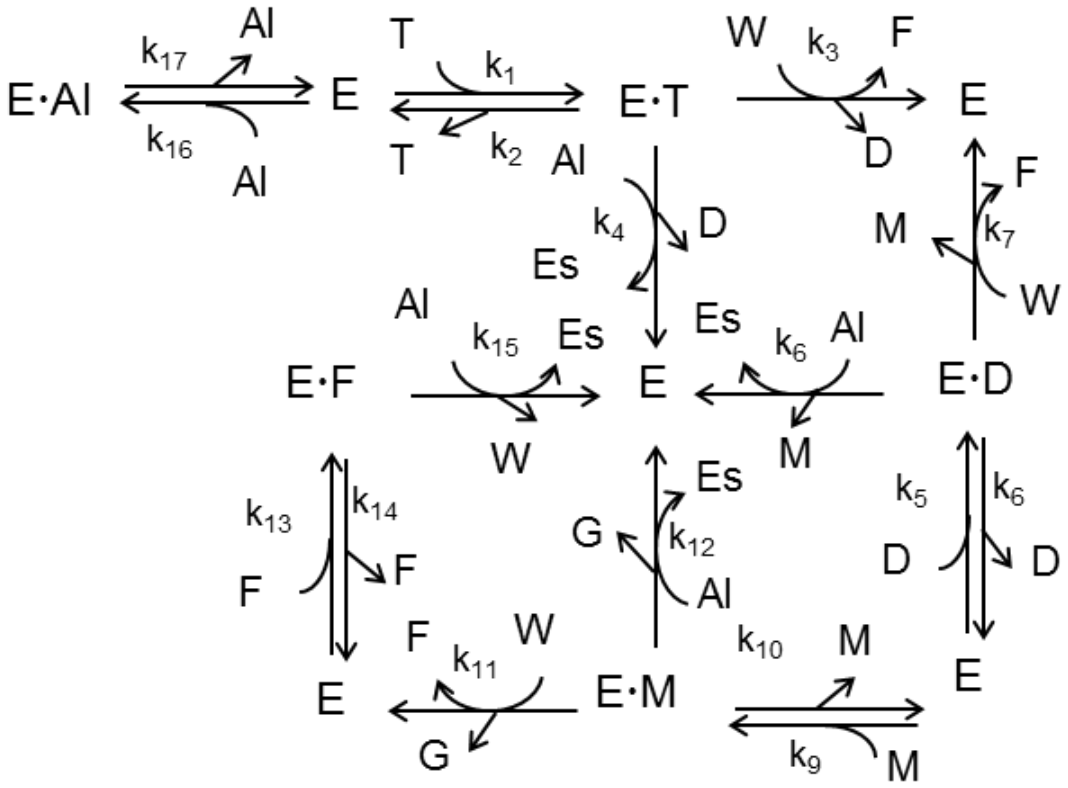

Figure 7.14. The conceptual scheme of the amended mechanism

The rate expressions have been developed by assuming that the hydrolysis and esterification reactions are rate limiting and the resulting rate equations are:

$$\frac{d[T]}{dt} = -(V_{mT}[W] + V_{eT}[Al])[T][E^*] \quad \textbf{(7.2)}$$

$$\frac{d[D]}{dt} = ((V_{mT}[W] + V_{eT}[Al])[T] - (V_{mD}[W] + V_{eD}[Al])[D])[E^*] \quad \textbf{(7.3)}$$

$$\frac{d[M]}{dt} = ((V_{mD}[W] + V_{eD}[Al])[D] - (V_{mM}[W] + V_{eM}[Al])[M])[E^*] \quad \textbf{(7.4)}$$

$$\frac{d[G]}{dt} = (V_{mM}[W] + V_{eM}[Al])[E^*] \quad \textbf{(7.5)}$$

$$\frac{d[F]}{dt} = \frac{-d[W]}{dt} = ((V_{mT}[T] + V_{mD}[D] + V_{mM}[M])[W] - V_{eEs}[F][Al])[E^*] \quad \textbf{(7.6)}$$

$$\frac{d[Es]}{dt} = \frac{-d[Al]}{dt} = (V_{eT}[T] + V_{eD}[D] + V_{eM}[M] + V_{eEs}[F])[Al][E^*] \quad \textbf{(7.7)}$$

Where the [E*] is:

$$[E^*] = \frac{[E_T]}{(1 + K_{mT}[T] + K_{mD}[D] + K_{mM}[M] + K_{mF}[F] + (\frac{Al}{K_I})} \quad \textbf{(7. 8)}$$

V_{mT}, V_{mD} and V_{mM} are the hydrolysis rate constants and are defined as $V_{mT} = k_3k_1/k_2$, $V_{mD} = k_7k_5/k_6$ and $V_{mM} = k_{11}k_9/k_{10}$. V_{eEs} is the esterification rate constant and is defined as $V_{eEs} = k_{15}k_{13}/k_{14}$. V_{eT}, V_{eD} and V_{eM} are the rate constants for transesterification and defined as $V_{eT} = k_4k_1/k_2$, $V_{eD} = k_8k_5/k_6$ and $V_{eM} = k_{12}k_9/k_{10}$. The equilibrium constants K_{mT}, K_{mD}, K_{mM}, K_{mF} and the inhibition constant K_I are defined as $K_{mT} = k_1/k_2$, $K_{mD} = k_5/k_6$, $K_{mM} = k_9/k_{10}$, $K_{mF} = k_{13}/k_{14}$ and $K_I = k_{17}/k_{16}$.

The unknown parameters were determined by fitting equations (7.2) to (7.8) to the batch experimental data using MATLAB according to the method described in Section 7.4.1.

7.3.3 Results using the Amended Kinetic Model

A comparison of the model and experimental water concentrations is shown in Figure 7.15. From these data it can be seen that the amended model allows water formation and there is a good agreement between the amended model and the experimental water concentrations although the model predicts a slightly higher water concentration. A comparison of the experimentally determined concentrations compared to those predicted by the model for the MG, DG, TG and FAME concentrations is shown in Figure 7.16. There is a reasonable fit between the experimental and model parameters.

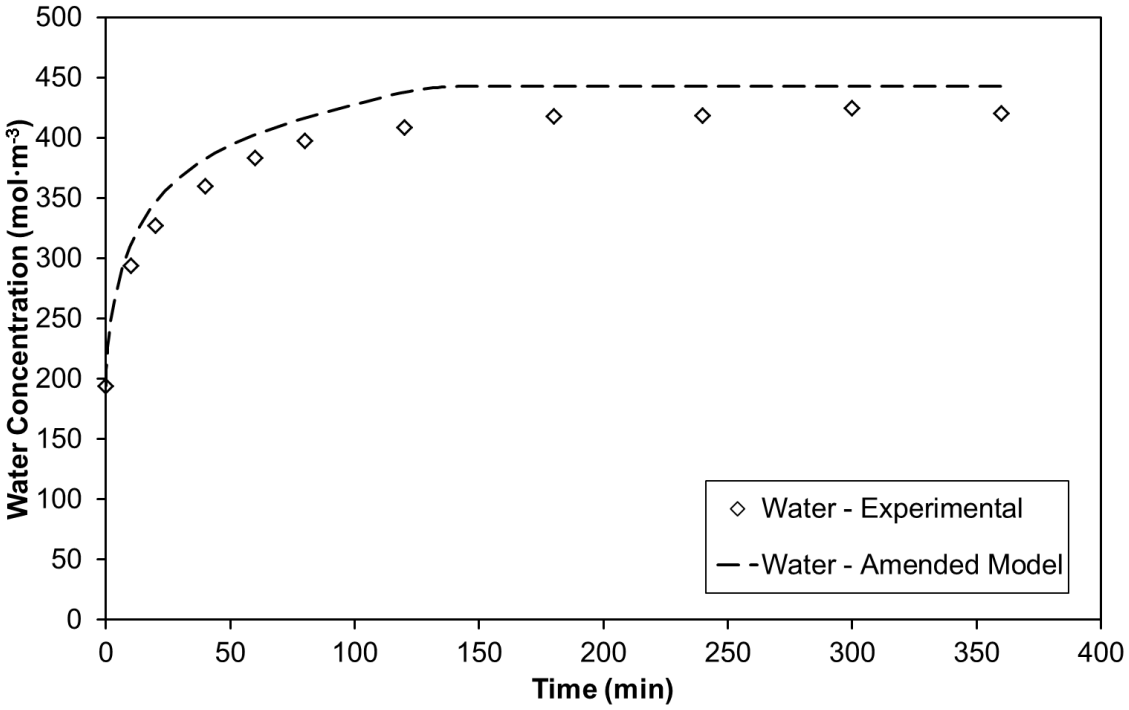

Figure 7.15. A comparison of the experimental and model water concentrations using the amended model.

In the case of the DG and MG concentrations the model developed by Cheirsilp et al. (2008) fits these concentrations better than the amended model. The amended model predicts a faster initial decrease in the concentration than the experimental data. One of the assumptions made as part of the model development was that all the DG species could be treated as a single component. However, it can be seen from Figures 7.7 and 7.8 that the 1, 2 and 1, 3 positional isomers react at different rates and the DG trend is the sum of these two trends. The model could be improved by allowing for both DG isomers. However this would increase the complexity of the model and substantially increase the complexity of the component analysis.

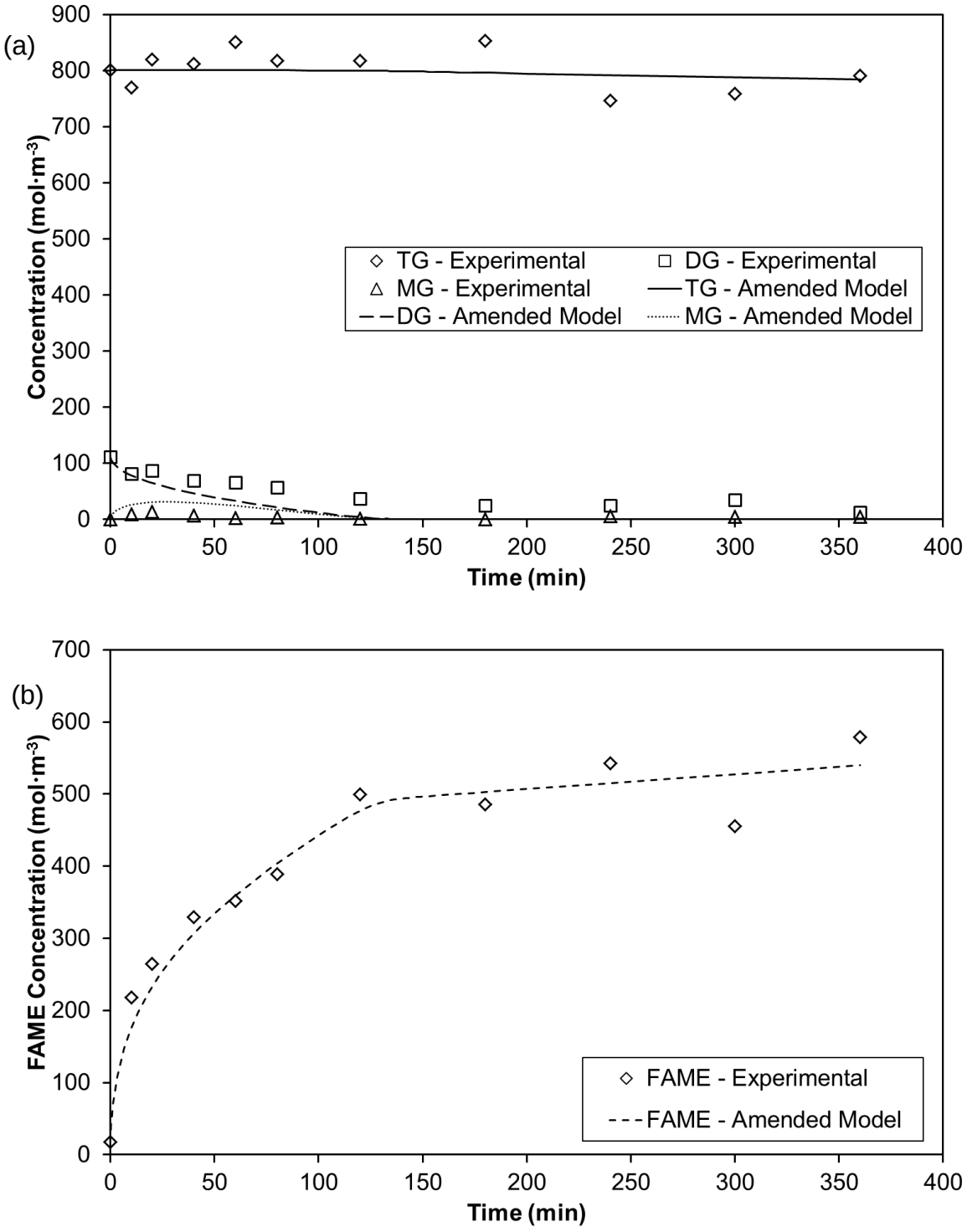

Figure 7.16. A comparison of the concentrations from the experiments compared to those predicted by the model with (a) the MG, DG and TG concentrations and (b) showing the FAME concentrations. The experiment was carried out at 50 °C using Novozyme 435.

The parameters predicted by the model for this system are shown in Table 7.4 and have been compared to the values found in the literature

(Cheirsilp et al. 2008). From these data it can be seen that there are substantial differences between these values, as expected, because the systems investigated are different. Novozyme 435 was used instead of immobilized *Pseudomonas sp*, methanol was used in place of ethanol, water was not added to the reaction mixture and the model has been modified to allow for water formation during the esterification reaction. Novozyme 435 is known to result in slow reactions with TGs (Tongboriboon et al. 2010; Ganesan et al. 2009) and the parameters for the TG reactions (V_{mT} and V_{eT}) are lower than the literature values. From these data it can be seen that the DGs and MGs react more readily than the TGs. As expected the esterification reaction rate constant (V_{es}) is greater than the literature value because Novozyme 435 has been shown to favour the esterification reaction (Tongboriboon et al. 2010). The value for the alcohol inhibition constant (K_I) is greater than the literature value and this can be accounted for because methanol was used instead of ethanol. The two catalysts exhibit different levels of alcohol tolerance. Overall the data indicate that Novozyme 435 can catalyse the transesterification reaction in parallel with the hydrolysis esterification reaction sequence.

Table 7.4. The Model Parameters

Parameters	Predicted Values ($mol^{-1}\cdot min^{-1}$)	Literature Values* ($mol^{-1}\cdot min^{-1}$)
V_{mT}	0.0130	1.27
V_{mD}	0.447	1.35
V_{mM}	78.6	3.25
V_{eEs}	48.4	23.1
V_{eT}	0.00430	45.9
V_{eD}	25.5	19.6
V_{eM}	18.5	16.1
K_{mT}	0.00770	0.482
K_{mD}	0.00290	0.387
K_{mM}	3.92	0.329
K_{mF}	0.00410	0.187
K_I	764	14.7

*Cheirsilp et al. (2008)

7.4 Conclusions

It was found that when Novozyme 435 is used as the esterification pretreatment catalyst for the preparation of biodiesel from UCO the amount of FAME formed was higher than expected (Chapter 6). It was proposed that this was due to transesterification side reactions and various liquid chromatography methods have been investigated to monitor the MG, DG and TG concentrations. It was found that Method 4 using UPLC and a TOF MS detector was most suitable for the analysis. It has been shown that this method has sufficient sensitivity to monitor the progress of specific isomers with the 1, 3 DG isomers being consumed faster than the 1, 2 isomer.

A series of batch experiments was subsequently monitored for the MG, DG, TG, FAME and FFAs concentrations and it was found that the MGs and DGs were reacting confirming the existence of side reactions at high temperatures. In addition it was found that while there was reduction in the TG concentration at higher temperatures, the rate was very slow.

Cheirslip et al. (2008) used kinetic modelling to show that enzyme catalysed reactions proceed with transesterification in parallel with the hydrolysis esterification sequence of reactions. The proposed model was amended to allow for water formation and it was found that there was a good fit between the proposed model and the experimental results. These results show Novozyme 435 can simultaneously catalyse the hydrolysis, esterification and transesterification reactions in UCO.

Chapter 8: Enzymatic Biodiesel Production

8.1 Introduction

Enzyme catalysts have been widely considered for the production of biodiesel (Enweremadu & Mbarawa 2009; Ganesan et al. 2009; Atadashi et al. 2013). One of the advantages of enzyme catalyst is that high conversions are possible at relatively benign operating conditions (Shahid & Jamal 2011). Another advantage is that the saponification side reactions, due to water and free fatty acids (FFAs), do not occur. The class of enzyme catalysts used to investigate biodiesel production are lipases (Semwal et al. 2011; Akoh et al. 2007). The function of lipases is to catalyse the breakdown of lipids by cleaving the carboxyl bond (Paiva et al. 2000; Souza et al. 2009). The lipases most frequently investigated for biodiesel production are a lipase from *Candida antarctica* lipase B and *Pseudomanas cepacia*. *P. cepacia* has recently been reclassified as *Burkholderia cepacia* (Torres et al. 2008) however for simplicity the name *P. cepacia* has been used for this work.

Lipases can be used in a free or immobilised form however given that the aim of this work is to investigate heterogeneous catalysts the focus will be on immobilised enzymes. A commercially available form of *C. antarctica* is Novozyme 435 with acrylic resin as the immobilisation support (Tongboriboon et al. 2010), and while it has been found that high conversions are possible a long reaction time is required (Al-Zuhair et al. 2009). Novozyme 435 has been investigated for the esterification pre-treatment reaction (Chapter 6) and is has been shown that the transesterification of triglycerides (TG) is very slow (Chapter 7).

The transesterification reaction catalysed by *P. cepacia* has been widely reported however most researchers have focused on immobilisation of the free enzyme (Li et al. 2011; Zheng et al. 2012). There are limited reports on a

commercially available form of *P. cepacia* immobilised on diatomaceous earth, known as Amano Lipase PS-IM and manufactured by Amano Lipase Inc. On this basis Amano Lipase PS-IM will be investigated for the transesterification reaction.

Esterification pre-treatment to convert the FFAs in used cooking oil (UCO) to fatty acid methyl esters (FAME), prior to transesterification, was discussed in Chapter 6. This is particularly relevant when base catalysts are used to catalyse the transesterification reaction because FFAs react with the catalysts leading to unwanted saponification side reactions (Enweremadu & Mbarawa 2009). Lipases are not affected by FFAs (Chen et al. 2009; Lam et al. 2010). In Chapter 7 it was shown that the simultaneous esterification of FFAs and transesterification of diglycerides (DG) and monoglycerides (MG) is possible using Novozyme 435. However the conversion of TGs, which make up the bulk of UCO, was relatively low and it is hoped that Amano Lipase PS-IM will be more effective at the transesterification of TGs. As a result it is proposed to carry out Amano Lipase PS-IM catalysed transesterification (enzymatic biodiesel production stage 1), followed by Novozyme 435 catalysed esterification and transesterification (enzymatic biodiesel production stage 2).

Enzymatic biodiesel production stage 1, using Amano Lipase PS-IM as the catalyst, is discussed in Section 8.2, starting with the effect of water on the FFAs concentration and TG conversion in Section 8.2.1. The TG conversion was calculated using the FAME concentration and the assumption that the UCO initially added is composed only of TGs which can be converted to FAME. The effect on TG conversion of the mole ratio and stepwise addition of methanol are discussed in Section 8.2.2. The effect of stirring speed, temperature and catalyst loading are discussed in Sections 8.2.3-8.2.5. Enzymatic biodiesel production stage 2 using Novozyme 435 as the catalyst is discussed in Section 8.3.

8.2 Enzymatic Biodiesel Production Stage 1

8.2.1 Effect of water

The effect of water addition, on conversion, using Amano Lipase PS-IM has been investigated and the results are given in Figure 8.1. There is approximately 0.53 wt% water initially present in the UCO in addition to the water added to the reaction mixture. From these data it can be seen that water is required in order for the reaction to proceed. Overall the FFAs concentration increases with increasing water addition. In comparison it can be seen from Figure 8.1 (b) that when sufficient water is added this results in a high TG conversion with a similar conversion for an addition of 5 and 10 vol%. Further increases in the amount of water result in a steady decrease in the TG conversion.

It has been shown that Amano Lipase PS-IM can catalyse transesterification, esterification and hydrolysis (Cheirsilp et al. 2008). These data suggest that as the water concentration increases the hydrolysis side reaction is favoured. It should be possible to convert the FFAs to FAME using Novozyme 435, thus increasing the TG conversion, however the aim of stage 1 is to maximise the TG conversion. Similar high TG conversions are achieved when 5 and 10 vol% water are added to the reaction mixture. The addition and subsequent removal of water will increase the costs and it is preferable to minimise the amount of water added. On this basis the optimum water addition is 5 vol%

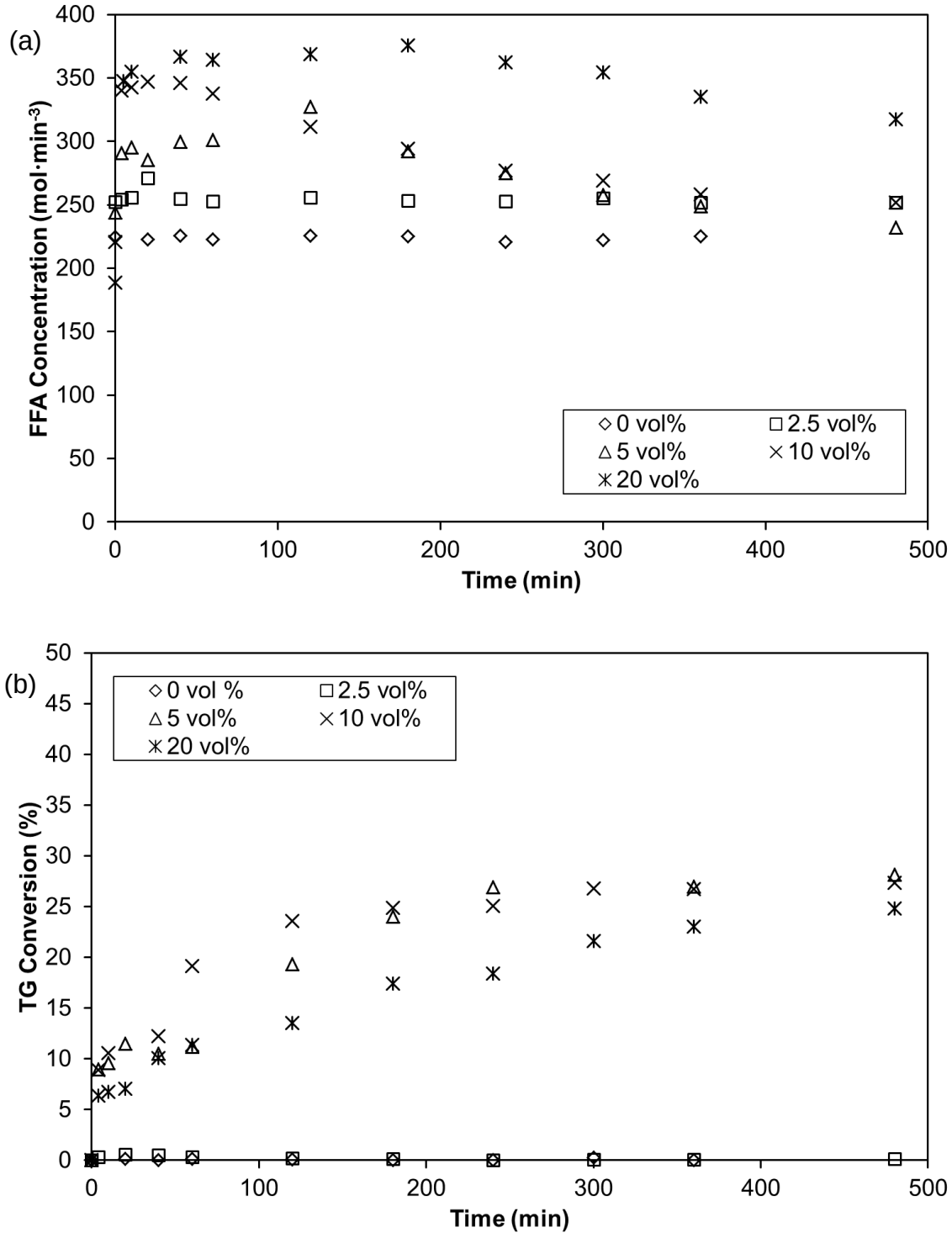

Figure 8.1. The effect of water addition on the (a) FFAs concentration and (b) the TG conversion using Amano Lipase PS-IM as the catalyst. (With a mole ratio of 3.12:1, a temperature of 40 °C, a catalyst loading of 0.786 wt% and a stirrer speed 500 rpm)

8.2.2 Effect of methanol

The effect of the methanol to TG mole ratio on TG conversion using Amano lipase PS-IM is shown in Figure 8.2. From these data it can be seen that Amano lipase PS-IM follows a similar trend to Novozyme 435 in that there is an optimum conversion. The catalyst is poisoned at higher values and for lower mole ratios there is insufficient methanol for conversion. Amano Lipase PS-IM has a higher methanol tolerance when compared to Novozyme 435. The methanol to FFAs mole ratio with Novozyme 435 was found to be 6.3:1. This corresponds to a methanol to TG mole ratio of 1.25:1. The water added when using Amano Lipase PS-IM will dilute the methanol and may increase the mole ratio that can be used. The optimum mole ratio is 3:1.

A TG conversion of 40% was achieved at the optimum mole ratio of 3:1. Shimada et al. (2002) showed that it is possible to overcome this problem and increase conversion using stepwise addition of methanol. The effect of stepwise addition of methanol is shown in Figure 8.3 with methanol added after 4 h. These data indicate that for the conditions investigated there is no additional conversion when methanol is added after 4 h of reaction time. It is possible that conversion could be improved with the right conditions. However, it can be seen from Figure 8.2 (b) that conversion is very sensitive to changes in the mole ratio and they may be difficult to identify. There are cases where the benefits of stepwise addition of alcohol are limited (Shah et al. 2004; Tongboriboon et al. 2010). An increase in TG conversion is not possible using stepwise addition of methanol at the conditions investigated.

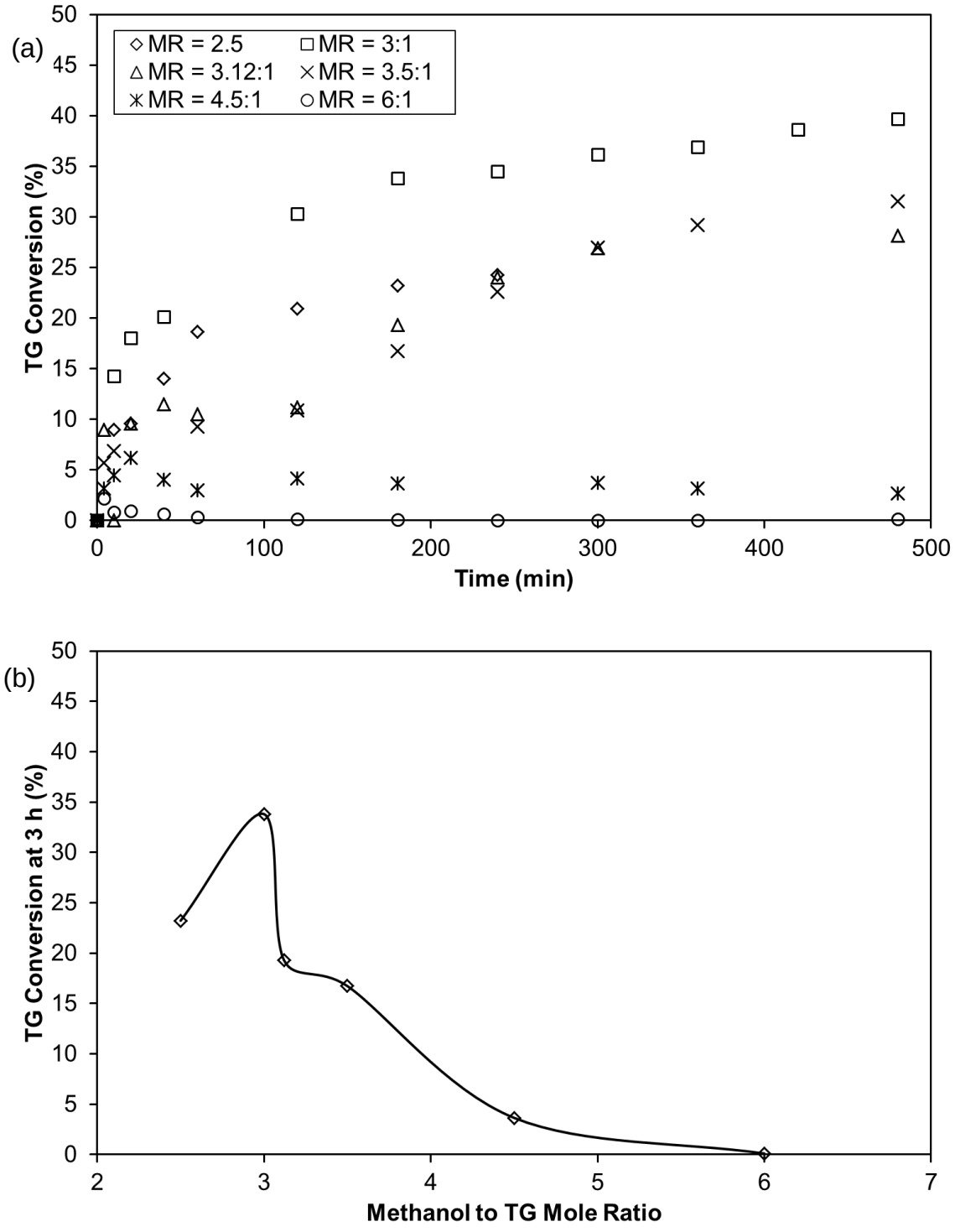

Figure 8.2. The effect of the methanol to TG mole ratio on TG conversion with (a) showing the overall conversion trend and (b) showing the conversion at 3h. (With water addition of 5 vol%, a temperature of 40 °C, 0.786 wt% and a stirrer speed 500 rpm)

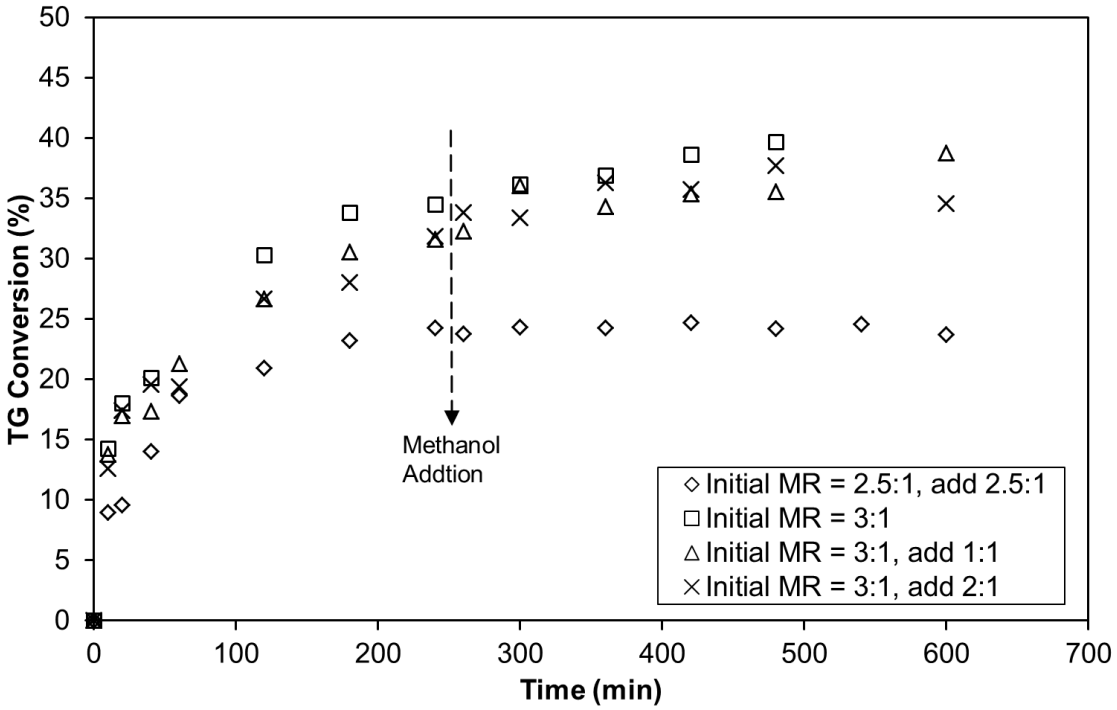

Figure 8.3. The effect of stepwise addition of methanol on TG conversion. (With water addition of 5 vol%, a temperature of 40 °C, a catalyst loading of 0.786 wt% and a stirrer speed 500 rpm)

8.2.3 Effect of stirring speed

The effect of stirring speed on TG conversion is shown in Figure 8.4. Increasing the stirring speed is expected to eliminate external mass transfer limitations and ensure the heterogeneous catalyst is well suspended. From these data it can be seen that with a stirring speed of 300 rpm the conversion is low indicating that there are external mass transfer limitations at these conditions. When the stirrer speed is increased to 700 rpm it can be seen that the conversion is slightly lower than a speed of 500 rpm. This can be explained in part by experimental error; however it is also possible that the high speed is damaging the catalyst particularly at longer reaction times. 500 rpm has been selected as the optimum stirrer speed because it gives the highest conversion at the lowest possible speed.

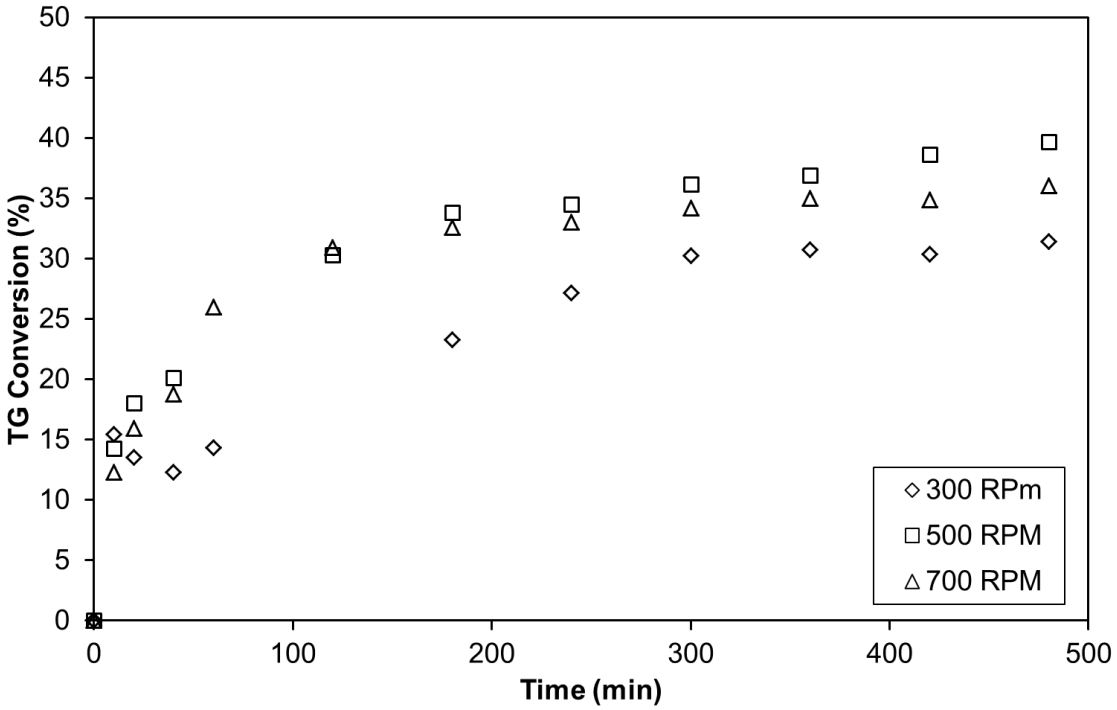

Figure 8.4. The effect of stirring speed on TG conversion. (With water addition of 5 vol%, a mole ratio of 3:1, a temperature of 40 °C and a catalyst loading of 0.786 wt%.)

8.2.4 Effect of temperature

The effect of temperature on the conversion of TGs is shown in Figure 8.5. From these data it can be seen there is a large drop in conversion when the temperature is increased to 50 °C. According to the manufacturer's data the activity of this catalyst should increase with increasing temperature up to 60 °C. The mole ratio is relatively high and it is expected that the reduction in conversion is due to a combination of the high temperature and a high mole ratio.

The TG conversion at 30 and 40 °C is relatively similar and allowing for experimental error the conversion could be considered to be the same. Given that the conversion is marginally higher at the lower temperature of 30 °C, this value has been selected as the optimum.

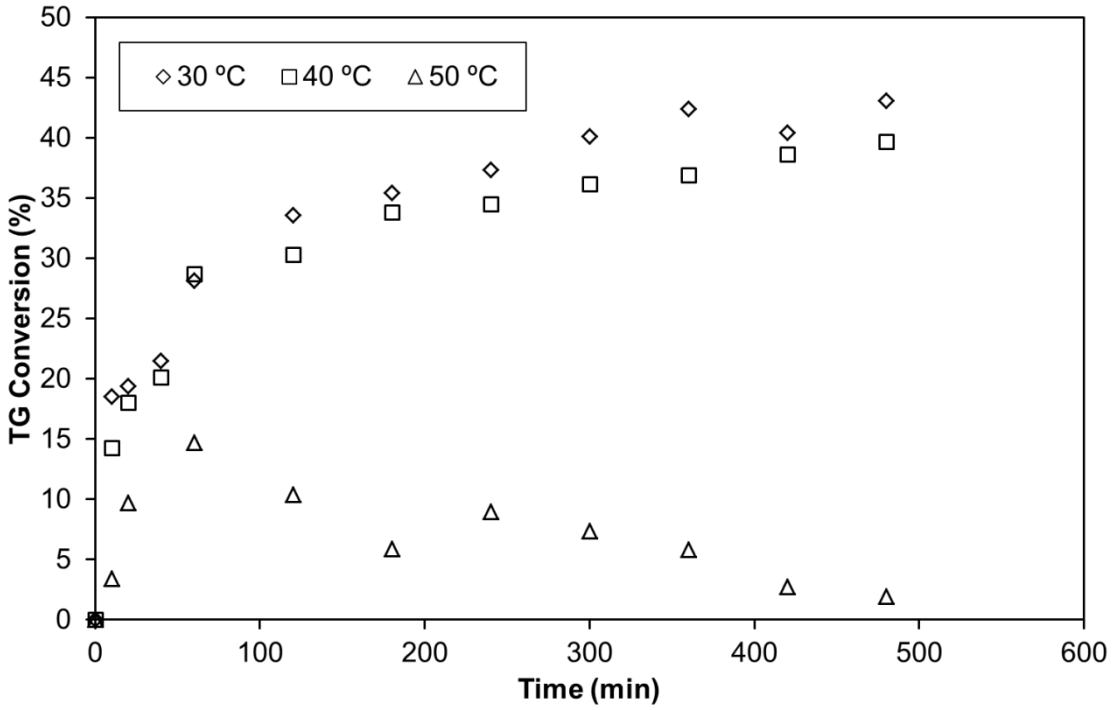

Figure 8.5. The effect of temperature on TG conversion. (With water addition of 5 vol%, a mole ratio of 3:1, a catalyst loading of 0.786 wt% and a stirrer speed of 500 rpm)

8.2.5 Effect of catalyst loading

The effect of catalyst loading on conversion is shown in Figure 8.6. From these data it can be seen that conversion increases with an increase in catalyst loading until a maximum is reached. At this point increasing the catalyst loading will not increase conversion because there are sufficient catalytic sites available to catalyse the reaction. On this basis a loading of 0.786 wt% has been identified as the optimum catalyst loading for this system.

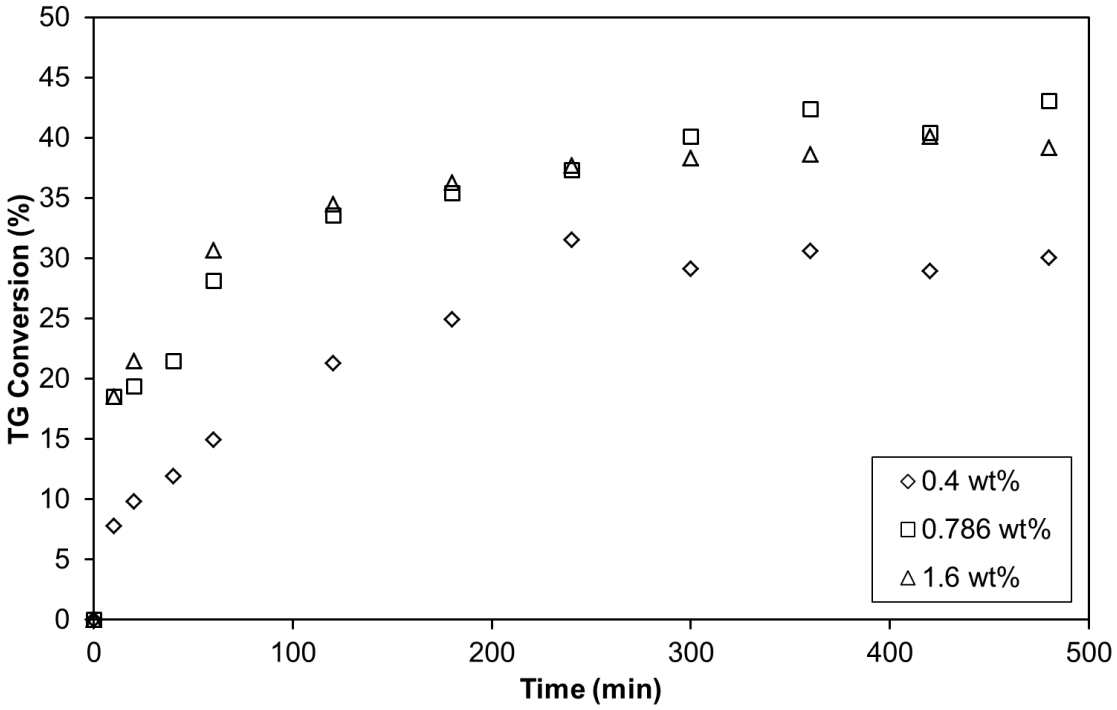

Figure 8.6. The effect of catalyst loading on TG conversion. (With water addition of 5 vol%, a mole ratio of 3:1, a temperature of 30 °C and a stirrer speed of 500 rpm)

8.3 Enzymatic Biodiesel Production Stage 2

Amano Lipase PS-IM has been investigated for the transesterification reaction to convert UCO to biodiesel. The reactions are not affected by the presence of FFAs and as a result UCO was used as the raw material. While the FFAs do not lead to the undesirable saponification side reaction during transesterification they still need to be removed from the final product in order to meet the biodiesel specifications. The esterification reaction can be used to convert the FFAs to biodiesel, thus increasing conversion. The FFAs concentration at the optimum reaction conditions is shown in Figure 8.7. From these data it can be seen that FFAs are formed at low reactions times and the concentration subsequently decreases steadily. After 8 h of reaction time the FFAs concentration is 200 mol·m^{-3}.

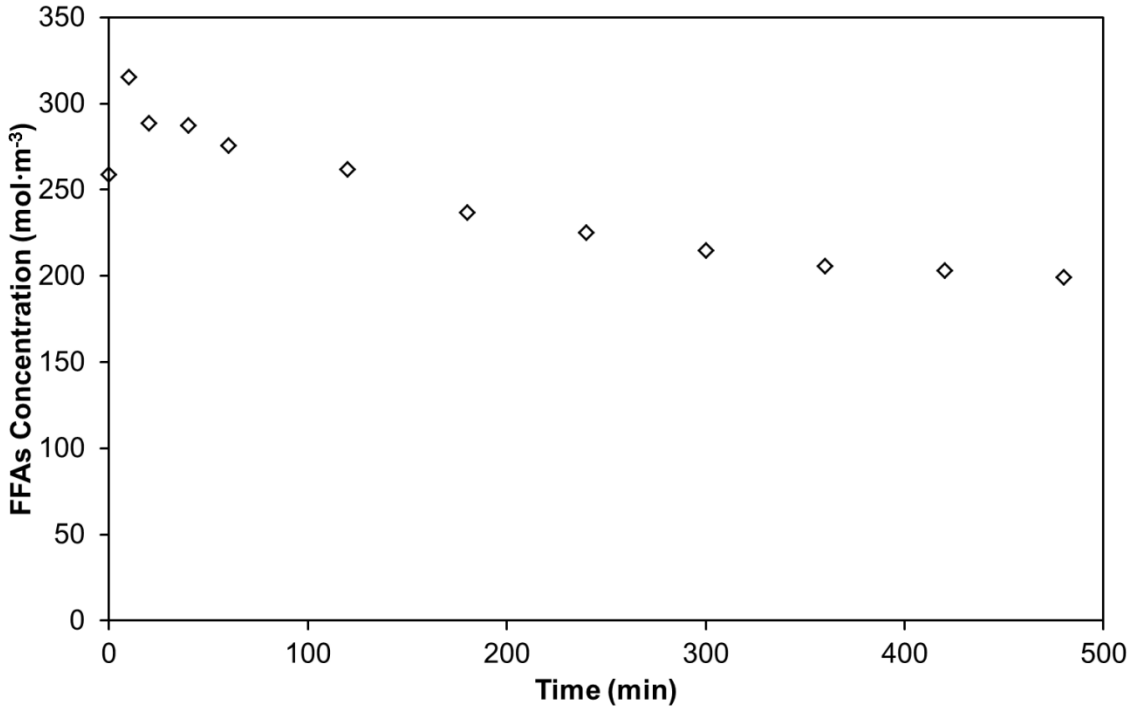

Figure 8.7. The FFAs concentration trend at optimum conditions. (With water addition of 5 vol%, a mole ratio of 3:1, a temperature of 30 °C, a catalyst loading of 0.789 wt% and a stirrer speed of 500 rpm)

In Chapter 7, Section 7.4, it was found that Novozyme 435 could simultaneously catalyse the esterification of FFAs and the transesterification of monoglycerides (MG) and diglycerides (DG). On this basis it is proposed that Novozyme 435 would be more suitable as a post-treatment catalyst for enzymatic biodiesel production, in order to convert the FFAs and any unreacted MGs, DGs to FAME. After transesterification the reaction mixture was separated from the catalyst by filtration and left in a separating funnel overnight. The reaction product separated into a UCO rich top layer and a glycerol rich bottom layer as shown in Chapter 5, Figure 5.8, vial B. The UCO rich layer contains the FAME produced during transesterification and is referred to as the stage 1 product. There is still some water and methanol in the stage 1 product. Rotary evaporation can be used to remove the methanol and water, however it may also remove some of the FAMEs. As a result experiments were carried out to determine if rotary evaporation was a necessary and suitable treatment step. The FAME concentration of the stage 1 product before and after drying was measured and it was found that there was a slight increase in the FAME

concentration which has been attributed to a slight decrease in the mass of the stage 1 product due to water and methanol removal.

A comparison of the FAME and FFAs concentration trend using the untreated and dried stage 1 product is shown in Figure 8.8. From these data it can be seen that more FAME is formed using the dried transesterification product. In addition while this is less clear from the scale the reduction in FFAs is greater using the dried stage 1 product. This indicates that the methanol and water remaining behind in the transesterification product inhibited the esterification and transesterification reactions.

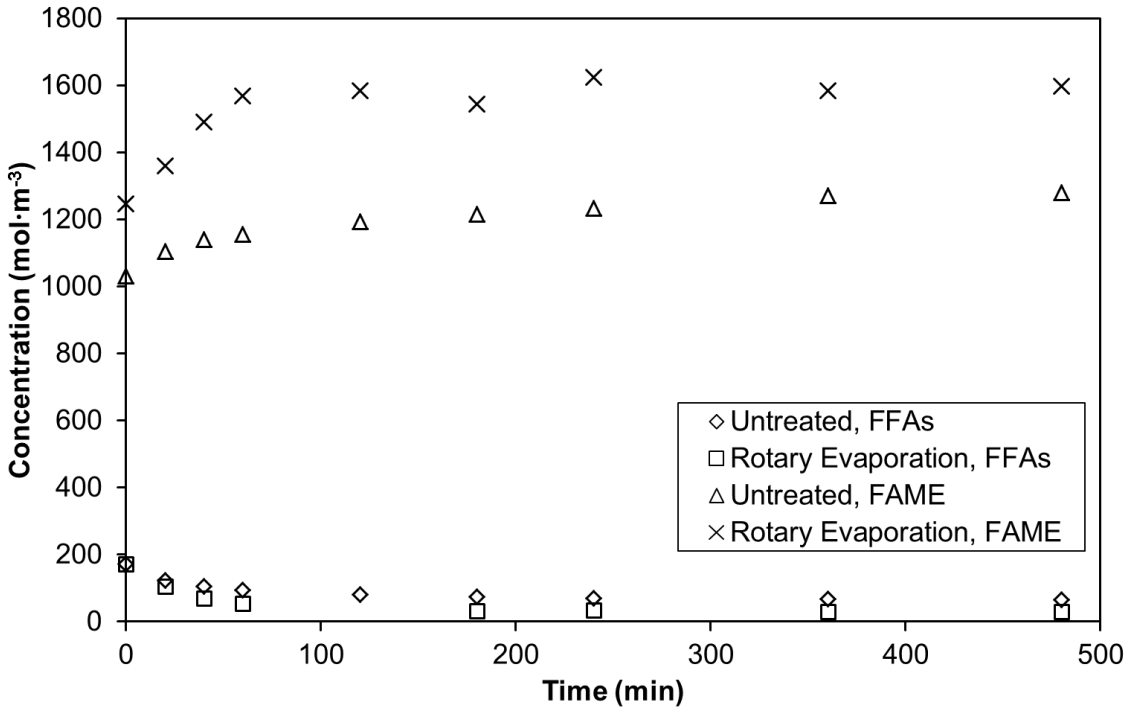

Figure 8.8. A comparison of the FFAs and FAME concentrations and the effect of raw material type when using Novozyme 435 for enzymatic biodiesel production stage 2. (With a methanol to TGs mole ratio of 1.25:1, a temperature of 50 °C, a catalyst loading of 1.00 wt% and a stirrer speed of 650 rpm)

From Figure 8.8 it can be seen that the amount of FAME formed is greater than the amount of FFAs consumed. Novozyme 435 can convert FFAs, MGs and DGs to FAME and in order to confirm this, the ratio of FAME formed to FFAs consumed has been calculated. The ratio of the untreated stage 1

product is 2.4:1 compared to a ratio of 2.5:1 for the dried stage 1 product. The esterification reaction converts one mole of FFAs to one mole of FAME, Chapter 1, Figure 1.2 and a ratio of 1:1 would be expected if esterification was the only reaction occurring during stage 2.

The overall conversion of TGs in the second stage is shown in Figure 8.9. From these data it can be seen that the TG conversion increases from 43% to 55% in the second stage. The TG conversion reaches 55% after 2 h of reaction time indicating that this time would be sufficient for stage 2.

From these data it can be seen that it is possible to improve conversion using Novozyme 435. However the overall conversion is still relatively low and the final product is not suitable for use as biodiesel. In addition, the FFAs concentration is also too high to meet the biodiesel standards. Stage 2 was carried out using the optimum conditions identified in Chapter 5 for the esterification pre-treatment reaction and further improvement may be possible in stage 2.

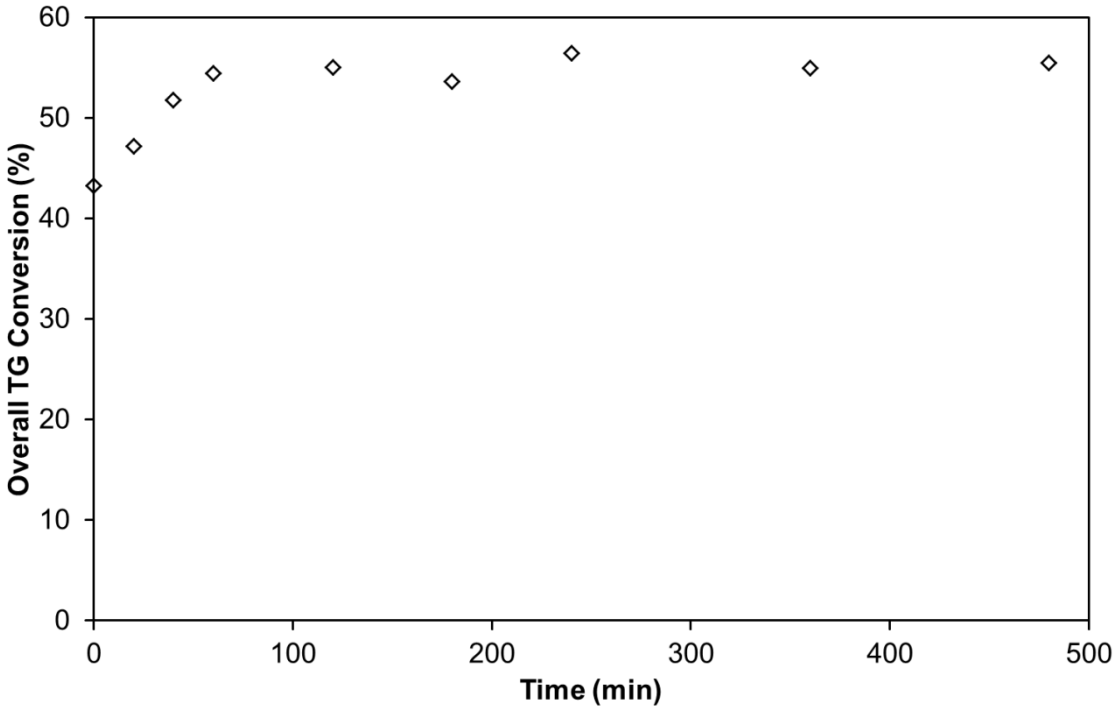

Figure 8.9. The overall TG conversion for enzymatic biodiesel production stage 2. (With a methanol to TGs mole ratio of 1.25:1, a temperature of 50 °C, a catalyst loading of 1.00 wt% and a stirrer speed of 650 rpm)

8.4 Conclusions

The enzymatic production of biodiesel from UCO has been investigated using Amano Lipase PS-IM in stage 1 and Novozyme 435 in stage 2. A detailed investigation to determine the optimum conditions for Amano Lipase PS-IM were carried out. It was found that the optimum conditions are the addition of 5 vol% water, a mole ratio of 3:1, a stirring speed of 500 rpm, a temperature of 30 °C and a catalyst loading of 0.789 wt% giving a conversion of 43%.

It was found that the conversion could be increased in stage 2 particularly when the stage 1 product was dried using rotary evaporation. The stage 2 batch experiments were carried out using the optimum conditions identified for Novozyme 435 in Chapter 5. It was found that a higher conversion was achieved when stage 1 product was dried using rotary evaporation and that the FFAs and FAME concentration indicated simultaneous esterification and transesterification reactions. The final TG conversion was 55% and could be achieved with 2 h of reaction time.

Chapter 9: Conclusions and Recommendations for Future Work

9.1 Conclusions

Potential improvements to the biodiesel production process have been investigated. In order to minimise the environmental impact, used cooking oil (UCO) was selected as the feedstock along with heterogeneous catalysts. The heterogeneous catalysts were selected on the basis that high yields were expected at relatively benign operating conditions. An ion-exchange resin (Purolite D5082) and an immobilised enzyme (Novozyme 435) were investigated for the esterification pre-treatment reaction and an immobilised enzyme (Amano Lipase PS-IM) was selected for the transesterification reaction.

A detailed characterisation of the fresh and used catalysts was carried out in order to gain a better understanding of the catalytic activity of the catalysts investigated (Chapter 4). This information was used to compare the catalysts types. This information was also used to compare fresh and used catalysts in order gain a better understanding of the changes and the data were linked to reusability studies (Chapter 6).

The UCO was characterised using various chemical and physical techniques (Chapter 5) and found to have a similar FFAs composition to soybean oil.

The optimum batch reaction conditions of the esterification pre-treatment reaction were investigated for Novozyme 435 and Purolite D5082 (Chapter 6). The optimum reaction conditions identified for Purolite D5082 were a temperature of 60 °C, a methanol to free fatty acid (FFA) mole ratio of 62:1, a catalyst loading of 5 wt% resulting in an FFAs conversion of 88% after 8 h of

reaction time. The optimum conditions identified for Novozyme 435 were a temperature of 50 °C, a mole ratio of 6.2:1 and a catalyst loading of 1 wt% resulting in a conversion of 90% after 8 h of reaction time.

The catalytic activity of Purolite D5082, Novozyme 435 and previously studied Purolite D5081 were compared and it was found that the highest conversion, of 97% after an 8 h reaction time, was possible using Purolite D5081 (Chapter 6). There are benefits to using Novozyme 435 because a similar conversion was possible using a much smaller mole ratio, a lower temperature and a shorter reaction time. In addition, it was found that the reaction rate was still relatively high at 30 °C indicating that this reaction could be carried out, without additional heating in some parts of the world.

It was proposed that side reactions were occurring during Novozyme 435 catalysed esterification pre-treatment (Chapter 6). In order to investigate this further an ultra performance liquid chromatography (UPLC-MS) method was developed (Chapter 7) to monitor the monoglyceride (MG), diglyceride (DG) and triglyceride (TG) concentrations. From the trends it could be seen that the diglycerides were being consumed leading to the formation and subsequent consumption of MGs there was very little change in the TG concentration. This confirmed the existence of side reactions.

A kinetic model was developed to investigate the reaction mechanism of Novzoyme 435 using the MG, DG, TG, fatty acid methyl ester (FAME) and FFA concentrations (Chapter 7). The parameters of this model were determined by fitting the model to experimental data and a reasonably good fit was achieved. According to this model, direct esterification was catalysed in parallel with sequential esterification hydrolysis reactions.

A two-step enzymatic biodiesel production process was investigated with the first stage catalysed by Amano Lipase PS-IM and the second stage catalysed by Novozyme 435 (Chapter 8). The process was investigated because the unwanted saponification side reactions do not occur with enzyme

catalysts (Chen et al. 2009; Atadashi et al. 2013) and Novozyme 435 has been shown to catalyse esterification and transesterification (Chapter 7). The optimum batch reaction conditions for the Amano Lipase PS-IM identified for the first step are addition of 5 vol% water, a temperature of 30 °C, a methanol to UCO mole ratio of 3:1 and a catalyst loading of 0.789 wt% resulting in a TG conversion of 43%. The Novozyme 435 catalysed second stage was carried using the optimum conditions identified in Chapter 6. When the oil layer from stage one was dried the final TG conversion was 55%.

Process options to minimise the environmental impact and improve the efficiency of biodiesel production have been investigated. It was found that high conversions were possible using Novozyme 435 and previously investigated Purolite D5081 for the esterification pre-treatment reaction. The highest conversion of 97% was achieved using Purolite D5081, however there were process benefits when using Novozyme 435 because the reaction could be carried out using a substantially lower mole ratio, a lower temperature and a shorter reaction time. Amano Lipase PS-IM was investigated for the transesterification reaction and the highest conversion was relatively low at 43%. This conversion was increased to 55% with a Novozyme 435 catalysed post-esterification reaction and further improvements may be possible

9.2 Recommendations for Future Work

The results of the experimental work indicate a number of areas that would be interesting for further research and are discussed below.

9.2.1 Investigate improvements to the analytical method for determining the MG, DG and TG concentrations

The analysis carried out using UPLC-MS, to determine the MG, DG and TG concentrations, and the subsequent kinetic modelling has provided some useful information on the catalytic activity of Novozyme 435. However, there is scope to improve the concentration data used for the modelling. The concentration data, particularly the TG data was scattered and the reliability of

the data could be improved by preparing the samples in triplicate although this will result in a substantial increase in the sample preparation and analysis times.

It may be necessary to consider an alternative analytical technique in order to determine MG, DG and TG concentrations. This work focused on the use of liquid chromatography for the analysis of the reaction products because it was deemed the most suitable method for the components which have a relatively low volatility. A gas chromatography method has been specified to determine MG, DG and TG concentrations in biodiesel (British Standard Online, 2011). This method has been designed to detect low levels of MG, DG and TGs in biodiesel, however it may be possible to amend this method for samples with much higher concentrations.

9.2.2 Improve the kinetic modelling parameters

If improvements are made to the quality of the MG, DG and TG data as discussed in Section 9.2.1, these data could be entered into the current model in order to improve the model parameters.

To date the modelling work has focused on a very narrow set of reaction conditions. For example, the modelling was carried out using the optimum methanol to FFAs mole ratio and assessing the model for a wide range of mole ratios would improve the robustness of the parameters particularly the methanol inhibition constant (K_i). The parameters have been calculated at various temperatures, however this could be improved by incorporating the Arrhenius equation into the model.

The kinetic model was developed to investigate the side reactions observed during the Novozyme 435 catalysed, esterification pre-treatment reaction. The same model could be applied to Amano Lipase PS-IM catalysed reactions. It would be interesting to compare the MG, DG and TG concentration data and model parameters for the two catalysts, in order to compare the catalytic activities and mechanisms.

9.2.3 Investigate improvements to the Enzymatic Biodiesel Production Process

A maximum TG conversion of 43% was achieved using Amano Lipase PS-IM, which is low compared to the results reported for similar catalysts (Li et al. 2011; Da Rós et al. 2010). A potential explanation for the low conversion is that there is a contaminant in the UCO inhibiting or poisoning the Amano Lipase PS-IM. For example Russbueldt & Hoelderich (2009) found that a mineral salt contaminant in a UCO was inhibiting the catalytic activity of an ion-exchange resin. Another explanation is that there are lipid components which cannot be converted to FAME by Amano Lipase PS-IM. Abidin (2012) was able to achieve a conversion of 75% using the same UCO and an anion exchange resin (Diaion PA306s). In similar way to Novozyme 435 it may be that Amano Lipase PS-IM is not able to catalyse the transesterification of one of the main lipid classes of MG, DG or TGs. Alternatively, one or more of the specific MG, DG or TG components may not be reacting. These factors could be investigated by carrying out the transesterification reaction using alternative vegetable oils, particularly virgin oils such as soybean or sunflower oil.

The UPLC-MS or another method could be used to monitor the MG, DG and TG trends and determine which components are being converted. In this case the UPLC-MS method may be the most suitable method because it can be used to monitor specific components and it may even be possible to identify and monitor specific isomers of MG, DG or TG components in the oil. This method was used to show that the 1,3 DG isomers reacted more readily than the 1,2 DG isomers for Novozyme 435 catalysed reactions (Chapter 7).

Amano Lipase PS-IM is composed of *Pseudomonas cepacia* (recently reclassified as *Burkholderia cepacia*) lipase immobilised on diatomaceous earth. Immobilisation of enzymes has been shown to affect the catalytic activity and while this can lead to an increase in conversion it does occasionally result in a decrease in conversion (Li et al. 2011; Zheng et al. 2012). The free lipase version of Amano Lipase PS-IM is Amano Lipase PS. The transesterification reaction could be carried out using the free enzyme. Amano Lipase PS could

also be immobilised using one of the techniques described in the literature (Zheng et al. 2012; Tongboriboon et al. 2010). A comparison of these results could be used to determine if the immobilisation technique is inhibiting the reaction.

Amano Lipase PS-IM is supplied as a fine powder which is not suitable for industrial applications particularly continuous flow applications. Alternative immobilisation techniques could be investigated to improve the conversion and industrial applicability of Amano Lipase PS-IM

The synergistic effect of mixing lipases with different catalytic activities has been reported (Tongboriboon et al. 2010) and it may be possible to mix Novozyme 435 and an immobilised Amano Lipase PS to improve the overall catalytic activity and increase conversion. However, a new set of optimum conditions would need to be identified because there are substantial differences in the water requirements and methanol tolerances for Amano Lipase PS-IM and Novozyme 435.

Continuous flow processes are generally considered more suitable for industrial applications. Development of a continuous flow process would follow logically from the work described above. The conversion and immobilisation techniques would need to be improved in order for this work to be viable. In addition, a good quality model would be useful to help design and develop an effective process.

9.2.4 Carry Out Detailed Economic and Lifecycle Analysis of Potential Processes

This work has focused on the experimental and technical aspects of biodiesel production. However, a complete analysis would need to take into account the economic and environmental aspects.

It is widely recognised that enzyme catalysts are expensive when compared to chemical catalysts (Li et al. 2011; Atadashi et al. 2013). In the

context of this work it was found that there are benefits to using Novozyme 435 in place of Purolite D5081 because the Novozyme 435 catalysed reaction can be carried out using less methanol, a lower temperature and a shorter reaction time and thus offers a number of environmental and economic benefits. On this basis, an economic assessment and life cycle analysis of the Novozyme 435 and Purolite D5082 catalysed esterification pre-treatment reactions would be interesting. A life cycle analysis should take into account difference in the processes used to manufacture the catalysts.

Chapter 10: References

Abidin, S.Z., Haigh, K.F. and Saha, B., 2012. Esterification of free fatty acids in used cooking oil using ion-exchange resins as catalysts: An efficient pretreatment method for biodiesel feedstock. *Industrial and Engineering Chemistry Research*, 51, pp.14653–14664.

Abidin, S.Z., 2012. *Production of Biodiesel from Used Cooking Oil (UCO) using Ion Exchange Resins as Catalysts*. PhD Loughborough University.

Agarwal, A.K. and Rajamanoharan, K., 2009. Experimental investigations of performance and emissions of *Karanja* oil and its blends in a single cylinder agricultural diesel engine. *Applied Energy*, 86, pp.106–112.

Akoh, C.C. et al., 2007. Enzymatic Approach to Biodiesel Production. *Journal of Agricultural and Food Chemistry*, 55, pp.8995–9005.

Al-Zuhair, S. et al., 2006. The effect of fatty acid concentration and water content on the production of biodiesel by lipase. *Biochemical Engineering Journal*, 30, pp.212–217.

Al-Zuhair, S., Fan, W. and Lim SJ, 2007. Proposed kinetic mechanism of the production of biodiesel from palm oil using lipase. *Process Biochemistry*, 42, pp.951–960.

Al-Zuhair, S., Dowaidar, A. and Kamal, H., 2009. Dynamic modelling of biodiesel production from simulated waste cooking oil using immobilized lipase. *Biochemical Engineering Journal*, 44, pp.256–262.

Andrijanto, E., Dawson, E. A., Brown, D.R., 2012. Hypercrosslinked polystyrene sulphonic acid catalysts for the esterification of free fatty acids in biodiesel synthesis. *Applied Catalysis B: Environmental*, 115-116, pp.261–268.
Arzamendi, G. et al., 2006. Monitoring of biodiesel production: Simultaneous analysis of the transesterification products using size-exclusion chromatography. *Chemical Engineering Journal*, 122, pp.31–40.

ASTM International, 2012. *D6751-12 Standard Specification for Biodiesel Fuel Blend Stock (B100) for Middle Distillate*. ASTM International [online] Available through Loughborough University Library: http://enterprise.astm.org/SUBSCRIPTION/search/sedl-search.html?query=ASTM%206751&sub=enterprise [Accessed on 30 July 2013]

Atadashi, I.M. et al., 2013. The effects of catalysts in biodiesel production: A review. *Journal of Industrial and Engineering Chemistry*, 19, pp.14–26.

Atadashi, I.M., Aroua, M.K. and Aziz, A.A., 2011. Biodiesel separation and purification: A review. *Renewable Energy*, 36, pp.437–443.

Azócar, L. et al., 2010. Improving fatty acid methyl ester production yield in a lipase-catalyzed process using waste frying oils as feedstock. *Journal of Bioscience and Bioengineering*, 109, pp.609–614.

Balat, M. and Balat, H., 2010. Progress in biodiesel processing. *Applied Energy*, 87, pp.1815–1835.

Barakos, N., Pasias, S. and Papayannakos, N., 2008. Transesterification of triglycerides in high and low quality oil feeds over an HT2 hydrotalcite catalyst. *Bioresource Technology*, 99, pp.5037–5042.

Bielansky, P. et al., 2011. Catalytic conversion of vegetable oils in a continuous FCC pilot plant. *Fuel Processing Technology*, 92, pp.2305–2311.

Bommarius, A.S. and Riebel, B., 2002. *Biocatalysis : fundamentals and applications*, Weinheim ; Cambridge: Wiley-VCH.

Brask, J. et al., 2011. Combining enzymatic esterification with conventional alkaline transesterification in an integrated biodiesel process. *Applied Biochemistry and Biotechnology*, 163, pp.918–27.

British Standards Institution, 2011, *BS EN 14105:2011 Fat and oil derivatives – fatty acid methyl esters (FAME) – determination of free and total glycerol and mono-, di- and triglyceride contents*, British Standards Online [online] Available through Loughborough University Library: https://bsol.bsigroup.com/Bibliographic/BibliographicInfoData/000000000030207064 [Accessed on 15 September 2013].

British Standards Institution, 2013. *BS EN 14214:2012 Liquid petroleum products — Fatty acid methyl esters (FAME) for use in diesel engines and heating applications — Requirements and test methods*. British Standards Online [online] Available through Loughborough University Library: https://bsol.bsigroup.com/en/My-BSI/My-Subscriptions/BSOL/Search/Search-Results/?src=s&s=c&snc=Y&bwc=F&q=EN%2014214&ib=1 [Accessed 30 July 2013].

Caetano, C.S. et al., 2009. Esterification of fatty acids to biodiesel over polymers with sulfonic acid groups. *Applied Catalysis A: General*, 359, pp.41–46.

Calabrò, V. et al., 2010. Kinetics of enzymatic trans-esterification of glycerides for biodiesel production. *Bioprocess and Biosystems Engineering*, 33, pp.701–710.

Canakci, M. and Gerpen, J. Van, 2001. Biodiesel production from oils and fats with high free fatty acids. *Transactions of the ASAE*, 44, pp.1429–1436.

Cao, F. et al., 2008. Biodiesel production from high acid value waste frying oil Catalyzed by superacid heteropolyacid. *Biotechnology and Bioengineering*, 101, pp.93–100.

Chabukswar, D.D., Heer, P.K.K.S. and Gaikar, V.G., 2013. Esterification of palm fatty acid distillate using heterogeneous sulfonated microcrystalline cellulose catalyst and its comparison with H2SO4 catalyzed reaction. *Industrial and Engineering Chemistry Research*, 52, pp.7316–7326.

Chang, H.-M. et al., 2005. Optimized synthesis of lipase-catalyzed biodiesel by Novozym 435. *Journal of Chemical Technology and Biotechnology*, 80, pp.307–312.

Cheirsilp, B., H-Kittikun, A. and Limkatanyu, S., 2008. Impact of transesterification mechanisms on the kinetic modeling of biodiesel production by immobilized lipase. *Biochemical Engineering Journal*, 42, pp.261–269.

Chen, J.-W. and Wu, W.-T., 2003. Regeneration of immobilized *Candida antarctica* lipase for transesterification. *Journal of Bioscience and Bioengineering*, 95, pp.466–469.

Chen, Y. et al., 2009. Synthesis of biodiesel from waste cooking oil using immobilized lipase in fixed bed reactor. *Energy Conversion and Management*, 50, pp.668–673.

Cordeiro, C.S. et al., 2008. A new zinc hydroxide nitrate heterogeneous catalyst for the esterification of free fatty acids and the transesterification of vegetable oils. *Catalysis Communications*, 9, pp.2140–2143.

Corro, G., Pal, U. and Tellez, N., 2013. Biodiesel production from *Jatropha curcas* crude oil using ZnO/SiO_2 photocatalyst for free fatty acids esterification. *Applied Catalysis B: Environmental*, 129, pp.39–47.

Da Rós, P.C.M. et al., 2010. Evaluation of the catalytic properties of *Burkholderia cepacia* lipase immobilized on non-commercial matrices to be used in biodiesel synthesis from different feedstocks. *Bioresource Technology*, 101, pp.5508–5516.

Demirbas, A. and Fatih Demirbas, M., 2011. Importance of algae oil as a source of biodiesel. *Energy Conversion and Management*, 52, pp.163–170.

Demirbas, A., 2009. *Biofuels Securing the Planet's Future Energy Needs*, New York, London: Springer.

Di Nicola, G. et al., 2008. Development and optimization of a method for analyzing biodiesel mixtures with non-aqueous reversed phase liquid chromatography. *Journal of Chromatography. A*, 1190, pp.120–126.

Di Serio, M. et al., 2007. Vanadyl phosphate catalysts in biodiesel production. *Applied Catalysis A: General*, 320, pp.1–7.

Di Serio, M. et al., 2008. Heterogeneous catalysts for biodiesel production. *Energy and Fuel*, 22, pp.207–217.

Dizge, N. and Keskinler, B., 2008. Enzymatic production of biodiesel from canola oil using immobilized lipase. *Biomass and Bioenergy*, 32, pp.1274–1278.

Dizge, N., Keskinler, B. and Tanriseven, A., 2009. Biodiesel production from canola oil by using lipase immobilized onto hydrophobic microporous styrene–divinylbenzene copolymer. *Biochemical Engineering Journal*, 44, pp.220–225.

Dossat, V., Combes, D. and Marty, A., 2002. Lipase-catalysed transesterification of high oleic sunflower oil. *Enzyme and Microbial Technology*, 30, pp.90–94.

Enweremadu, C.C. and Mbarawa, M.M., 2009. Technical aspects of production and analysis of biodiesel from used cooking oil—A review. *Renewable and Sustainable Energy Reviews*, 13, pp.2205–2224.

European Parliament and Council Directive 2009/28/EC of 23 April 2009 *on the promotion of the use of energy from renewable sources and amending and subsequently repealing Directives 2001/77/EC and 2003/30/EC (Text with EEA relevance*. [online] Available at: http://eur-lex.europa.eu/LexUriServ/LexUriServ.do?uri=CELEX:32009L0028:EN:NOT [Accessed on 29 July 2013].

Feng, Y. et al., 2010. Biodiesel production using cation-exchange resin as heterogeneous catalyst. *Bioresource Technology*, 101, pp.1518–1521.

Ferrão-Gonzales, A.D. et al., 2011. Thermodynamic analysis of the kinetics reactions of the production of FAME and FAEE using Novozyme 435 as catalyst. *Fuel Processing Technology*, 92, pp.1007–1011.

Foresti, M.L. et al., 2008. Kinetic modeling of enzymatic ethyl oleate synthesis carried out in biphasic systems. *Applied Catalysis A: General*, 334, pp.65–72.

Ganesan, D., Rajendran, A., Thangavelu, V., 2009. An overview on the recent advances in the transesterification of vegetable oils for biodiesel production using chemical and biocatalysts. *Reviews in Environmental Science and Biotechnology*, 8, pp.367–394.

Gay, M., Lee, J. and Goh, E., 2011. Analysis of Biodiesel Fuel Using UPLC/Xevo G2 QTof. *Waters Corporation*, pp.1–7.

Georgogianni, K.G. et al., 2009a. Transesterification of rapeseed oil for the production of biodiesel using homogeneous and heterogeneous catalysis. *Fuel Processing Technology*, 90, pp.1016–1022.

Georgogianni, K.G. et al., 2009b. Transesterification of soybean frying oil to biodiesel using heterogeneous catalysts. *Fuel Processing Technology*, 90, pp.671–676.

Gog, A. et al., 2012. Biodiesel production using enzymatic transesterification – Current state and perspectives. *Renewable Energy*, 39, pp.10–16.

Guo, F. et al., 2010. Calcined sodium silicate as solid base catalyst for biodiesel production. *Fuel Processing Technology*, 91, pp.322–328.

Haas, M.J. et al., 2006. A process model to estimate biodiesel production costs. *Bioresource Technology*, 97, pp.671–8.

Haas, M.J., 2005. Improving the economics of biodiesel production through the use of low value lipids as feedstocks: vegetable oil soapstock. *Fuel Processing Technology*, 86, pp.1087–1096.

Haigh, K.F. et al., 2013. Comparison of Novozyme 435 and Purolite D5081 as heterogeneous catalysts for the pretreatment of used cooking oil for biodiesel production. *Fuel*, 111, pp.186–193.

Haigh, K.F. et al., n.d. Kinetics of the Pre-treatment of used cooking oil using Novozyme 435 for biodiesel production. *Chemical Engineering Research and Design*. Submitted

Halim, S. and Harunkamaruddin, A., 2008. Catalytic studies of lipase on FAME production from waste cooking palm oil in a *tert*-butanol system. *Process Biochemistry*, 43, pp.1436–1439.

Hama, S. et al., 2011. Enzymatic packed-bed reactor integrated with glycerol-separating system for solvent-free production of biodiesel fuel. *Biochemical Engineering Journal*, 55, pp.66–71.

Hameed, B.H., Lai, L.F. and Chin, L.H., 2009. Production of biodiesel from palm oil (*Elaeis guineensis*) using heterogeneous catalyst: An optimized process. *Fuel Processing Technology*, 90, pp.606–610.

Hara, M., 2009. Environmentally benign production of biodiesel using heterogeneous catalysts. *ChemSusChem*, 2, pp.129–35.

Hazar, H. and Aydin, H., 2010. Performance and emission evaluation of a CI engine fueled with preheated raw rapeseed oil (RRO)–diesel blends. *Applied Energy*, 87, pp.786–790.

Helwani, Z. et al., 2009a. Solid heterogeneous catalysts for transesterification of triglycerides with methanol: A review. *Applied Catalysis A: General*, 363, pp.1–10.

Helwani, Z. et al., 2009b. Technologies for production of biodiesel focusing on green catalytic techniques: A review. *Fuel Processing Technology*, 90, pp.1502–1514.

Hishamuddin, E., 2009. *Partitioning of triacylglycerols in the fractional crystallisation of palm oil*. PhD Loughborough University.

Holcapek, M. et al., 1999. Analytical monitoring of the production of biodiesel by high-performance liquid chromatography with various detection methods. *Journal of Chromatography. A*, 858, pp.13–31.

Huang, Y., Zheng, H. and Yan, Y., 2010. Optimization of lipase-catalyzed transesterification of lard for biodiesel production using response surface methodology. , pp.504–515.

Huber, G.W., O'Connor, P. and Corma, A., 2007. Processing biomass in conventional oil refineries: Production of high quality diesel by hydrotreating vegetable oils in heavy vacuum oil mixtures. *Applied Catalysis A: General*, 329, pp.120–129.

Issariyakul, T. et al., 2007. Production of biodiesel from waste fryer grease using mixed methanol/ethanol system. *Fuel Processing Technology*, 88, pp.429–436.

Jitputti, J. et al., 2006. Transesterification of crude palm kernel oil and crude coconut oil by different solid catalysts. *Chemical Engineering Journal*, 116, pp.61–66.

Kaieda, M. et al., 2001. Effect of methanol and water contents on production of biodiesel fuel from plant oil catalyzed by various lipases in a solvent-free system. *Journal of bioscience and bioengineering*, 91, pp.12–15.

Kataoka, S. et al., 2010. Microreactor with mesoporous silica support layer for lipase catalyzed enantioselective transesterification. *Green Chemistry*, 12, pp.331–337.

Khor, G.K. et al., 2010. Thermodynamics and inhibition studies of Lipozyme TL IM in biodiesel production via enzymatic transesterification. *Bioresource Technology*, 101, pp.6558–6561.

Knothe, G., 2005. Fuel Properties. In G. Knothe, ed. *The Biodiesel Handbook*. AOCS, pp. 76–164.

Knothe, G., 2010. Biodiesel and renewable diesel: A comparison. *Progress in Energy and Combustion Science*, 36, pp.364–373.

Koda, R. et al., 2010. Ethanolysis of rapeseed oil to produce biodiesel fuel catalyzed by *Fusarium heterosporum* lipase-expressing fungus immobilized whole-cell biocatalysts. *Journal of Molecular Catalysis B: Enzymatic*, 66, pp.101–104.

Komers, K. et al., 1998. Biodiesel fuel from rapeseed oil, methanol, and KOH. Analytical methods in research and production. *Lipid /Fett*, 100, pp.507–512.

Korunic, Z., 1998. Review Diatomaceous Earths , a Group of Natural Insecticides. *Journal of Stored Products Research*, 34, pp.87–97.

Köse, O., Tüter, M. and Ayşe Aksoy, H., 2002. Immobilized Candida antarctica lipase-catalyzed alcoholysis of cotton seed oil in a solvent-free medium. *Bioresource Technology*, 83, pp.125–129.

Kouzu, M. et al., 2009. Heterogeneous catalysis of calcium oxide used for transesterification of soybean oil with refluxing methanol. *Applied Catalysis A: General*, 355, pp.94–99.

Kraai, G.N. et al., 2008. Kinetic studies on the Rhizomucor miehei lipase catalyzed esterification reaction of oleic acid with 1-butanol in a biphasic system. *Biochemical Engineering Journal*, 41, pp.87–94.

Kulkarni, M.G. and Dalai, A.K., 2006. Waste cooking oil - An economical source for biodiesel : A review. *Industrial and Engineering Chemistry Research*, pp.2901–2913.

Kumari, V., Shah, S. and Gupta, M.N., 2007. Preparation of biodiesel by lipase-catalyzed transesterification of high free fatty acid containing oil from *Madhuca indica*. *Energy and Fuels*, 21, pp.368–372.

Lam, M.K., Lee, K.T. and Mohamed, A.R., 2010. Homogeneous, heterogeneous and enzymatic catalysis for transesterification of high free fatty acid oil (waste cooking oil) to biodiesel: a review. *Biotechnology Advances*, 28, pp.500–518.

Lee, J.H. et al., 2010. Development of batch and continuous processes on biodiesel production in a packed-bed reactor by a mixture of immobilized *Candida rugosa* and *Rhizopus oryzae* lipases. *Applied Biochemistry and Biotechnology*, 161, pp.365–371.

Lee, P.J. and Di Gioia, A.J., 2007. Acquity UPLC/ELS/UV: One methodology for FFA, FAME and TAG analysis of biodiesel. *Waters Corporation*.

Li, J. et al., 2012. Biodiesel production from yellow horn (*Xanthoceras sorbifolia Bunge*.) seed oil using ion exchange resin as heterogeneous catalyst. *Bioresource Technology*, 108, pp.112–118.

Li, N.-W., Zong, M.-H. and Wu, H., 2009. Highly efficient transformation of waste oil to biodiesel by immobilized lipase from *Penicillium expansum*. *Process Biochemistry*, 44, pp.685–688.

Li, S.-F. et al., 2011. *Pseudomonas cepacia* lipase immobilized onto the electrospun PAN nanofibrous membranes for biodiesel production from soybean oil. *Journal of Molecular Catalysis B: Enzymatic*, 72, pp.40–45.

Li, Y., Bao, G. and Wang, H., 2008. Determination of 11 fatty acids and fatty acid methyl esters in biodiesel using ultra performance liquid chromatography. *Chinese Journal of Chromatography*, 26, pp.494–498.

Limmanee, S. et al., 2013. Mixed oxides of Ca, Mg and Zn as heterogeneous base catalysts for the synthesis of palm kernel oil methyl esters. *Chemical Engineering Journal*, 225, pp.616–624.

Liu, Y. et al., 2009. Solubility Measurement for the Reaction Systems in Pre-Esterification of High Acid Value *Jatropha curcas* L. Oil. *Journal of Chemical and Engineering Data*, 54, pp.1421–1425.

López, D.E. et al., 2008. Esterification and transesterification using modified-zirconia catalysts. *Applied Catalysis A: General*, 339, pp.76–83.

Maher, K.D. and Bressler, D.C., 2007. Pyrolysis of triglyceride materials for the production of renewable fuels and chemicals. *Bioresource Technology*, 98, pp.2351–68.

Mahmud, M.S. et al., 2010. Kinetic analysis of oleic acid esterification using lipase as catalyst in a microaqueous environment. *Industrial and Engineering Chemistry Research*, 49, pp.1071–1078.

Marchetti, J.M., Miguel, V.U. and Errazu, A.F., 2007. Heterogeneous esterification of oil with high amount of free fatty acids. *Fuel*, 86, pp.906–910.

Mbaraka, I., 2003. Organosulfonic acid-functionalized mesoporous silicas for the esterification of fatty acid. *Journal of Catalysis*, 219, pp.329–336.

McMaster, M.C., 2007. *HPLC a practical user's guide* 2nd ed., John Wiley.

Meher, L.., Dharmagadda, V.S.S. and Naik, S.N., 2006a. Optimization of alkali-catalyzed transesterification of *Pongamia pinnata* oil for production of biodiesel. *Bioresource Technology*, 97, pp.1392–1397.

Meher, L.., Vidya Sagar, D. and Naik, S.., 2006b. Technical aspects of biodiesel production by transesterification—a review. *Renewable and Sustainable Energy Reviews*, 10, pp.248–268.

Melero, J.A., Iglesias, J. and Morales, G., 2009a. Heterogeneous acid catalysts for biodiesel production: current status and future challenges. *Green Chemistry*, 11, pp.1285–1308.

Melero, J.A. et al., 2009b. Biodiesel production with heterogeneous sulfonic acid-functionalized mesostructured catalysts. *Energy and Fuels*, 23, pp.539–547.

Melero, J.A. et al., 2010. Storage stability and corrosion studies of renewable raw materials and petrol mixtures: A key issue for their co-processing in refinery units. *Fuel*, 89, pp.554–562.

Noiroj, K. et al., 2009. A comparative study of KOH/Al2O3 and KOH/NaY catalysts for biodiesel production via transesterification from palm oil. *Renewable Energy*, 34, pp.1145–1150.

Noureddini, H., Gao, X. and Philkana, R.S., 2005. Immobilized *Pseudomonas cepacia* lipase for biodiesel fuel production from soybean oil. *Bioresource Technology*, 96, pp.769–77.

Orçaire, O., Buisson, P. and Pierre, A.C., 2006. Application of silica aerogel encapsulated lipases in the synthesis of biodiesel by transesterification reactions. *Journal of Molecular Catalysis B: Enzymatic*, 42, pp.106–113.

Ozbay, N., Oktar, N. and Tapan, N., 2008. Esterification of free fatty acids in waste cooking oils (WCO): Role of ion-exchange resins. *Fuel*, 87, pp.1789–1798.

Paiva, A.L., Balcão, V.M. and Malcata, F.X., 2000. Kinetics and mechanisms of reactions catalyzed by immobilized lipases. *Enzyme and Microbial Technology*, 27, pp.187–204.

Park, Y.-M. et al., 2010. Esterification of used vegetable oils using the heterogeneous WO3/ZrO2 catalyst for production of biodiesel. *Bioresource Technology*, 101 Suppl, pp.S59–S61.

Patil, P.D., Gude, V.G. and Deng, S., 2009. Biodiesel production from *Jatropha Curcas*, waste cooking, and *Camelina sativa* Oils. *Industrial and Engineering Chemistry Research*, 48, pp.10850–10856.

Raita, M. et al., 2011. Biocatalytic esterification of palm oil fatty acids for biodiesel production using glycine-based cross-linked protein coated microcrystalline lipase. *Journal of Molecular Catalysis B: Enzymatic*, 73, pp.74–79.

Ramos, M.J. et al., 2008. Transesterification of sunflower oil over zeolites using different metal loading: A case of leaching and agglomeration studies. *Applied Catalysis A: General*, 346, pp.79–85.

Russbueldt, B.M.E. and Hoelderich, W.F., 2009. New sulfonic acid ion-exchange resins for the preesterification of different oils and fats with high content of free fatty acids. *Applied Catalysis A: General*, 362, pp.47–57.

Santori, G. et al., 2009. Quantitation of Compounds in Biodiesel Mixtures with Reversed-Phase Liquid Chromatography. *Energy and Fuels*, 23, pp.3783–3789.

Semwal, S. et al., 2011. Biodiesel production using heterogeneous catalysts. *Bioresource Technology*, 102, pp.2151–2161.

Shah, S. and Gupta, M.N., 2007. Lipase catalyzed preparation of biodiesel from *Jatropha* oil in a solvent free system. *Process Biochemistry*, 42, pp.409–414.

Shah, S., Sharma, S. and Gupta, M.N., 2004. Biodiesel preparation by lipase-catalyzed transesterification of *Jatropha* Oil. *Energy and Fuels*, 18, pp.154–159.

Shahid, E.M. and Jamal, Y., 2011. Production of biodiesel: A technical review. *Renewable and Sustainable Energy Reviews*, 15, pp.4732–4745.

Sharma, Y.C., Singh, B. and Korstad, J., 2011. Latest developments on application of heterogenous basic catalysts for an efficient and eco friendly synthesis of biodiesel: A review. *Fuel*, 90, pp.1309–1324.

Shibasaki-Kitakawa, N. et al., 2007. Biodiesel production using anionic ion-exchange resin as heterogeneous catalyst. *Bioresource Technology*, 98, pp.416–421.

Shimada, Y. et al., 2002. Enzymatic alcoholysis for biodiesel fuel production and application of the reaction to oil processing. *Journal of Molecular Catalysis B: Enzymatic*, 17, pp.133–142.

Shu, Q. et al., 2007. Synthesis of biodiesel from soybean oil and methanol catalyzed by zeolite beta modified with La3+. *Catalysis Communications*, 8, pp.2159–2165.

Sim, J.H., Kamaruddin, A.H. and Bhatia, S., 2010. Biodiesel (FAME) productivity, catalytic efficiency and thermal stability of Lipozyme TL IM for crude palm oil transesterification with methanol. *Journal of the American Oil Chemists' Society*, 87, pp.1027–1034.

Šimáček, P. et al., 2011. Premium quality renewable diesel fuel by hydroprocessing of sunflower oil. *Fuel*, 90, pp.2473–2479.

Singare, P.U., Lokhande, R.S. and Madyal, R.S., 2011. Thermal Degradation Studies of Some Strongly Acidic Cation Exchange Resins. , 1, pp.45–54.

Smith, B., 1999. *Infrared Spectral Interpretation*, Boca Raton: CRC Press.

Soumanou, M., 2003. Improvement in lipase-catalyzed synthesis of fatty acid methyl esters from sunflower oil. *Enzyme and Microbial Technology*, 33, pp.97–103.

Souza, M.S. et al., 2009. Biodiesel synthesis via esterification of feedstock with high content of free fatty acids. *Applied Biochemistry and Biotechnology*, 154, pp.74–88.

Srivastava, R.K. and Albertsson, A., 2005. High-molecular-weight poly(1,5-dioxepan-2-one) via enzyme-catalyzed ring-opening polymerization. *Journal of Polymer Science: Part A: Polymer Chemistry* , 43, pp.4206–4216.

Stuart, B., 2004. *Infrared Spectroscopy: Fundamentals and Applications*, Chichester: John Wiley and Sons, Ltd.

Su, E. and Wei, D., 2008. Improvement in lipase-catalyzed methanolysis of triacylglycerols for biodiesel production using a solvent engineering method. *Journal of Molecular Catalysis B: Enzymatic*, 55, pp.118–125.

Sun, S. et al., 2013. Kinetic study on lipase catalyzed trans-esterification of palm oil and dimethyl carbonate for biodiesel production. *Journal of Renewable and Sustainable Energy*, 5, p.1-7.

Talukder, M.M.R., Wu, J.C. and Chua, L.P.-L., 2010a. Conversion of waste cooking oil to biodiesel via enzymatic hydrolysis followed by chemical esterification. *Energy and Fuels*, 24, pp.2016–2019.

Talukder, M.M.R. et al., 2010b. Two-step lipase catalysis for production of biodiesel. *Biochemical Engineering Journal*, 49, pp.207–212.

Talukder, M.M.R. et al., 2009. Comparison of Novozym 435 and Amberlyst 15 as heterogeneous catalyst for production of biodiesel from palm fatty acid distillate. *Energy and Fuels*, 23, pp.1–4.

Tariq, M., Ali, S. and Khalid, N., 2012. Activity of homogeneous and heterogeneous catalysts, spectroscopic and chromatographic characterization of biodiesel: A review. *Renewable and Sustainable Energy Reviews*, 16, pp.6303–6316.

Tesser, R. et al., 2010. Kinetics and modeling of fatty acids esterification on acid exchange resins. *Chemical Engineering Journal*, 157, pp.539–550.

Tian, H. et al., 2008. Alternative processing technology for converting vegetable oils and animal fats to clean fuels and light olefins. *Chinese Journal of Chemical Engineering*, 16, pp.394–400.

Tongboriboon, K., Cheirsilp, B. and H-Kittikun, A., 2010. Mixed lipases for efficient enzymatic synthesis of biodiesel from used palm oil and ethanol in a solvent-free system. *Journal of Molecular Catalysis B: Enzymatic*, 67, pp.52–59.

Torres, C.F. et al., 2008. A predictive kinetic study of lipase-catalyzed ethanolysis reactions for the optimal reutilization of the biocatalyst. *Biochemical Engineering Journal*, 42, pp.105–110.

Tran, D.-T. et al., 2012. Enzymatic transesterification of microalgal oil from *Chlorella vulgaris* ESP-31 for biodiesel synthesis using immobilized *Burkholderia* lipase. *Bioresource Technology*, 108, pp.119–27.

Trubiano, G., Borio, D. and Errazu, A., 2007. Influence of the operating conditions and the external mass transfer limitations on the synthesis of fatty acid esters using a Candida antarctica lipase. *Enzyme and Microbial Technology*, 40, pp.716–722.

Türkan, A. and Kalay, S., 2006. Monitoring lipase-catalyzed methanolysis of sunflower oil by reversed-phase high-performance liquid chromatography: Elucidation of the mechanisms of lipases. *Journal of Chromatography. A*, 1127, pp.34–44.

Urban, J., Svec, F. and Fréchet, J.M.J., 2012. A monolithic lipase reactor for biodiesel production by transesterification of triacylglycerides into fatty acid methyl esters. *Biotechnology and Bioengineering*, 109, pp.371–80.

Watanabe, Y. et al., 2007. Enzymatic production of fatty acid methyl esters by hydrolysis of acid oil Followed by esterification. *Journal of the American Oil Chemists' Society*, 84, pp.1015–1021.

Wen, Z. et al., 2010. Synthesis of biodiesel from vegetable oil with methanol catalyzed by Li-doped magnesium oxide catalysts. *Applied Energy*, 87, pp.743–748.

Williams, P.J.L.B. and Laurens, L.M.L., 2010. Microalgae as biodiesel and biomass feedstocks: Review and analysis of the biochemistry, energetics and economics. *Energy and Environmental Science*, 3, p.554.

Willis, W.M. and Marangoni, A.G., 2008. Enzymatic Interesterification. In C. C. Akoh and D. B. Min, eds. *Food Lipids: Chemistry, Nutrition and Biotechnology*. Boca Raton, London, New York: CRC Press, pp. 807–840.

Wyatt, V.T. et al., 2005. Fuel properties and nitrogen oxide emission levels of biodiesel produced from animal fats. *Journal of the American Oil Chemists' Society*, 82, pp.585–591.

Xie, W. and Huang, X., 2006. Synthesis of biodiesel from soybean oil using heterogeneous KF/ZnO catalyst. *Catalysis Letters*, 107, pp.53–59.

Xie, W. and Li, H., 2006. Alumina-supported potassium iodide as a heterogeneous catalyst for biodiesel production from soybean oil. *Journal of Molecular Catalysis A: Chemical*, 255, pp.1–9.

Xu, Y., Du, W. and Liu, D., 2005. Study on the kinetics of enzymatic interesterification of triglycerides for biodiesel production with methyl acetate as the acyl acceptor. *Journal of Molecular Catalysis B: Enzymatic*, 32, pp.241–245.

Yadav, G. and Manjula Devi, K., 2004. Immobilized lipase-catalysed esterification and transesterification reactions in non-aqueous media for the synthesis of tetrahydrofurfuryl butyrate: comparison and kinetic modeling. *Chemical Engineering Science*, 59, pp.373–383.

Yagiz, F., Kazan, D. and Akin, A., 2007. Biodiesel production from waste oils by using lipase immobilized on hydrotalcite and zeolites. *Chemical Engineering Journal*, 134, pp.262–267.

Yan, S., Salley, S. and Simonng, K., 2009. Simultaneous transesterification and esterification of unrefined or waste oils over ZnO-La_2O_3 catalysts. *Applied Catalysis A: General*, 353, pp.203–212.

Yin, L.-J. et al., 2010. Hydrolysis of *Chlorella* by *Cellulomonas* sp. YJ5 Cellulases and Its Biofunctional Properties. *Journal of Food Science*, 75, pp.H317–H323.

Yoo, H.-Y. et al., 2011. A novel alkaline lipase from *Ralstonia* with potential application in biodiesel production. *Bioresource Technology*, 102, pp.6104–6111.

Zabeti, M., Wan Daud, W.M.A. and Aroua, M.K., 2009. Activity of solid catalysts for biodiesel production: A review. *Fuel Processing Technology*, 90, pp.770–777.

Zagorodni, A.A., 2007. *Ion exchange materials : properties and applications*, Oxford: Elsevier.

Zhang, S. et al., 2010. Rapid microwave-assisted transesterification of yellow horn oil to biodiesel using a heteropolyacid solid catalyst. *Bioresource Technology*, 101, pp.931–6.

Zheng, J. et al., 2012. Lipase-coated K_2SO_4 micro-crystals: preparation, characterization, and application in biodiesel production using various oil feedstocks. *Bioresource Technology*, 110, pp.224–31.

Zhou, H., Lu, H. and Liang, B., 2006. Solubility of multicomponent systems in the biodiesel broduction by transesterification of *Jatropha curcas* L. oil with methanol. *Journal of Chemical and Engineering Data*, 51, pp.1130–1135.

Appendix A: MATLAB Code

A1. Overall Description

A typical example of the MATLAB code used to carry out the kinetic modelling is given in Sections A2 – A4. The overall code used to carry out the kinetic modelling is given in Section A2. This section of code is used to load the required data and input the initial estimate for the parameters. This code can also be modified to use previously calculated parameters and specify the number of loops.

This code then calls the objection function using “fminsearch”. The objective function is given in Section A3. This determines the difference between the model and the experimental data and condenses the difference into a single value, and shows how close the model is to the experimental data. No weighting of the results has been used. The objective function uses “ode23s” to solve the differential equations given in the model. The model has been written up as a separate file given in Section A4.

A2. The overall code; “Enzyme_parm_est_T”

```
global texp Yexp x0 t0 tf ET  plot_res Y time

ThesisData50c;  % loads data
texp = Time;   % time in min
Yexp = Exp1;

ET = 8.33e-5;  %mol/m3, based on the Thielmann paper with
supporting calculation in the softback book

% Initial concentration ???

  x0 = Exp1(:,1)';

  t0 = 0;
  tf = texp(end);  % min

OPTIONS = optimset('display','iter','maxiter',50);

plot_res = 1;
```

```
X0_param = [0.5  0.5   2     4     0.5   3     3     1     1     1
      1     5];   %Cheirslip constants (mol-1.min-1)
%X0_param = Xoptim;


[Xoptim,FVAL,EXITFLAG,OUTPUT] = fminsearch(@(x) Enz_obj_est(x),
X0_param, OPTIONS);

%LB = zeros(1,12);
%UB = ones(1,12)*inf;
%[Xoptim,FVAL,EXITFLAG,OUTPUT] = fmincon(@(x) Enz_obj_est(x),
X0_param,[],[],[],[],LB,UB,[],OPTIONS)

%plot_res = 0;
figure
Enz_obj_est(Xoptim)
```

A3. The Objective Function; “Enz_obj_est”

```
function fobj = Enz_obj_est(param)

global texp Yexp t0 tf x0 ET plot_res Y time


[time, Y] = ode23s(@enzyme_model_T, [t0 tf], x0, [], param);

%linear interpolation
Ymodel = [interp1(time,Y,texp)]';

fobj = sum(sum((Ymodel - Yexp).^2))*10;  %need to double check
the form of this equation - not sure about double sum

if plot_res
  plot(time, Y, texp, Yexp, 'ro')
  title('Model Data'), xlabel('Time [min]'),
ylabel('Concentration???')
  %legend('model results', 'experimental data')
  drawnow
end
```

A4. The Model; “enzyme_model_T”

```
function dx = enzyme_model_T(t,x,k)
global ET


%Modified Cheirslip model
%R = 8.31;
%k1 = k(1)*exp(-k(2)/R/T)
```

```
dx(1) = -(k(1)*x(6) + k(5)*x(7))*x(1)* (ET / (1 + k(8)*x(1) +
k(9)*x(2) + k(10)*x(3) + k(11)*x(5) + x(7)/k(12)));
dx(2) = ((k(1)*x(6) + k(5)*x(7))*x(1) - (k(2)*x(6) +
k(6)*x(7))*x(2))*(ET / (1 + k(8)*x(1) + k(9)*x(2) + k(10)*x(3) +
k(11)*x(5) + x(7)/k(12)));
dx(3) = ((k(2)*x(6) + k(6)*x(7))*x(2) - (k(3)*x(6) +
k(7)*x(7))*x(3))*(ET / (1 + k(8)*x(1) + k(9)*x(2) + k(10)*x(3) +
k(11)*x(5) + x(7)/k(12)));
dx(4) = (k(3)*x(6) + k(7)*x(7)*x(3))*(ET / (1 + k(8)*x(1) +
k(9)*x(2) + k(10)*x(3) + k(11)*x(5) + x(7)/k(12)));
dx(5) = ((k(1)*x(1) + k(2)*x(2) + k(3)*x(3))*x(6) -
k(4)*x(5)*x(7))*(ET / (1 + k(8)*x(1) + k(9)*x(2) + k(10)*x(3) +
k(11)*x(5) + x(7)/k(12)));
dx(6) = -((k(1)*x(1) + k(2)*x(2) + k(3)*x(3))*x(6) -
k(4)*x(5)*x(7))*(ET / (1 + k(8)*x(1) + k(9)*x(2) + k(10)*x(3) +
k(11)*x(5) + x(7)/k(12))); %modified water equation
dx(7) = -(k(5)*x(1) + k(6)*x(2) + k(7)*x(3) +
k(4)*x(5))*x(7)*(ET / (1 + k(8)*x(1) + k(9)*x(2) + k(10)*x(3) +
k(11)*x(5) + x(7)/k(12)));
dx(8) = -dx(7);   % I'm not sure about this.  Need to check the
maths and maybe amend the model

dx = dx(:);
```

Appendix B: Publications

B1. Journal Papers

Haigh, K.F. et al., 2013. Comparison of Novozyme 435 and Purolite D5081 as heterogeneous catalysts for the pretreatment of used cooking oil for biodiesel production. *Fuel*, 111, pp.186–193.

Haigh, K.F. et al., n.d. Kinetics of the Pre-treatment of used cooking oil using Novozyme 435 for biodiesel production. *Chemical Engineering Research and Design*. Submitted

Abidin, S.Z., Haigh, K.F. and Saha, B., 2012. Esterification of free fatty acids in used cooking oil using ion-exchange resins as catalysts: An efficient pretreatment method for biodiesel feedstock. *Industrial and Engineering Chemistry Research*, 51, pp.14653–14664.

B2. Conferences Papers

Haigh KF, Abidin SZ, Saha B, and Vladisavljević GT, 2012. Pretreatment of used cooking oil for the preparation of biodiesel using heterogeneous catalysis. *Progress in Colloid and Polymer Science*. 139, pp19-22.

Haigh KF, Saha B, Vladisavljević GT and Reynolds JC, 2012. Kinetics of the pre-treatment of used cooking oil using Novozyme 435 for Biodiesel Production. *Procedia Engineering*, 42, pp1106-1113.

B3. Conferences

Haigh KF, Abidin SZ, Vladisavljević GT and Saha B, 4-6 July 2011. Environmentally Benign Biodiesel Production by Heterogeneous Catalysis. *UK Colloids 2011: An international colloid and surface science symposium*, Poster presentation.

Haigh KF, Saha B, Vladisavljević GT, Reynolds JC and Nagy ZK, 25 – 29 August 2012. Kinetics of the Pre-treatment of Used Cooking Oil using Novozyme 435 for Biodiesel Production. *CHISA 2012*, Prague, Czech Republic. Oral presentation.

Haigh KF, Abidin SZ, Vladisavljević GT, Reynolds J and Saha B. 11 December 2012. Comparison of the catalytic performance of Novozyme 435 and Purolite D5081 for the esterification pre-treatment of used cooking oil for biodiesel production. *Catalysis for energy, University of Birmingham*, Oral presentation.

Saha, B., Abidin, SZ and Haigh, K.F. 19-21 September 2012. Ion exchange resins catalysed esterification of free fatty acids in used cooking oil with methanol: An efficient pre-treatement method for biodiesel production. *IEX 2012: The international ion exchange conference*. Queens College Cambridge, Oral Presentation.